



KTH Electrical Engineering

Fundamental Limits in Wireless Wideband Networking

TAN TAI DO

Doctoral Thesis in Telecommunications
Stockholm, Sweden 2015

TRITA-EE 2015:84
ISSN 1653-5146
ISBN 978-91-7595-721-0

KTH, School of Electrical Engineering
Communication Theory Department
SE-100 44 Stockholm
SWEDEN

Akademisk avhandling som med tillstånd av Kungl Tekniska högskolan framlägges till offentlig granskning för avläggande av teknologie doktorsexamen i telekommunikation 09 November 2015, kl. 13.15 i hörsal Q1, Kungl Tekniska Högskolan, Osquldas väg 10, Stockholm.

© 2015 Tan Tai Do, unless otherwise noted.

Tryck: Universitetsservice US AB

Abstract

The rapid growth of the wireless communication industry recently does not only bring opportunities but also challenges on developing radio technologies and solutions that can support high data rate as well as reliable and efficient communications. Two fundamental factors that limit the transmission rate are the available transmit energy and the available bandwidth. In this thesis, we investigate fundamental limits on energy and bandwidth efficiencies in wireless wideband networking. The framework and results can be used for performance assessment, design, and development of practical cellular networks.

First, we study the energy efficiency of a bidirectional broadcast channel in the wideband regime, i.e., where the bandwidth tends to infinity and the spectral efficiency is disregarded. In particular, we consider a transmit strategy for a Gaussian MIMO bidirectional broadcast channel that maximizes the energy efficiency, i.e., minimizes the energy required to reliably transmit one information bit. A closed-form solution of the optimal transmit covariance matrix is derived, which shows that using a single beam transmit strategy is optimal. Additionally, an extension to a multi-pair Gaussian MIMO bidirectional broadcast channel is studied, in which we propose a simple transmit strategy motivated from the optimal transmit strategy for the single user-pair setup. We show that serving a selected user-pair with full power is optimal in the sense of maximizing the achievable energy efficiency. Discussions on the optimality of the proposed transmit scheme for the multi-pair setup are also provided.

Next, we study the bandwidth efficiency of another wireless wideband network, in which the available bandwidth is large but still finite. Accordingly, we consider the bandwidth efficiency limit of an uplink wideband CDMA channel. Various realistic assumptions such as asynchronous transmission, inter-symbol interference, continuous-time waveform transmitted signal, etc. are incorporated into the problem formulation. In order to tackle the problems that arise with those assumptions, we derive an equivalent discrete-time channel model based on sufficient statistics for optimal decoding of the transmitted messages with perfect channel knowledge. The capacity regions are then characterized using the equivalent channel model. In addition, an extension to a system with imperfect channel state information and mismatched filtering at the receiver is considered. Achievable rate regions are characterized considering two different assumptions on decoding strategy, i.e., the optimal decoding based on the actual statistics of channel estimation errors and the sub-optimal approach treating the estimation errors as additive worst-case noise. Moreover, we also present a low-complexity receiver for the uplink wideband CDMA channel, which is based on a decision feedback equalizer structure.

Sammanfattning

Den snabba tillväxten av kommunikationsindustrin den senare tiden skapar inte bara möjligheter men även utmaningar för att utveckla radioteknologier och lösningar som kan stödja höga datahastigheter såväl som tillförlitlig och effektiv kommunikation. Två grundläggande faktorer som begränsar överföringshastigheten är den tillgängliga sändarenergien samt bandbredden. I denna uppsats undersöker vi grundläggande begränsningar för energi- och bandbredd-effektivitet i trådlösa bredbandsnätverk. Detta ramverk och dessa resultat kan användas för prestandautvärdering, design och utveckling av mobilnät i praktiken.

Först studerar vi energieffektiviteten i en dubbelriktad broadcastkanal i bredbandsområdet, d.v.s. där bandbredden går mot oändlighet och spektrumeffektivitet ej beaktas. Speciellt så uppmärksammar vi en sändningsstrategi för en Gaussisk MIMO dubbelriktad kanal som maximerar energieffektiviteten, d.v.s. den energi som behövs för att tillförlitligt överföra en enda informationsbit. Ett slutet uttryck för den optimala sändarkovariansmatrisen härleds, vilken visar att det är optimalt att använda bara ett enda strålknippe. Dessutom studeras en utvidgning till en flerparig Gaussisk MIMO dubbelriktad broadcast kanal, för vilken vi föreslår en enkel sändningsstrategi motiverat utifrån den optimala sändningsstrategin för enanvändarparkonfigurationen. Vi visar att det är optimalt att betjäna ett utvalt användarpär med full effekt, d.v.s. optimal i meningen att det maximerar den möjligt uppnåbara energieffektiviteten. Diskussioner avseende optimalitet av det föreslagna sändningsschemat för flerparkonfigurationen ges också.

Därefter studerar vi bandbreddseffektiviteten hos ett annat trådlöst bredbandsnätverk, där den tillgängliga bandbredden är stor men ändå begränsad. Således studerar vi bandbreddseffektivitets-begränsningar för en wideband CDMA kanal i upplänk. Olika realistiska antaganden såsom asynkron överföring, störningar symboler emellan, sändarsignaler med tidskontinuerlig vågform, etc. ingår i problemformuleringen. För att hantera de problem som uppstår med dessa antaganden, så härleder vi en motsvarande tidsdiskret kanal modell baserad på tillräcklig statistik för optimal avkodning av det sända meddelandet med perfekt kanalkunskap. Kapacitetsområden karaktäriseras sedan med motsvarande ekvivalenta kanal modell. Dessutom beaktas en utvidgning till ett system med osäker kanalstatusinformation och icke-optimal filtrering vid mottagaren. Uppnåeliga datahastighetsområden karaktäriseras avseende två olika antaganden om avkodningsstrategi, d.v.s. optimal avkodningen baserat på den faktiska statistiken hos kanaluppskattningfelet och den icke-optimala metoden som hanterar uppskattningsfel som ett värsta-fall med brus. Utöver det så presenterar vi även en lågkomplexitetsmottagare för wideband CDMA kanalen i upplänk, vilken bygger på en beslutsdriven utjämnarstruktur med återkoppling.

Acknowledgments

I would like to take this opportunity to acknowledge all those who have supported me in the development of this thesis.

First and foremost, I would like to express my deepest gratitude to my advisor and co-advisor, Prof. Mikael Skoglund and Prof. Tobias Oechtering for their attentive supervision and careful guidance. Mikael gave me the opportunity to join the Communication Theory Lab., which not only led to this thesis but also laid the ground for my future career. I am grateful for his openness, insightful suggestions and feedbacks, and supports through my years of study. Tobias has a major role in the completion of this thesis. He has invested a lot of time in supervising me. Whenever I need help, Tobias's door was open. His careful advices have always been invaluable, e.g., to improve the quality of my writing, which was surely not an easy task. His sound knowledge, enthusiasm, and the sense of responsibility makes him a great mentor. I am very thankful to him for invaluable discussions and lessons both on research and life.

I would like to thank Prof. Su Min Kim and Dr. Gunnar Peters, who had supported me a lot during the projet with Huawei Tech. Sweden AB. I have learnt a lot from their knowledge and experience. In particular, I am very much indebted to Prof. Su Min Kim for his useful comments and his valuable help since the start of our collaboration.

I wish to thank all faculty and students in the Communication Theory Lab. for creating a wonderful working environment. I am thankful to Prof. Lars K. Rasmussen, Prof. Ming Xiao, Prof. Ragnar Thobaben, and Dr. Saikat Chatterjee for their excellent lectures and for giving me valuable suggestions on various occasions. Special thanks to Hieu Do, Kittipong Kittichokechai, Ali Zaidi, Zhao Wang, Nan Li, Cao Le Phuong for many wonderful moments and events we have had together. I had a wonderful time in Stockholm with many good friends. I want to thank all my friends, in particular I want to mention Majid Gerami, Haopeng Li, Du Liu, Efthymios Stathakis, Hadi Ghauch, Farshad Naghibi, Leefke Dössel, Frederic Gabry, Mattias Andersson, Dennis Sundman, Jinfeng Du, Peter Larsson, Amirpasha Shirazinia, Maksym Girnyk, Nicolas Schrammar, Ahmed Zaki, Minh Thanh Vu, and Zuxing Li.

I am grateful to Annika Augustsson, Irene Kindblom, Raine Tiivel, and the IT support team for making things run smoothly from my first day in KTH. I am indebted to Efthymios Stathakis, Minh Thanh Vu, Zhao Wang, Hadi Ghauch, and Cao Le Phuong for their time and effort in proofreading part of the thesis and for giving me helpful comments and feedbacks.

I would like to thank Prof. Olav Tirkkonen from Aalto University for acting as opponent for this thesis. Thanks are due to Prof. Erik Ström from Chalmers University, Prof. Ana Isabel Pérez-Neira from Technical University of Catalonia, and Prof. Mikael Sternad from Uppsala University for acting on the grading committee, and Prof. Lars K. Rasmussen for the thesis review.

My gratitude is extended to my teachers and friends from Vietnam and South Korea. I would like to thank all my teachers, especially, Mr. Tran Trong Hung, who closely guided me from high school and Prof. Yun Hee Kim, who led me to the first step on my research. I am grateful to Dr. Le-Nam Tran and his family for helping me from my first day in Stockholm. I would like to thank Hien Ngo and Dr. Duong Quang Trung for both technical and non-technical discussions during my PhD study.

Most importantly, I would like to thank my beloved parents, parents in law, sisters, sisters in law, brothers, brothers in law, nieces and nephews. I am indebted to my small family, especially my wife. Without her love and encouragement I would not be able to get to the point of writing these lines.

Tan Tai Do
Stockholm, November 2015

Contents

Contents	ix
1 Introduction	1
1.1 Organization and Contributions of the Thesis	2
1.2 Copyright Notice	5
1.3 Abbreviations	6
2 Background	9
2.1 Preliminaries	9
2.2 Fundamental Constraints in High Data Rate Communications . .	13
2.3 Bidirectional Broadcast Channel	18
2.4 Wideband CDMA System	21
3 Single Pair MIMO Bidirectional Broadcast Channel in the Wideband Regime	27
3.1 Related Works and Motivation	27
3.2 Problem Setup	29
3.3 Optimal Transmit Strategy	32
3.4 Energy Efficiency and Fairness	35
3.5 Wideband Slope	42
3.6 Chapter Conclusion	44
3.7 Appendices	44
4 Multi-pair MIMO Bidirectional Broadcast Channel in the Wideband Regime	51
4.1 Related Works and Motivation	51
4.2 Problem Setup	52
4.3 Optimal Transmit Strategy	56
4.4 Energy Efficiency and Fairness Issue	59
4.5 Optimality	61
4.6 Chapter Conclusion	62
4.7 Appendices	63

5	Uplink WCDMA Channel with Perfect CSIR	65
5.1	Related Works and Motivation	66
5.2	Problem Setup	68
5.3	Capacity Characterization	72
5.4	Capacity Approximation	76
5.5	Numerical Characterization	83
5.6	Asymptotic Performance	86
5.7	Chapter Conclusion	89
5.8	Appendices	89
6	Uplink WCDMA Channel with Imperfect CSIR	97
6.1	Related Works and Motivation	97
6.2	Problem Setup	99
6.3	Achievable Rate Regions	104
6.4	Numerical Results	109
6.5	Chapter Conclusion	113
6.6	Appendices	113
7	Uplink WCDMA Channel with Decision Feedback Equalizer	119
7.1	Related Works and Motivation	119
7.2	Problem Setup	120
7.3	MMSE DFE for Gaussian Input	121
7.4	DFE for Finite Constellation Input	127
7.5	Linear Filters	129
7.6	Numerical Examples	131
7.7	Chapter Conclusion	135
8	Conclusion	137
8.1	Summary	137
8.2	Discussion	139
	Bibliography	141

Introduction

Communication, especially radio communication has extensive impacts on our society nowadays. The developing history of radio communication has been quite long since the first radio experiments [Bon95] of Guglielmo Marconi in the 1890s till now. During this period, mobile technology has evolved from a deluxe service for some selected individuals to a global communication system with almost 7 billions mobile-cellular subscriptions worldwide [ITU14]. With the rapid growth of wireless networks in recent years, radio communication is not simply used for telephone calls, but also for advanced communications such as interactive download and upload applications, digital television, real-time-gaming applications and so on. This is an underlying force that drives the mobile communication industry as well as researcher societies to develop radio technologies/solutions that can support high data rate communications in a reliable and efficient way.

As it will be clarified later, two main fundamental factors that limit the transmitted data rate are the available transmit energy and the available bandwidth. In order to increase the transmission rate, one has to increase the transmit energy and/or the available bandwidth.

For a given limited bandwidth, a straight-forward solution for higher transmission rates is to use a higher-order modulation scheme, i.e., the modulation alphabet is extended to include more signaling alternatives and allow more bits of information to be transmitted per modulation symbol. This will increase the spectral efficiency and thus improving the transmission rate for a given available bandwidth. However, the use of higher-order modulation leads to several drawbacks such as reduced robustness to noise and interference, large peak-to-average power ratios and high transmit power requirements. For instance, higher-order modulations such as 16QAM or 64QAM require a much higher signal-to-noise ratio (SNR) to maintain the same bit-error probability compared to BPSK. As it has been shown in [DPSB08] that transmission with high spectral efficiency is fundamentally energy inefficient in the sense that it requires un-proportionally high SNR for a given data rate. Supporting a relatively high transmission rate for a limited bandwidth is only possible when a very high SNR is available at the receiver, for example in a

small-cell with low traffic load or where mobile users are close to the base station. However, this is against the target of extending the coverage for future cellular networks.

An alternative solution is to widen the transmission bandwidth, which is the favourite solution for current 3GPP wireless standards such as wideband code division multiple access (WCDMA) Universal Mobile Telecommunications System (UMTS), High Speed Packet Access (HSPA) or Long-Term Evolution (LTE) [3GPP, HT04]. However, the transmission bandwidth is often a scarce and expensive resource. It is not cheap to allocate a sufficiently large portion of spectrum for a very wideband transmission, especially in the lower-frequency bands. A larger transmission bandwidth also results in higher complexity of the radio equipments at base stations and mobile terminals. For instance, a wider transmission bandwidth requires a higher sampling rate, more complicated digital-to-analog and analog-to-digital converters, and more complex front-end digital signal processing. Moreover, extending the transmission bandwidth will increase the corruption of the transmitted signal due to the frequency selectivity of channel, which leads to a higher error rate for a given SNR.

Therefore, knowing the fundamental limits and balancing the energy efficiency and spectral efficiency are important tasks in designing a communication network. Motivated from developing trends and challenges of current radio technologies, we study fundamental limits in wireless wideband networks. In particular, we focus on the energy and spectral efficiency aspects of such networks. The study in this thesis can be used as a framework for the performance assessment, design, and development of current and future cellular networks. The contributions and outline of the thesis are as follows.

1.1 Organization and Contributions of the Thesis

We divide the main contents of the thesis into two parts, focusing on the energy efficiency and the spectral efficiency, respectively. In the first part, we consider the energy efficiency aspect of Gaussian MIMO bidirectional broadcast channels in the wideband regime with a single user-pair setup in Chapter 3 and with a multiple user-pair setup in Chapter 4. In the second part, we focus on the spectral efficiency aspect of uplink wideband CDMA channels with perfect channel state information at the receiver (CSIR) in Chapter 5, with imperfect CSIR in Chapter 6, and with decision feedback equalizers in Chapter 7. The contents and contributions of each chapter are summarized as follows.

Chapter 2

We start with Chapter 2 by summarizing preliminary knowledge related to the thesis including some information theoretical definitions, fundamental limits in high data rate communications, bi-directional broadcast channels, and wideband CDMA

systems. Those basic concepts serve as a background for studying the problems in the subsequent chapters.

Part 1

This part consists of two chapters: Chapter 3 and Chapter 4.

Chapter 3

In Chapter 3, we study the energy efficiency of a single pair bidirectional broadcast channel in the wideband regime. In particular, we consider the optimal transmit strategy for a Gaussian MIMO bidirectional broadcast channel that maximizes the energy efficiency, i.e., minimizing the energy required to reliably transmit one information bit, so called minimum energy per bit (MEpB). A closed-form solution of the optimal transmit covariance matrix is derived, which shows that a single beam transmit strategy is optimal. Transmit strategies for some special cases are also analyzed. The multi-user setting leads to a multi-dimensional MEpB region, in which the trade-off between individual and system performances can be clearly observed. Lastly, the fairness versus energy efficiency trade-off is also discussed.

Chapter 4

As a natural extension from Chapter 3, in this chapter we examine the energy efficiency of a bidirectional broadcast channel with multiple user-pairs. In this chapter, we propose a transmit strategy, which is motivated from the optimal transmit strategy for the single user-pair setup. An achievable wideband rate region and an achievable energy per bit region are provided. In order to characterize the boundaries of those regions, the optimal transmit covariance matrix is designed in the sense of maximizing the achievable wideband weighted sum-rate. The result shows that a single beam transmission aiming for only one selected user-pair is optimal. The discussions with respect to the optimality of the proposed scheme include individual MEpB achievability and a conjecture on the MEpB region.

The materials in Part 1 are based on

- [DOS11] T. T. Do, T. J. Oechtering, and M. Skoglund, “Optimal transmission for the MIMO bidirectional broadcast channel in the wideband regime,” in *Proc. 12th IEEE Int. Workshop on Signal Process. Adv. in Wireless Commun. (SPAWC2011)*, Jun. 2011.
- [DOS12] T. T. Do, T. J. Oechtering, and M. Skoglund, “Achievable energy per bit for the multi-pair MIMO bidirectional broadcast channel,” in *Proc. 18th European Wireless Conference (EW2012)*, Apr. 2012.

- [DOS13] T. T. Do, T. J. Oechtering, and M. Skoglund, “Optimal transmission for the MIMO bidirectional broadcast channel in the wideband regime,” *IEEE Trans. Signal Process.*, vol. 61, no. 20, pp. 5103 - 5116, Oct. 2013.

Part 2

This part consists of three chapters: Chapter 5, Chapter 6, and Chapter 7.

Chapter 5

Chapter 5 investigates the spectral efficiency, i.e., capacity limit of an uplink WCDMA channel assuming that perfect channel state information (CSI) is available at the receiver. Various realistic assumptions such as asynchronous transmission, inter-symbol interference, continuous-time waveform transmitted signal, etc. are incorporated into problem. An equivalent discrete-time channel model is derived based on sufficient statistics for optimal decoding of the transmitted messages. Capacity regions are then characterized using the equivalent channel considering both finite constellation and Gaussian distributed input signals. The capacity with finite sampling is also provided to exemplify performance loss due to a specific post-processing at the receiver. We also propose an approximation algorithm to evaluate the capacity when dimensions of the system are large. Moreover, we analyze the asymptotic capacity when the signal-to-noise ratio tends to infinity. The conditions to simultaneously achieve the individual capacities are derived, which reveal the impact of the signature waveform space, channel frequency selectivity and signal constellation on the system performance.

Chapter 6

In this chapter, we continue with the capacity limit of an uplink WCDMA channel but assume that only imperfect CSI is available at the receiver. A discrete-time equivalent channel model is derived assuming mismatched filtering using the imperfect CSI at the receiver. Achievable rate regions are then characterized considering two different assumptions on decoding strategy, i.e., an optimal decoding strategy based on the specific statistics of channel estimation error and a sub-optimal decoding strategy treating the signal associated with channel estimation error as worst-case noise. Numerical results are provided to show that one can enhance the performance by exploiting the knowledge on the statistics of the channel estimation error. Simulations also assess the effect of the imperfectness on the achievable rate, which reveal that finite constellation inputs are less sensitive to the estimation accuracy than Gaussian input, especially in the high SNR regime.

Chapter 7

In this chapter, we consider a low-complexity decoding strategy for the uplink WCDMA channel. We start with a minimum mean square error (MMSE) decision

feedback equalizer (DFE) structure, which is a capacity-lossless receiver structure for Gaussian channels with Gaussian distributed input. After showing that the MMSE DFE receiver achieves the sum-capacity for a simple two-user setup, we apply it to our WCDMA model. In addition to the MMSE DFE receiver, we consider two other linear DFEs: matched filter DFE and decorrelator DFE. Based on three different DFEs, which have low-complexity receiver structures, we derive the achievable sum-rates for both Gaussian distributed and finite constellation inputs. Since the inter-stream interferences are not Gaussian in general, in this chapter we propose two decoding strategies for the DFE motivated from the decoding schemes in Chapter 6: i) per-stream optimal decoding that uses the true transition probability density function of each stream and ii) per-stream sub-optimal decoding that treats the inter-stream interferences as Gaussian noise.

The materials in Part 2 are based on

- [DOKP14] T. T. Do, T. J. Oechtering, S. M. Kim, and G. Peters, “Capacity analysis of continuous-time time-variant asynchronous uplink wideband CDMA system,” in *Proc. 80th IEEE Veh. Technol. Conf. (VTC2014-Fall)*, Sep. 2014.
- [DKO⁺ed] T. T. Do, S. M. Kim, T. J. Oechtering, M. Skoglund, and G. Peters, “Waveform domain framework for capacity analysis of uplink WCDMA systems,” *EURASIP Journal on Wireless Commun. and Networking*, 2015, conditionally accepted.
- [DKOP15] T. T. Do, S. M. Kim, T. J. Oechtering, and G. Peters, “Capacity analysis of uplink WCDMA systems with imperfect channel state information,” in *Proc. 81th IEEE Veh. Technol. Conf. (VTC2015-Spring)*, May 2015.
- [DOK⁺ed] T. T. Do, T. J. Oechtering, S. M. Kim, M. Skoglund, and G. Peters, “Uplink waveform channel with imperfect channel state information and finite constellation inputs,” *IEEE Trans. Wireless Commun.*, 2015, submitted.
- [KDOP15] S.M. Kim, T. T. Do, T. J. Oechtering, and G. Peters, “On the entropy computation of large complex gaussian mixture distributions,” *IEEE Trans. Signal Process.*, vol. 63, no. 17, pp. 4710 - 4723, Sep. 2015. The conference version [KDOP14] was presented in SSP-2014.

1.2 Copyright Notice

As specified in Section 1.1, parts of the material presented in this thesis are partly verbatim based on the thesis author’s joint works which are previously published or submitted to conferences and journals held by or sponsored by the Institute of

Electrical and Electronics Engineer (IEEE) and the European Association for Signal Processing (EURASIP). IEEE and EURASIP hold the copyright of the published papers and will hold the copyright of the submitted papers if they are accepted. Materials (e.g., figure, graph, table, or textual material) are reused in this thesis with permission.

1.3 Abbreviations

3GPP	3rd generation partnership project
AWGN	Additive white Gaussian noise
BPSK	Binary phase-shift keying
CDMA	Code division multiple access
CSI	Channel state information
CSIR	Channel state information at the receiver
DFE	Decision feedback equalizer
DMC	Discrete memoryless channel
EpB	Energy per bit
GMR	Gaussian mixture reduction
HSPA	High speed packet access
i.i.d.	Independent and identically distributed
I/Q	In-phase/quadrature
ISI	Inter-symbol interference
KKT	Karush-Kuhn-Tucker
LPF	Low pass filter
LTE	Long-Term Evolution
MAC	Multiple access channel
MAP	Maximum a posteriori
MEpB	Minimum energy per bit
MF	Matched filtering
MIMO	Multiple input multiple output
MISO	Multiple input single output
ML	Maximum likelihood
MMSE	Minimum mean square error
MRC	Maximal ratio combining
OVSF	Orthogonal variable spreading factor
pdf	Probability density function
PHY	Physical layer
pmf	Probability mass function

psd	Power spectral density
QAM	Quadrature amplitude modulation
QPSK	Quadrature phase-shift keying
RRC	Root raised cosine
SIC	Successive interference cancellation
SIMO	Single input multiple output
SISO	Single input single output
SNR	Signal-to-noise ratio
SRRC	Square root raised cosine
UMTS	Universal mobile telecommunications system
WCDMA	Wideband code division multiple access
w.r.t.	With respect to

Background

This chapter provides preliminary knowledge, which serves as a background for studying the problems in the subsequent chapters. We will introduce basic concepts including preliminary definitions, fundamental limits in high data rates communications, bidirectional broadcast channel and wideband CDMA systems.

2.1 Preliminaries

We first introduce definitions of *entropy* and *mutual information*, which are the two most important elements in defining channel capacity. In the following, some relevant concepts are presented including Markov chain, data processing inequality and sufficient statistic.

2.1.1 Entropy and mutual information

Definition 2.1 (Entropy [CT06]). Let X be a discrete random variable with finite alphabet \mathcal{X} and a probability mass function (pmf) $p_X(x)$. The *entropy* of X , denoted by $H(X)$, is defined as

$$H(X) = - \sum_{x \in \mathcal{X}} p_X(x) \log p_X(x). \quad (2.1)$$

The unit of $H(X)$ depends on the base of the logarithm. $H(X)$ is measured in *bits* if the logarithm is to the base 2, and is measured in *nats* if the logarithm is to the natural base e . Entropy can be interpreted as a measure of uncertainty, for instance, $H(X)$ measures amount of uncertainty of the random variable X .

Definition 2.2 (Conditional entropy [CT06]). Let X and Y be two discrete random variables with finite alphabets \mathcal{X} and \mathcal{Y} , and a joint pmf $p_{XY}(x, y)$. The conditional

entropy of Y given X , denoted by $H(Y|X)$, is defined as

$$H(Y|X) = - \sum_{x \in \mathcal{X}} \sum_{y \in \mathcal{Y}} p_{XY}(x, y) \log_{Y|X} p(y|x). \quad (2.2)$$

Conditional entropy $H(Y|X)$ measures amount of uncertainty of the random variable Y remained after observing X .

Definition 2.3 (Mutual information, discrete case [CT06]). Let X and Y be two discrete random variables with finite alphabets \mathcal{X} , \mathcal{Y} and joint pmf $p_{XY}(x, y)$. The mutual information between X and Y , denoted by $I(X; Y)$, is defined as

$$I(X; Y) = \sum_{x \in \mathcal{X}} \sum_{y \in \mathcal{Y}} p_{XY}(x, y) \log \frac{p_{XY}(x, y)}{p_X(x)p_Y(y)}, \quad (2.3)$$

where $p_X(x)$ and $p_Y(y)$ are the marginal pmfs of X and Y , respectively. Mutual information can be interpreted as amount of information shared between two random variables. For instance, $I(X; Y)$ measures amount of information about X one can infer from observing Y , or equivalent amount of information about Y one can infer from observing X .

Definition 2.4 (Conditional mutual information [CT06]). Let X , Y , and Z be discrete random variables with finite alphabets \mathcal{X} , \mathcal{Y} , \mathcal{Z} and a joint pmf $P_{X,Y,Z}(x, y, z)$. The conditional mutual information between X and Y conditioned on Z , denoted by $I(X; Y|Z)$, is defined as

$$I(X; Y|Z) = \sum_{x,y,z} P_{X,Y,Z}(x, y, z) \log \frac{P_{X,Y|Z}(x, y|z)}{P_{X|Z}(x|z)P_{Y|Z}(y|z)}. \quad (2.4)$$

Conditional mutual information $I(X; Y|Z)$ represents amount of information about X one can infer from observing Y given that Z is already known.

These aforementioned definitions for entropy and mutual information are given for a pair or a triple of random variables. However, similar definitions apply for multiple random variables with corresponding joint distributions.

Lemma 2.1 (Properties of entropy H and mutual information I [CT06]). *The following are some basic properties of entropy and mutual information.*

- *Non-negativity:* $H(X) \geq 0$.
- *Conditioning reduces entropy:* $H(X|Y) \leq H(X)$.
- *Chain rule:* $H(X^n) = \sum_{i=1}^n H(X_i|X^{i-1}) = \sum_{i=1}^n H(X_i|X_{i+1}^n)$.
- *Upper bound:* $H(X) \leq \log |\mathcal{X}|$, with equality iff X is uniformly distributed over \mathcal{X} .

- *Non-negativity:* $I(X; Y) \geq 0$.
- *Relation to entropy:* $I(X; Y|Z) = H(X|Z) - H(X|Y, Z)$.
- *Self information:* $I(X; X) = H(X)$.
- *Chain rule:* $I(X^n; Y^n|Z^n) = \sum_{i=1}^n I(X_i; Y^n|Z^n, X^{i-1})$.

The following definitions apply to continuous random variables.

Definition 2.5 (Differential entropy [CT06]). Let X be a continuous random variable that admits a probability density function (pdf) $f_X(x)$. The *differential entropy* of X , denoted by $h(X)$, is defined as

$$h(X) = - \int_{\mathcal{S}_X} f_X(x) \log f_X(x) dx, \quad (2.5)$$

where \mathcal{S}_X is the support of X .

Definition 2.6 (Conditional differential entropy [CT06]). Let X and Y be continuous random variables that admit a joint pdf $f_{XY}(x, y)$. The conditional differential entropy of X given Y , denoted by $h(X|Y)$, is defined as

$$h(X|Y) = - \int_{\mathcal{S}_{XY}} f_{XY}(x, y) \log f_{X|Y}(x|y) dx dy, \quad (2.6)$$

where \mathcal{S}_{XY} is the support of (X, Y) .

Definition 2.7 (Mutual information, continuous case [CT06]). Let X and Y be continuous random variables that admit a joint pdf $f_{XY}(x, y)$. The mutual information between X and Y , denoted by $I(X; Y)$, is defined as

$$I(X; Y) = \int_{\mathcal{S}_{XY}} f_{XY}(x, y) \log \frac{f_{XY}(x, y)}{f_X(x)f_Y(y)} dx dy, \quad (2.7)$$

where \mathcal{S}_{XY} is the support of (X, Y) , and $f_X(x)$ and $f_Y(y)$ are the marginal pdf's of X and Y , respectively¹.

¹For general random variables, the mutual information is defined as

$$I(X; Y) = \int_{\mathcal{S}_{XY}} \left(\log \frac{dP_{XY}}{d(P_X \times P_Y)} \right) dP_{XY},$$

where P_{XY} , P_X , and P_Y are the probability distributions of (X, Y) , X , and Y , respectively. $\frac{dP_{XY}}{d(P_X \times P_Y)}$ denotes the Radon-Nikodym derivative of the joint probability measure P_{XY} with respect to the product measure $P_X \times P_Y$ [Gra09]. Furthermore, we define $H(X) = I(X; X)$.

From the definitions it is clear that

$$I(X; Y) = H(X) - H(X|Y) = H(Y) - H(Y|X) \quad (2.8)$$

for discrete random variables, and

$$I(X; Y) = h(X) - h(X|Y) = h(Y) - h(Y|X) \quad (2.9)$$

for continuous random variables.

2.1.2 Markov chain, data processing inequality and sufficient statistics

Definition 2.8 (Markov chain [CT06]). We use $X - Y - Z$ to denote that (X, Y, Z) forms a Markov chain, that is, their joint pmf can be factorized as $P_{X,Y,Z}(x, y, z) = P_{X,Y}(x, y)P_{Z|Y}(z|y)$ or $P_{X,Y,Z}(x, y, z) = P_{X|Y}(x|y)P_{Y,Z}(y, z)$.

Markov chains are related to the concept of *conditional independence*. For example, $X - Y - Z$ implies that X is conditionally independent of Z given Y . We can see that it has a symmetry property, i.e., $X - Y - Z$ implies $Z - Y - X$. In the following, we state a few other properties satisfied by a Markov chain or conditional independence.

Lemma 2.2 (Properties satisfied by Markov chain [CT06]). *Let (X, Y, Z, W) be discrete random variables.*

- *Decomposition: $X - Y - (Z, W)$ implies $X - Y - Z$.*
- *Weak union: $X - Y - (Z, W)$ implies $X - (Y, Z) - W$.*
- *Contraction: $X - Y - Z$ and $X - (Y, Z) - W$ imply $X - Y - (Z, W)$.*
- *Intersection: $X - (Y, Z) - W$ and $X - (Y, W) - Z$ imply $X - Y - (Z, W)$, where the intersection is valid only for strictly positive probability distributions.*

Lemma 2.3 (Data processing inequality [CT06]). *If $X - Y - Z$, then $I(X; Y) \geq I(X; Z)$. In particular, if $Z = f(Y)$, we have $I(X; Y) \geq I(X; f(Y))$. This implies that any processing of the data Y cannot increase information about X .*

2.1.3 Sufficient statistic

Definition 2.9 (Sufficient statistic [CT06]). Let $\{f_\theta(x)\}$ be a family of probability mass functions indexed by θ , X be a sample from a distribution in this family, and $T(X)$ be any statistic (function of the sample). Then $T(X)$ is said to be a sufficient statistic relative to the family $\{f_\theta(x)\}$ if X is independent of θ given $T(X)$ for any distribution on θ , i.e., $\theta - T(X) - X$ forms a Markov chain.

This is the same as the condition for equality in the data processing inequality,

$$I(\theta; X) = I(\theta; T(X))$$

for any distribution on θ . In other words, a sufficient statistic preserves the mutual information.

2.2 Fundamental Constraints in High Data Rate Communications

We continue with fundamental constraints in a point-to-point channel communication including the spectral efficiency and energy efficiency trade-off and their behaviors in the wideband regime.

2.2.1 Capacity of a point-to-point channel

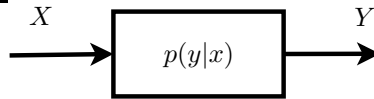


Figure 2.1: Point-to-point discrete memoryless channel.

The basic target of communication is to reliably transmit a message from a transmitter to a receiver over a communication channel. In practice, the communication channels are disturbed by noise, interference or propagation from the environment. One of the most basic communication channel is the point-to-point discrete memoryless channel (DMC) depicted in Figure 2.1. In this figure, X denotes the channel input, Y denotes the channel output and the transition probability mass function $p(y|x)$ captures the characteristics of the channel. It is well known that the channel capacity, which describes the supremum of all achievable rate that can be reliably transmitted over the channel, of the point-to-point DMC in Figure 2.1 is given as follows.

Theorem 2.2.1 (Capacity of a point-to-point DMC [CT06]). *The capacity of a point-to-point DMC is given by*

$$C = \sup_{p(x)} I(X; Y), \quad (2.10)$$

where supremum is equal to maximum if the set \mathcal{X} is finite, i.e., $|\mathcal{X}| < \infty$.

The channel model in Figure 2.1 and result in Theorem 2.2.1 are universal in the sense that they can describe any point-to-point DMC. In the literature, one of the most common models that is widely studied in information theory and communication theory is the Gaussian point-to-point channel. In this channel, the signal

sent by the transmitter is corrupted by additive white Gaussian noise (AWGN). An example of the Gaussian point-to-point channel is depicted in Figure 2.2. The signal model of this can be described as

$$Y = X + N,$$

where N is additive white Gaussian noise, i.e., $N \sim \mathcal{N}(0, N_0/2)$.

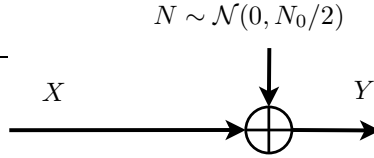


Figure 2.2: Gaussian point-to-point channel.

The capacity of the Gaussian point-to-point channel is given by the famous Shannon channel capacity formula as follow.

Theorem 2.2.2 (Capacity of a Gaussian point-to-point channel [CT06]). *The capacity of a Gaussian point-to-point channel is given by*

$$C = B \log_2 \left(1 + \frac{P}{BN_0} \right) \quad (\text{bits/s}), \quad (2.11)$$

where B (in Hz) is the available bandwidth, P (in watts) is the received signal power, $N_0/2$ (in watts/Hz) is the two-sided noise power spectral density.

2.2.2 Spectral efficiency and energy efficiency trade-off

It can be seen from the capacity formula in Theorem 2.2.2 that two fundamental factors that limit the achievable rate are the available bandwidth B and the signal-to-noise ratio P/N (we define $N := BN_0$ (watts) as the noise power).

Let us assume that we transmit with a certain rate R (in bits/s) and E_b (in joules/bit) is the received energy per bit. Then, the received power P can be expressed as $P = E_b R$ and the achievable rate R can be bounded by

$$\begin{aligned} R \leq C &= B \log_2 \left(1 + \frac{P}{BN_0} \right) \\ &= B \log_2 \left(1 + \frac{E_b R}{N_0 B} \right). \end{aligned} \quad (2.12)$$

Let us define $\gamma := \frac{R}{B}$ as the *spectral efficiency*. Following from (2.12), we have a lower bound on $\frac{E_b}{N_0}(R)$, i.e., the received energy per information bit for reliable

communicating at rate R , normalized by the noise power density as

$$\begin{aligned} \frac{E_b}{N_0}(R) &\geq \frac{2^{R/B} - 1}{R/B} \\ &= \frac{2^\gamma - 1}{\gamma}. \end{aligned} \quad (2.13)$$

We note that the equality in (2.13) holds when data is transmitted with a transmission rate equals to the capacity, i.e., $R = C$. Let us define $\frac{E_b}{N_0}(C) := \frac{2^\gamma - 1}{\gamma}$, then $\frac{E_b}{N_0}(C)$ is the required received energy per information bit for reliable communications at channel capacity, which describes the *energy efficiency*.²

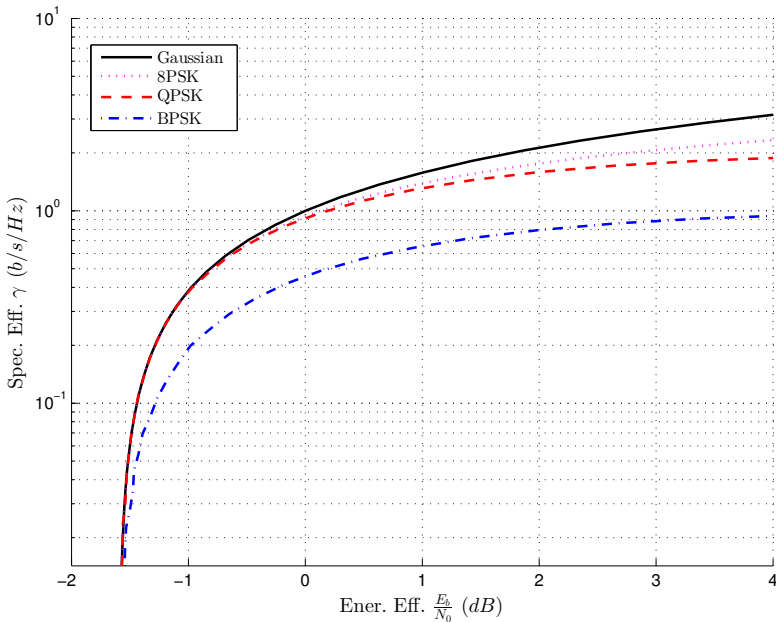


Figure 2.3: Spectral efficiency and energy efficiency trade-off.

Figure 2.3 illustrates the trade-off between the spectral efficiency and the energy efficiency of a Gaussian point-to-point channel. For comparison, the spectral and energy efficiencies trade-offs with finite constellation inputs (BPSK, QPSK, 8PSK)

²Rigorously, the energy efficiency should be defined by the inversion $1/\frac{E_b}{N_0}$, i.e., the number of bits that can be reliably transmitted per energy unit. However, in this thesis, we will use $\frac{E_b}{N_0}$ to represent the energy efficiency as it is consistent with the literature on communication in the wideband regime, which focuses on the minimum energy per bit.

are also included. We can see that for the spectral efficiency less than one, i.e., the transmission rate is smaller than the available bandwidth, the required energy per bit increases slightly with the spectral efficiency. However, when the transmission rate is larger than the available bandwidth, a slight increase in the transmission rate (for a fixed bandwidth) requires a much higher received energy per bit. This implies that when the transmission rate is in the same order or larger than the available bandwidth, any further increase of the data rate, without a corresponding increasing bandwidth, requires a much larger increase in the received energy.

2.2.3 Minimum energy per bit

We note that $\frac{E_b}{N_0}(C)$ is the required received energy per information bit, i.e., energy efficiency for reliable communications with spectral efficiency $\gamma = C/B$. We now wonder how much energy efficiency can be achieved given that one disregards the spectral efficiency or in extreme case when $B \rightarrow \infty$, i.e., $\gamma = 0$?

Since the capacity in (2.11) is a monotonically increasing function of the available bandwidth B , the energy per bit $\frac{E_b}{N_0}(C) = \frac{P}{CN_0}$ for given P is decreasing with the increase of B . Therefore, the *minimum energy per bit* (MEpB) required for reliable communication is given by

$$\frac{E_b}{N_{0 \min}} = \lim_{B \rightarrow \infty} \frac{P}{N_0 C}. \quad (2.14)$$

This is a key measurement in the wideband regime and has been studied for a general class of channels in [Ver02]. Accordingly, the MEpB can be derived as [Ver02]

$$\frac{E_b}{N_{0 \min}} = \frac{\log_e 2}{\dot{C}(0)},$$

where $\dot{C}(0)$ is the derivative at 0 of the capacity function with respect to (w.r.t.) P/N_0 . Moreover, it has been shown in [Ver02] that for a Gaussian point-to-point channel, the MEpB is $\frac{E_b}{N_{0 \min}} = \log_e 2 = -1.59 \text{ dB}$ and Gaussian inputs are not mandatory to achieve this MEpB. In this thesis, we will study the MEpB for Gaussian MIMO bidirectional broadcast channels where the concept of MEpB needs to be extended to a multi-user setting, in which one has to deal with multiple transmit powers and rates instantaneously.

It is worth noting that when the available bandwidth B approaches infinity, the spectral efficiency tends to zero, however, the capacity C does not vanish. Hence, we define the limit of C when $B \rightarrow \infty$ as the *wideband capacity* C , i.e.,

$$C = \lim_{B \rightarrow \infty} C. \quad (2.15)$$

Then, the MEpB can be calculated as the ratio of the power P and the wideband rate normalized by the noise power N_0

$$\frac{E_b}{N_{0 \min}} = \frac{P}{N_0 C} \quad (2.16)$$

and the *achievable energy per bit* (EpB) when the data is transmitted at rate R is given by

$$\frac{E_b}{N_0} = \frac{P}{N_0 R}, \quad (2.17)$$

where $R = \lim_{B \rightarrow \infty} R$ is the *achievable wideband rate*.

Remark 2.1. For distinction, throughout this thesis, we use the italic letter C (or R) to denote the capacity (or achievable rate) and the normal letter C (or R) to denote the wideband capacity (or achievable wideband rate).

2.2.4 Wideband slope

The minimum energy per bit is achieved with infinite bandwidth B , i.e., zero spectral efficiency. However, as discussed in [Ver02], another important performance metric in the wideband regime is the *wideband slope*, i.e., the slope of the spectral efficiency curve versus $\frac{E_b}{N_0}$ in the low energy per bit regime. When the spectral efficiency is small but non-zero, the wideband slope, measured in bits/s/Hz/(3 dB), evaluates the growth speed of the spectral efficiency w.r.t. the EpB. In other words, the wideband slope characterizes the trade-off between the spectral efficiency and EpB (or the bandwidth versus power trade-off) in the wideband regime.

For a point-to-point channel, the wideband slope is defined as [Ver02]

$$\begin{aligned} S_0 &= \lim_{\frac{E_b}{N_0} \rightarrow \frac{E_b}{N_{0 \min}}} \frac{C}{10 \log 10 \frac{E_b}{N_0}(C) - 10 \log 10 \frac{E_b}{N_{0 \min}}} \\ &= \lim_{B \rightarrow \infty} \frac{C}{10 \log 10 \frac{E_b}{N_0}(C) - 10 \log 10 \frac{E_b}{N_{0 \min}}}. \end{aligned} \quad (2.18)$$

Figure 2.4 shows the spectral efficiency curve versus $\frac{E_b}{N_0}$ in the linear scale. It shows that although the MEpBs are the same for different input signals, the wideband slopes depend on the input signals. In particular, the wideband slope is larger for higher modulation orders and largest for Gaussian input. This is reasonable and expected as the higher modulation order is used, the higher spectral efficiency can be achieved.

Similar to the MEpB, in this thesis we also study the wideband slope in a multi-user concept, where both the individual and system wideband slopes are considered.

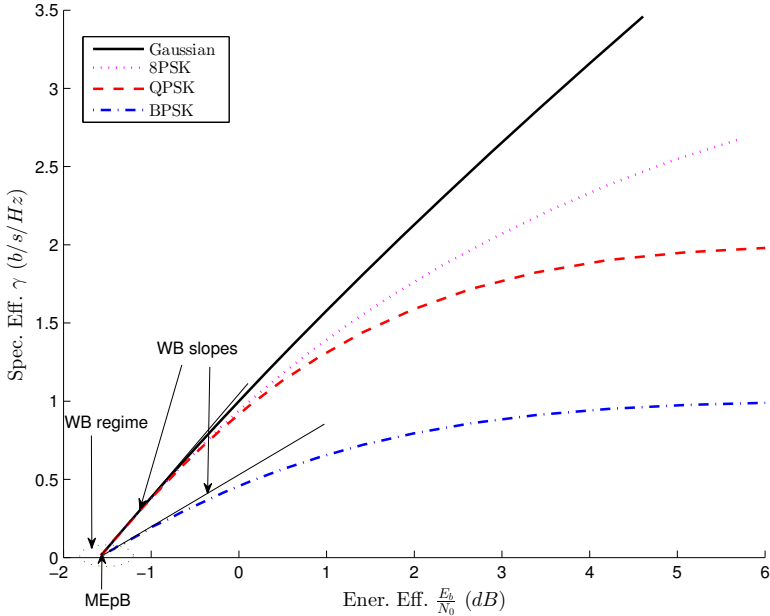


Figure 2.4: Spectral efficiency and energy efficiency trade-off.

2.3 Bidirectional Broadcast Channel

Recently, cooperative communication has attracted considerable attention due to its potential which could lead to extend the coverage and mitigate fading effects of wireless networks. In cooperative systems, the conventional one-way relaying with half-duplex protocol suffers some loss in the overall spectral efficiency since two phases are needed for the transmission from source to destination. In order to compensate for this, *bidirectional relaying* has been proposed [LJS06, RW07], also called *two-way relaying*, where two nodes want to exchange their messages through the support of a relay node, see [KMT08, OSBB08, OWB09, OJWB09] for further references.

In a two phases decode-and-forward bidirectional relaying system, during the first phase, so called multiple-access (MAC) phase, both users transmit their messages to the relay, which are decoded at the relay before a processed signal is broadcasted to users in the second phase, namely the broadcast phase. Since the optimal transmit strategy for the MAC phase is well known, we concentrate on the broadcast phase in this thesis, which is called *bidirectional broadcast channel* due to the side information from the previous MAC phase [OSBB08, OWB09, OJWB09].

Figure 2.5 illustrates the system model of a bidirectional relaying channel where

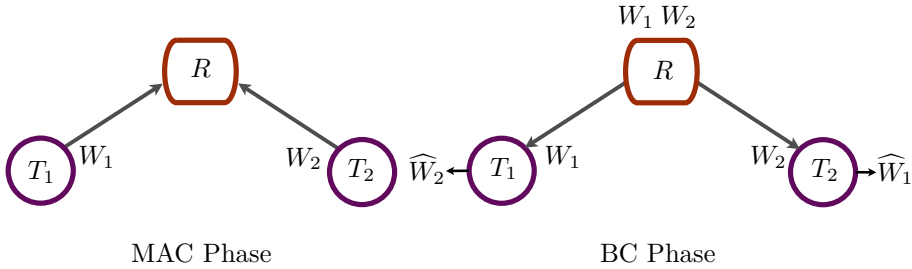


Figure 2.5: Bidirectional relaying channel.

2 users/terminals T_1, T_2 want to exchange their messages with the support from the relay R . Terminal T_1 want to transmit message W_1 and desires W_2 from T_2 . After the MAC phase, we assume that the relay can successfully decode both W_1 and W_2 . In the broadcast phase, the relay forwards W_1, W_2 and each user tries to decode its desired message using the corresponding received signal and its side information (its own message).

The optimal coding scheme and capacity region for a bidirectional broadcast channel have been derived in [OSBB08]. The following theorem from [OSBB08] describes the capacity of a bidirectional broadcast channel.

Theorem 2.3.1 (Capacity of bidirectional broadcast channel [OSBB08]). *The capacity region of the discrete memoryless bidirectional broadcast channel is the set of all rate pairs $[R_1, R_2]$ satisfying*

$$R_1 \leq I(X; Y_1 | U), \quad R_2 \leq I(X; Y_2 | U), \quad (2.19)$$

for random variables U, X, Y_1, Y_2 drawn from the joint probability mass function $p(u)p(x|u)p(y_1 y_2 | x)$.

In the above theorem, U is an auxiliary random variable, X is the encoded message from W_1, W_2 at the relay and Y_1 and Y_2 are the received signals at users (more details and rigorous definitions of W_1, W_2, U, X, Y_1 , and Y_2 can be found in [OSBB08]). The optimal coding strategy for the bidirectional broadcast channel is similar to the superposition coding strategy of the degraded broadcast channel [CT06], but both receivers can subtract the interference (self-interference) when decoding their desired messages. The capacity achieving code for the bidirectional broadcast channel is also similar to the network coding using a bitwise XOR operation [WCK05, FBW06]. But the achievable rates using the network coding approach are limited by the worst receiver.

The result in Theorem 2.3.1 is for a general discrete memoryless bidirectional broadcast channel, which is extended to a Gaussian MIMO bidirectional broadcast channel in [WOB⁺08]. Accordingly, Gaussian transmitted signal is shown to be optimal and achieves the capacity region of the Gaussian MIMO bidirectional broadcast channel as in the following theorem.

Theorem 2.3.2 (Capacity of Gaussian MIMO bidirectional broadcast channel [WOB⁺08]). *The capacity region of the Gaussian MIMO bidirectional broadcast channel is given by*

$$\mathcal{C} := \bigcup_{\mathbf{Q}: \text{tr}(\mathbf{Q}) \leq P, \mathbf{Q} \succeq 0} \mathcal{V}([R_1(\mathbf{Q}), R_2(\mathbf{Q})]), \quad (2.20)$$

where $\mathcal{V}(\cdot)$ is the downward positive comprehensive hull [BS08], which is defined by $\mathcal{V}([x_1, x_2, \dots, x_n]) \triangleq \{\mathbf{y} \in \mathbb{R}_+^n : y_i \leq x_i, i = 1, 2, \dots, n\}$ and $[R_1(\mathbf{Q}), R_2(\mathbf{Q})]$ is the rate pair for given \mathbf{Q} described by

$$R_k(\mathbf{Q}) = \log \det \left(\mathbf{I} + \frac{1}{\sigma^2} \mathbf{H}_k \mathbf{Q} \mathbf{H}_k^\dagger \right), \quad k = 1, 2,$$

where $\text{tr}(\mathbf{Q}) \leq P$, \mathbf{H}_k , $k = 1, 2$ are channel matrices from the relay to the terminals and σ^2 is the noise power.

The capacity region for the Gaussian MIMO case can not be given in a closed-form because of its complicated structure. Normally, the boundary of the capacity region is characterized using convex optimization. For instance, the optimal transmit strategies for the bidirectional broadcast channel with multiple antennas have been studied for Gaussian channels in [OWB09, OJWB09], where the optimal covariance matrices for the Gaussian transmit vector signals are derived. Based on the capacity formula in Theorem 2.3.2, in this thesis, we will also derive the optimal transmit strategy for the Gaussian MIMO bidirectional broadcast channel but in the wideband regime, which leads to a closed-form solution.

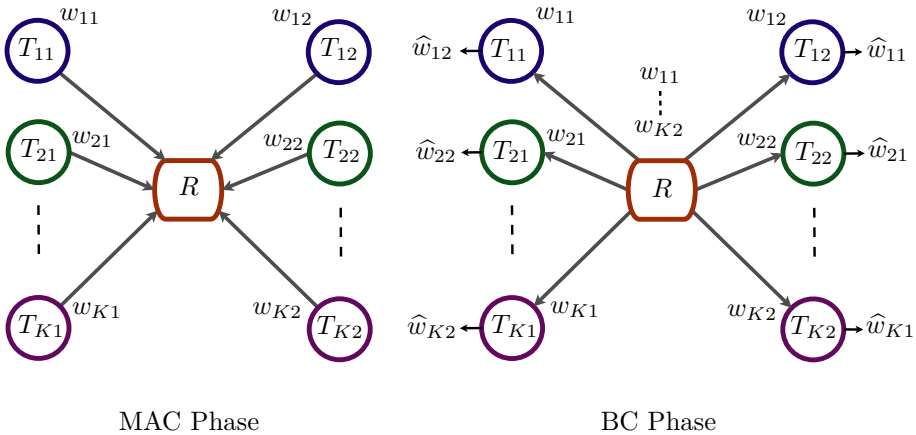


Figure 2.6: Multi-pair bidirectional relay channel.

In addition to the traditional two-way relaying, multi-way relaying has been proposed and studied [GYGP13, OKJ10, AKSH09, KSD10, CY09], where more than

two users would like to communicate with each other via the support of relay. Within this, multi-pair bidirectional relaying [AKSH09, CY09] is a special case, where two users of each pair want to exchange their messages together and do not desire messages from the other pairs. Figure 2.6 depicts a multi-pair bidirectional relaying system. In this network, user T_{k1} and T_{k2} of pair k would like to exchange the messages together and consider the messages from other pairs as interferences. In this thesis, we also study the fundamental limit of a multi-pair bidirectional broadcast channel in the wideband regime. However, unlike the single pair bidirectional broadcast channel, the capacity region of a multi-pair bidirectional broadcast channel is still unknown. There are several efforts on finding the capacity of this channel, but all of them have only been successful on deriving capacity bounds so far [AKSH09, CY09, KSD10], to the best of our knowledge. Therefore, the approach of using the capacity formula to derive the optimal transmit strategy as for the single pair setup can not be used here. We instead propose a reasonable coding scheme and then analyze its optimality in the wideband regime using capacity bounds of the multi-pair bidirectional broadcast channel.

2.4 Wideband CDMA System

Code division multiple access (CDMA) has become standard in several wireless communication systems from IS-95, UMTS WCDMA to HSPA, and so on [DBK⁺98, 3GPtm, HT04]. Although being introduced more than fifty years ago, CDMA is still largely employed and developed nowadays due to its various advantages such as enabling universal frequency reuse, improving handoff performance by soft-handoff and mitigating the effects of interference and fading. Thus, assessing performance of such networks is of significant practical importance.

Since the physical layer (PHY) defines the fundamental capacity limit of the uplink WCDMA channel [HT04], we focus on operations of the uplink WCDMA PHY. Figure 2.7 describes operational procedure of the uplink WCDMA PHY based on the 3GPP release 11 specification [3GPtm]. Since our main objective is to analyze the spectral efficiency, i.e., the capacity of the uplink WCDMA channel, the implemented channel coding scheme is beyond scope of this thesis, so that we focus on the shaded part as the effective WCDMA channel.

Figure 2.8 illustrates the multiplexing of a user's data stream in a K -user uplink WCDMA system with M data streams and spreading factor N . The baseband transmit signal for the k -th user is expressed as

$$x_k(t) = \left(\sqrt{E_k} \sum_{i=1}^{\infty} \sum_{m=1}^M d_{ki}^I \frac{1}{\sqrt{N}} \sum_{n=0}^{N-1} c c_k^m[n] p(t - iT_s - nT_c) \right. \\ \left. + j \sqrt{E_k} \sum_{i=1}^{\infty} \sum_{m=1}^M d_{ki}^Q \frac{1}{\sqrt{N}} \sum_{n=0}^{N-1} c c_k^m[n] p(t - iT_s - nT_c) \right)$$

$$+ j \sqrt{E_k^c} \sum_{i=1}^{\infty} d_{ki}^c \frac{1}{\sqrt{N_c}} \sum_{n=0}^{N_c-1} c c_k^c[n] p(t - iT_s^c - nT_c) \Big) \odot sc_k, \quad (2.21)$$

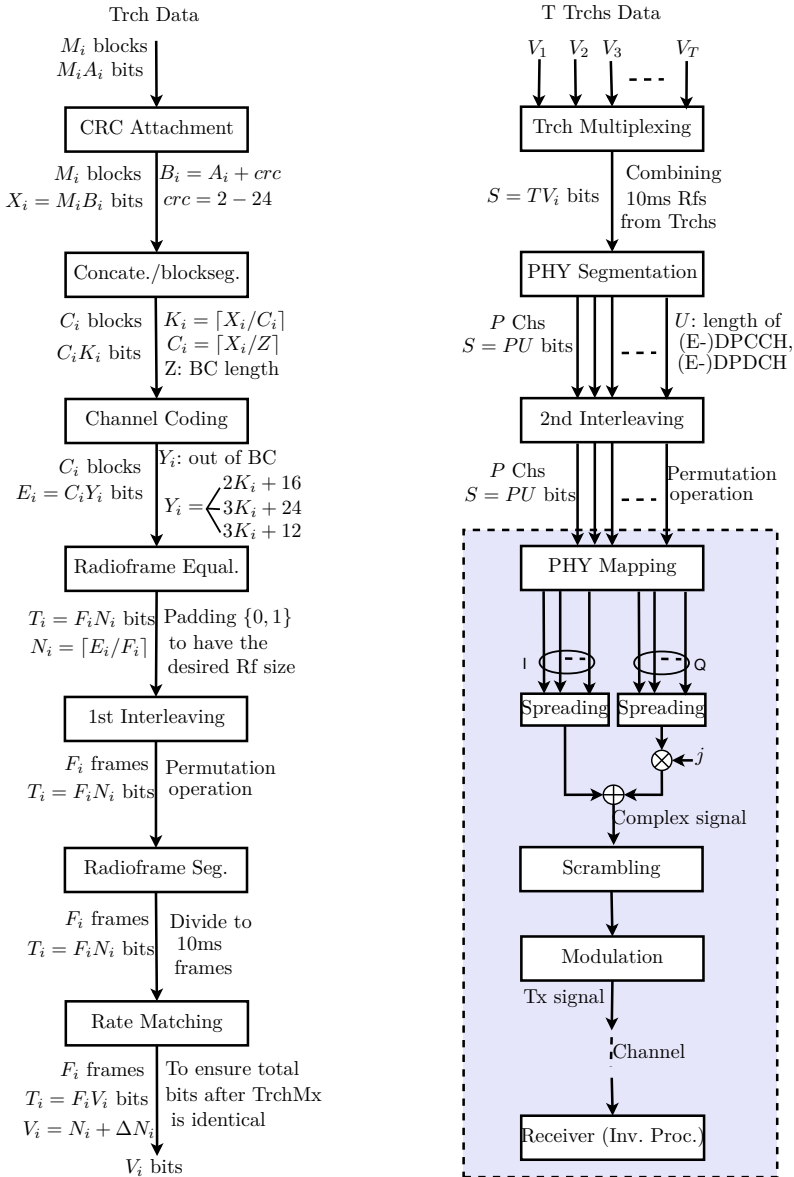


Figure 2.7: Physical layer model of the uplink WCDMA system.

where

- E_k and E_k^c denote the transmit energy of the k -th user for the (enhanced-) dedicated physical data channels ((E-)DPDCHs) and the (enhanced-)dedicated physical control channel ((E-)DPCCH), respectively.
- d_{ki}^{Im} and d_{ki}^{Qm} are the transmitted symbols in I and Q branches for the (E-) DPDCHs of the k -th user.
- d_{ki}^c is the i -th control symbol of the k -th user in the (E-)DPCCH.
- $cc_k^m[\cdot]$ and $cc_k^c[\cdot]$ denote the antipodal real-valued channelization codes (i.e., spreading codes, $cc_k^m[\cdot], cc_k^c[\cdot] \in \{-1, +1\}$) for the m -th (E-)DPDCH and the (E-)DPCCH, respectively.
- T_s and T_s^c denote the symbol durations for the (E-)DPDCHs and (E-)DPCCH. T_c denotes the chip duration.
- N_c denotes the spreading factor of the (E-)DPCCH (e.g., $N_c = 256$ in the uplink WCDMA system).
- $p(t)$ denotes the pulse shape of a chip waveform which is the squared-root-raised-cosine (SRRC) pulse with roll-off factor 0.22 in the WCDMA system.
- \odot denotes the element-by-element multiplication operator.
- sc_k is the scrambling code sequence of the k -th user.

The main characteristics of an uplink WCDMA channel are described by effects of modulation, multiplexing, spreading, scrambling, and the wireless channel itself. Quadrature amplitude modulation (QAM) schemes are used for the modulation of the uplink WCDMA system. The spreading and scrambling code sequences according to the 3GPP standard for the uplink WCDMA system are summarized as follows [3GPP, HT04]:

- Spreading code (channelization code)
 - For the (E-)DPDCH
 - * $N = 2, 4$ for multicode CDMA (multiple (E-)DPDCHs).
 - * $N = 4 \dots 256$ for single DPDCH.
 - * Each (E-)DPDCH pair (in I and Q branches) uses the same channelization code.
 - For the (E-)DPCCH
 - * The first code of the orthogonal variable spreading factor (OVSF) codes with $N = 256$ is used (i.e., 1 symbol = $66.7 \mu\text{s}$).
- Scrambling code (user-specific code)

- Long scrambling codes based on Gold sequence (38400 chips = 10 ms, e.g., 150 symbols with $N = 256$) are used if the base station uses a traditional RAKE receiver.
- Short scrambling codes (256 chips = $66.7\mu\text{s}$) are used for advanced receivers.

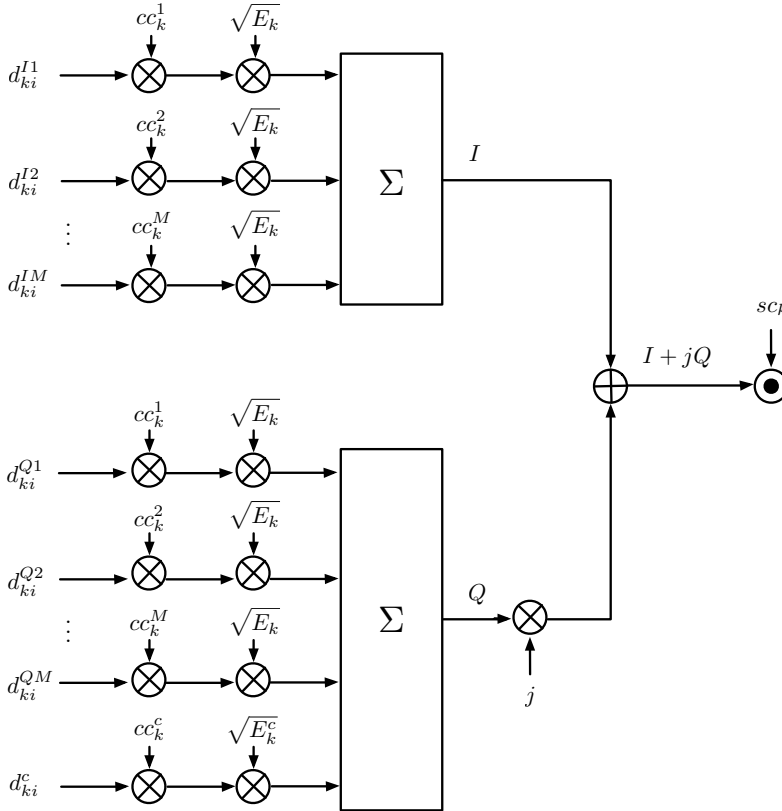


Figure 2.8: Multiplexing of (E-)DPDCHs and a (E-)DPCCH for the k -th user in an uplink WCDMA system.

Since the control symbols in the (E-)DPCCH are modulated using a much higher spreading factor, i.e., $N_c = 256$ (compared to the values of N are about 2 or 4), it is expected that they can be reliably decoded first. Then the interference from control symbols in the multiplexed received signal is removed using the concept of successive interference cancellation. Accordingly, in this thesis, we neglect the control data symbols in the transmitted signal model. Let $d_{ki}^m = d_{ki}^{Im} + jd_{ki}^{Qm}$ be

the complex input symbol. Then the transmitted signal for the k -th user can be rewritten as

$$\begin{aligned} x_k(t) &= \sqrt{E_k} \left(\sum_{i=1}^{\infty} \sum_{m=1}^M d_{ki}^m \frac{1}{\sqrt{N}} \sum_{n=0}^{N-1} cc_k^m[n] p(t - iT_s - nT_c) \right) \odot sc_k \\ &= \sqrt{\frac{E_k}{N}} \sum_{i=1}^{\infty} \sum_{m=1}^M d_{ki}^m \sum_{n=0}^{N-1} c_{ki}^m[n] p(t - iT_s - nT_c), \end{aligned} \quad (2.22)$$

where we define $c_{ki}^m[n] = cc_k^m[n]cs_k[iN + n]$, in which $cc_k^m[\cdot] \in \{-1, +1\}$ denotes the *real*-valued channelization code sequence for the m -th data stream of the k -th user, and $cs_k[\cdot] \in \{(\pm 1, \pm j)/\sqrt{2}\}$ denotes the *complex*-valued scrambling code sequence for the k -th user.

Typically, most of the existing research on CDMA start with the equivalent discrete time channel considering the transmit signal as a vector of transmitted symbols d_{ki}^m . However, as the argued in [Aul10], this does not always reflect the operation of a physical channel medium correctly. Motivated from a practical perspective, in this thesis, we start from a continuous time signal as given in (2.22) when studying WCDMA systems.

Moreover, if we denote $s_{ki}^m(t) = \frac{1}{\sqrt{N}} \sum_{n=0}^{N-1} c_{ki}^m[n] p(t - (i-1)T_s - nT_c)$ as the signature waveform, the transmitted signal in (2.22) can be rewritten as

$$x_k(t) = \sqrt{E_k} \sum_{i=1}^{\infty} \sum_{m=1}^M d_{ki}^m s_{ki}^m(t). \quad (2.23)$$

This is the common transmitted signal model for a continuous-time waveform channel [Gal68, Chap. 8], which can be used to describe the signal model of various practical systems. Therefore, although our study focuses on the WCDMA systems, the framework and results can be easily extended or applied to other wireless standards.

Single Pair MIMO Bidirectional Broadcast Channel in the Wideband Regime

In this chapter, we study the energy efficiency of a *single pair* Gaussian MIMO bidirectional broadcast channel, in which two users exchange their messages together via the support of a relay. Starting from the capacity formula of the Gaussian MIMO bidirectional broadcast channel [WOB⁺08], we derive the optimal transmit strategy for the channel *in the wideband regime*. In order to characterize the boundaries of the wideband capacity and energy per bit regions, the transmit strategy at the relay is designed to maximize the wideband weighted sum-rate. A closed-form solution of the optimal transmit covariance matrix is derived, which shows that a single beam transmit strategy is optimal. The fairness versus energy efficiency trade-off is also discussed in the end of this chapter.

3.1 Related Works and Motivation

As mentioned in Chapter 2, bidirectional relaying, so called two-way relaying inherits the advantages of cooperative communication such as extending the coverage and mitigating the fading effect of wireless networks while overcoming its spectral inefficiency, especially in a half-duplex cooperative system. Since the MAC phase of the bidirectional relaying system is well investigated, the broadcast phase, which is also called *bidirectional broadcast channel* has drawn more attention recently [LJS06, RW07, OSBB08, WOB⁺08, OWB09, OJWB09]. In [OSBB08], the capacity and the optimal transmit strategy for a discrete memoryless bidirectional broadcast channel were derived, which shown that the channel capacity could be achieved by a coding strategy similar to the superposition coding for the degraded broadcast channel. The results are then extended to Gaussian multiple antennas systems. In [WOB⁺08], the authors derived the capacity region for a Gaussian MIMO bidirectional broadcast channel, which is achieved by Gaussian vector input signals. In [OWB09, OJWB09], the optimal transmit strategies, i.e., the optimal transmit covariance matrices of the Gaussian vector input signals for the Gaussian

bidirectional broadcast channels with multiple antennas have been studied.

In addition, wideband regime analysis has also drawn considerably research interest since it provides a lower bound on the energy per bit (EpB) ratio in a system. This is in particular worth to know in wireless networks operating with relatively low EpB and spectral efficiency such as satellite, sensor network, smart house, and so on. In the landmark paper [Ver02], Verdú studied the system performance in the wideband regime through the minimum energy per bit (MEpB) required to maintain reliable communication and the wideband slope of the spectral efficiency curve. Since then, several additional studies have focused on the wideband or respectively low SNR regime [SSBNS08, BXB08, MLTV10, ZJW⁺10, UYHMX10].

In a multi-user setting the concept of MEpB needs to be extended because in general one has to deal with multiple rates for different users. To this end, it is reasonable either to take an individual point of view or to look at it from a system point of view. In [MLTV10], the authors considered the MEpB for each user with different power allocations as well as the MEpB of the whole system based on the total power and sum rate in a MIMO uplink channel. Assuming all users transmit at the same target rate is another approach to investigate the MEpB of a multi-user multiple access channel (MAC) [UYHMX10]. Recently, in [JKV09, JKV11], Verdú et al. considered the broadcast channel with cooperating receivers and common message only, where the MEpB for the single user has been derived as a lower bound for the MEpB of the whole system. Indeed, the MEpB metric becomes more involved in the downlink setup since one has to deal with both the energy efficiency and fairness issues when a single transmit power budget is used to serve different users instantaneously. In this chapter, we show that the individual EpBs of users lead to a multi-dimensional region, in which the trade-off between individual and system performances can be clearly observed. This allows us to identify several relevant transmit strategies, which take fairness conditions into account. With the exception of [PRS03, Kel97, JL05, JBN10], a focus on energy efficiency taking fairness into account is so far not common in the literature. However, we consider it as an important aspect.

Chapter 3 is organized as follows. Section 3.2 introduces the system model and defines the capacity as well as the energy per bit regions in the wideband regime. In Section 3.3, we derive the optimal transmit strategy for the Gaussian MIMO bidirectional broadcast channel, which characterizes the boundaries of the wideband capacity and the energy per bit regions. Transmit strategies for some special cases are also presented in this section. The energy efficiency and fairness issues are considered in Section 3.4. Section 3.5 studies the individual and system wideband slopes, which are achieved from the proposed transmit strategy. Finally, numerical results and the conclusion are given in the end of the chapter.

3.2 Problem Setup

Let us consider a Gaussian MIMO bidirectional relaying system which consists of two users and one supporting relay as depicted in Figure 3.1. User i ($i = 1, 2$) is called T_i and is equipped with n_i antennas. The users communicate with their counterpart with support from the relay which is equipped with n_r antennas. We assume that a decode-and-forward protocol is used and the relay successfully decodes the messages from both users in the MAC phase. In this chapter we concentrate on the broadcast phase where the relay forwards a re-encoded composition of the decoded messages to the users.

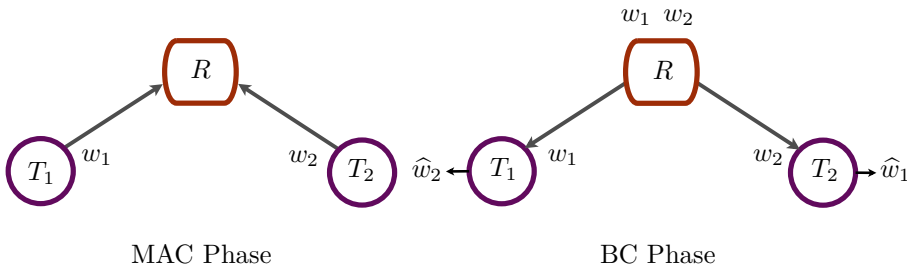


Figure 3.1: Bidirectional relay channel.

Let w_1 and w_2 denote the messages from the users, which are independent and known at the relay. We assume that T_1 knows w_1 and desires w_2 and T_2 knows w_2 and desires w_1 . In order to forward $\nu = [w_1, w_2]$ to both users, the relay uses the capacity achieving coding scheme proposed in [WOB⁺08] to encode ν into the transmitted signal vector $\mathbf{x} \in \mathbb{C}^{n_r \times 1}$. We assume that $\mathbb{E}\{\mathbf{x}\mathbf{x}^\dagger\} = \mathbf{Q}$, where \mathbf{Q} is semi-positive definite and satisfies the power constraint $\text{tr}(\mathbf{Q}) \leq P$.

Let us denote $\mathbf{H}_i \in \mathbb{C}^{n_i \times n_r}$, $i = 1, 2$ as the multiplicative channel matrices between the relay and users. The received signal at each user is then obtained as

$$\mathbf{y}_i = \mathbf{H}_i \mathbf{x} + \mathbf{n}_i, \quad i = 1, 2,$$

where $\mathbf{y}_i \in \mathbb{C}^{n_i \times 1}$ is the received signal at T_i and $\mathbf{n}_i \in \mathbb{C}^{n_i \times 1}$ is the additive Gaussian noise vector at T_i , whose elements are independent and identically distributed according to $\mathcal{CN}(0, \sigma_0^2)$.

We assume that perfect channel state information is available at the relay and all users. The spectral efficiency (in bits per second per Hertz) for T_i , $i = \{1, 2\}$, decoding $w_{\bar{i}}$ ($\bar{i} \in \{1, 2\} \setminus \{i\}$) while knowing w_i , in the Gaussian MIMO bidirectional broadcast channel given \mathbf{Q} can be obtained as [WOB⁺08]

$$S_i(\mathbf{Q}) = \log_2 \left| \mathbf{I}_{n_i} + \frac{1}{\sigma_0^2} \mathbf{H}_i \mathbf{Q} \mathbf{H}_i^\dagger \right|, \quad i = 1, 2, \quad (3.1)$$

where $|\cdot|$ and † denote the matrix determinant and Hermitian transpose operations, respectively.

3.2.1 Wideband capacity region

Let B denote the available bandwidth and $N_0/2$ is the noise power spectral density. Then the noise power can be rewritten as $\sigma_0^2 = BN_0$. Heuristically,¹ if we fix the transmit power P and sample at the Nyquist rate, the power per sample and the SNR are then $P/2B$ and P/BN_0 , respectively. Thus, in the wideband regime, as the bandwidth B tends to infinity, the available power per sample and SNR tend to zero. Because of that, the wideband regime is also often called the *low power regime* or *low SNR regime* [LTV03, CTV04, MLTV10, UYHMX10]. For a given transmit covariance matrix \mathbf{Q} , the achievable wideband rate (in bits per second) for each user is obtained by

$$\begin{aligned} R_i(\mathbf{Q}) &= \lim_{B \rightarrow \infty} B \log_2 \left| \mathbf{I}_{n_i} + \frac{1}{BN_0} \mathbf{H}_i \mathbf{Q} \mathbf{H}_i^\dagger \right| \\ &= \lim_{B \rightarrow \infty} B (\log_2 e) \left[\frac{1}{BN_0} \text{tr}(\mathbf{H}_i \mathbf{Q} \mathbf{H}_i^\dagger) - \frac{1}{2(BN_0)^2} \text{tr}((\mathbf{H}_i \mathbf{Q} \mathbf{H}_i^\dagger)^2) + o\left(\frac{1}{B^2}\right) \right] \\ &= \frac{\log_2 e}{N_0} \text{tr}(\mathbf{H}_i \mathbf{Q} \mathbf{H}_i^\dagger), \quad i = 1, 2. \end{aligned} \quad (3.2)$$

In (3.2), the Taylor expansion of the matrix function in (3.1) developed for $\frac{1}{B} \rightarrow 0$ was used. The first order approximation of the spectral efficiency (or the zero order approximation of the wideband rate), with respect to (w.r.t.) $\text{snr} = P/BN_0$ (or w.r.t. $\frac{1}{B}$ for fixed P/N_0), is sufficient for deriving the MEpB [Ver02]. Moreover, we define the wideband capacity region of the Gaussian MIMO bidirectional broadcast channel as

$$\mathcal{C} := \bigcup_{\mathbf{Q}: \text{tr}(\mathbf{Q}) \leq P, \mathbf{Q} \succeq 0} \mathcal{V}([R_1(\mathbf{Q}), R_2(\mathbf{Q})]), \quad (3.3)$$

where $\mathcal{V}(\cdot)$ is the downward positive comprehensive hull [BS08], which is defined by $\mathcal{V}([x_1, x_2, \dots, x_n]) \triangleq \{\mathbf{y} \in \mathbb{R}_+^n : y_i \leq x_i, i = 1, 2, \dots, n\}$.

3.2.2 Energy per bit region

The wideband regime leads to the MEpB, the lowest energy per information bit which is required to maintain reliable communication in a system. Moreover, the EpBs and EpB² region can be characterized from the wideband rate and wideband capacity region as follow.

From a transmitter point of view, one may be interested in the required energy spent by the relay to transmit one bit in total to all users for a given \mathbf{Q} . This

¹A rigorous coding theorem for a bandlimited system would require arguments following Wyner as done in [Wyn66].

²More precisely, we can call "wideband EpB" as we consider the wideband regime and the EpB is derived from the wideband rate.

quantity can be described by the *system EpB*, which we define as

$$\frac{E_{b,s}(\mathbf{Q})}{N_0} = \frac{P}{N_0 R_s(\mathbf{Q})}, \quad (3.4)$$

where $R_s(\mathbf{Q}) = R_1(\mathbf{Q}) + R_2(\mathbf{Q})$ is the wideband sum-rate for a given transmit covariance matrix \mathbf{Q} .

From a receiver point of view, one may be interested in the required energy spent by the relay to transmit one bit to a certain user for a given \mathbf{Q} . Accordingly, we define this ratio as the *individual EpB*, which is given by

$$\frac{E_{bi}(\mathbf{Q})}{N_0} = \frac{P}{N_0 R_i(\mathbf{Q})}, i = 1, 2. \quad (3.5)$$

In general, the individual energy efficiency is not maximized with the same \mathbf{Q} for all users simultaneously; we face a vector optimization problem. Thus, it is reasonable to consider the trade-offs between users through the EpB vector $[\frac{E_{b1}(\mathbf{Q})}{N_0}, \frac{E_{b2}(\mathbf{Q})}{N_0}]$. All possible trade-offs are fully described by the multi-dimensional EpB region,³ i.e.,

$$\mathcal{E} = \bigcup_{\mathbf{Q}: \text{tr}(\mathbf{Q}) \leq P, \mathbf{Q} \succeq 0} \bar{\mathcal{V}} \left(\left[\frac{E_{b1}(\mathbf{Q})}{N_0}, \frac{E_{b2}(\mathbf{Q})}{N_0} \right] \right), \quad (3.6)$$

where $\bar{\mathcal{V}}(\cdot)$ is the upward positive comprehensive hull [BS08], which is defined by $\bar{\mathcal{V}}([x_1, x_2, \dots, x_n]) \triangleq \{\mathbf{y} \in \mathbb{R}_+^n : y_i \geq x_i, i = 1, 2, \dots, n\}$. Obviously, $\frac{E_{bi}(\mathbf{Q})}{N_0}$ is a decreasing function of $R_i(\mathbf{Q})$, which is positive and continuous. Therefore, the boundary of the EpB region \mathcal{E} is characterized by the curved section of the boundary of the wideband capacity region \mathcal{C} , for which we will derive the optimal transmit strategies in the next section.

Remark 3.1. [Minimum EpB vector] For a point-to-point channel, the MEpB describes the required EpB when a system operates at the wideband capacity. For a multi-user system, the concept of MEpB is generalized to a multi-dimensional MEpB vector, which corresponds to an optimal operating point on the boundary of the EpB region. Since each optimal EpB vector corresponds to a Pareto optimal rate vector on the wideband capacity region, we define the *MEpB vector* as $\xi(\mathbf{Q}_{opt}) = \left[\frac{E_{b1}(\mathbf{Q}_{opt})}{N_0}, \frac{E_{b2}(\mathbf{Q}_{opt})}{N_0} \right]$, where \mathbf{Q}_{opt} is an optimal covariance matrix corresponding to a Pareto optimal wideband rate vector $[R_1(\mathbf{Q}_{opt}), R_2(\mathbf{Q}_{opt})]$ on the boundary of the wideband capacity region.

³More precisely, we could call it the “wideband EpB region” as we consider the wideband regime and the EpB is derived from the wideband rate.

3.3 Optimal Transmit Strategy

In this section, we characterize the wideband capacity and EpB regions defined in the previous section. To this end, we derive the optimal transmit strategies, which achieve the MEpB pairs/vectors as well as the operating points on the boundary of the wideband capacity region. Since the wideband capacity region \mathcal{C} is convex, its boundary is characterized by the wideband weighted sum-rate maxima. Let $\gamma \in [0, 1]$ denote the weighting factor. The wideband weighted sum-rate is then given by

$$\begin{aligned} R(\mathbf{Q}, \gamma) &= \gamma R_1(\mathbf{Q}) + (1 - \gamma) R_2(\mathbf{Q}) \\ &= \frac{\log_2 e}{N_0} \left[\gamma \text{tr}(\mathbf{H}_1 \mathbf{Q} \mathbf{H}_1^\dagger) + (1 - \gamma) \text{tr}(\mathbf{H}_2 \mathbf{Q} \mathbf{H}_2^\dagger) \right]. \end{aligned}$$

Our goal is now to find the optimal transmit covariance matrix \mathbf{Q} for a given γ , which can be formulated through the following optimization problem

$$\begin{aligned} \max \quad & f(\mathbf{Q}) = \gamma \text{tr}(\mathbf{H}_1 \mathbf{Q} \mathbf{H}_1^\dagger) + (1 - \gamma) \text{tr}(\mathbf{H}_2 \mathbf{Q} \mathbf{H}_2^\dagger) \\ \text{s.t.} \quad & \text{tr}(\mathbf{Q}) \leq P, \\ & \mathbf{Q} \succeq 0, \end{aligned} \quad (3.7)$$

where $\mathbf{Q} \succeq 0$ defines the positive semidefinite matrix \mathbf{Q} . In the following theorem, we provide a characterization of an optimal covariance matrix which maximizes (3.7).

Theorem 3.3.1. *Let $\mathcal{H} = [\sqrt{\gamma} \mathbf{H}_1^T \quad \sqrt{1 - \gamma} \mathbf{H}_2^T]^T \in \mathbb{C}^{(n_1 + n_2) \times n_r}$ be the equivalent channel matrix and let $\mathbf{w} \in \mathbb{C}^{n_r \times 1}$ be the normalized eigenvector corresponding to the maximum eigenvalue of $\mathcal{H}^\dagger \mathcal{H}$. An optimal covariance matrix $\mathbf{Q}_{\text{opt}}(\gamma)$ which maximizes (3.7) is given by*

$$\mathbf{Q}_{\text{opt}}(\gamma) = P \mathbf{w} \mathbf{w}^\dagger. \quad (3.8)$$

Proof. Based on a basic transformation of the trace function $\text{tr}(\mathbf{A}^\dagger \mathbf{X} \mathbf{C}) + \text{tr}(\mathbf{B}^\dagger \mathbf{X} \mathbf{D}) = \text{tr}([\mathbf{A} \ \mathbf{B}]^\dagger \mathbf{X} [\mathbf{C} \ \mathbf{D}])$, the objective function $f(\mathbf{Q})$ can be rewritten as

$$f(\mathbf{Q}) = \text{tr}(\mathcal{H} \mathbf{Q} \mathcal{H}^\dagger).$$

The optimization problem in (3.7) becomes

$$\begin{aligned} \max \quad & \text{tr}(\mathcal{H} \mathbf{Q} \mathcal{H}^\dagger) \\ \text{s.t.} \quad & \text{tr}(\mathbf{Q}) \leq P, \\ & \mathbf{Q} \succeq 0. \end{aligned} \quad (3.9)$$

Since \mathbf{Q} is a covariance matrix, it is a non-negative semi-definite Hermitian matrix. Therefore, let \mathbf{Q} and $\mathcal{H}^\dagger \mathcal{H}$ have the eigenvalue decompositions

$$\begin{aligned} \mathbf{Q} &= \mathbf{U}_q \mathbf{\Lambda}_q \mathbf{U}_q^\dagger, \\ \mathcal{H}^\dagger \mathcal{H} &= \mathbf{U}_h \mathbf{\Lambda}_h \mathbf{U}_h^\dagger, \end{aligned}$$

where \mathbf{U}_q and \mathbf{U}_h are unitary matrices, $\mathbf{\Lambda}_q$ and $\mathbf{\Lambda}_h$ are diagonal matrices whose diagonal elements are the eigenvalues of \mathbf{Q} and $\mathcal{H}^\dagger \mathcal{H}$, respectively. Without loss of generality, we assume that the diagonal elements of $\mathbf{\Lambda}_q$ and $\mathbf{\Lambda}_h$ are ordered from largest to smallest value. As in [ASDG06], the maximization of (3.9) is obtained when $\mathbf{\Lambda}_q = \text{diag}\{P, 0, \dots, 0\}$ and $\mathbf{U}_q = \mathbf{U}_h$. Therefore, the optimal covariance matrix $\mathbf{Q}_{opt}(\gamma)$ is given by the eigenvector \mathbf{w} corresponding to the maximum eigenvalue of $\mathcal{H}^\dagger \mathcal{H}$ as in (3.8). \square

Theorem 3.3.1 shows that there exists an optimal transmit covariance matrix $\mathbf{Q}_{opt}(\gamma)$ of rank one. Thus, an optimal transmit strategy is a single beam along the principal eigenvector of the matrix $\mathcal{H}^\dagger \mathcal{H}$, which depends on the channel matrices \mathbf{H}_i ($i = 1, 2$) and the weighting factor γ . This result is similar to the single beam optimality of a point-to-point MIMO channel in the low SNR regime [TV05, Ch. 7], i.e., the optimal policy is to allocate all power to the strongest eigenmode. Moreover, the maximum wideband weighted sum-rate can be obtained as

$$R(\gamma) = \frac{P \log_2 e}{N_0} \lambda_{\max}(\gamma), \quad (3.10)$$

where $\lambda_{\max}(\gamma)$ is the maximum eigenvalue of the equivalent matrix $\mathcal{H}^\dagger \mathcal{H}$ for the given weighting factor γ .

In the following, we look at the transmit strategies for some special cases. The transmit strategy for the SIMO and SISO cases ($n_r = 1$) is trivial since it is optimal to transmit with full power from the single antenna of the relay. Thus, we focus on the optimal transmit strategy for the MISO case ($n_1 = n_2 = 1, n_r \geq 1$) and a MIMO case where we consider the special configuration $n_1 = n_2 = n_r = 2$.

3.3.1 MISO channels

Let the column vectors $\mathbf{h}_1, \mathbf{h}_2$ denote the multiplicative channels from the relays to the users in the MISO case, i.e.,

$$y_i = \mathbf{h}_i^T \mathbf{x} + n_i, \quad i = 1, 2.$$

Then the optimal beamforming vector is derived from the directions of the channels from the relay to the users, which is stated in the following theorem.

Theorem 3.3.2. *For the MISO channels with the unit vectors $\mathbf{u}_1 = \mathbf{h}_1 / \|\mathbf{h}_1\|$ and $\mathbf{u}_2 = \mathbf{h}_2 / \|\mathbf{h}_2\|$ with $\rho = |\mathbf{u}_1^\dagger \mathbf{u}_2| \in (0, 1)$, an optimal beamforming vector \mathbf{w} is given by*

$$\mathbf{w} = \epsilon_1 \mathbf{u}_1 + \epsilon_2 e^{-j\varphi} \mathbf{u}_2, \quad (3.11)$$

where $\varphi = \arg(\mathbf{u}_1^\dagger \mathbf{u}_2)$ and $(\epsilon_1, \epsilon_2) \in \mathbb{R}_+^2$ which are defined as

$$\begin{aligned}\epsilon_1 &= \frac{\rho\lambda}{\sqrt{(1-\rho^2)\lambda^2 - 2\mu_2(1-\rho^2)\lambda + \mu_2^2}}, \\ \epsilon_2 &= \frac{\mu_2 - \lambda}{\sqrt{(1-\rho^2)\lambda^2 - 2\mu_2(1-\rho^2)\lambda + \mu_2^2}},\end{aligned}\quad (3.12)$$

with $\mu_1 = \gamma\|\mathbf{h}_1\|^2$, $\mu_2 = (1-\gamma)\|\mathbf{h}_2\|^2$, and λ is given by

$$\lambda = \frac{(\mu_1 + \mu_2) - \sqrt{(\mu_1 + \mu_2)^2 - 4\mu_1\mu_2(1-\rho^2)}}{2(1-\rho^2)}.\quad (3.13)$$

Proof. The proof for this theorem is given in Appendix 3.7.A. \square

The parallel and orthogonal channels scenarios, i.e., $\rho \in \{0, 1\}$ are omitted in Theorem 3.3.2. We will consider these trivial cases later. Theorem 3.3.2 shows that the optimal transmit strategy is to transmit into the vector space spanned by $\{\mathbf{u}_1, \mathbf{u}_2\}$ and the beamforming vector is expressed as the linear combination of two channel directions. Moreover, it is interesting to see that the phase difference of the coefficients is fixed and independent of the pre-determined weighting factor.

Next, the optimal transmit strategies for parallel and orthogonal channels are considered.

Orthogonal channels ($\rho = 0$): The transmit strategies can be categorized into three cases based on the values of μ_i , $i = 1, 2$, which is directly related to the weighting factor γ and channel realizations \mathbf{h}_i , $i = 1, 2$.

– If $\mu_1 < \mu_2$: The optimal beamforming vector is parallel with the direction of the channel \mathbf{h}_2 , i.e., $(\epsilon_1 = 0, \epsilon_2 = 1)$.

– If $\mu_1 > \mu_2$: The optimal beamforming vector is parallel with the direction of the channel \mathbf{h}_1 , i.e., $(\epsilon_1 = 1, \epsilon_2 = 0)$.

– If $\mu_1 = \mu_2$: Any feasible power split (ϵ_1, ϵ_2) maximizes the weighted sum-rate.

This can be roughly understood that the optimal transmit strategy for the orthogonal channels is to transmit with full power to the user, which has the better “weighted gain” μ_i .

Parallel channels ($\rho = 1$): In this case, the directions of the two channels coincide. Thus, any parameter pair $(\epsilon_1 = 1 - \epsilon_2 \in [0, 1])$ leads to the same wideband weighted sum-rate.

3.3.2 2×2 MIMO channels

Determining the beamforming vector \mathbf{w} is the most complex task in our transmit strategy design for a MIMO system. It requires the characterization of the principal eigenvector of the equivalent matrix. A closed-form expression for such vector could reduce the design complexity remarkably. However, the derivation of the maximal eigenvalue and its eigenvector corresponds to finding the roots of polynomial

equations. Accordingly, here we can derive a closed-form of the optimal transmit beamforming vector for the case which corresponds to the second order polynomials, i.e., 2×2 MIMO channels. Let

$$\mathbf{H}_1 := \begin{bmatrix} a_1 & b_1 \\ c_1 & d_1 \end{bmatrix}, \quad \mathbf{H}_2 := \begin{bmatrix} a_2 & b_2 \\ c_2 & d_2 \end{bmatrix},$$

with $a_1, b_1, c_1, d_1, a_2, b_2, c_2, d_2 \in \mathbb{C}$. Then the equivalent channel matrix, given a weighting factor γ , is defined as

$$\mathcal{H}^\dagger \mathcal{H} := \begin{bmatrix} \mathbf{a} & \mathbf{b} \\ \mathbf{c} & \mathbf{d} \end{bmatrix},$$

with

$$\begin{aligned} \mathbf{a} &= \gamma|a_1|^2 + \gamma|c_1|^2 + (1-\gamma)|a_2|^2 + (1-\gamma)|c_2|^2, \\ \mathbf{b} &= \gamma a_1^* b_1 + \gamma c_1^* d_1 + (1-\gamma) a_2^* b_2 + (1-\gamma) c_2^* d_2, \\ \mathbf{c} &= \gamma a_1 b_1^* + \gamma c_1 d_1^* + (1-\gamma) a_2 b_2^* + (1-\gamma) c_2 d_2^*, \\ \mathbf{d} &= \gamma|b_1|^2 + \gamma|d_1|^2 + (1-\gamma)|b_2|^2 + (1-\gamma)|d_2|^2. \end{aligned}$$

After some basic algebraic manipulations, the largest eigenvalue of $\mathcal{H}^\dagger \mathcal{H}$ can be obtained as

$$\lambda_1 = \frac{\mathbf{a} + \mathbf{d}}{2} + \sqrt{\left(\frac{\mathbf{a} + \mathbf{d}}{2}\right)^2 - (\mathbf{a}\mathbf{d} - \mathbf{b}\mathbf{c})}.$$

Accordingly, the beamforming vector corresponding to the largest eigenvalue of $\mathcal{H}^\dagger \mathcal{H}$ is given in a closed-form as

$$\mathbf{w} = \frac{1}{\sqrt{\mathbf{c}^2 + (\lambda_1 - \mathbf{a})^2}} \begin{bmatrix} \mathbf{c} \\ \lambda_1 - \mathbf{a} \end{bmatrix}.$$

This implies that for a 2×2 MIMO channel, the transmit strategy is to transmit using both antennas, except the trivial cases with $b_1 = d_1 = 1 - \gamma = 0$, $b_2 = d_2 = \gamma = 0$ and $b_1 = d_1 = b_2 = d_2 = 0$. In these cases, the maximal eigenvalue λ_1 equals to \mathbf{a} (since $\mathbf{b} = \mathbf{d} = 0$) and the beamforming vector becomes $\mathbf{w} = [1 \ 0]^T$. This is similar to the SIMO and SISO cases with full power transmission using a single antenna only.

3.4 Energy Efficiency and Fairness

As the system (energy) efficiency and fairness are often two conflicting targets, one should pay attention to both when designing the system. The idea is to choose

an appropriate transmit strategy that can achieve a certain goal, i.e., to maximize energy efficiency, to maximize fairness, or to balance the desire for high energy efficiency with fairness among users. In our optimization problem, the transmit strategy can be flexibly adjusted to meet the desired performance. Indeed, by setting the weighting factor γ in (3.7) properly, we can obtain all Pareto optimal operating points on the boundary of the EpB region, which correspond to different energy efficiency and fairness criteria. In this section, we focus on some transmit strategies corresponding to some well-known resource allocation approaches.

3.4.1 Utility maximization

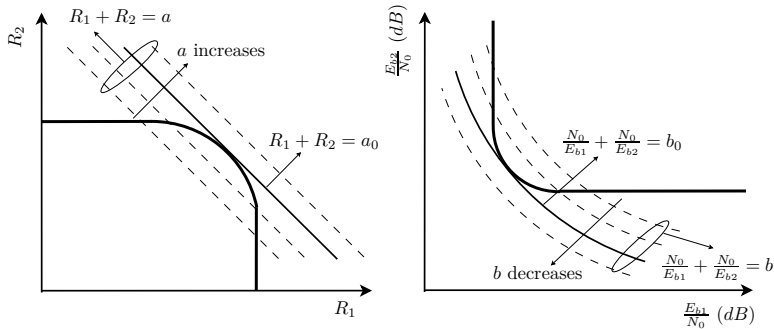


Figure 3.2: Graphical illustration of the utility maximization operating point. In the wideband rate domain on the left, this point is represented by the point of contact between the wideband rate region's boundary and a certain curve in the curve family $R_1 + R_2 = a, \forall a \in \mathbb{R}$, i.e., $R_1 + R_2 = a_0$. In the EpB domain on the right, this point is the point of contact between the EpB region's boundary and the curve family $\frac{N_0}{E_{b1}} + \frac{N_0}{E_{b2}} = b, \forall b \in \mathbb{R}$.

A common approach is to opt for the transmit strategy which maximizes the utility of the transmitter/relay. As mentioned above, the system EpB reflects the energy efficiency at the transmitter in the wideband regime. Therefore, the transmit covariance matrix $\mathbf{Q}_{opt}(\gamma)$ is chosen such that the system EpB is smallest (or the wideband sum-rate is maximized) regardless of the fairness between users. This is achieved by employing the beamforming transmission which corresponds to the weighting factor $\gamma = 0.5$. Indeed, the original wideband weighted sum-rate optimization problem (3.7) becomes the sum-rate maximization problem when $\gamma = 0.5$. Figure 3.2 gives a graphical illustration for this operating point on the boundaries of the wideband capacity region (on the left figure) and the EpB region (on the right figure). The maximal wideband sum-rate is then obtained as double of the wideband weighted sum-rate, i.e.,

$$R_s(\mathbf{Q}_{opt}(0.5)) = 2 \frac{P \log_2 e}{N_0} \lambda_{\max}(0.5),$$

where $\lambda_{\max}(0.5)$ is the maximal eigenvalue of the equivalent channel matrix $\mathcal{H}^\dagger \mathcal{H}$ given $\gamma = 0.5$. Therefore, the system EpB is given by

$$\frac{E_{b,s}}{N_0} \min = \frac{P}{N_0 R_s(\mathbf{Q}_{opt}(0.5))} = \frac{\log_e 2}{2\lambda_{\max}(0.5)}. \quad (3.14)$$

This is the minimum amount of energy spent by the transmitter to transmit one information bit in total to both users, which denotes the so called *system MEpB*.

This transmit strategy is optimal in term of exploiting the resource most efficiently (or system MEpB achieving). It may still somewhat meet the fairness expectation if the channel qualities of users are similar. However, when the channel qualities are unbalanced, it is likely that a user having a much better channel will be allocated most of the system resources while the other may be under-served.

3.4.2 Single user optimization

Next, let us consider a transmission approach that achieves the *individual MEpB*, i.e., the minimum energy cost for delivering one information bit to a certain user. For instance, the individual MEpB for user 1 can be achieved by employing the optimization (3.7) with the corresponding weighting factor $\gamma = 1$. The optimal transmit strategy becomes beamforming along the principal eigenvector of user 1's channel matrix, $\mathbf{Q}_{opt}(1) = P\mathbf{v}_1^\dagger \mathbf{v}_1$, where \mathbf{v}_1 is the eigenvector corresponding to the maximum eigenvalue of $\mathbf{H}_1^\dagger \mathbf{H}_1$. The corresponding EpB pair is then given by

$$\frac{E_{b1}}{N_0} \min_{opt1} = \frac{\log_e 2}{\lambda_{1\max}}, \quad \frac{E_{b2}}{N_0} \min_{opt1} = \frac{\log_e 2}{\text{tr}(\mathbf{H}_2 \mathbf{Q}_{opt}(1) \mathbf{H}_2^\dagger)},$$

where $\lambda_{1\max}$ is the maximal eigenvalue of $\mathbf{H}_1^\dagger \mathbf{H}_1$ and $\frac{E_{b1}}{N_0} \min_{opt1}$ is the individual MEpB for user 1.

Similarly, the individual MEpB for user 2 can be achieved by setting $\gamma = 0$ and beamforming along the principal eigenvector of user 2's channel matrix. The optimal EpB pair is then given by

$$\frac{E_{b1}}{N_0} \min_{opt2} = \frac{\log_e 2}{\text{tr}(\mathbf{H}_1 \mathbf{Q}_{opt}(0) \mathbf{H}_1^\dagger)}, \quad \frac{E_{b2}}{N_0} \min_{opt2} = \frac{\log_e 2}{\lambda_{2\max}},$$

with $\lambda_{2\max}$ is the maximal eigenvalue of $\mathbf{H}_2^\dagger \mathbf{H}_2$ and $\frac{E_{b2}}{N_0} \min_{opt2}$ is the individual MEpB for user 2.

In order to achieve the individual MEpB for a certain user, the beamforming vector was adjusted to the direction of the principal eigenvector of its channel matrix, regardless of the channel of the other user. This could lead to the starvation of the other user if the correlation between the channels is too small. This motivates to take fairness issues into account next.

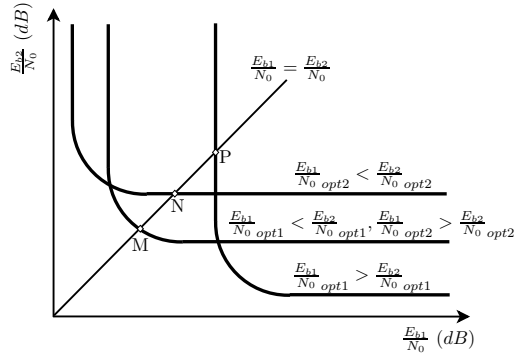


Figure 3.3: Graphical illustration of the max-min fairness operating point. When $\frac{E_{b1}}{N_0 \text{ opt1}} < \frac{E_{b2}}{N_0 \text{ opt1}}$ and $\frac{E_{b1}}{N_0 \text{ opt2}} > \frac{E_{b2}}{N_0 \text{ opt2}}$, the optimal point M is on the curved section of the EpB region's boundary. Otherwise, the optimal points N and P are not on the curved sections.

3.4.3 Max-min fairness optimization

Although the utility maximization and single user optimization can achieve the system MEpB and the individual MEpBs, respectively, those transmit strategies have the drawback that there could be a user that is extremely under-served if the difference between channel (in the terms of quality and uncorrelation) is large. On the other side, maximum fairness is achieved by a transmit strategy that leads to the same individual EpB for both users, i.e.,

$$\frac{E_{b1}(\mathbf{Q}_{opt}(\gamma_f))}{N_0} = \frac{E_{b2}(\mathbf{Q}_{opt}(\gamma_f))}{N_0}. \quad (3.15)$$

This EpB pair corresponds to the max-min fairness point. Here, γ_f denotes the chosen weighting factor that achieves the max-min fairness operating point. As shown in the illustration in Figure 3.3, this EpB pair is on the curved section of the boundary of EpB region if and only if $\frac{E_{b1}}{N_0 \text{ opt1}} < \frac{E_{b2}}{N_0 \text{ opt1}}$ and $\frac{E_{b1}}{N_0 \text{ opt2}} > \frac{E_{b2}}{N_0 \text{ opt2}}$. Otherwise, the max-min fairness optimal EpB pair is given by $\frac{E_{b1}}{N_0 f} = \frac{E_{b2}}{N_0 f} = \max\left\{\frac{E_{b1}}{N_0 \text{ opt1}}, \frac{E_{b2}}{N_0 \text{ opt2}}\right\}$.

In the utility maximization and single user optimization transmission approaches, the choice of the corresponding weighting factors is simple and follows straightforward from the desired targets ($\gamma = 0.5$ for sum-rate maximization, $\gamma \in \{0, 1\}$ for single user optimization). However, in max-min fairness optimization, the weighting factor which results in (3.15) is not obviously obtained. In general, γ_f can be found by a single dimension grid search on the interval $[0, 1]$. In case of MISO channels, the weighting factor γ_f and the corresponding beamforming coefficients $\{\epsilon_{1f}, \epsilon_{2f}\}$ can be determined based on the following proposition.

Proposition 3.4.1. *For MISO channels with $\|\mathbf{h}_1\| > \rho\|\mathbf{h}_2\|$ and $\|\mathbf{h}_2\| > \rho\|\mathbf{h}_1\|$, in order to achieve the max-min fairness operating point, the weighting factor γ and the beamforming coefficients $\{\epsilon_1, \epsilon_2\}$ in (3.11) are chosen as*

$$\gamma_f = \frac{\|\mathbf{h}_2\|(\|\mathbf{h}_2\| - \rho\|\mathbf{h}_1\|)}{\|\mathbf{h}_1\|^2 + \|\mathbf{h}_2\|^2 - 2\rho\|\mathbf{h}_1\|\|\mathbf{h}_2\|}, \quad (3.16)$$

$$\epsilon_{1f} = \frac{1}{\sqrt{1 + 2\rho a + a^2}}, \epsilon_{2f} = a\epsilon_{1f}, \quad (3.17)$$

where $a = (\|\mathbf{h}_1\| - \rho\|\mathbf{h}_2\|)/(\|\mathbf{h}_2\| - \rho\|\mathbf{h}_1\|)$.

Proof. The proof for this proposition is given in Appendix 3.7.B. \square

For MISO channels, the constraints $\|\mathbf{h}_1\| > \rho\|\mathbf{h}_2\|$ and $\|\mathbf{h}_2\| > \rho\|\mathbf{h}_1\|$ are equivalent to the conditions $\frac{E_{b1}}{N_0}_{opt1} < \frac{E_{b2}}{N_0}_{opt1}$ and $\frac{E_{b1}}{N_0}_{opt2} > \frac{E_{b2}}{N_0}_{opt2}$, respectively. Thus, Proposition 3.4.1 characterizes the beamforming vectors for the max-min fairness operating points, which lie on the curved section of the EpB region's boundary. For $\|\mathbf{h}_1\| \leq \rho\|\mathbf{h}_2\|$ (or $\|\mathbf{h}_2\| \leq \rho\|\mathbf{h}_1\|$), the beamforming vector is chosen as the principal eigenvector of $\mathbf{h}_1^\dagger \mathbf{h}_1$ (or $\mathbf{h}_2^\dagger \mathbf{h}_2$) and the achieved max-min fairness EpB pair is $\frac{E_{b1}}{N_0}_f = \frac{E_{b2}}{N_0}_f = \frac{\log_e 2}{\lambda_{1 \max}}$ (or $\frac{E_{b1}}{N_0}_f = \frac{E_{b2}}{N_0}_f = \frac{\log_e 2}{\lambda_{2 \max}}$).

Remark 3.2. A generalization of the max-min fairness criterion is the fixed EpB ratio constraint, where the transmit strategy is chosen so that the ratio between individual EpBs of users is fixed as $\frac{E_{b1}(\mathbf{Q}_{opt}(\gamma_\alpha))}{N_0} / \frac{E_{b2}(\mathbf{Q}_{opt}(\gamma_\alpha))}{N_0} = \alpha$, α is a pre-defined constant. For the MISO case, the optimal beamforming vector and its corresponding weighting factor γ_α can be then directly determined from Proposition 3.4.1 with $\|\mathbf{h}_1\|$ being replaced by $\alpha\|\mathbf{h}_1\|$.

3.4.4 Proportional fairness optimization

The transmit strategies that have been discussed so far either try to achieve the maximum fairness or to achieve the system MEpB and individual MEpBs while sacrificing the fairness. Now, let us consider a transmit strategy which balances the energy efficiency with the fairness among users by employing the proportional fairness criterion [Kel97, JL05]. This transmit strategy is characterized by the objective

$$\max_{0 \leq \gamma \leq 1} \sum_{i=1}^2 \log(R_i(\mathbf{Q}_{opt}(\gamma))) = \log\left(\max_{0 \leq \gamma \leq 1} \prod_{i=1}^2 R_i(\mathbf{Q}_{opt}(\gamma))\right).$$

A graphical illustration for this operating point on the boundaries of the wideband capacity and EpB regions can be found in Figure 3.4. Let γ_{pf} denote the weighting

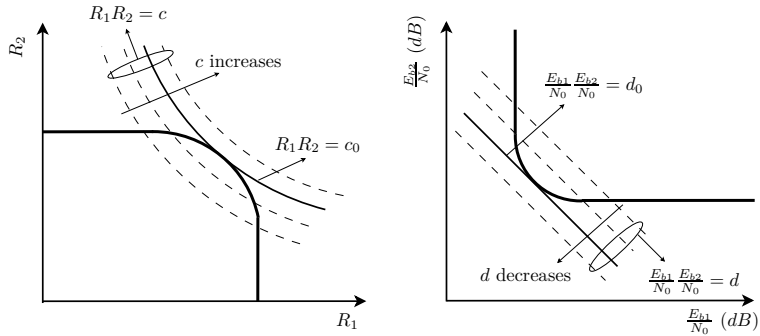


Figure 3.4: Graphical illustration of the proportional fairness operating point. In the wideband rate domain on the left, this point is represented by the point of contact between the wideband rate region's boundary and a certain curve in the curve family $R_1R_2 = c, \forall c \in \mathbb{R}$, i.e., $R_1R_2 = c_0$. In the EpB domain on the right, this point is the point of contact between the EpB region's boundary and the curve family $\frac{E_{b1}}{N_0} \frac{E_{b2}}{N_0} = d, \forall d \in \mathbb{R}$, which are linear in the decibel (dB) scale.

factor which leads to proportional fairness operating point, i.e.,

$$\begin{aligned} \gamma_{pf} &= \arg \max_{0 \leq \gamma \leq 1} (R_1(\mathbf{Q}_{opt}(\gamma))R_2(\mathbf{Q}_{opt}(\gamma))) \\ &= \arg \min_{0 \leq \gamma \leq 1} \left(\frac{E_{b1}(\mathbf{Q}_{opt}(\gamma))}{N_0} \frac{E_{b2}(\mathbf{Q}_{opt}(\gamma))}{N_0} \right). \end{aligned} \quad (3.18)$$

Similar to the max-min fairness transmission approach, the optimal weighting factor γ_{pf} can be solved by an one dimension grid search on the interval $[0, 1]$. In the case of MISO channels, γ_{pf} and the coefficients $\{\epsilon_{1pf}, \epsilon_{2pf}\}$ can be computed based on the following proposition.

Proposition 3.4.2. *For MISO channels, in order to achieve the proportional fairness operating point, the weighting factor γ and the beamforming coefficients $\{\epsilon_1, \epsilon_2\}$ in (3.11) are chosen as*

$$\gamma_{pf} = \frac{\|\mathbf{h}_2\|^2}{\|\mathbf{h}_1\|^2 + \|\mathbf{h}_2\|^2}, \quad (3.19)$$

$$\epsilon_{1pf} = \epsilon_{2pf} = \frac{1}{\sqrt{2(1 + \rho)}}. \quad (3.20)$$

Proof. The proof for this proposition is given in Appendix 3.7.C. \square

Unlike in the max-min fairness case, the proportional fairness operating point always lies on the curved section of the boundaries of the capacity and the EpB regions, which is illustrated in Figure 3.4. The point of interest is the contact point between the EpB region's boundary and the tangential line in the family

$\{\frac{E_{b1}}{N_0} \frac{E_{b2}}{N_0} = d\}_d$, which corresponds to the optimal d_0 . Moreover, since the achievable rates of users are proportional with their channel gains (as shown in (3.7.A.4) and (3.7.A.5)), using (3.20), we have $R_1(\mathbf{Q}_{opt}(\gamma_{pf}))/\|\mathbf{h}_1\|^2 = R_2(\mathbf{Q}_{opt}(\gamma_{pf}))/\|\mathbf{h}_2\|^2$, which reflects the proportional fairness objective.

Figure 3.5 shows the wideband capacity and the EpB regions of an AWGN bidirectional broadcast channel, whose boundaries include all the operating points which have been discussed in this section. We assume that the power constraint is $P/N_0 = 1$ and we have $n_1 = n_2 = 1$ and $n_r = 2$ antennas at the users and the relay. The channel between user 1 and the relay is fixed as $\mathbf{h}_1 = [1 \ 1 + i]$, whereas three possible cases are considered for the channel from the relay to user 2: $\mathbf{h}_2 = 0.8[1 \ 1 + i]$ ($\mathbf{h}_2 \parallel \mathbf{h}_1$ and $\rho = 1$), $\mathbf{h}_2 = 0.8[1 + i \ 1]$ ($\rho = 2/3$) and $\mathbf{h}_2 = 0.8[1 - i \ -1]$ ($\mathbf{h}_2 \perp \mathbf{h}_1$ and $\rho = 0$).

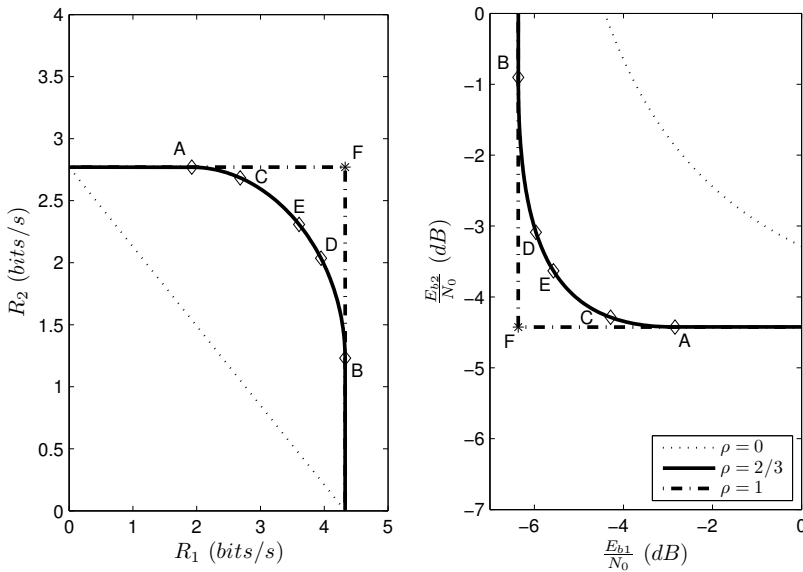


Figure 3.5: Wideband capacity (on the left) and EpB (on the right) regions for a bidirectional broadcast channel. The points A and B represent the single optimal rate pairs, C is the operating point for max-min fairness optimization, D is the utility maximization point, and E corresponds to the proportional fairness case. F is the best rate pair achieved by parallel channels. The dotted curves are the boundaries for the regions assuming orthogonal channels.

3.5 Wideband Slope

In addition to the MEpB, another important metric in the wideband regime is the wideband slope [Ver02], i.e., the slope of the spectral efficiency curve at low EpB. When the spectral efficiency is small but non-zero, the wideband slope, measured in bits/s/Hz/(3 dB), evaluates the growth speed of the spectral efficiency according to EpB. In other words, the wideband slope characterizes the trade-off between the spectral efficiency and EpB (or the bandwidth versus power trade-off) in the wideband regime. This section analyzes the wideband slope that can be achieved from the proposed transmit strategy. Similar to the EpB, the wideband slope is also considered from both user and system perspectives.

3.5.1 Individual wideband slope

We first consider the *individual wideband slope*, which reflects the trade-off between the individual spectral efficiency and the required EpB for each user. According to [Ver02], the individual wideband slope given \mathbf{Q} can be defined as

$$\mathcal{S}_{0i}(\mathbf{Q}) = \left. \frac{-2[\dot{S}_i(\mathbf{Q})]^2}{\ddot{S}_i(\mathbf{Q})} \right|_{\text{snr}=0}, \quad i = 1, 2,$$

where $\dot{S}_i(\mathbf{Q})$ and $\ddot{S}_i(\mathbf{Q})$ are the first and second derivatives of the individual spectral efficiency function $S_i(\mathbf{Q})$ w.r.t. the SNR, $\text{snr} = P/BN_0$, respectively. Moreover, the spectral efficiency for each user in (3.1) can be written as a function of the SNR as

$$S_i(\mathbf{Q}) = \log_2 e \left[\frac{\text{snr}}{P} \text{tr}(\mathbf{H}_i \mathbf{Q} \mathbf{H}_i^\dagger) - \frac{1}{2} \left(\frac{\text{snr}}{P} \right)^2 \text{tr}((\mathbf{H}_i \mathbf{Q} \mathbf{H}_i^\dagger)^2) + o(\text{snr}^2) \right].$$

Therefore, the individual wideband slope can be obtained as

$$\mathcal{S}_{0i}(\mathbf{Q}) = \frac{2 \left[\text{tr}(\mathbf{H}_i \mathbf{Q} \mathbf{H}_i^\dagger) \right]^2}{\text{tr}((\mathbf{H}_i \mathbf{Q} \mathbf{H}_i^\dagger)^2)}, \quad i = 1, 2. \quad (3.21)$$

Now, let us recall the transmit strategies which maximize the wideband weighted sum-rate, i.e., beamforming transmit strategy with $\mathbf{Q} = \mathbf{Q}_{opt}(\gamma) = P\mathbf{w}\mathbf{w}^\dagger$. From the commutative property of the trace operation, we have

$$\begin{aligned} \left(\text{tr}(\mathbf{H}_i \mathbf{Q}_{opt}(\gamma) \mathbf{H}_i^\dagger) \right)^2 &= \left(\text{tr}(P \mathbf{H}_i \mathbf{w} \mathbf{w}^\dagger \mathbf{H}_i^\dagger) \right)^2 \\ &= \left(\text{tr}(P \mathbf{w}^\dagger \mathbf{H}_i^\dagger \mathbf{H}_i \mathbf{w}) \right)^2 \\ &= (P \mathbf{w}^\dagger \mathbf{H}_i^\dagger \mathbf{H}_i \mathbf{w})^2 \end{aligned}$$

and

$$\begin{aligned}
\text{tr} \left((\mathbf{H}_i \mathbf{Q}_{opt}(\gamma) \mathbf{H}_i^\dagger)^2 \right) &= \text{tr} \left((P \mathbf{H}_i \mathbf{w} \mathbf{w}^\dagger \mathbf{H}_i^\dagger)^2 \right) \\
&= \text{tr} \left((P \mathbf{w}^\dagger \mathbf{H}_i^\dagger \mathbf{H}_i \mathbf{w})^2 \right) \\
&= (P \mathbf{w}^\dagger \mathbf{H}_i^\dagger \mathbf{H}_i \mathbf{w})^2.
\end{aligned}$$

Therefore,

$$\mathcal{S}_{0i}(\mathbf{Q}_{opt}(\gamma)) = 2, \quad i = 1, 2.$$

This implies that when the transmit strategy is designed to maximize the wideband weighted sum-rate (or achieve the MEpB vector on the boundary of the EPB region), then we achieve the individual wideband slope which equals to the one of a Gaussian point-to-point channel [Ver02].

3.5.2 System wideband slope

Next, let us continue with the slope of the system spectral efficiency curve at low EpB, which is the so called *system wideband slope*. In the wideband regime, this entity characterizes the trade-off between the overall bandwidth requirement and the power consumption at the relay. Similar to the individual wideband slope, the system wideband slope can be obtained from the derivatives of the system spectral efficiency as

$$\mathcal{S}_{0,s}(\mathbf{Q}) = \frac{-2[\dot{S}_s(\mathbf{Q})]^2}{\ddot{S}_s(\mathbf{Q})} \Big|_{\text{snr}=0},$$

where $S_s(\mathbf{Q})$ is the system spectral efficiency. The system spectral efficiency is defined by the sum of the individual spectral efficiencies, $S_s(\mathbf{Q}) = S_1(\mathbf{Q}) + S_2(\mathbf{Q})$. Therefore,

$$\begin{aligned}
\mathcal{S}_{0,s}(\mathbf{Q}) &= \frac{-2[\dot{S}_1(\mathbf{Q}) + \dot{S}_2(\mathbf{Q})]^2}{\ddot{S}_1(\mathbf{Q}) + \ddot{S}_2(\mathbf{Q})} \Big|_{\text{snr}=0} \\
&= \frac{2 \left[\text{tr}(\mathbf{H}_1 \mathbf{Q} \mathbf{H}_1^\dagger + \mathbf{H}_2 \mathbf{Q} \mathbf{H}_2^\dagger) \right]^2}{\text{tr} \left((\mathbf{H}_1 \mathbf{Q} \mathbf{H}_1^\dagger)^2 + (\mathbf{H}_2 \mathbf{Q} \mathbf{H}_2^\dagger)^2 \right)}. \tag{3.22}
\end{aligned}$$

Moreover, when $\mathbf{Q} = \mathbf{Q}_{opt}(\gamma) = P \mathbf{w} \mathbf{w}^\dagger$, the numerator of (3.22) equals to $2 \left(\sum_{i=1}^2 P \mathbf{w}^\dagger \mathbf{H}_i^\dagger \mathbf{H}_i \mathbf{w} \right)^2$ and the denominator equals to $\sum_{i=1}^2 (P \mathbf{w}^\dagger \mathbf{H}_i^\dagger \mathbf{H}_i \mathbf{w})^2$. From the Cauchy-Schwarz inequality, we have

$$\mathcal{S}_{0,s}(\mathbf{Q}_{opt}(\gamma)) \leq 4.$$

The inequality is tight if and only if $\text{tr}(\mathbf{H}_1 \mathbf{Q}_{opt}(\gamma) \mathbf{H}_1^\dagger) = \text{tr}(\mathbf{H}_2 \mathbf{Q}_{opt}(\gamma) \mathbf{H}_2^\dagger)$, which corresponds to the max-min fairness operating point. This implies that among the beamforming transmit strategies, which achieve the Pareto optimal operating points on the boundaries of the wideband capacity and EpB regions, the max-min fairness transmit strategy supports the best system wideband slope.

3.6 Chapter Conclusion

This chapter has considered the capacity and EpB limits of a Gaussian MIMO bidirectional broadcast channel in the wideband regime. The optimal transmit strategy which maximizes the wideband weighted sum-rate has been presented, which characterizes the boundaries of the wideband capacity and EpB regions. The closed-form solution of the optimal transmit covariance matrix shows that a single beam transmit strategy is optimal. This result is analogous to the single beam optimality of a point-to-point MIMO system in the low SNR regime. For MISO channels the optimal beamforming vector can be expressed as the linear combination of the channel directions. The vector optimization problem formulation allowed us to take fairness issues into account when designing the transmit strategy. By setting the weighting factor properly, we can achieve different optimal operating points corresponding to different energy efficiency and fairness criteria.

3.7 Appendices

3.7.A Proof of Theorem 3.3.2

Theorem 3.3.2 can be proved by the following three steps.

Step 1: We first prove by contradiction that the optimal beamforming is to transmit into the vector space $\text{span}\{\mathbf{u}_1, \mathbf{u}_2\}$. The proof is based on the idea in [OWB09]. Suppose that the optimal transmit vector can be expressed as

$$\mathbf{w} = a_1 \mathbf{u}_1 + a_2 \mathbf{u}_2 + a_3 \mathbf{u}_3, \quad (3.7.A.1)$$

where $(a_1, a_2, a_3) \in \mathbb{C}^3$, $|a_3| > 0$, $\mathbf{u}_3 \perp \text{span}\{\mathbf{u}_1, \mathbf{u}_2\}$ and $\text{tr}(\mathbf{Q}_{opt}(\gamma)) = P \text{tr}(\mathbf{w} \mathbf{w}^\dagger) = P$. The wideband rate of user i , $i = 1, 2$, is given by

$$\begin{aligned} R_i(\mathbf{Q}_{opt}(\gamma)) &= \frac{\log_2 e}{N_0} \text{tr}(\mathbf{h}_i^\dagger \mathbf{Q}_{opt}(\gamma) \mathbf{h}_i) \\ &= \frac{P \log_2 e}{N_0} |\mathbf{h}_i^\dagger \mathbf{w}|^2 \\ &= \frac{P \log_2 e}{N_0} |\mathbf{h}_i^\dagger (a_1 \mathbf{u}_1 + a_2 \mathbf{u}_2 + a_3 \mathbf{u}_3)|^2 \\ &= \frac{P \log_2 e}{N_0} |\mathbf{h}_i^\dagger (a_1 \mathbf{u}_1 + a_2 \mathbf{u}_2)|^2, \end{aligned} \quad (3.7.A.2)$$

where the last equality follows from $\mathbf{h}_i^\dagger \mathbf{u}_3 = 0$, $i = 1, 2$. So, with $\tilde{\mathbf{w}} = \frac{a_1 \mathbf{u}_1 + a_2 \mathbf{u}_2}{\sqrt{1 - |a_3|}}$ we obtain a larger wideband rate

$$\begin{aligned} \frac{P \log_2 e}{N_0} |\mathbf{h}_i^\dagger \tilde{\mathbf{w}}|^2 &= \frac{P \log_2 e}{N_0(1 - |a_3|)} |\mathbf{h}_i^\dagger (a_1 \mathbf{u}_1 + a_2 \mathbf{u}_2)|^2 \\ &> \frac{P \log_2 e}{N_0} |\mathbf{h}_i^\dagger (a_1 \mathbf{u}_1 + a_2 \mathbf{u}_2)|^2 \\ &= R_i(\mathbf{Q}_{opt}(\gamma)). \end{aligned}$$

This is a contradiction to the assumption that \mathbf{w} defined in (3.7.A.1) is the optimal beamforming. Thus, the optimal beamforming vector can be described as

$$\mathbf{w} = a_1 \mathbf{u}_1 + a_2 \mathbf{u}_2.$$

Step 2: Next, we prove that $\{a_1, a_2\}$ can be simplified as real factors and a phase difference. Since $\mathbf{Q}_{opt}(\gamma) = P \mathbf{w} \mathbf{w}^\dagger$ is unchanged under a phase rotation of the beamforming vector \mathbf{w} , without loss of the generality, we can consider $a_1 = \epsilon_1$ and $a_2 = \epsilon_2 e^{j\theta}$, $\epsilon_1, \epsilon_2 \in \mathbb{R}_+$. Then the power constraint reads as

$$\text{tr}(\mathbf{w} \mathbf{w}^\dagger) = \epsilon_1^2 + \epsilon_2^2 + 2\epsilon_1 \epsilon_2 \rho \cos(\varphi + \theta) = 1. \quad (3.7.A.3)$$

The wideband rate for user 1 becomes

$$\begin{aligned} R_1(\mathbf{Q}_{opt}(\gamma)) &= \frac{P \log_2 e}{N_0} |\mathbf{h}_1^\dagger \mathbf{w}|^2 \\ &= \frac{P \log_2 e}{N_0} \|\mathbf{h}_1\| \|\mathbf{u}_1^\dagger (\epsilon_1 \mathbf{u}_1 + \epsilon_2 e^{j\theta} \mathbf{u}_2)\|^2 \\ &= \frac{P \log_2 e}{N_0} \|\mathbf{h}_1\|^2 |\epsilon_1 \mathbf{u}_1^\dagger \mathbf{u}_1 + \epsilon_2 e^{j\theta} \mathbf{u}_1^\dagger \mathbf{u}_2|^2 \\ &= \frac{P \log_2 e}{N_0} \|\mathbf{h}_1\|^2 |\epsilon_1 + \epsilon_2 e^{j\theta} \rho e^{j\varphi}|^2 \\ &= \frac{P \log_2 e}{N_0} \|\mathbf{h}_1\|^2 (\epsilon_1^2 + \epsilon_2^2 \rho^2 + 2\epsilon_1 \epsilon_2 \rho \cos(\varphi + \theta)) \\ &= \frac{P \log_2 e}{N_0} \|\mathbf{h}_1\|^2 (1 - \epsilon_2^2 (1 - \rho^2)). \end{aligned} \quad (3.7.A.4)$$

Similarly,

$$R_2(\mathbf{Q}_{opt}(\gamma)) = \frac{P \log_2 e}{N_0} \|\mathbf{h}_2\|^2 (1 - \epsilon_1^2 (1 - \rho^2)). \quad (3.7.A.5)$$

It follows from (3.7.A.3) that for any $\theta \neq -\varphi$ we can decrease ϵ_1, ϵ_2 (so that $R_1(\mathbf{Q}_{opt}(\gamma))$ and $R_2(\mathbf{Q}_{opt}(\gamma))$ increase) while satisfying (3.7.A.3) by adjusting θ to $\theta = -\varphi$. Thus, $\theta = -\varphi$ is the optimal phase difference of the coefficients.

Step 3: Finally, we derive the exact value of ϵ_1, ϵ_2 corresponding to our optimal wideband weighted sum-rate as the functions of γ and \mathbf{h}_i , $i = 1, 2$. Substituting

$\mathbf{Q}_{opt}(\gamma) = P\mathbf{w}\mathbf{w}^\dagger$ and $\mathbf{w} = \varepsilon_1\mathbf{u}_1 + \varepsilon_2e^{-j\varphi}\mathbf{u}_2$ in (3.7), the optimal coefficients $\{\varepsilon_1, \varepsilon_2\}$ are solutions of the following optimization problem

$$\begin{aligned} \max \quad & f(\varepsilon_1, \varepsilon_2) = \gamma P\|\mathbf{h}_1\|^2(1 - \varepsilon_2^2(1 - \rho^2)) + (1 - \gamma)P\|\mathbf{h}_2\|^2(1 - \varepsilon_1^2(1 - \rho^2)) \\ \text{s.t.} \quad & \varepsilon_1^2 + \varepsilon_2^2 + 2\varepsilon_1\varepsilon_2\rho = 1, \\ & \varepsilon_1 \geq 0, \varepsilon_2 \geq 0. \end{aligned} \quad (3.7.A.6)$$

Recalling the definitions $\mu_1 = \gamma\|\mathbf{h}_1\|^2$ and $\mu_2 = (1 - \gamma)\|\mathbf{h}_2\|^2$, the objective function in (3.7.A.6) can be rewritten as

$$f(\varepsilon_1, \varepsilon_2) = P(\mu_1 + \mu_2) - P(1 - \rho^2)[\mu_2\varepsilon_1^2 + \mu_1\varepsilon_2^2]. \quad (3.7.A.7)$$

Therewith, the optimization problem in (3.7.A.6) becomes

$$\begin{aligned} \min \quad & g(\varepsilon_1, \varepsilon_2) = \mu_2\varepsilon_1^2 + \mu_1\varepsilon_2^2 \\ \text{s.t.} \quad & \varepsilon_1^2 + \varepsilon_2^2 + 2\varepsilon_1\varepsilon_2\rho = 1, \\ & \varepsilon_1 \geq 0, \varepsilon_2 \geq 0. \end{aligned} \quad (3.7.A.8)$$

The Lagrangian duality function [BV04] associated with this optimization problem is given by

$$L(\varepsilon_1, \varepsilon_2, \lambda, \nu_1, \nu_2) = (\mu_2\varepsilon_1^2 + \mu_1\varepsilon_2^2) - \lambda(\varepsilon_1^2 + \varepsilon_2^2 + 2\rho\varepsilon_1\varepsilon_2 - 1) - \nu_1\varepsilon_1 - \nu_2\varepsilon_2.$$

The primal $\{\varepsilon_1, \varepsilon_2\}$ and dual $\{\lambda^*, \nu_1^*, \nu_2^*\}$ optimal coefficients are then characterized by the Karush-Kuhn-Tucker (KKT) optimality conditions

$$\partial L(\varepsilon_1, \varepsilon_2, \lambda^*, \nu_1^*, \nu_2^*)/\partial \varepsilon_1 = 2\mu_2\varepsilon_1 - 2\lambda^*\varepsilon_1 - 2\rho\lambda^*\varepsilon_2 - \nu_1^* = 0, \quad (3.7.A.9a)$$

$$\partial L(\varepsilon_1, \varepsilon_2, \lambda^*, \nu_1^*, \nu_2^*)/\partial \varepsilon_2 = 2\mu_1\varepsilon_2 - 2\lambda^*\varepsilon_2 - 2\rho\lambda^*\varepsilon_1 - \nu_2^* = 0, \quad (3.7.A.9b)$$

$$\varepsilon_1^2 + \varepsilon_2^2 + 2\rho\varepsilon_1\varepsilon_2 - 1 = 0, \quad (3.7.A.9c)$$

$$\nu_1^* \geq 0, \nu_2^* \geq 0, \quad (3.7.A.9d)$$

$$\nu_1^*\varepsilon_1 = 0, \nu_2^*\varepsilon_2 = 0. \quad (3.7.A.9e)$$

Two solutions $\{\varepsilon_1 = 0, \varepsilon_2 = 1\}$ and $\{\varepsilon_1 = 1, \varepsilon_2 = 0\}$ are easy to obtain.

When $\{\varepsilon_1 \neq 0, \varepsilon_2 \neq 0\}$, it follows from (3.7.A.9e) that $\nu_1^* = \nu_2^* = 0$. Thus, from (3.7.A.9a) and (3.7.A.9b), we have $\frac{\varepsilon_1}{\varepsilon_2} = \frac{\rho\lambda^*}{\mu_2 - \lambda^*}$ and $\frac{\varepsilon_1}{\varepsilon_2} = \frac{\mu_1 - \lambda^*}{\rho\lambda^*}$. Combining these two conditions we get

$$(1 - \rho^2)\lambda^{*2} - (\mu_1 + \mu_2)\lambda^* + \mu_1\mu_2 = 0.$$

From the initial assumption that $\rho \notin \{0, 1\}$, we obtain two possible values for the optimal λ^*

$$\lambda^* = \frac{(\mu_1 + \mu_2) \pm \sqrt{(\mu_1 + \mu_2)^2 - 4\mu_1\mu_2(1 - \rho^2)}}{2(1 - \rho^2)}.$$

However, from (3.7.A.9a) and (3.7.A.9b) we have

$$(\mu_2 - \lambda^*)\epsilon_1 = \rho\lambda^*\epsilon_2 \geq 0, \quad (3.7.A.10a)$$

$$(\mu_1 - \lambda^*)\epsilon_2 = \rho\lambda^*\epsilon_1 \geq 0, \quad (3.7.A.10b)$$

where “ ≥ 0 ” comes from the assumptions $\epsilon_1, \epsilon_2 \in \mathbb{R}_+$, $\rho = |\mathbf{u}_1^\dagger \mathbf{u}_2| \in (0, 1)$ and $\lambda^* \geq 0$ (from two possible roots for λ^*). Thus, we have that $\lambda^* \leq \min\{\mu_1, \mu_2\}$ and we choose $\lambda^* = \lambda$ as in (3.13). Substituting $\epsilon_2 = \frac{\mu_2 - \lambda^*}{\rho\lambda^*}\epsilon_1$ (from (3.7.A.10a)) into (3.7.A.9c) and solving for ϵ_1, ϵ_2 gives (3.12).

Overall, three (ϵ_1, ϵ_2) pairs are found that satisfy the KKT optimality conditions: $(0, 1)$, $(1, 0)$ and (ϵ_1, ϵ_2) . Now we determine the optimal solution by comparing the corresponding objective values of the optimization problem in (3.7.A.8) for those three solutions. We have

$$g(\epsilon_1, \epsilon_2) = \mu_2\epsilon_1^2 + \mu_1\epsilon_2^2.$$

From (3.7.A.9a) and (3.7.A.9b) we have

$$\mu_2\epsilon_1^2 = \lambda^*(\epsilon_1 + \rho\epsilon_2)\epsilon_1, \quad (3.7.A.11)$$

$$\mu_1\epsilon_2^2 = \lambda^*(\epsilon_2 + \rho\epsilon_1)\epsilon_2. \quad (3.7.A.12)$$

Summing (3.7.A.11) and (3.7.A.12) then using $\epsilon_1^2 + \epsilon_2^2 + 2\rho\epsilon_1\epsilon_2 = 1$ (from (3.7.A.9c)), we get

$$g(\epsilon_1, \epsilon_2) = \mu_2\epsilon_1^2 + \mu_1\epsilon_2^2 = \lambda^* \leq \min\{\mu_1, \mu_2\} = \min\{g(0, 1), g(1, 0)\}.$$

Thus, $\{\epsilon_1, \epsilon_2\}$ in Theorem 3.3.2 is an optimal solution.

3.7.B Proof of Proposition 3.4.1

Under the conditions $\|\mathbf{h}_1\| > \rho\|\mathbf{h}_2\|$ and $\|\mathbf{h}_2\| < \rho\|\mathbf{h}_1\|$, we consider the max-min fairness optimal points on the curved section which satisfy (3.15). Combining (3.15), (3.7.A.4), (3.7.A.5) and the constraint $\mathbf{w}^\dagger \mathbf{w} = 1$ we obtain

$$\|\mathbf{h}_1\|^2(1 - \epsilon_{2f}^2(1 - \rho^2)) = \|\mathbf{h}_2\|^2(1 - \epsilon_{1f}^2(1 - \rho^2)), \quad (3.7.B.1)$$

$$\epsilon_{1f}^2 + \epsilon_{2f}^2 + 2\rho\epsilon_{1f}\epsilon_{2f} = 1 \quad (3.7.B.2)$$

Substituting “1”s in (3.7.B.1) by the left-hand side of (3.7.B.2) we get

$$\|\mathbf{h}_1\|^2(\rho\epsilon_{2f} + \epsilon_{1f})^2 = \|\mathbf{h}_2\|^2(\rho\epsilon_{1f} + \epsilon_{2f})^2.$$

Thus, we have

$$\epsilon_{2f} = \frac{\|\mathbf{h}_1\| - \rho\|\mathbf{h}_2\|}{\|\mathbf{h}_2\| - \rho\|\mathbf{h}_1\|}\epsilon_{1f}. \quad (3.7.B.3)$$

This is the second equality of (3.17) with $a = \frac{\|\mathbf{h}_1\| - \rho \|\mathbf{h}_2\|}{\|\mathbf{h}_2\| - \rho \|\mathbf{h}_1\|}$. Substituting ϵ_{2f} from (3.7.B.3) into (3.7.B.2) and solving for ϵ_{1f} we get

$$\epsilon_{1f} = \frac{1}{\sqrt{1 + 2\rho a + a^2}}.$$

Next we find the corresponding weighting factor γ_f . Since the max-min fairness optimal point is on the boundary of the EpB region, $\{\epsilon_{1f}, \epsilon_{2f}\}$ satisfy (3.7.A.9a) and (3.7.A.9b). Accordingly, we have

$$\frac{\mu_2}{\mu_1} = \frac{(1 - \gamma_f)\|\mathbf{h}_2\|^2}{\gamma_f\|\mathbf{h}_1\|^2} = \frac{\epsilon_{2f}(\epsilon_{1f} - \rho\epsilon_{2f})}{\epsilon_{1f}(\epsilon_{2f} - \rho\epsilon_{1f})} = \frac{1 - \rho a}{1 - \rho/a}. \quad (3.7.B.4)$$

Solving (3.7.B.4) for γ_f gives (3.16).

3.7.C Proof of Proposition 3.4.2

Rewriting the objective function in (3.18) as a function of $\{\varepsilon_1, \varepsilon_2\}$, we have

$$\begin{aligned} R_1(\mathbf{Q}_{opt}(\gamma))R_2(\mathbf{Q}_{opt}(\gamma)) &= \|\mathbf{h}_1\|^2\|\mathbf{h}_2\|^2(1 - \varepsilon_2^2(1 - \rho^2))(1 - \varepsilon_1^2(1 - \rho^2)) \\ &= \|\mathbf{h}_1\|^2\|\mathbf{h}_2\|^2(1 - \rho^2)((1 - \rho^2)\varepsilon_1^2\varepsilon_2^2 - \varepsilon_1^2 - \varepsilon_2^2 + \frac{1}{1 - \rho^2}). \end{aligned}$$

The coefficients $\{\epsilon_{1pf}, \epsilon_{2pf}\}$ which lead to the proportional fairness optimal point are then the solutions of the following optimization problem

$$\max \quad (1 - \rho^2)\varepsilon_1^2\varepsilon_2^2 - \varepsilon_1^2 - \varepsilon_2^2 \quad (3.7.C.1)$$

$$s.t. \quad \varepsilon_1^2 + \varepsilon_2^2 + 2\rho\varepsilon_1\varepsilon_2 = 1, \quad (3.7.C.2)$$

$$\varepsilon_1 \geq 0, \varepsilon_2 \geq 0. \quad (3.7.C.3)$$

The objective function becomes $(1 - \rho^2)\varepsilon_1^2\varepsilon_2^2 + 2\rho\varepsilon_1\varepsilon_2 - 1$ by substitution of the first constraint $\varepsilon_1^2 + \varepsilon_2^2 = 1 - 2\rho\varepsilon_1\varepsilon_2$. Thus the objective function is an increasing function w.r.t. $\varepsilon_1\varepsilon_2$ (as $\varepsilon_1 \geq 0, \varepsilon_2 \geq 0$). Moreover, $\varepsilon_1\varepsilon_2 = (1 - \varepsilon_1^2 - \varepsilon_2^2)/(2\rho)$ is a decreasing function w.r.t. $(\varepsilon_1^2 + \varepsilon_2^2)$. Thus, the optimal solutions of (3.7.C.1) can be solved by the following problem

$$\min \quad \varepsilon_1^2 + \varepsilon_2^2$$

$$s.t. \quad \varepsilon_1^2 + \varepsilon_2^2 + 2\rho\varepsilon_1\varepsilon_2 = 1,$$

$$\varepsilon_1 \geq 0, \varepsilon_2 \geq 0.$$

This optimal problem is a special case of the optimal problem (3.7.A.8) with $\mu_1 = \mu_2 = 1$. Therefore, the optimal solution can be obtained as

$$\epsilon_{1pf} = \epsilon_{2pf} = \frac{1}{\sqrt{2(1 + \rho)}}.$$

Furthermore, since this operating point is on the boundary of the EpB region, (3.7.A.9a)-(3.7.A.9e) hold. Combining this with $\epsilon_1 = \epsilon_2$, we get $\mu_1 = \mu_2$. Therefore, the weighting factor can be obtained as

$$\gamma_{pf} = \frac{\|\mathbf{h}_2\|^2}{\|\mathbf{h}_1\|^2 + \|\mathbf{h}_2\|^2}.$$

Multi-pair MIMO Bidirectional Broadcast Channel in the Wideband Regime

In the previous chapter, we have considered the optimal transmit strategy and energy efficiency limits for a single pair Gaussian MIMO bidirectional broadcast channel. From the single pair scenario, a natural question is whether the proposed transmit strategy could be applied to a more general model with multiple user-pairs and a single relay. This is an example model for a cellular network, where many pairs of users want to communicate together with the support of a base station (as a relay) under the presence of interference from other user-pairs who are also communicating together through the support of the same base station. In this chapter, we propose a simple transmit strategy for a *multi-pair Gaussian MIMO bidirectional broadcast channel* in the wideband regime, which is motivated from the optimal transmit strategy for the single user-pair case. Further discussions with respect to the optimality of the proposed scheme are provided including individual MEpB achievability and a conjecture on the MEpB region.

4.1 Related Works and Motivation

As an extension to the traditional two-way relaying system, multi-way relaying has been proposed and studied [GYGP13, OKJ10, AKSH09, KSD10, CY09], where more than two users exchange information among themselves via the support of relay. Within this, multi-pair bidirectional relaying [AKSH09, KSD10, CY09] is a special case, where two users of each pair want to exchange the messages together, regarding the signals from other pairs as interference. In the single pair setup, the interference from the other user is cancelled using the side information at each user. Thus, this can be considered as a noise-limited system. However, in a multi-pair bidirectional broadcast channel, the side information at each user is not enough for cancelling all interference from all other users. Therefore, multi-pair bidirectional broadcast channel is a noise- and interference-limited system in general.

In a two phase decode-and-forward multi-pair MIMO bidirectional relaying sys-

tem. During the first phase, so called MAC phase, all users transmit their messages to the relay, which are decoded at the relay before they are re-encoded and broadcasted to the users in the second phase, namely the broadcast phase. Similar to Chapter 3, we concentrate on the broadcast phase in this chapter, constituting a called *the multi-pair bidirectional broadcast channel* due to the broadcasting nature and the side information at the receiver.

The most common way to characterize the MEpB is to use the derivative evaluated at zero SNR of the capacity function [Ver02, LTV03, CTV04]. This approach is not possible in most multi-terminal systems since the capacity for such channels with finite bandwidth is often unknown. For some special scenarios of the multi-pair bidirectional relay system, there have been some attempts to find bounds on the capacity region. In [AKSH09], the capacity for a deterministic channel has been studied. In [KSD10], achievable rate regions and a cut-set outer bound have been derived. However, the capacity region for a multi-pair Gaussian MIMO bidirectional channel is still an open problem.

To face these challenges from the communication theory point of view, we consider a simple coding strategy for the decoded messages at the relay. The achievable wideband rate and energy per bit regions for the proposed scheme are then analyzed. Since the achievable wideband rate and energy per bit regions are proved to be convex, their boundaries are characterized by optimal transmit strategies, which maximize the wideband weighted sum-rates. Similar to the single pair scenario, the weighting factors can be used to find and discuss the fairness versus energy efficiency trade-off. Discussions on the optimality of the proposed coding strategy are then provided, in which the individual pair MEpB and a conjecture on the MEpB are considered.

The rest of the chapter is organized as follows. Section 4.2 presents the system model and defines the achievable wideband rate region and the achievable EpB region. In Section 4.3, the optimal transmit strategy for the AWGN multi-pair MIMO bidirectional broadcast channel is considered and a closed-form of the optimal transmit covariance matrix is derived. The energy efficiency versus fairness issue is provided in Section 4.4. Discussions on the optimality of the proposed scheme are given in Section 4.5. Finally, some conclusions are given in the end of the chapter.

4.2 Problem Setup

We consider a multi-pair bidirectional relaying system which consists of K pairs of user and a supporting relay as depicted in Figure 4.1. User i of pair k is called T_{ki} and is equipped with n_{ki} ($k = 1, \dots, K; i = 1, 2$) antennas. The relay is equipped with n_r antennas. Under the assumption that the relay has successfully decoded the messages from all users in the MAC phase, we concentrate on the broadcast phase, where the relay forwards a re-encoded composition of decoded messages to the users.

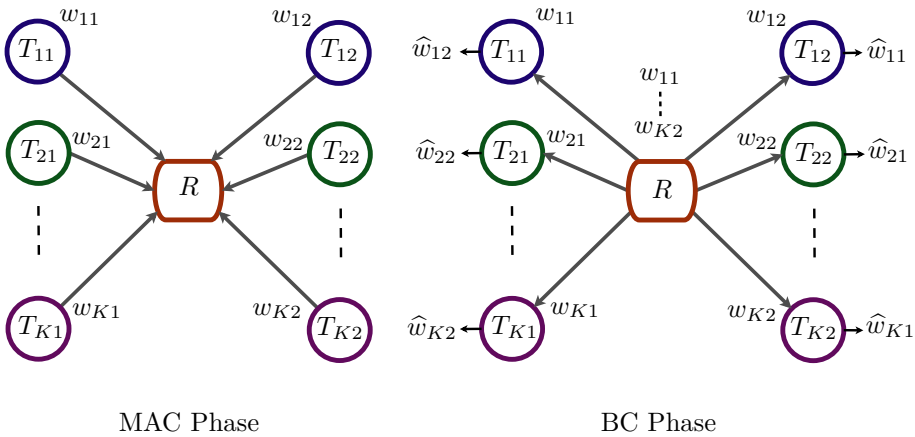


Figure 4.1: Multi-pair bidirectional relay channel.

Let $\{w_{11}, w_{12}, \dots, w_{K1}, w_{K2}\}$ denote the messages from the users, which are pairwise independent and known at the relay after the MAC phase. We assume that T_{k1} transmits w_{k1} and desires w_{k2} from T_{k2} . In the opposite direction, T_{k2} transmits w_{k2} and desires w_{k1} from T_{k1} . In order to send the message $\nu_k = [w_{k1}, w_{k2}]$ to pair k , i.e., $\{T_{k1}, T_{k2}\}$, the relay uses the transmit vector $\mathbf{x}_k \in \mathbb{C}^{n_r \times 1}$. We consider an encoding scheme which combines the single pair capacity achieving strategy [WOB⁺08] with superposition coding [TV05]. To this end, the relay encodes ν_k into \mathbf{x}_k for each pair and then broadcasts the superposition of all \mathbf{x}_k ($k = 1, \dots, K$) as in Figure 4.2. Thus, the transmitted signal at the relay is $\mathbf{x} = \sum_{k=1}^K \mathbf{x}_k$, which has to satisfy the total power constraint $\mathbb{E}\{\mathbf{x}^\dagger \mathbf{x}\} = \sum_{k=1}^K \text{tr}(\mathbf{Q}_k) \leq P_{tot}$, where $\mathbb{E}\{\mathbf{x}_k \mathbf{x}_k^\dagger\} = \mathbf{Q}_k$.

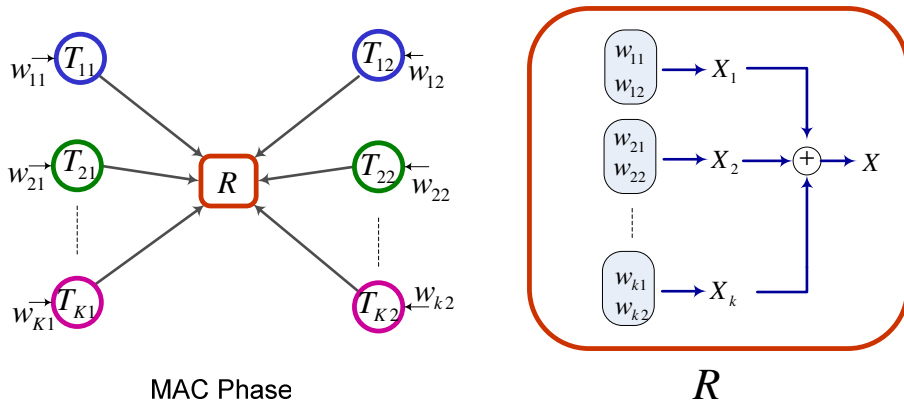


Figure 4.2: Proposed coding strategy at relay after the MAC phase.

The multiplicative channel matrix between the relay and T_{ki} is denoted by $\mathbf{H}_{ki} \in \mathbb{C}^{n_{ki} \times n_r}$. Then the received signal at each user is given as

$$\mathbf{y}_{ki} = \mathbf{H}_{ki} \mathbf{x} + \mathbf{n}_{ki}, \forall k = 1, \dots, K, i = 1, 2, \quad (4.1)$$

where \mathbf{n}_{ki} denotes the additive Gaussian noise vector at T_{ki} , whose elements are independent and identically distributed according to $\mathcal{CN}(0, \sigma_0^2)$.

We assume that perfect channel state information is available at the relay and all users. In the broadcast phase, user T_{ki} knows its own message w_{ki} and only tries to decode the unknown message $w_{k\bar{i}}$ ($\bar{i} = \{1, 2\} \setminus i$) from its counterpart $T_{k\bar{i}}$ using w_{ki} as side information. Each user simply considers the signal for all other pairs as additional additive Gaussian noise. Thus the achievable rate for each user is given by the capacity of a Gaussian point-to-point channel [TV05]. Given the set of transmit covariance matrices $\mathcal{Q} = \{\mathbf{Q}_1, \mathbf{Q}_2, \dots, \mathbf{Q}_K\}$, the spectral efficiency (in bits per second per Hertz) of T_{ki} is then obtained as

$$S_{ki}(\mathcal{Q}) = \log_2 \left| \mathbf{I}_{n_{ki}} + \mathbf{H}_{ki} \mathbf{Q}_k \mathbf{H}_{ki}^\dagger \Phi_{ki}^{-1} \right|, \forall k = 1, \dots, K, i = 1, 2, \quad (4.2)$$

where $|\cdot|$ denotes the determinant operation and Φ_{ki} is the interference-plus-noise covariance matrix at T_{ki} , i.e.,

$$\Phi_{ki} = \sum_{j=1, j \neq k}^K \mathbf{H}_{ki} \mathbf{Q}_j \mathbf{H}_{ki}^\dagger + \sigma_0^2 \mathbf{I}_{n_{ki}}, \forall k = 1, \dots, K, i = 1, 2.$$

4.2.1 Achievable wideband rate region

Let B denote the available bandwidth of the system and $N_0/2$ is the noise power spectral density. Then the noise power can be rewritten as $\sigma_0^2 = BN_0$. In the wideband regime, as the bandwidth goes to infinity, the available power per sample and the SNR tend to zero. By applying Taylor expansion for the matrix function (4.2), the wideband rate (in bits per second) for each user is given by

$$\begin{aligned} R_{ki}(\mathcal{Q}) &= \lim_{B \rightarrow \infty} BS_{ki}(\mathcal{Q}) \\ &= \lim_{B \rightarrow \infty} \frac{\log_2 e}{N_0} \left[\text{tr} \left(\mathbf{H}_{ki} \mathbf{Q}_k \mathbf{H}_{ki}^\dagger \right) - \left[\frac{1}{2} \text{tr} \left(\left(\mathbf{H}_{ki} \mathbf{Q}_k \mathbf{H}_{ki}^\dagger \right)^2 \right) \right. \right. \\ &\quad \left. \left. + \text{tr} \left(\mathbf{H}_{ki} \mathbf{Q}_k \mathbf{H}_{ki}^\dagger \left(\sum_{j \neq k} \mathbf{H}_{ki} \mathbf{Q}_j \mathbf{H}_{ki}^\dagger \right) \right) \right] \frac{1}{BN_0} + o \left(\frac{1}{(BN_0)^2} \right) \right], \end{aligned} \quad (4.3)$$

for all $k=1, \dots, K, i=1, 2$.

Eq.(4.3) shows that the zeroth order approximation of the wideband rate of each user (w.r.t. $\frac{1}{B}$) does not depend on the interference from the other pairs. Since the first order approximation of the spectral efficiency (or the zeroth order approximation of the wideband rate) is sufficient to characterize the MEpB as shown

in [Ver02]. It is interesting to note that the inter-pair interference has no impact on the achievable EpB. Therefore, it is reasonable to expect that the proposed transmit scheme, which is designed to be optimal for the individual pair, is good enough to achieve the MEpB of the Gaussian multi-pair MIMO bidirectional broadcast channel.

Accordingly, let us define the achievable wideband rate region as

$$\mathcal{R}_a = C_o \left(\bigcup_{\mathcal{Q}: \sum_{k=1}^K \text{tr}(\mathbf{Q}_k) \leq P_{tot}} \mathbf{R}(\mathcal{Q}) \right), \quad (4.4)$$

where $C_o(\cdot)$ denotes the convex hull of the union of all achievable wideband rate vectors $\mathbf{R}(\mathcal{Q}) = (\mathbf{R}_{11}(\mathcal{Q}), \mathbf{R}_{12}(\mathcal{Q}), \dots, \mathbf{R}_{K2}(\mathcal{Q})) \in \mathbb{R}^{2K}$ for a given \mathcal{Q} .

4.2.2 Achievable Energy per Bit region

Similar to the single pair case in Chapter 3, we define the achievable system EpB and individual achievable EpBs¹ for the Gaussian multi-pair MIMO bidirectional broadcast channel as in the following.

Let us define the achievable *system EpB* as the required energy spent by the relay to reliably transmit one bit in total to all users. For given \mathcal{Q} , this quantity is given by

$$\frac{E_{b,s}(\mathcal{Q})}{N_0} = \frac{P_{tot}}{N_0 \mathbf{R}_s(\mathcal{Q})}, \quad (4.5)$$

where $\mathbf{R}_s(\mathcal{Q}) = \sum_{k=1}^K \sum_{i=1}^2 \mathbf{R}_{ki}(\mathcal{Q})$ is the wideband sum-rate given the set of transmit covariance matrices \mathcal{Q} .

Similarly, we define the achievable *individual user EpB* as the required energy spent by the relay to reliably transmit one bit to a desired user. For given \mathcal{Q} , the achievable EpB for each user is given by

$$\frac{E_{b,ki}(\mathcal{Q})}{N_0} = \frac{P_{tot}}{N_0 \mathbf{R}_{ki}(\mathcal{Q})}, \forall k = 1, \dots, K, i = 1, 2. \quad (4.6)$$

For a point-to-point channel, the MEpB describes the required EpB when the system operates at the wideband capacity, i.e., the capacity when $B \rightarrow \infty$. In the context of a multi-pair system with multiple users, we define the achievable EpB vector $\xi(\mathcal{Q}) = \left(\frac{E_{b,11}(\mathcal{Q})}{N_0}, \frac{E_{b,21}(\mathcal{Q})}{N_0}, \dots, \frac{E_{b,K2}(\mathcal{Q})}{N_0} \right)$, which represents the required EpBs when the system operates at the corresponding achievable wideband rate $\mathbf{R}(\mathcal{Q}) = (\mathbf{R}_{11}(\mathcal{Q}), \mathbf{R}_{12}(\mathcal{Q}), \dots, \mathbf{R}_{K2}(\mathcal{Q})) \in \mathbb{R}^{2K}$ for a given \mathcal{Q} . Then the *achievable*

¹More precisely, we can call "achievable wideband EpB" as we consider the wideband regime and the EpB is derived from the wideband rate.

EpB region is the convex hull of the union of all achievable wideband rate vectors $\xi(\mathcal{Q})$ according to \mathcal{Q} as

$$\mathcal{E}_a = C_o \left(\bigcup_{\mathcal{Q}, \sum_{k=1}^K \text{tr}(\mathbf{Q}_k) \leq P_{tot}} \xi(\mathcal{Q}) \right). \quad (4.7)$$

Since $\frac{E_{b,ki}(\mathcal{Q})}{N_0}$ is a decreasing function with respect to $R_{ki}(\mathcal{Q})$ and is a one-by-one mapping from $R_{ki}(\mathcal{Q})$, the boundary of the achievable EpB region \mathcal{E}_a can be determined by the curved section of the boundary of the achievable wideband rate region \mathcal{R}_a , which will be characterized in the next section.

4.3 Optimal Transmit Strategy

Since the achievable wideband rate region in (4.4) is convex as shown in the Appendix 4.7.A, its boundary is characterized by the maximal weighted sum-rate. In this section, the optimal² transmit strategies, i.e., the transmit covariance matrices which achieve the weighted sum-rate maximum, are considered. Let $\Gamma = \{\gamma_1, \gamma_2, \dots, \gamma_K, \gamma_{11}, \gamma_{12}, \dots, \gamma_{K1}, \gamma_{K2}\}$ denote the set of weighting factors, then the wideband weighted sum-rate can be written as

$$\begin{aligned} R(\mathcal{Q}, \Gamma) &= \sum_{k=1}^K \gamma_k \left(\gamma_{k1} R_{k1}(\mathcal{Q}) + \gamma_{k2} R_{k2}(\mathcal{Q}) \right) \\ &= \frac{\log_2 e}{N_0} \sum_{k=1}^K \gamma_k \left(\gamma_{k1} \text{tr}(\mathbf{H}_{k1} \mathbf{Q}_k \mathbf{H}_{k1}^\dagger) + \gamma_{k2} \text{tr}(\mathbf{H}_{k2} \mathbf{Q}_k \mathbf{H}_{k2}^\dagger) \right). \end{aligned} \quad (4.8)$$

The right-hand side of (4.8) follows from (4.3) with $\frac{1}{BN_0} \rightarrow 0$. Each realization of the weighting factor Γ represents the tangential direction of a supporting hyperplane [BV04] of the achievable wideband rate region. Moreover, Γ reflects the priorities between pairs and users. In this concept, we use the coefficients $(\gamma_1, \gamma_2, \dots, \gamma_K)$ to represent the priorities among pairs and $(\gamma_{11}, \gamma_{12}, \dots, \gamma_{K1}, \gamma_{K2})$ to represent the priorities between users of each pair. We assume that they satisfy

$$\begin{aligned} \gamma_1 + \gamma_2 + \dots + \gamma_K &= 1, \gamma_k \geq 0 \\ \gamma_{k1} + \gamma_{k2} &= 1, \gamma_{ki} \geq 0, \forall k = 1, \dots, K, i = 1, 2. \end{aligned}$$

By varying the weighting factors, we achieve different optima corresponding to different operating points on boundary of the achievable wideband rate region.

²This is optimal in the sense of achieving the boundary of the achievable wideband rate region in (4.4) assuming that the proposed coding scheme in Section 4.2 (motivated from the capacity achieving coding scheme for single pair setup) is used. This may not be optimal in the sense of achieving the wideband capacity of the system.

Our goal is now to find the set of optimal transmit covariance matrices \mathcal{Q} which can be formulated through the following optimization problem

$$\begin{aligned} \max_{\mathcal{Q}} \quad & f(\mathcal{Q}, \Gamma) = \sum_{k=1}^K \gamma_k \left(\gamma_{k1} \text{tr}(\mathbf{H}_{k1} \mathbf{Q}_k \mathbf{H}_{k1}^\dagger) + \gamma_{k2} \text{tr}(\mathbf{H}_{k2} \mathbf{Q}_k \mathbf{H}_{k2}^\dagger) \right) \\ \text{s.t.} \quad & \sum_{k=1}^K \text{tr}(\mathbf{Q}_k) \leq P_{tot}, \\ & \mathbf{Q}_k \succeq 0, \quad \forall k = 1, \dots, K. \end{aligned} \quad (4.9)$$

In the following theorem, we show that this optimization problem can be solved by a single pair optimal transmit strategy in Chapter 3.

Theorem 4.3.1. *A solution of the optimization problem (4.9) is given by*

$$\mathcal{Q}^* = \{\mathbf{0}, \mathbf{0}, \dots, \mathbf{Q}_{\tilde{k}}^*, \dots, \mathbf{0}\},$$

where \tilde{k} is defined as

$$\tilde{k} = \arg \max_k \max_{\mathbf{Q}: \mathbf{Q} \succeq 0, \text{tr}(\mathbf{Q})=1} \gamma_k \sum_{i=1}^2 \gamma_{ki} \text{tr}(\mathbf{H}_{ki} \mathbf{Q} \mathbf{H}_{ki}^\dagger),$$

and

$$\mathbf{Q}_k^* = P_{tot} \arg \max_{\mathbf{Q}: \mathbf{Q} \succeq 0, \text{tr}(\mathbf{Q})=1} \sum_{i=1}^2 \gamma_{\tilde{k}i} \text{tr}(\mathbf{H}_{\tilde{k}i} \mathbf{Q} \mathbf{H}_{\tilde{k}i}^\dagger).$$

Proof. Let $\mathbf{Q}_k = P_k \mathbf{Q}_{k0}$ with \mathbf{Q}_{k0} is a normalized covariance matrix, i.e., $\text{tr}(\mathbf{Q}_{k0}) = 1$. Then the objective function of (4.9) becomes

$$f(\mathcal{Q}, \Gamma) = \sum_{k=1}^K P_k \mu_k(\mathbf{Q}_{k0})$$

where

$$\mu_k(\mathbf{Q}_{k0}) := \gamma_k \sum_{i=1}^2 \gamma_{ki} \text{tr}(\mathbf{H}_{ki} \mathbf{Q}_{k0} \mathbf{H}_{ki}^\dagger).$$

Suppose $\mathcal{Q}^* = \{\mathbf{Q}_1^*, \mathbf{Q}_2^*, \dots, \mathbf{Q}_K^*\}$ is the optimal transmit strategy and $\mathbf{Q}_k^* = P_k^* \mathbf{Q}_{k0}^*$. Without loss of generality we assume that the order $\mu_1^* \geq \mu_2^* \geq \dots \geq \mu_K^*$ where

$$\mu_k^* = \max_{\mathbf{Q}_{k0}} \mu_k(\mathbf{Q}_{k0}) = \mu_k(\mathbf{Q}_{k0}^*). \quad (4.10)$$

Then the result is proved by contradiction. Assuming that there exists a *strictly better* transmit strategy $\mathbf{Q}^* = \{P'_1 \mathbf{Q}_{10}^*, P'_2 \mathbf{Q}_{20}^*, \dots, P'_K \mathbf{Q}_{K0}^*\}$ with the power allocation ($P'_1 = (1 - \sum_{k=2}^K \varepsilon_k) P_{tot}$, $P'_2 = \varepsilon_2 P_{tot}$, $P'_3 = \varepsilon_3 P_{tot}$, \dots , $P'_K = \varepsilon_K P_{tot}$) and $(\varepsilon_2, \varepsilon_3, \dots, \varepsilon_K) \neq \mathbf{0}_{K-1}$. We have

$$\begin{aligned} f(\mathbf{Q}^*, \Gamma) &= \sum_{k=1}^K P'_k \mu_k^* \\ &= (1 - \sum_{k=2}^K \varepsilon_k) P_{tot} \mu_1^* + \sum_{k=2}^K \varepsilon_k \mu_k^* \\ &= P_{tot} \mu_1^* - \sum_{k=2}^K (\mu_1^* - \mu_k^*) \varepsilon_k \\ &\leq P_{tot} \mu_1^* = f(\mathbf{Q}^*, \Gamma) \end{aligned}$$

This contradicts with the assumption to be strictly better, i.e. “>”. Thus, $\mathbf{Q}^* = \{\mathbf{Q}_1^*, \mathbf{0}, \dots, \mathbf{0}\}$ with $P_1 = P_{tot}$ is the optimal transmit strategy. In general, $\mathbf{Q}^* = \{\mathbf{0}, \mathbf{0}, \dots, \mathbf{Q}_{\tilde{k}}^*, \dots, \mathbf{0}\}$ is the optimal transmit strategy with the desired user pair \tilde{k} is determined as follows

$$\begin{aligned} \tilde{k} &= \arg \max_k \mu_k^* \\ &= \arg \max_k \max_{\mathbf{Q}: \mathbf{Q} \succeq 0, \text{tr}(\mathbf{Q})=1} \gamma_k \sum_{i=1}^2 \gamma_{ki} \text{tr}(\mathbf{H}_{ki} \mathbf{Q} \mathbf{H}_{ki}^\dagger) \end{aligned}$$

and the corresponding optimal transmit covariance matrix is given by

$$\begin{aligned} \mathbf{Q}_{\tilde{k}}^* &= P_{tot} \mathbf{Q}_{k0}^* \\ &= P_{tot} \arg \max_{\mathbf{Q}: \mathbf{Q} \succeq 0, \text{tr}(\mathbf{Q})=1} \sum_{i=1}^2 \gamma_{\tilde{k}i} \text{tr}(\mathbf{H}_{\tilde{k}i} \mathbf{Q} \mathbf{H}_{\tilde{k}i}^\dagger). \end{aligned}$$

□

This implies that in the wideband regime, we can always maximize the weighted sum-rate by serving only a selected user-pair with full power. Each rate point at the intersection with the rates axis, i.e., $(0, \dots, 0, R_{\tilde{k}1}(\mathbf{Q}_{\tilde{k}}^*), R_{\tilde{k}2}(\mathbf{Q}_{\tilde{k}}^*), 0, \dots, 0)$, on the boundary of the achievable wideband rate region is optimal for a range of weighting factors for which we have $\mu_{\tilde{k}}^* = \max_k \mu_k^*$. We also note that when $\mu_k^* = \mu_t^*$ ($k \neq t$), either pair k or pair t is served or time-sharing between them, we achieve the same maximal wideband weighted sum-rate.

Next, we are looking more closely on the optimal transmit covariance matrix $\mathbf{Q}_{\tilde{k}}^*$ and how to choose the optimal serving pair \tilde{k} . To this end, we first find the optimal value $\mu_{\tilde{k}}^*$ and its corresponding \mathbf{Q}_{k0}^* in (4.10), which are resulted from the

following optimization problem

$$\begin{aligned} \max_{\mathbf{Q}_{k0}} \quad & \gamma_{k1} \text{tr}(\mathbf{H}_{k1} \mathbf{Q}_{k0} \mathbf{H}_{k1}^\dagger) + \gamma_{k2} \text{tr}(\mathbf{H}_{k2} \mathbf{Q}_{k0} \mathbf{H}_{k2}^\dagger) \\ \text{s.t.} \quad & \text{tr}(\mathbf{Q}_{k0}) = 1, \\ & \mathbf{Q}_{k0} \succeq 0. \end{aligned} \quad (4.11)$$

A closed-form solution of problem (4.11) can be derived as done for the single pair scenario considered in Section 3.3 of the previous chapter. It follows that, the optimal normalized transmit covariance matrix \mathbf{Q}_{k0}^* is given by

$$\mathbf{Q}_{k0}^* = \mathbf{w}_k \mathbf{w}_k^\dagger, \quad (4.12)$$

where \mathbf{w}_k denotes the eigenvector corresponding to the maximum eigenvalue of the Hermitian matrix $\mathcal{H}_k^\dagger \mathcal{H}_k$ with $\mathcal{H}_k := [\sqrt{\gamma_{k1}} \mathbf{H}_{k1}^T \quad \sqrt{\gamma_{k2}} \mathbf{H}_{k2}^T]^T \in \mathbb{C}^{(n_{k1}+n_{k2}) \times n_r}$ is the equivalent channel matrix for pair k . Since the normalized optimal transmit covariance matrix \mathbf{Q}_{k0}^* is of rank one, the optimal transmit strategy is a single beam along the principal eigenvector of the equivalent matrix $\mathcal{H}_k^\dagger \mathcal{H}_k$, which depends only on the channel coefficients and weighting factors of the served pair.

Moreover, the value of μ_k^* is simply given by

$$\mu_k^* = \gamma_k \lambda_{k,\max}(\Gamma),$$

where $\lambda_{k,\max}(\Gamma)$ is the maximal eigenvalue of the equivalent matrix $\mathcal{H}_k^\dagger \mathcal{H}_k$ given that the set of weighting factors Γ are chosen. Accordingly, the optimal serving pair \tilde{k} in Theorem 4.3.1 can be determined as

$$\tilde{k} = \arg \max_k \gamma_k \lambda_{k,\max}(\Gamma).$$

We can see that for a given set of weighting factors Γ , the optimal transmit strategy is quite straight-forward: We first define the maximum eigenvalue $\lambda_{k,\max}(\Gamma)$, $k = 1, \dots, K$ for all pairs, comparing all after weighting them with γ_k , $k = 1, \dots, K$ to determine the optimal serving pair \tilde{k} , then beaming along the principal eigenvector of the chosen pair.

Next, we consider the transmit strategies for some interesting optimal points, in which the set of weighting factors Γ has to be pre-determined to satisfy certain criterion related to the fairness issue.

4.4 Energy Efficiency and Fairness Issue

Similar to the single pair case, by setting the weighting factors properly, one can obtain different operating points on the boundary of the EpB region, corresponding to different priorities and fairness criteria. Moreover, in a multi-pair setup, the energy efficiency and fairness trade-off involves both the fairness issue among pairs (by setting γ_k) and among users of each pair (by setting $\gamma_{\tilde{k}i}$). In the following, we

consider the transmit strategies corresponding to some well-known operating points. Since the concept is similar to Chapter 3, in this chapter we only briefly provide the results including how to pre-determine the weighting factors and beaming technique for each case. More details on the intuitions and motivations can be found in the previous chapter.

4.4.1 Utility maximization

When sacrificing all the fairness within the system (among pairs as well as between users of each pair), the highest energy efficiency can be achieved by choosing $\gamma_k = 1/K$ and $\gamma_{ki} = 0.5, \forall k, i$. By doing this, the optimization problem (4.9) becomes equivalent to sum-rate maximization. The system EpB is then obtained as

$$\frac{E_{b,s}}{N_0} \min = \frac{\log_e 2}{\max_k(\lambda_{k,\max})}. \quad (4.13)$$

where $\lambda_{k,\max}$ is the maximal eigenvalue of the equivalent matrix $\mathcal{H}_k^\dagger \mathcal{H}_k$ of k -th pair when $\gamma_{k1} = \gamma_{k2}$. This is the minimum amount of required energy to reliably transmit one bit in total to all users regardless the realization of Γ , or one could say this is the *system minimum energy per bit*.

4.4.2 Single user optimization

In the single user optimality scenario, the highest priority for (k,i) -th user can be achieved by setting $\gamma_k = 1$ and $\gamma_{ki} = 1$. Accordingly, the optimal transmit strategy becomes beamforming along the principal eigenvector of the (k,i) -th user channel matrix \mathbf{H}_{ki} . The individual EpB is then achieved as

$$\frac{E_{b,ki}}{N_0} \min = \frac{\log_e 2}{\lambda_{ki,\max}}, \quad (4.14)$$

where $\lambda_{ki,\max}$ denotes the maximal eigenvalue of the single user matrix $\mathbf{H}_{ki}^\dagger \mathbf{H}_{ki}$. This is the minimum amount of required energy to reliably transmit one bit to the desired user regardless the realization of Γ , or one could say this is the *individual minimum energy per bit*.

4.4.3 Max-min fairness optimization

A reasonable fairness criterion is that all users operate at the same energy efficiency (or the same rate). This point corresponds to the max-min fairness point or egalitarian solution.

In order to achieve this operating point, we first need to achieve fairness among users of each pair. To this end, the weighting factors within pair $(\gamma_{k1}, \gamma_{k2})$ need to be set so that the normalized optimal covariance matrix \mathbf{Q}_{k0}^* leads to $\text{tr}(\mathbf{H}_{k1} \mathbf{Q}_{k0}^* \mathbf{H}_{k1}^\dagger) =$

$\text{tr}(\mathbf{H}_{k2}\mathbf{Q}_{k0}^*\mathbf{H}_{k2}^\dagger)$. This can be solved by one dimension grid search on γ_{ki} (or in closed-form as in Section 3.4 for MISO case).

Next, additional time-sharing between pairs can be used to achieve the same wideband rate for all users. In addition to using time-sharing, an alternative method to achieve fairness among pairs is to set the weighting factors between pair $(\gamma_1, \dots, \gamma_K)$ so that $\mu_1^* = \mu_2^* = \dots = \mu_K^*$ (in order to get a max-min fairness operating point, which is in the boundary of the EpB region), then setting the transmit power $P_k, k = 1, \dots, K$ such that $R_{ki}(\mathbf{Q}^*, \Gamma) = R_{ti}(\mathbf{Q}^*, \Gamma) (\forall k \neq t)$.

4.5 Optimality

As mentioned from Section 4.2, the proposed coding scheme is extended from the capacity achieving coding scheme for a single pair setup. It is not guaranteed that the proposed coding scheme is optimal for a multi-pair system. In this section, we analyze the optimality of the proposed scheme in the wideband regime. Unlike the single pair case, the capacity region of the multi-pair bidirectional broadcast channel is still unknown. The optimality of the proposed scheme will be investigated through the gap of the achievable wideband rate region \mathcal{R}_a and outer bounds for the wideband capacity.

4.5.1 The individual pair MEpB

Let us recall two important properties of the proposed coding scheme: i) It is based on the optimal coding strategy for the single pair set up and ii) It is optimal to transmit with full power to only one pair of users. Therefore, one can expect that the proposed scheme can achieve the *individual pair MEpB* (so the individual user MEpB), i.e., the corner points of the MEpB region (and the corner points of the wideband capacity region) can be reached.

In order to verify this, we first consider an outer bound for the wideband capacity region. Let us consider the cut around the relay and pair k . For any achievable wideband rate vector $\mathbf{R} = (R_{11}, R_{12}, \dots, R_{K2}) \in \mathbb{R}^{2K}$, the rate pair (R_{k1}, R_{k2}) has to be inside the individual pair capacity region \mathcal{C}_k , where \mathcal{C}_k is the capacity region for the single pair bidirectional broadcast channel, with the power constraints P_{tot} , i.e.,

$$\mathcal{C}_k = \bigcup_{\mathbf{Q}_k: \text{tr}(\mathbf{Q}_k) \leq P_{tot}} (R_{k1}^0(\mathbf{Q}_k), R_{k2}^0(\mathbf{Q}_k)),$$

where

$$R_{ki}^0(\mathbf{Q}_k) = \lim_{B \rightarrow \infty} B \log_2 |\mathbf{I}_{n_{ki}} + \mathbf{H}_{ki}\mathbf{Q}_k\mathbf{H}_{ki}^\dagger|, \quad i = 1, 2, \quad (4.15)$$

Therefore, \mathcal{C}_k is an outer bound for the wideband capacity of the multi-pair bidirectional broadcast channel.

Let us now consider an optimal point on the boundary of the achievable wideband rate region \mathcal{R}_a , which corresponds to the case where pair k is served with full power. From (4.3) and (4.15), we have $R_{ki}(\mathbf{Q}_k^*) = R_{ki}^0(\mathbf{Q}_k^*)$ where \mathbf{Q}_k^* is the optimal transmit covariance matrix corresponding to an optimal point on the boundary of \mathcal{R}_a and \mathcal{C}_k . In other words, the boundary of the achievable wideband rate region reaches the wideband capacity boundary at the optimal rate points $(0, \dots, 0, R_{k1}(\mathbf{Q}_k^*), R_{k2}(\mathbf{Q}_k^*), 0, \dots, 0)$. Thus, $(\frac{P_{tot}}{N_0 R_{k1}(\mathbf{Q}_k^*)}, \frac{P_{tot}}{N_0 R_{k2}(\mathbf{Q}_k^*)})$ is the MEpB of pair k . Moreover, the individual user MEpB can also be achieved by setting the weighting factors within pair k as $(\gamma_{k1} = 1, \gamma_{k2} = 0)$ or $(\gamma_{k1} = 0, \gamma_{k2} = 1)$.

4.5.2 A conjecture on the wideband capacity region

It is expected that the wideband capacity outer bound in (4.15) is loose in general since it is only restricted by the wideband rate constraints of a single pair. The Taylor expansion in (4.3) motivates us to think about a potential outer bound of the wideband capacity region, where the individual wideband rates are interference free, i.e.,

$$\mathcal{C}_{\text{conj}} = C_o \left(\bigcup_{\mathcal{Q}} \mathbf{R}^0(\mathcal{Q}) \right) \quad (4.16)$$

where $\mathbf{R}^0(\mathcal{Q}) = (R_{11}^0, R_{12}^0, \dots, R_{K1}^0, R_{K2}^0)$ is the rate vector with

$$R_{ki}^0 = \lim_{B \rightarrow \infty} B \log_2 \left| \mathbf{I} + \mathbf{H}_{ki} \mathbf{Q}_k \mathbf{H}_{ki}^\dagger \right|, i = 1, 2; k = 1, 2, \dots, K \quad (4.17)$$

for a set of positive semi-definite matrices $\mathcal{Q} = \{\mathbf{Q}_1, \mathbf{Q}_2, \dots, \mathbf{Q}_K\}$ which satisfy $\sum_{k=1}^K \text{tr}(\mathbf{Q}_k) \leq P_{tot}$.

If $\mathcal{C}_{\text{conj}}$ is really a capacity outer bound, by using the Taylor expansion on (4.17), we can see that the achievable wideband rate region \mathcal{R}_a coincides with the wideband capacity outer bound and is the wideband capacity region. Accordingly, the EpB vectors on the boundary of the achievable EpB region \mathcal{E}_a are the MEpB vectors of the Gaussian multi-pair MIMO bidirectional broadcast channel as the wideband capacity is sufficient to characterize the MEpB [HM10].

4.6 Chapter Conclusion

This chapter considered achievable wideband rates and EpBs of a Gaussian multi-pair MIMO bidirectional broadcast channel, which can be achieved by a simple coding strategy, motivated by the optimal coding scheme for a single pair setup in Chapter 3. It is interesting that the boundaries of the achievable wideband rate and EpB regions can be achieved by serving only one selected user-pair with full power. Although the capacity region (so the wideband capacity and MEpB regions) of the Gaussian multi-pair MIMO bidirectional broadcast channel is still unknown, it has

been shown that the proposed coding scheme can achieve the corner points in the boundaries of the wideband capacity and MEpB regions. Due to the independency of the approximated wideband rates on the inter-pair interference, we have the conjecture that the proposed coding scheme is optimal in sense of achieving the wideband capacity region.

4.7 Appendices

4.7.A Convexity of \mathcal{R}_a

Consider two rate vectors $\mathbf{R}(\mathcal{Q}^1), \mathbf{R}(\mathcal{Q}^2) \in \mathcal{R}_a$, with $\mathcal{Q}^1, \mathcal{Q}^2 \in \mathbb{M}$, where $\mathbf{R}(\mathcal{Q}^j) = [\mathbf{R}_{11}(\mathcal{Q}^j), \dots, \mathbf{R}_{K2}(\mathcal{Q}^j)]$, $j \in \{1, 2\}$ and

$$R_{ki}(\mathcal{Q}^j) = \frac{\log_2 e}{N_0} \text{tr}(\mathbf{H}_{ki} \mathbf{Q}_k^j \mathbf{H}_{ki}^\dagger), \quad i, j \in \{1, 2\}, k = 1, \dots, K.$$

Let $\mathbf{R}(t) = [\mathbf{R}_{11}(t), \dots, \mathbf{R}_{K2}(t)]$. We will show that the rate vector $\mathbf{R}(t) = t\mathbf{R}(\mathcal{Q}^1) + (1-t)\mathbf{R}(\mathcal{Q}^2) \in \mathcal{R}_a$ for all $t \in [0, 1]$. We have

$$\begin{aligned} R_{ki}(t) &= tR_{ki}(\mathcal{Q}^1) + (1-t)R_{ki}(\mathcal{Q}^2) \\ &= t \frac{\log_2 e}{N_0} \text{tr}(\mathbf{H}_{ki} \mathbf{Q}_k^1 \mathbf{H}_{ki}^\dagger) + (1-t) \frac{\log_2 e}{N_0} \text{tr}(\mathbf{H}_{ki} \mathbf{Q}_k^2 \mathbf{H}_{ki}^\dagger) \\ &= \frac{\log_2 e}{N_0} \text{tr}(\mathbf{H}_{ki} (t\mathbf{Q}_k^1 + (1-t)\mathbf{Q}_k^2) \mathbf{H}_{ki}^\dagger) \\ &= \frac{\log_2 e}{N_0} \text{tr}(\mathbf{H}_{ki} \mathbf{Q}_k^t \mathbf{H}_{ki}^\dagger), \end{aligned}$$

where $\mathbf{Q}_k^t = t\mathbf{Q}_k^1 + (1-t)\mathbf{Q}_k^2$. Let $\mathcal{Q}^t = \{\mathbf{Q}_1^t, \dots, \mathbf{Q}_K^t\}$. Since $\mathbf{Q}_k^j \succeq 0$, $j \in \{1, 2\}$, $k = 1, \dots, K$, we have $\mathbf{Q}_k^t \succeq 0$, $k=1, \dots, K$. Moreover,

$$\begin{aligned} \sum_{k=1}^K \text{tr}(\mathbf{Q}_k^t) &= t \sum_{k=1}^K \text{tr}(\mathbf{Q}_k^1) + (1-t) \sum_{k=1}^K \text{tr}(\mathbf{Q}_k^2) \\ &\leq tP_{tot} + (1-t)P_{tot} = P_{tot}. \end{aligned}$$

Thus, we can rewrite $\mathbf{R}(t)$ as $\mathbf{R}(t) = \mathbf{R}(\mathcal{Q}^t) = [\mathbf{R}_{11}(\mathcal{Q}^t), \dots, \mathbf{R}_{K2}(\mathcal{Q}^t)]$ with $\mathcal{Q}^t \in \mathbb{M}$. This shows that $\mathbf{R}(t) \in \mathcal{R}_a$ for all $t \in [0, 1]$. Therefore, \mathcal{R}_a is convex.

Uplink WCDMA Channel with Perfect CSIR

In the first part of the thesis, we have focused on the energy efficiency aspect of the Gaussian MIMO bidirectional broadcast channel. We have investigated the minimum energy per bit, which describes the required energy per information bit for reliable communication when the spectral efficiency is disregarded, i.e., the available bandwidth is infinite. In the second part of this thesis, we will focus on the spectral efficiency aspect of another kind of wireless wideband network, where the system setup is relevant for practical cellular networks in which the available bandwidth is large but still finite. In particular, we analyze the spectral efficiency, i.e., capacity¹ limit of an uplink wideband CDMA channel.

In this chapter, we begin the second part of the thesis by considering an uplink WCDMA channel with the assumption of perfect CSI at the receiver. Various realistic assumptions are incorporated into the system model, which make the framework and results valuable for the performance assessment of real cellular networks such as: continuous-time waveform transmitted signal, time-variant spreading sequences, asynchronous transmission, multi-code CDMA system with inter-symbol interference (ISI) over frequency-selective channels. In order to make the analysis more convenient, an equivalent discrete-time channel model is derived based on sufficient statistics for optimal decoding of the transmitted messages. Capacity regions are then characterized using the equivalent channel. Unlike most previous research on channel capacity, we focus on the capacity with finite constellation inputs and use the capacity for Gaussian distributed input as a benchmark for comparison. The capacity with finite sampling is provided to exemplify performance loss due to specific post-processing at the receiver. An approximation algorithm is also proposed to evaluate the capacity when dimensions of the system are large. Moreover, we analyze the asymptotic capacity when the signal-to-noise ratio goes to infinity. The conditions to simultaneously achieve the asymptotic individual capacities are de-

¹In order to be consistent with the literature on multi-user networks, we will use the metrics “capacity” and “capacity region” instead of “spectral efficiency” and “spectral efficiency region”. One can easily convert the capacity to spectral efficiency by normalizing the capacity unit in bits/s/Hz.

rived, which reveal the impact of the signature waveform space, channel frequency selectivity and signal constellation on the asymptotic performance.

5.1 Related Works and Motivation

In the literature, the fundamental limits of multi-user CDMA systems have been mostly studied under the assumptions of synchronous, time-invariant (each user uses the same spreading sequence for all data symbols), and/or random spreading sequences [RM94, VA99, MM12, VS99, TH99, PZSY13]. In [RM94, VA99, MM12], the optimal spreading sequences and capacity limits for synchronous CDMA have been studied with a discrete-time signal model. A more theoretical approach on CDMA capacity analysis has been pursued in [VS99, TH99, PZSY13] by modeling the spreading sequences with random sequences. However the assumption of perfect synchronization between users is not realistic, especially for a cellular CDMA uplink. Moreover, in practice, time-variant spreading sequences with Gold or Kasami codes [DBK⁺98, 3GPTm, HT04] are often used rather than time-invariant or random spreading sequences.

The capacity limit of a CDMA system with symbol-asynchronous transmission (the symbol epochs of the signal are not aligned at the receiver) has also been studied in [Ver89, UY04, LUE05, CMD10]. In [Ver89], Verdú studied the capacity region of an uplink time-invariant CDMA system with ISI by exploiting the asymptotic properties of Toeplitz matrices. In [UY04, LUE05], the authors studied user and sum capacities of a symbol-asynchronous CDMA system but with chip-synchronous transmission (the timing of the chip epochs are aligned) assumption, which made the analysis tractable using a discrete-time model. In [CMD10], the spectral efficiency of an asynchronous CDMA system has been considered while neglecting the ISI by assuming a large spreading factor.

There have been several studies trying to deal with continuous-time asynchronous CDMA systems. However, most of them focus on other performance metrics than capacity (e.g., error probability considering different detection algorithms) [WP99, YYU02, LGW04, FCC⁺09, CDL09]; time-invariant CDMA [YC10] or asynchronous CDMA but with an ISI-free assumption [AH13]. The capacity analysis for a practical CDMA cellular network with continuous-time waveform transmitted signal, time-variant spreading sequences, asynchronous transmission is complicate due to the following reasons: First, an equivalent discrete-time signal model is difficult to arrive at due to the asynchronization between symbols and chips. Next, for a time-variant spreading CDMA system, the approach based on the asymptotic properties of Toeplitz forms [Gra72], which is crucial for the capacity analysis of ISI channels [Ver89, HM88], cannot be employed since the varying of spreading sequence destroys the Toeplitz structure of the equivalent channel matrix.

Motivated by the fact that most existing research on multi-user CDMA capacity has focused on theoretical analysis with simplified system assumptions, in this chapter, we analyze the capacity limit of a WCDMA system with more realistic

assumptions, which make the results more valuable for the performance assessment of the practical cellular networks. In more detail, we consider a continuous-time waveform transmitted signal, time-variant, asynchronous, multi-code CDMA system with ISI over frequency-selective channels. We first derive sufficient statistics for decoding the transmitted symbols based on the continuous-time received signal, which provides us a discrete-time signal model. The capacity can then be analyzed using the discrete-time model since sufficient statistics preserve the mutual information [CT06, Chap. 2]. Next, we numerically characterize the capacity region when the input signal is given by finite constellations, e.g., BPSK, QAM, and so on with a uniform input distribution, which are widely used in current real cellular networks. Additionally, we provide the capacity region when the input signal follows a Gaussian distribution, which is the optimal input distribution for additive Gaussian noise channels. Accordingly, the Gaussian capacity offers a capacity outer bound for the real WCDMA cellular networks using finite constellation inputs.

Due to the data processing inequality [CT06, Chap. 2], the mutual information between input and output does not increase through post-processing at the receiver. Given the capacity bounds measured directly at the receive antenna of a real system, we can now assess the capacity performance loss due to a specific post-processing at the receiver. Here, we continue to investigate the capacity performance loss due to sampling, which is a traditional discretization approach in practical systems. The sampled capacity is derived considering sampling at the receiver after passing through an ideal low pass filter (LPF) with a finite bandwidth. Note that in the real cellular networks, since the sampling window is often finite, perfect reconstruction of a band-limited signal is not guaranteed even if the sampling rate is equal to Nyquist rate [Lap09, Chap. 8]. Such impact on the capacity is also investigated in this work.

In general, the capacity region of a channel with finite constellation input is numerically computed via Monte Carlo simulation because a closed-form expression does not exist. However, the computations are related to distributions of Gaussian mixture random vectors, whose number of components increases exponentially with the dimensions of the system. This makes the capacity evaluations for large systems intractable due to prohibitive computational complexity. In order to tackle this problem, we propose an effective approximation algorithm based on sphere decoding to find the approximate capacity for large MIMO system with finite constellation input.

Moreover, we analyze the asymptotic sum-capacity when the SNR goes to infinity, for which we derive the conditions on the signature waveforms so that on every link to the base station, the individual capacity is achieved simultaneously. To this end, we first derive a *sufficient condition*, which holds for all kinds of input signals including signals based on finite and infinite constellations. Next, once again, we motivate our study from a practical perspective by focusing on finite constellation input signals. Accordingly, a *necessary condition* to simultaneously achieve the individual capacities with finite constellation input signal, which takes the signal constellation structure into account, is derived. Those results are particularly useful

for spreading sequence design in real WCDMA cellular networks.

The rest of the chapter is organized as follows. Section 5.2 presents the signal model where sufficient statistics and an equivalent matrix representation are derived. In Section 5.3, the capacity analysis is provided considering finite constellation and Gaussian distributed input signals. The approximate algorithm to evaluate the capacity is presented in Section 5.4. Numerical results are given in Section 5.5. Section 5.6 analyzes the asymptotic capacity when SNR tends to infinity. Finally, Section 5.7 concludes the chapter.

5.2 Problem Setup

Since the PHY defines the fundamental capacity limit of the uplink WCDMA channel [HT04], we focus on a signal model reflecting the operations of the uplink WCDMA PHY based on the 3GPP release 11 specification [3GPPtm].

Specifically, let us consider a K -user multi-code WCDMA system with M codes for each I/Q branch and spreading factor N_{sf} . Then, the transmitted signal for user k can be expressed as

$$x_k(t) = \sqrt{E_k} \sum_{i=1}^N \sum_{m=1}^M d_{ki}^m s_{ki}^m(t), k = 1, \dots, K, \quad (5.1)$$

where N denotes the number of transmitted symbols from each user, E_k is the transmit power of user k , d_{ki}^m is the i -th symbol of the m -th stream of user k , $\mathbb{E}\{|d_{ki}^m|^2\} = 1$, and

$$s_{ki}^m(t) = \frac{1}{\sqrt{N_{\text{sf}}}} \sum_{n=0}^{N_{\text{sf}}-1} c_{ki}^m[n] p(t - (i-1)T_s - nT_c)$$

is the *signature waveform* assigned to d_{ki}^m , where $p(t)$ is the *chip waveform* with unit power and finite bandwidth B ,² T_s and T_c are the symbol and chip durations, respectively, and $c_{ki}^m[n]$ denotes the spreading sequence which satisfies $\sum_{n=0}^{N_{\text{sf}}-1} |c_{ki}^m[n]|^2 = N_{\text{sf}}$. In a CDMA system with time-variant spreading sequences, each user uses a different spreading sequence $\{c_{ki}^m[n]\}_n$ for each transmitted symbol d_{ki}^m . This corresponds to a practical cellular CDMA network with long scrambling codes, in which the effective spreading sequence varies between symbols.

In this part, we assume a tapped-delay line channel model³ with L multi-paths

²In theory, a band-limited signal requires infinite time to transmit. However, in practical WCDMA systems, chip waveforms with fast decaying sidelobes (e.g., root raised cosine (RRC) and squared-root raised cosine (SRRC) pulses) are used and truncated by the length of several chip intervals.

³It is worth noting that even though the channel impulse response is assumed to be time-invariant as similar to [Ver89, HM88], the Toeplitz structure of the equivalent channel matrix is not maintained because of the variation of the spreading sequences over symbols in a time-variant CDMA system.

[Ver98, Chap. 2] as follow

$$h_k(t) = \sum_{l=1}^L g_{kl} \delta(t - \tau_{kl}), k = 1, \dots, K,$$

where g_{kl} and τ_{kl} denote the channel coefficient and the propagation delay for the l -th path of the channel for user k , respectively. Then the received signal is given by

$$\begin{aligned} r(t) &= \sum_{k=1}^K h_k(t) * x_k(t - \lambda_k) + n(t) \\ &= \sum_{k=1}^K \sum_{i=1}^N \sum_{m=1}^M \sqrt{E_k} d_{ki}^m \sum_{l=1}^L g_{kl} s_{ki}^m(t - \lambda_k - \tau_{kl}) + n(t), \end{aligned} \quad (5.2)$$

where λ_k denotes the time delay of the transmitted signal from user k , the symbol $*$ denotes the convolution operation, and $n(t)$ represents the additive white Gaussian noise with a two-sided power spectral density (psd) $N_0/2 = \sigma^2$.

5.2.1 Sufficient Statistic

Since a sufficient statistic for decoding the transmitted messages preserves the capacity of the system, the capacity of a continuous-time channel can be computed using a sufficient statistic [CT06, Chap. 2], [Gal68, Chap. 8]. To this end, let us define the transmitted symbol vectors $\mathbf{d}_{ki} := [d_{ki}^1, \dots, d_{ki}^M]^T \in \mathbb{C}^{M \times 1}$ (for each stream), $\mathbf{d}_k := [\mathbf{d}_{k1}^T, \dots, \mathbf{d}_{kN}^T]^T \in \mathbb{C}^{NM \times 1}$ (for each user), and $\mathbf{d} := [\mathbf{d}_1^T, \dots, \mathbf{d}_K^T]^T \in \mathbb{C}^{KNM \times 1}$ (for all users), where $(\cdot)^T$ denotes the transpose operation. Further, let us define $\mu(t; \mathbf{d})$ as the received signal without noise, i.e.,

$$\mu(t; \mathbf{d}) := \sum_{k=1}^K \sum_{i=1}^N \sum_{m=1}^M \sqrt{E_k} d_{ki}^m \sum_{l=1}^L g_{kl} s_{ki}^m(t - \lambda_k - \tau_{kl}).$$

The problem of optimal decoding of \mathbf{d} is similar to the detection problem in [Ver98, Proposition 3.2] (see [LGW04] for a similar approach based on the Cameron-Martin formula [Poo94, Chap. VI]). Accordingly, the optimal decision⁴ can be made using the following decision variables

$$\Phi(\mathbf{d}) = 2\Re \left\{ \int_{-\infty}^{\infty} \mu(t; \mathbf{d})^* r(t) dt \right\} - \int_{-\infty}^{\infty} [\mu(t; \mathbf{d})]^2 dt, \quad (5.3)$$

⁴In [Ver98, Proposition 3.2], the hypotheses are equiprobable and the optimal decision is based on maximum of $\Phi(\mathbf{d})$ (ML criterion). In general, the optimal decision is based on MAP criterion, which includes $\log(p(\mathbf{d}))$ into $\mu(t; \mathbf{d})$. However, this additional term is independent of $r(t)$. Therefore, we do not have to include it in the sufficient statistic.

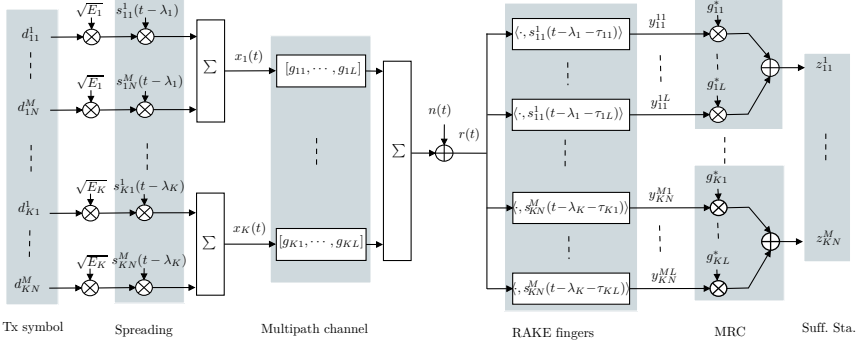


Figure 5.1: Diagram of the implementation to obtain the sufficient statistic from the continuous-time received signal of a K -user uplink WCDMA system with M codes for each I/Q branch over a L -tap frequency-selective channel.

where $\Re\{\cdot\}$ denotes the real part of a complex value and $(\cdot)^*$ denotes the complex conjugate operation. Since the second term of (5.3) does not depend on the received signal $r(t)$, we can drop it. Therewith, the sufficient statistic is based on the first term of (5.3), which can be rewritten as

$$2\Re \left\{ \sum_{k=1}^K \sum_{i=1}^N \sum_{m=1}^M \sqrt{E_k} d_{ki}^{m*} \sum_{l=1}^L g_{kl}^* \int_{-\infty}^{\infty} r(t) s_{ki}^m(t - \lambda_k - \tau_{kl})^* dt \right\}.$$

Let us denote $y_{ki}^{ml} := \int_{-\infty}^{\infty} r(t) s_{ki}^m(t - \lambda_k - \tau_{kl})^* dt$ and $z_{ki}^m := \sum_{l=1}^L g_{kl}^* y_{ki}^{ml}$, then $\{z_{ki}^m\}_{k,i,m}$ is a sufficient statistic for decoding \mathbf{d} based on $r(t)$. It is shown that the received signal passing through a bank of matched filters, where the received signal is matched to the delayed versions of the signature waveforms, results in a sufficient statistic for decoding \mathbf{d} based on $r(t)$. Figure 5.1 illustrates an implementation to obtain the sufficient statistic from the continuous-time received signal. This has a RAKE receiver structure [Pro95, Chap. 14], including RAKE matched fingers following by maximal ratio combining (MRC).

Let $\rho_{(kiml)}^{(k'i'm'l')}$ be the cross-correlation function between the signature waveforms defined as

$$\begin{aligned} \rho_{(kiml)}^{(k'i'm'l')} &= \int_{-\infty}^{\infty} s_{ki}^m(t - \lambda_k - \tau_{kl})^* s_{k'i'}^{m'}(t - \lambda_{k'} - \tau_{k'l'}) dt \\ &= \frac{1}{N_{\text{sf}}} \sum_{n=0}^{N_{\text{sf}}-1} \sum_{n'=0}^{N_{\text{sf}}-1} c_{ki}^m[n]^* c_{k'i'}^{m'}[n'] R_p \left(\frac{n-n'}{N_{\text{sf}}} T_s + (i-i') T_s \right. \\ &\quad \left. + (\tau_{kl} - \tau_{k'l'}) + (\lambda_k - \lambda_{k'}) \right), \end{aligned} \quad (5.4)$$

where $R_p(\tau) = \int_{-\infty}^{\infty} p(t)^* p(t + \tau) dt$ is the autocorrelation function of the chip

waveform. Then the sufficient statistics can be expressed as

$$z_{ki}^m = \sum_{l=1}^L \sum_{k'=1}^K \sum_{i'=1}^N \sum_{m'=1}^M \sum_{l'=1}^L \sqrt{E_{k'}} d_{k'i'}^{m'} g_{kl}^* g_{k'l'} \rho_{(kiml)}^{(k'i'm'l')} + n_{ki}^m, \forall k, m, i, \quad (5.5)$$

where $n_{ki}^m := \sum_{l=1}^L g_{kl}^* \int_{-\infty}^{\infty} n(t) s_{ki}^m(t - \lambda_k - \tau_{kl})^* dt$ is the equivalent noise term associated with z_{ki}^m after matched filtering.

5.2.2 Matrix Representation of the Sufficient Statistic

A matrix canonical form is useful to characterize the capacity based on a sufficient statistic. Hence, in this subsection we express the sufficient statistics $\{z_{ki}^m\}_{k,i,m}$ derived in (5.5) as an equivalent matrix equation.

First of all, let \mathbf{g}_k denote the multi-path fading coefficients for user k , $\mathbf{g}_k = [g_{k1}, g_{k2}, \dots, g_{kL}]^T \in \mathbb{C}^{L \times 1}$, $k = 1, \dots, K$. Then the equivalent channel gain matrix for user k with M codes in each I/Q branch can be written as

$$\bar{\mathbf{G}}_k = \text{blkdiag}(\underbrace{\mathbf{g}_k, \dots, \mathbf{g}_k}_{M \text{ vectors}}) \in \mathbb{C}^{ML \times M},$$

where $\text{blkdiag}(\cdot)$ denotes the block diagonal matrix operation, i.e., $\bar{\mathbf{G}}_k$ is a $ML \times M$ block matrix with M vectors \mathbf{g}_k in the diagonal. Therewith, the (cross-)channel matrix corresponding to the i' -th symbols of user k' at the transmitter and the matched filters for i -th symbols of user k at the receiver can be expressed as

$$\mathbf{H}_{ki}^{k'i'} = \bar{\mathbf{G}}_k^\dagger \mathbf{R}_{ki}^{k'i'} \bar{\mathbf{G}}_{k'} \in \mathbb{C}^{M \times M}, \quad (5.6)$$

where $(\cdot)^\dagger$ denotes the Hermitian transpose and $\mathbf{R}_{ki}^{k'i'}$ is the $ML \times ML$ correlation matrix of the signature waveforms for the i -th symbols of user k and the i' -th symbols of user k' , i.e.,

$$\mathbf{R}_{ki}^{k'i'} = \begin{bmatrix} \rho_{(ki11)}^{(k'i'11)} & \cdots & \rho_{(ki11)}^{(k'i'1L)} & \cdots & \rho_{(ki11)}^{(k'i'ML)} \\ \vdots & \vdots & \vdots & \vdots & \vdots \\ \rho_{(kiML)}^{(k'i'11)} & \cdots & \rho_{(kiML)}^{(k'i'1L)} & \cdots & \rho_{(kiML)}^{(k'i'ML)} \end{bmatrix} \in \mathbb{C}^{ML \times ML}.$$

Then we obtain the equivalent received signal corresponding to the matched filters for the i -th symbols of user k as follows

$$\mathbf{z}_{ki} = \sum_{i'=1}^N (\sqrt{E_k} \mathbf{H}_{ki}^{k'i'} \mathbf{d}_{k'i'} + \sum_{k' \in \mathcal{S} \setminus \{k\}} \sqrt{E_{k'}} \mathbf{H}_{ki}^{k'i'} \mathbf{d}_{k'i'}) + \mathbf{n}_{ki},$$

where $\mathbf{z}_{ki} = [z_{ki}^1 \cdots z_{ki}^M]^T \in \mathbb{C}^{M \times 1}$ and $\mathbf{n}_{ki} = [n_{ki}^1 \cdots n_{ki}^M]^T \in \mathbb{C}^{M \times 1}$.

Moreover, let us define the equivalent (cross-)channel matrix corresponding to user k' at the transmitter and the matched filters for user k at the receiver as

$$\mathbf{H}_k^{k'} = \begin{bmatrix} \mathbf{H}_{k1}^{k'1} & \mathbf{H}_{k1}^{k'2} & \cdots & \mathbf{H}_{k1}^{k'N} \\ \vdots & \vdots & \vdots & \vdots \\ \mathbf{H}_{kN}^{k'1} & \mathbf{H}_{kN}^{k'2} & \cdots & \mathbf{H}_{kN}^{k'N} \end{bmatrix} \in \mathbb{C}^{NM \times NM}. \quad (5.7)$$

Then the received signal corresponding to the matched filters for user k can be expressed by

$$\mathbf{z}_k = \sqrt{E_k} \mathbf{H}_k^k \mathbf{d}_k + \sum_{k' \in \mathcal{S} \setminus \{k\}} \sqrt{E_{k'}} \mathbf{H}_k^{k'} \mathbf{d}_{k'} + \mathbf{n}_k, \quad (5.8)$$

where $\mathbf{z}_k = [\mathbf{z}_{k1}^T, \dots, \mathbf{z}_{kN}^T]^T$ and $\mathbf{n}_k = [\mathbf{n}_{k1}^T, \dots, \mathbf{n}_{kN}^T]^T$. Next, we stack all the (cross-)channel matrices $\mathbf{H}_k^{k'}$, $k' = 1, \dots, K$, to obtain the equivalent channel matrix corresponding to user k as

$$\mathbf{H}_k = [\mathbf{H}_1^k{}^T, \mathbf{H}_2^k{}^T, \dots, \mathbf{H}_K^k{}^T]^T \in \mathbb{C}^{KNM \times NM}.$$

Finally, let us define $\mathbf{z} = [\mathbf{z}_1^T, \dots, \mathbf{z}_K^T]^T \in \mathbb{C}^{KNM \times 1}$ and $\mathbf{n} = [\mathbf{n}_1^T, \dots, \mathbf{n}_K^T]^T \in \mathbb{C}^{KNM \times 1}$. Then the sufficient statistics can be expressed in a matrix equation as follows

$$\mathbf{z} = \sum_{k=1}^K \sqrt{E_k} \mathbf{H}_k \mathbf{d}_k + \mathbf{n}. \quad (5.9)$$

This description corresponds to a traditional discrete-time vector-valued MAC. Moreover, it is shown in Appendix 5.8.A that the equivalent noise vector \mathbf{n} is a complex Gaussian random vector with zero mean and covariance matrix $\sigma^2 \mathbf{H}$ with $\mathbf{H} = [\mathbf{H}_1, \dots, \mathbf{H}_K] \in \mathbb{C}^{KNM \times KNM}$.

5.3 Capacity Characterization

In this section, we analyze the capacity of the continuous-time uplink WCDMA channel in (5.2). Recall that \mathbf{z} is the sufficient statistic for optimal (i.e., capacity preserving) decoding \mathbf{d} based on $r(t)$. Any coding scheme which achieves the capacity of the channel with input \mathbf{d} and output $r(t)$ can also be employed to the channel with input \mathbf{d} and output \mathbf{z} by performing the optimal decoding based on \mathbf{z} instead of $r(t)$. Therefore, the channel capacity is preserved when the continuous-time output $r(t)$ is replaced by the sufficient statistic \mathbf{z} . Thus, we can focus on the capacity of the equivalent discrete-time channel in (5.9), which is given by the capacity of a discrete memoryless MAC [Ahl71].

Let us define R_1, R_2, \dots, R_K as the maximum number of bits that can be reliably transmitted from user 1, user 2, ..., user K per block of N symbols. The capacity

region of the uplink WCDMA channel is then characterized by the closure of the convex hull of the union of all achievable rate vectors (R_1, R_2, \dots, R_K) satisfying [Ahl71], [CT06, Chapter 15]

$$\sum_{k \in \mathcal{J}} R_k \leq I(\mathbf{d}_{\mathcal{J}}; \mathbf{z} | \mathbf{d}_{\mathcal{J}^c}), \quad (5.10)$$

for all index subsets $\mathcal{J} \subseteq \{1, \dots, K\}$ and some joint pmf $p(\mathbf{d}) = \prod_{k=1}^K p(\mathbf{d}_k)$, where \mathcal{J}^c denotes the complement of \mathcal{J} and $\mathbf{d}_{\mathcal{J}} = \{\mathbf{d}_k : k \in \mathcal{J}\}$.

We now characterize the uplink WCDMA capacity region considering two specific input signals: finite constellation with uniformly distributed input and Gaussian distributed input.

Remark 5.1.

- The capacity in (5.10) is defined for a given channel impulse response and the assumption that a message is coded over sufficiently many blocks of N symbols using the same spreading sequences for all blocks while neglecting the effect of inter-block interference.
- The quantities in the right-hand sides of (5.10) describe the number of bits that can be reliably transmitted per block of N symbols. One can express the capacity in bits/s by normalizing with $1/T$, $T = NT_s$, or in bits/s/Hz by normalizing with $1/TB$.

5.3.1 Finite Constellation Input

When the input signal vector \mathbf{d}_k at each user is independently taken from a finite constellation set \mathcal{M}^{NM} , $|\mathcal{M}| = M_c$, with equal probability, i.e., $p(\mathbf{d}_k) = \frac{1}{M_c^{NM}}$, $\forall k \in \{1, \dots, K\}$, then the rate constraints in (5.10) can be rewritten as

$$\begin{aligned} \sum_{k \in \mathcal{J}} R_k &\leq I(\mathbf{d}_{\mathcal{J}}; \mathbf{z} | \mathbf{d}_{\mathcal{J}^c}) \\ &= h(\mathbf{z} | \mathbf{d}_{\mathcal{J}^c}) - h(\mathbf{z} | \mathbf{d}_{\mathcal{J}} \mathbf{d}_{\mathcal{J}^c}) = h(\mathbf{z}_{\mathcal{J}}) - h(\mathbf{n}) \\ &= -\mathbb{E} \{\log_2(f(\mathbf{z}_{\mathcal{J}}))\} - \log_2(\det(\pi e \sigma^2 \mathbf{H})) \end{aligned} \quad (5.11)$$

for all $\mathcal{J} \subseteq \{1, \dots, K\}$ with $\mathbf{z}_{\mathcal{J}} := \sum_{k \in \mathcal{J}} \sqrt{E_k} \mathbf{H}_k \mathbf{d}_k + \mathbf{n}$. $\mathbf{z}_{\mathcal{J}}$ is a Gaussian mixture random vector with pdf

$$f(\mathbf{z}_{\mathcal{J}}) = \sum_{\mathbf{d}_{\mathcal{J}}^{(i)} \in \mathcal{M}^{|\mathcal{J}|NM}} p(\mathbf{d}_{\mathcal{J}} = \mathbf{d}_{\mathcal{J}}^{(i)}) \cdot f(\mathbf{z}_{\mathcal{J}} | \mathbf{d}_{\mathcal{J}} = \mathbf{d}_{\mathcal{J}}^{(i)}), \quad (5.12)$$

where $p(\mathbf{d}_{\mathcal{J}} = \mathbf{d}_{\mathcal{J}}^{(i)}) = \frac{1}{M_c^{|\mathcal{J}|NM}}$ and $f(\mathbf{z}_{\mathcal{J}} | \mathbf{d}_{\mathcal{J}} = \mathbf{d}_{\mathcal{J}}^{(i)})$ is the conditional pdf of $\mathbf{z}_{\mathcal{J}}$ given $\mathbf{d}_{\mathcal{J}}$. Let us denote $\mathbf{E}_{\mathcal{J}} \mathbf{H}_{\mathcal{J}} \mathbf{d}_{\mathcal{J}} := \sum_{k \in \mathcal{J}} \sqrt{E_k} \mathbf{H}_k \mathbf{d}_k$, where $\mathbf{E}_{\mathcal{J}}$ is the power

allocation matrix $\mathbf{E}_{\mathcal{J}} := \text{blkdiag}(\{\sqrt{E_k}\mathbf{I}_{NM}\}_{k \in \mathcal{J}})$ and $\mathbf{H}_{\mathcal{J}}$ is the sub-matrix of \mathbf{H} after removing $\mathbf{H}_{k'}, \forall k' \in \mathcal{J}^c$. Then $f(\mathbf{z}_{\mathcal{J}}|\mathbf{d}_{\mathcal{J}} = \mathbf{d}_{\mathcal{J}}^{(i)})$ is the pdf of a complex Gaussian random vector with mean $\mathbf{E}_{\mathcal{J}}\mathbf{H}_{\mathcal{J}}\mathbf{d}_{\mathcal{J}}^{(i)}$ and covariance matrix $\sigma^2\mathbf{H}$, i.e.,

$$f(\mathbf{z}_{\mathcal{J}}|\mathbf{d}_{\mathcal{J}} = \mathbf{d}_{\mathcal{J}}^{(i)}) = \frac{\exp\left(-\left(\mathbf{z}_{\mathcal{J}} - \mathbf{E}_{\mathcal{J}}\mathbf{H}_{\mathcal{J}}\mathbf{d}_{\mathcal{J}}^{(i)}\right)^\dagger (\sigma^2\mathbf{H})^{-1} \left(\mathbf{z}_{\mathcal{J}} - \mathbf{E}_{\mathcal{J}}\mathbf{H}_{\mathcal{J}}\mathbf{d}_{\mathcal{J}}^{(i)}\right)\right)}{\pi^{KNM} \cdot \det(\sigma^2\mathbf{H})}.$$

Typically, the capacity region of a channel with finite constellation input is numerically characterized via Monte Carlo simulation because a closed-form expression does not exist. It is worth noting that in order to calculate the first term of (5.11), one has to average over all possible $M_c^{|\mathcal{J}|NM}$ input symbols (up to M_c^{KNM} for sum-rate) according to (5.12). However, when M_c and/or N are too large, this task becomes intractable due to computational complexity. In MIMO channels with finite constellation input, a similar problem occurs when the input alphabet set or the number of antennas is too large, e.g., 64-QAM or 8×8 MIMO [HtB03]. In order to tackle this problem, we propose an effective approximation algorithm based on sphere decoding approach to find the approximate capacity for large MIMO system with finite constellation input. We use it in the numerical results section (Section 5.5) to compute approximations on the capacity curves for large N . The specific details about the algorithm will be presented in Section 5.4.

5.3.2 Gaussian Input

If the input signal vector \mathbf{d}_k of each user follows a zero mean complex Gaussian distribution with unit input power constraint, i.e., $\mathbf{d}_k \sim \mathcal{CN}(\mathbf{0}, \mathbf{I}_{NM}), \forall k = 1, \dots, K$, then the capacity region is characterized by the rate vectors (R_1, R_2, \dots, R_K) satisfying

$$\sum_{k \in \mathcal{J}} R_k \leq \log \det \left(\mathbf{I}_{NM} + \sum_{k \in \mathcal{J}} \frac{E_k}{\sigma^2} \mathbf{H}_k^\dagger \mathbf{H}^{-1} \mathbf{H}_k \right) \quad (5.13)$$

for all $\mathcal{J} \subseteq \{1, \dots, K\}$. Since the Gaussian distributed input is the optimal input for a given mean power constraint, the capacity region defined in (5.13) serves as an outer bound for the capacity region with a practically motivated input, i.e., finite constellation input as discussed in Section 5.3.1.

5.3.3 Capacity with Sampling

Since the matched filtering at the receiver yields a sufficient statistic, the uplink WCDMA capacity achieved by any other receiver structures is upper bounded by the capacity achieved by the sufficient statistic using matched filtering. Regarding the capacity regions in Sections 5.3.1 and 5.3.2 as benchmarks for the performance assessment, we now analyze the uplink WCDMA capacity achieved by sampling

to evaluate the capacity performance loss due to specific post-processing at the receiver.

For sampling at the receiver, we assume that out-of-band noise is first suppressed by an ideal LPF with bandwidth B , which has the same bandwidth as the transmitted signal. Then the received signals are uniformly sampled at every time instance t_n , $n = 1, \dots, N_{\text{sp}}$, where N_{sp} is finite. As a result, the sampled received signal at time t_n is given by

$$r_n := r_{\text{lp}}(t_n) = \sum_{k=1}^K \sum_{m=1}^M \sum_{i=1}^N d_{ki}^m \sum_{l=1}^L g_{kl} s_{\text{lp},ki}^m(t_n - \lambda_k - \tau_{kl}) + n_{\text{lp}}(t_n), \quad n = 1, \dots, N_{\text{sp}},$$

where $r_{\text{lp}}(t)$, $s_{\text{lp},ki}^m(t)$, and $n_{\text{lp}}(t)$ denote the outputs of $r(t)$, $s_{ki}^m(t)$, and $n(t)$ passing through the LPF, respectively. We have $s_{\text{lp},ki}^m(t) = s_{ki}^m(t)$ since the ideal LPF has the same bandwidth as the transmitted signal, i.e., bandwidth of $s_{ki}^m(t)$. Denoting the effective signature waveform by $\bar{s}_{ki}^m(t) := \sum_{l=1}^L g_{kl} s_{ki}^m(t - \lambda_k - \tau_{kl})$, the sampled received signal can be expressed as

$$r_n = \sum_{k=1}^K \sum_{m=1}^M \sum_{i=1}^N \sqrt{E_k} \bar{s}_{ki}^m(t_n) d_{ki}^m + n_{\text{lp}}(t_n), \quad n = 1, \dots, N_{\text{sp}}.$$

Next, let us denote the sampling signature waveform matrix corresponding to user k by

$$\bar{\mathbf{S}}_k = \begin{bmatrix} \bar{s}_{k1}^1(t_1) & \bar{s}_{k1}^2(t_1) & \cdots & \bar{s}_{kN}^M(t_1) \\ \bar{s}_{k1}^1(t_2) & \bar{s}_{k1}^2(t_2) & \cdots & \bar{s}_{kN}^M(t_2) \\ \vdots & \vdots & \vdots & \vdots \\ \bar{s}_{k1}^1(t_{N_{\text{sp}}}) & \bar{s}_{k1}^2(t_{N_{\text{sp}}}) & \cdots & \bar{s}_{kN}^M(t_{N_{\text{sp}}}) \end{bmatrix} \in \mathbb{C}^{N_{\text{sp}} \times NM},$$

and the sampled received signal and sampled noise vectors by

$$\begin{aligned} \mathbf{r}_{\text{sp}} &= [r_1, r_2, \dots, r_{N_{\text{sp}}}]^T \in \mathbb{C}^{N_{\text{sp}} \times 1}, \\ \mathbf{n}_{\text{sp}} &= [n_{\text{lp}}(t_1), n_{\text{lp}}(t_2), \dots, n_{\text{lp}}(t_{N_{\text{sp}}})]^T \in \mathbb{C}^{N_{\text{sp}} \times 1}. \end{aligned}$$

Then the sampled received signal can be written in an equivalent matrix form as

$$\mathbf{r}_{\text{sp}} = \sum_{k=1}^K \sqrt{E_k} \bar{\mathbf{S}}_k \mathbf{d}_k + \mathbf{n}_{\text{sp}}, \quad (5.14)$$

Since $n(t)$ is a complex Gaussian random process with zero mean and psd $N_0/2 = \sigma^2$ over whole frequency bands, after passing through the ideal LPF with bandwidth B , the noise process $n_{\text{lp}}(t)$ becomes a stationary zero mean Gaussian process [WJ65, Chap. 3] with the auto-correlation function

$$R_{\text{lp}}(\tau) = N_0 B \text{sinc}(2B\tau),$$

where $\text{sinc}(\cdot)$ is the normalized sinc function. Therefore, the sampled additive noise vector \mathbf{n}_{sp} is a zero mean complex Gaussian random vector with covariance matrix $\mathbf{R}_{\text{sp}} = [r_{ij}]_{\{i,j\}}$, $i, j = 1, 2, \dots, N_{\text{sp}}$,

$$r_{ij} = R_{\text{lp}}(t_i - t_j), \quad i, j = 1, 2, \dots, N_{\text{sp}}. \quad (5.15)$$

The capacities with sampling are then similarly obtained as in (5.11) and (5.13) with some small modifications: The equivalent matrix \mathbf{H}_k needs to be replaced by $\bar{\mathbf{S}}_k$, the noise covariance matrix $\sigma^2 \mathbf{H}$ needs to be replaced by \mathbf{R}_{sp} . Accordingly, let us define $R_1^{\text{sp}}, R_2^{\text{sp}}, \dots, R_K^{\text{sp}}$ as the maximum number of bits that can be reliably transmitted from user 1, user 2, ..., user K per block of N symbols assuming sampling is employed at the receiver. The sampling capacity is then characterized by⁵

$$\sum_{k \in \mathcal{J}} R_k^{\text{sp}} \leq \log \det \left(\mathbf{I}_{N_{\text{sp}}} + \sum_{k \in \mathcal{J}} E_k \bar{\mathbf{S}}_k^\dagger \mathbf{R}_{\text{sp}}^{-1} \bar{\mathbf{S}}_k \right), \quad \forall \mathcal{J} \subseteq \{1, \dots, K\}, \quad (5.16)$$

for Gaussian input signal and

$$\sum_{k \in \mathcal{J}} R_k^{\text{sp}} \leq -\mathbb{E} \left\{ \log_2 (f(\mathbf{r}_{\mathcal{J}}^{\text{sp}})) \right\} - \log_2 (\det (\pi e \mathbf{R}_{\text{sp}})), \quad \forall \mathcal{J} \subseteq \{1, \dots, K\}, \quad (5.17)$$

for finite constellation input signal, where $\mathbf{r}_{\mathcal{J}}^{\text{sp}} := \sum_{k \in \mathcal{J}} \sqrt{E_k} \bar{\mathbf{S}}_k \mathbf{d}_k + \mathbf{n}_{\text{sp}}$ is a Gaussian mixture random vector.

5.4 Capacity Approximation

In this section, we develop an approximation algorithm to evaluate the capacity of the uplink WCDMA channel when the system dimensions are large. As pointed out in Section 5.3.1, evaluating the rate constraints in (5.11) is related to computing the distributions of the Gaussian mixture random vectors, whose number of components increase exponentially with the dimensions of the system. Let us consider the rate constraint in (5.11) for the achievable sum-rate,⁶ which is computed based on the following Gaussian mixture distribution

$$f(\mathbf{z}) = \sum_{i=1}^{M_c^{N_t}} p(\mathbf{d}^{(i)}) f(\mathbf{z} | \mathbf{d} = \mathbf{d}^{(i)}), \quad (5.18)$$

⁵Similarly to the capacity achieved by sufficient statistic, the quantities in the right-hand sides of (5.16) and (5.17) describe the number of bits that can be reliably transmitted per block of N symbols. One can express the capacity in bits/s by normalizing with $1/T$, $T = NT_s$, or in bits/s/Hz by normalizing with $1/TB$.

⁶We are focussing on the most complex case with the achievable sum-rate. The rate constraint for the individual rates and subset sum-rates can be computed as the special case of the achievable sum-rate.

where $f(\mathbf{z}|\mathbf{d} = \mathbf{d}^{(i)})$ is the pdf of a complex Gaussian random vector with mean $\mathbf{H}\mathbf{E}\mathbf{d}^{(i)}$ and covariance matrix $\sigma^2\mathbf{H}$, i.e., $\mathcal{CN}(\mathbf{H}\mathbf{E}\mathbf{d}^{(i)}, \sigma^2\mathbf{H})$, M_c is the number of constellation points, and $N_t = KNM$ denotes the transmitted block size. When K, N, M have comparatively large values, the computation of the true distribution $f(\mathbf{z})$ is intractable. The main idea to deal with this problem is to approximate the Gaussian mixture distribution in (5.18) and use it for the computation of the rate constraint. One of the most popular approximating approaches is Gaussian mixture reduction (GMR), which has been extensively studied in the fields of data fusion and tracking applications [CWPS11, AK12, HH08, SH09, HBDWH08]. The concept of GMR is to approximate the true Gaussian mixture distribution by another Gaussian mixture distribution with much smaller number of components, i.e.,

$$f(\mathbf{z}) = \sum_{i=1}^{N_{\text{true}}} w_i f_i(\mathbf{z}) \approx \hat{f}(\mathbf{z}) = \sum_{i=1}^{N_{\text{red}}} w_i f_i(\mathbf{z}), \quad N_{\text{red}} \ll N_{\text{true}}, \quad (5.19)$$

where N_{true} and N_{red} denote the total number of components of the true distribution and the number of reduced components of the approximate distribution, respectively. w_i denotes the weighting factor of the i -th component, and $\mathbf{z}_i \sim \mathcal{CN}(\mu_i, \sigma_i^2)$. If we replace N_{true} , w_i , and $f(\mathbf{z}_i)$ by $M_c^{N_t}$, $p(\mathbf{d}^{(i)})$, and $f(\mathbf{z}|\mathbf{d} = \mathbf{d}^{(i)})$, respectively, this GMR problem is exactly same as our approximation problem. The performance of GMR highly depends on the criterion of choosing the N_{red} components. Here, we will propose an GMR algorithm, in which the selected components are chosen based on the sphere decoding approach [DGC03, MGDC06].

5.4.1 Sphere Decoding Inspired Approximation

Sphere decoding is an efficient tree search algorithm to find a transmit vector with the shortest distance (or lowest cost value) among all possible transmit vectors [DGC03, MGDC06]. The crucial point is that the algorithm does not go through all possible transmit vectors. Our proposed approach to obtaining the closest neighboring Gaussian components will exactly exploit this algorithmic idea so that we do not have to go through all possible components. The sphere decoder approach dynamically adds components following a smart algorithmic approach.

The objective of the traditional sphere decoder is to find the single best component with the smallest distance. Our objective is to find the N_{SD} closest neighboring components to be added up for the approximation of $f(\mathbf{z})$. The complexity of the approximation grows with the number of selected components.

Again, we start with the sufficient statistic in matrix-form from (5.8.C.2) of Appendix 5.8.C

$$\mathbf{z} = \mathbf{H}\mathbf{E}\mathbf{d} + \mathbf{n}, \quad (5.20)$$

where $\mathbf{n} \sim \mathcal{CN}(0, \sigma^2\mathbf{H})$. Since a full rank linear operation does not change the mutual information [CT06], we first perform a pre-whitening operation by multiplying

$\mathbf{H}^{-\frac{1}{2}}$ in both sides. Then, the whitened sufficient statistics are given by

$$\tilde{\mathbf{z}} = \mathbf{H}^{-\frac{1}{2}} \mathbf{z} = \mathbf{H}^{\frac{1}{2}} \mathbf{E} \mathbf{d} + \tilde{\mathbf{n}}, \quad (5.21)$$

where $\tilde{\mathbf{n}}$ is a white Gaussian noise vector, i.e., $\tilde{\mathbf{n}} \sim \mathcal{CN}(0, \sigma^2 \mathbf{I})$. In order to apply the sphere decoding idea, we perform QR-factorization of the channel matrix, i.e., $\mathbf{H}^{\frac{1}{2}} \mathbf{E} = \mathbf{Q} \mathbf{R}$ where $\mathbf{R} \in \mathbb{C}^{N_t \times N_t}$ is the upper triangular matrix and $\mathbf{Q} \in \mathbb{C}^{N_t \times N_t}$ has orthogonal columns of unit norm. Hence, using the QR-factorization, the channel model in (5.21) can be equivalently rewritten as

$$\mathbf{v} = \mathbf{R} \mathbf{d} + \mathbf{w}, \quad (5.22)$$

where $\mathbf{v} = \mathbf{Q}^\dagger \tilde{\mathbf{z}}$ and $\mathbf{w} = \mathbf{Q}^\dagger \tilde{\mathbf{n}}$. Then the ML detection problem of the sphere decoder reads as follows

$$\hat{\mathbf{d}}_{ML} = \arg \min_{\mathbf{d} \in \mathcal{D}} \|\mathbf{v} - \mathbf{R} \mathbf{d}\|^2, \quad (5.23)$$

where $\mathcal{D} = \{\mathbf{d}^{(1)}, \dots, \mathbf{d}^{(N_t)}\}$ denotes the set of all possible input symbol vectors. Due to the invariance of the Euclidean norm under unitary rotations, problem (5.23) is equivalent to the ML detection problem for the equivalent channel in (5.20). The sphere decoder solves Eq. (5.23) by searching over all vectors, $\mathbf{d} \in \mathcal{D}$, satisfying a spherical constraint, i.e.,

$$\|\mathbf{v} - \mathbf{R} \mathbf{d}\|^2 \leq \zeta^2, \quad (5.24)$$

where ζ denotes the search threshold called *search radius*. Basically, if ζ is sufficiently large, at least one vector satisfies the constraint in (5.24) and the vector with the smallest distance will be the ML estimate. Different from the conventional detection problem, our goal is not to find only the best vector but a set of the closest vectors which then specifies the most relevant components. Accordingly, as ζ increases, we find more components satisfying (5.24) which leads to a more accurate approximation of the distribution, $\hat{f}(\mathbf{z})$. At the same time the complexity of a search exponentially increases [HV05, JO05]. Therefore, ζ is an important parameter which needs to be carefully chosen. A graphical illustration of the sphere criterion can be seen in Figure 5.2.

In the perspective of algorithm design, the sphere decoder is implemented through a constrained tree search in order to reduce the search complexity [DGC03, MGDC06]. To this end, we reformulate (5.24) as follows

$$\|\mathbf{v} - \mathbf{R} \mathbf{d}\|^2 = \sum_{i=1}^{N_t} |v_i - \sum_{j=i}^{N_t} r_{ij} \hat{d}_j|^2 \leq \zeta^2, \quad (5.25)$$

where r_{ij} , v_i , and \hat{d}_j denote the (i, j) -th element of \mathbf{R} , the i -th entry of \mathbf{v} , and the j -th entry of $\hat{\mathbf{d}}$, respectively. Thus, a necessary and sufficient condition for (5.24)

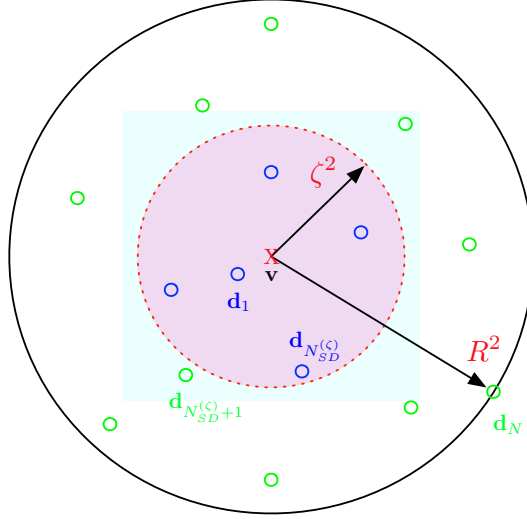


Figure 5.2: Graphical illustration of the sphere criterion.

to hold is given by

$$\sum_{i=N_t-k+1}^{N_t} |v_i - \sum_{j=i}^{N_t} r_{ij} \hat{d}_j|^2 \leq \zeta^2, \quad \forall k = 1, \dots, N_t. \quad (5.26)$$

Due to the upper triangular structure of \mathbf{R} , the inequality (5.26) for a given k is only a constraint on $d_{N_t-k+1}, \dots, d_{N_t}$. Hence, if $k = 1$, the inequality (5.26) becomes

$$|v_{N_t} - r_{N_t N_t} \hat{d}_{N_t}|^2 \leq \zeta^2. \quad (5.27)$$

This depth $k = 1$ corresponds to the root node in the search tree which is searched first. Similarly, for $k = 2, \dots, N_t$, Eq. (5.26) is equivalent to

$$\left| v_{N_t-k+1} - \sum_{j=N_t-k+1}^{N_t} r_{ij} \hat{d}_{N_t-k+1} \right|^2 \leq \zeta^2 - c_{k-1}, \quad (5.28)$$

where $c_{k-1} = \sum_{i=N_t-k+2}^{N_t} |v_i - \sum_{j=i}^{N_t} r_{ij} \hat{d}_i|^2$ denotes the cost value of the previous $(k-1)$ -th depth. The depth $k = N_t$ corresponds to the leaf nodes in the search tree. The relevant components $\hat{\mathbf{d}}^{(i)}$ are then given by those leaf nodes which satisfy the constraint. Moreover, if the cost value exceeds the search radius at the middle depth of the search tree, the below branches are pruned which can significantly reduce the search complexity. One simple tree search for $N_t = 3$, BPSK, and $\alpha = 2$

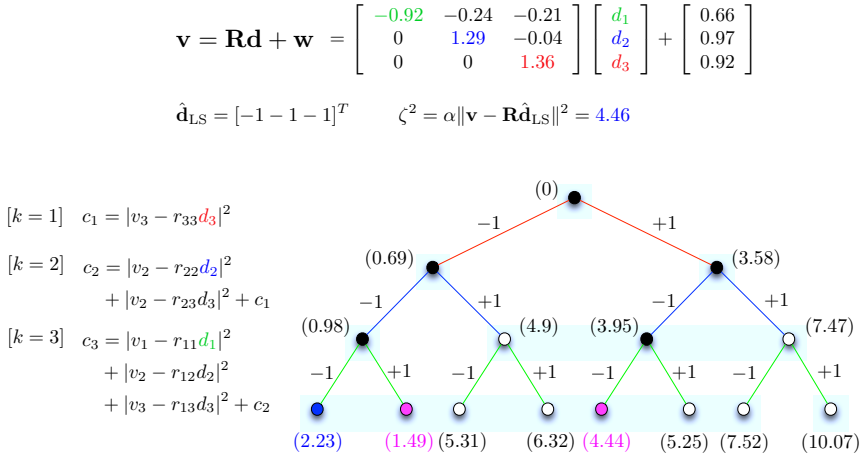


Figure 5.3: Graphical illustration of a tree search example.

can be seen in Figure 5.3. In this example, three nodes with the cost values less than the radius have been selected without going through all the possible nodes.

As mentioned above, the choice of the search radius is important with respect to accuracy and complexity. In the conventional sphere decoding, the initial search radius is set to a sufficiently large value and it is dynamically adjusted to a smaller value after finding at least one component. This dynamic adjustment of the search radius significantly reduces the search complexity. This is relevant to the sphere decoder because it only aims to find the best vector with the smallest distance. However, since the aim of our approximation problem is to find all neighboring components within a certain range, we set the search radius to a certain fixed value which takes both accuracy and complexity into account. In order to find the initial search radius we propose a solution based on least squares with a diagonalized channel assumption

$$\hat{\mathbf{d}}_{\text{LS}} = \arg \min_{\hat{\mathbf{d}} \in \mathcal{D}} \sum_{i=1}^{N_t} |v_i - r_{ii}\hat{d}_i|^2, \quad (5.29)$$

where $\hat{\mathbf{d}} = [\hat{d}_1, \dots, \hat{d}_{N_t}]^T$, $\hat{d}_i \in \mathcal{M}$ in which \mathcal{M} denotes the set of constellation points of a given QAM modulation. Hence, we set the initial search radius to be

$$\zeta^2 = \alpha \|\mathbf{v} - \mathbf{R}\hat{\mathbf{d}}_{\text{LS}}\|^2, \quad (5.30)$$

where $\alpha \geq 1$ denotes a control parameter used to trade off the accuracy and complexity. If we increase α parameter, we obtain a more accurate approximation at the cost of higher complexity. Even if this least squares-based criterion does not guarantee to yield always the closest component, it offers the closest component at

high SNR region and it guarantees to yield at least one component with a sufficiently small value for the search radius. This is because, when $\alpha \geq 1$, the sphere decoding finds at least the component based on least squares, $\hat{\mathbf{d}}_{\text{LS}}$, which is one of the all possible input symbol vectors, i.e., $\hat{\mathbf{d}}_{\text{LS}} \in \mathcal{D}$, through comparisons stated in Eq. (5.25).

Let \mathcal{D}_{SD} be the set of input symbol vectors which satisfy the sphere decoding constraint. Then the approximated pdf based on the sphere decoding inspired approximation algorithm is given as follows

$$\hat{f}_{\text{SD}}(\mathbf{z}) = \sum_{\mathbf{d}^{(i)} \in \mathcal{D}_{\text{SD}}} \frac{1}{M_c^{N_t}} f(\mathbf{z} | \mathbf{d} = \mathbf{d}^{(i)}), \quad (5.31)$$

where $f(\mathbf{z} | \mathbf{d} = \mathbf{d}^{(i)}) = \mathcal{CN}(\mathbf{H}^{1/2} \mathbf{E} \mathbf{d}^{(i)}, \sigma^2 \mathbf{I})$ and $p(\mathbf{d}^{(i)}) = \frac{1}{M_c^{N_t}}$ follows from the assumed uniform input distribution of the uplink WCDMA system.

The above approximation offers a lower bound on the Gaussian mixture pdf $f(\mathbf{z})$ since this sphere decoding inspired approximation just adds up parts of Gaussian components among the total number of Gaussian components, i.e.,

$$\begin{aligned} \hat{f}_{\text{SD}}(\mathbf{z}) &= \sum_{\mathbf{d}^{(i)} \in \mathcal{D}_{\text{SD}}} \frac{1}{M_c^{N_t}} f(\mathbf{z} | \mathbf{d} = \mathbf{d}^{(i)}) \\ &\leq \sum_{\mathbf{d}^{(i)} \in \mathcal{D}} \frac{1}{M_c^{N_t}} f(\mathbf{z} | \mathbf{d} = \mathbf{d}^{(i)}) = f(\mathbf{z}), \end{aligned} \quad (5.32)$$

where \mathcal{D} denotes the set of all possible input symbol vectors with its cardinality $|\mathcal{D}| = M_c^{N_t}$ and $f(\mathbf{z})$ is the exact pdf of \mathbf{z} . Therefore, the approximated achievable sum-rate is actually an upper bound for the achievable sum-rate as

$$\begin{aligned} C = I(\mathbf{z}; \mathbf{d}) &= - \int_{-\infty}^{\infty} f(\mathbf{z}) \log_2(f(\mathbf{z})) d\mathbf{z} - \log_2(\det(\pi e \sigma^2 \mathbf{H})) \\ &\leq - \int_{-\infty}^{\infty} f(\mathbf{z}) \log_2(\hat{f}_{\text{SD}}(\mathbf{z})) d\mathbf{z} - \log_2(\det(\pi e \sigma^2 \mathbf{H})) = \hat{C}_{\text{SD}}. \end{aligned} \quad (5.33)$$

Note that this sphere decoding inspired upper bound provides a much tighter upper bound as the parameter α increases. Especially, as α goes to infinity, it gives the exact capacity, i.e.,

$$\lim_{\alpha \rightarrow \infty} \hat{C}_{\text{SD}} = C, \quad (5.34)$$

since $\lim_{\alpha \rightarrow \infty} \mathcal{D}_{\text{SD}} = \mathcal{D}$.

5.4.2 Enhanced Search Algorithm

To reduce the tree search complexity for the sphere decoding motivated algorithm, we additionally consider columns ordering based on the Euclidean norm [DGC03].

The core idea is to sort the columns of the effective channel matrix $\mathbf{H}^{\frac{1}{2}}\mathbf{E}$ after the pre-whitening according to their Euclidean norms in a non-decreasing order.

The search tree is constructed based on the upper triangular matrix \mathbf{R} obtained from the QR factorization of the effective channel matrix, i.e., $\mathbf{QR} = \mathbf{H}^{\frac{1}{2}}\mathbf{E}$. The bottom diagonal element of \mathbf{R} corresponds to the root node and the first row elements of \mathbf{R} correspond to the leaf nodes in the search tree. Therefore, if we sort the elements of \mathbf{R} so that the lower positioned diagonal element has a larger value, it is assumed that the probability that nodes near the root node are pruned during a tree search of the sphere decoding increases. Since the pruning operation reduces unnecessary searches in the tree, it significantly reduces the search complexity. Sphere decoding experiments show that the above columns ordering of the effective channel matrix efficiently reduces the complexity of the search algorithm.

The columns ordering is realized by employing a column ordering permutation matrix $\mathbf{\Pi}$, which is generated so as to order the columns of the pre-whitened effective channel matrix $\mathbf{H}^{\frac{1}{2}}\mathbf{E}$ in a non-decreasing order with respect to its Euclidean norm. Then, the sufficient statistic is given by

$$\mathbf{z} = \mathbf{H}^{\frac{1}{2}}\mathbf{E}\mathbf{\Pi}\mathbf{\Pi}^{-1}\mathbf{d} + \mathbf{n}. \quad (5.35)$$

Now, we perform the QR factorization for $\mathbf{H}^{\frac{1}{2}}\mathbf{E}\mathbf{\Pi}$ instead of $\mathbf{H}^{\frac{1}{2}}\mathbf{E}$. Thus, the equivalent sufficient statistics after the QR factorization can be equivalently rewritten as

$$\mathbf{v} = \tilde{\mathbf{Q}}^{\dagger}\mathbf{z} = \tilde{\mathbf{R}}\tilde{\mathbf{d}} + \tilde{\mathbf{w}}, \quad (5.36)$$

where $\tilde{\mathbf{Q}}\tilde{\mathbf{R}} = \mathbf{H}^{\frac{1}{2}}\mathbf{E}\mathbf{\Pi}$, $\tilde{\mathbf{d}} = \mathbf{\Pi}^{-1}\mathbf{d}$, and $\tilde{\mathbf{w}} = \tilde{\mathbf{Q}}^{\dagger}\mathbf{n}$. Note that in our pre-whitened channel matrix $\mathbf{H}^{\frac{1}{2}}\mathbf{E}$, diagonal terms have the most dominant norm values compared to off-diagonal terms in the same row. Hence, this columns ordering based on Euclidean norm increases the possibility that an upper diagonal term has a larger norm value in the sorted upper triangular matrix $\tilde{\mathbf{R}}$. Similarly to the previous sphere decoder motivated approximation algorithm we now use (5.36) to construct the search tree to find the most relevant neighboring components which satisfy the sphere radius constraint. Thereby, we acquire the N_{red} closest elements by a post-processing $\mathbf{d} = \mathbf{\Pi}\tilde{\mathbf{d}}$.

The overall algorithm of the sphere decoding inspired approximation algorithm including the columns ordering based on Euclidean norm is specified as in Algorithm 5.1, where $\mathcal{U}(\mathcal{M}^{N_t})$ denotes the uniform distribution on the N_t -dimension Cartesian product of the constellation points set \mathcal{M} and $\hat{h}(\mathbf{z})$ is the Monte-Carlo integration approximation of $h(\mathbf{z})$.

Algorithm 5.1: Sphere Decoding Inspired Approximation Algorithm	
01:	(Initialization) Generate \mathbf{H} and set $\alpha \geq 1$
02:	(Pre-whitening) $\tilde{\mathbf{H}} = \mathbf{H}^{\frac{1}{2}} \mathbf{E}$
03:	(Columns ordering) $\tilde{\mathbf{H}}' = \tilde{\mathbf{H}} \mathbf{\Pi}$ where $\mathbf{\Pi}$ so that $\tilde{\mathbf{H}}' = \text{sort}(\ \tilde{\mathbf{H}}(:, j)\) \forall j$ in an increasing order
04:	(QR factorization) $\mathbf{QR} = \tilde{\mathbf{H}}'$ (Numerical integration by a Monte-Carlo method)
05:	for $j = 1 : N_d$
06:	Generate $\mathbf{d}^{(j)} = \sqrt{snr} \cdot m$ where $m \sim \mathcal{U}(\mathcal{M}^{N_t})$
07:	for $i = 1 : N_z$
08:	Generate $\mathbf{n}^{(i)}$ where $\mathbf{n}^{(i)} \sim \mathcal{CN}(0, \mathbf{I})$
09:	$\mathbf{z}^{(i)} = \tilde{\mathbf{H}} \mathbf{d}^{(j)} + \mathbf{n}^{(i)}$
10:	$\mathbf{v}^{(i)} = \mathbf{Q}^{\dagger} \mathbf{z}^{(i)}$
11:	(LS-based symbol vector) $\hat{\mathbf{d}}_{\text{LS}} = \arg \min_{\hat{\mathbf{d}} \in \mathcal{D}} \sum_{k=1}^{N_t} v_k^{(i)} - r_{kk} \hat{d}_k ^2$
12:	(Initial sphere radius) $\zeta^2 = \alpha \ \mathbf{v}^{(i)} - \mathbf{R} \hat{\mathbf{d}}_{\text{LS}}\ ^2$
13:	(SD tree search) $\tilde{\mathcal{D}}_{\text{SD}} = \{\hat{\mathbf{d}} : \ \mathbf{v}^{(i)} - \mathbf{R} \hat{\mathbf{d}}\ ^2 \leq \zeta^2\}$
14:	$\mathcal{D}_{\text{SD}} = \{\mathbf{d} : \mathbf{d} = \mathbf{\Pi} \tilde{\mathbf{d}}, \tilde{\mathbf{d}} \in \tilde{\mathcal{D}}_{\text{SD}}\}$
15:	$\hat{f}_{\text{SD}}^{(i,j)} \triangleq \sum_{\mathbf{d} \in \mathcal{D}_{\text{SD}}} \frac{1}{M_c^{N_t}} \mathcal{CN}(\tilde{\mathbf{H}} \mathbf{d}, \sigma^2 \mathbf{I})$
16:	end
17:	end
18:	$\hat{h}(\mathbf{z}) = -\frac{1}{N_d \cdot N_z} \sum_{i=1}^{N_z} \sum_{j=1}^{N_d} \log_2 \left(\hat{f}_{\text{SD}}^{(i,j)} \right)$
19:	$\hat{C}_{SD} = \hat{h}(\mathbf{z}) - \log_2 (\det(\pi e \sigma^2 \mathbf{H}))$

5.5 Numerical Characterization

In this subsection, we numerically characterize the capacity for a two-user uplink WCDMA system. For numerical experiments, we set the parameters which are close to those in a real uplink UMTS system as specified in [3GPtm]: time-variant CDMA with OVSF codes and Gold sequences, spreading factor $N_{\text{sf}} = 4$, SRRC chip waveform $p(t)$ with roll-off factor 0.22, and uniform power allocation $E_1/\sigma^2 = E_2/\sigma^2 = \text{SNR}$. In simulations, we employ a time-invariant multipath channel with $L = 3$ taps, a relative path-amplitude vector $\mathbf{a} = [0, -1.5, -3]$ dB, a relative path-phase vector $\boldsymbol{\theta} = [0, \frac{\pi}{3}, \frac{2\pi}{3}]$, and path-delay vector $\boldsymbol{\tau} = [0, \frac{T_c}{2}, T_c]$. Thus, the l -th element of the path-coefficient vector \mathbf{g}_1 is given by $a_l \cdot e^{j\theta_l} / \|\mathbf{a}\|$ where a_l is the l -th element of \mathbf{a} and θ_l is the l -th element of vector $\boldsymbol{\theta}$, and $\mathbf{g}_2 = \sqrt{2} \mathbf{g}_1$. In addition, we use fixed user delays which are randomly drawn within a symbol time once at the

beginning of simulations, i.e., $\lambda_k \sim \mathcal{U}(0, T_s)$.

Figure 5.4 illustrates the capacity of a two-user uplink UMTS system with $N = 2$ and $M = 1$ for 4-QAM (QPSK) input (from Section 5.3.1) and Gaussian distributed input (from Section 5.3.2) signals. The left-hand side sub-figure presents the sum- and individual capacities for Gaussian and 4-QAM input signals. The individual capacities R_2 are larger than R_1 since we set $\mathbf{g}_2 = \sqrt{2}\mathbf{g}_1$. The right-hand side sub-figure shows the capacity regions with 4-QAM input for several values of SNR. As expected, the capacity region enlarges as the SNR increases. Moreover, as the SNR tends to infinity, the capacity region converges to the corresponding source entropy outer bound (i.e., 2 bits/symbol individual rates and 4 bits/symbol sum-rate for the two-user channel with 4-QAM input). It is interesting that the maximal individual rates (2 bits/symbol) can be achieved simultaneously, i.e., the sum-rate constraint is asymptotically inactive in the high SNR regime. A deeper analysis on this asymptotic behavior will be given in the next section.

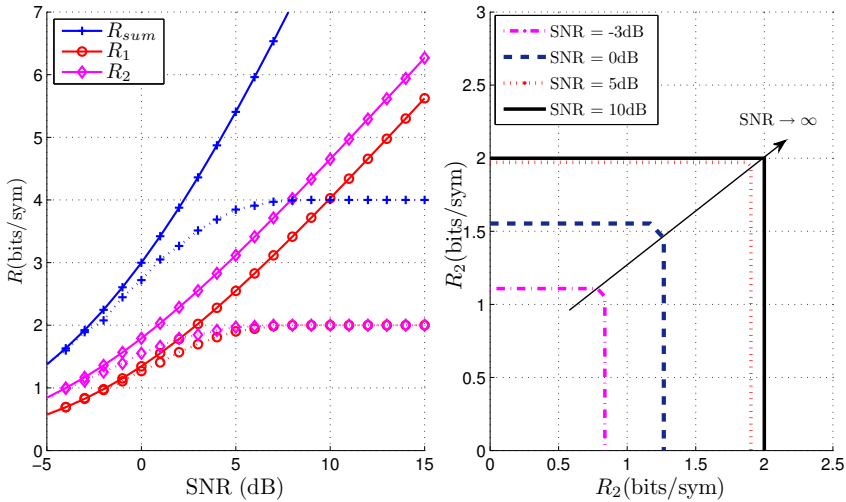


Figure 5.4: Capacity curves and capacity regions for a two-user setup with $N = 2$ and $M = 1$. On the left-hand side, the solid lines represent the capacities with Gaussian input and the dotted lines represent the capacities with 4-QAM input. All the capacities are normalized by $1/N$.

Figure 5.5 shows the achievable sum-rates for larger block length ($N = 32$) and two codes ($M = 2$) in each I/Q branch. The achievable sum-rates with finite constellation input are computed using the approximation algorithm as in Section 5.4. In this figure, both the achievable sum-rates achieved by sufficient statistic (from Sections 5.3.1, 5.3.2) and by sampling (from Section 5.3.3) are included. For achievable sum-rates using sampling, the experiments with sampling rate lower than the

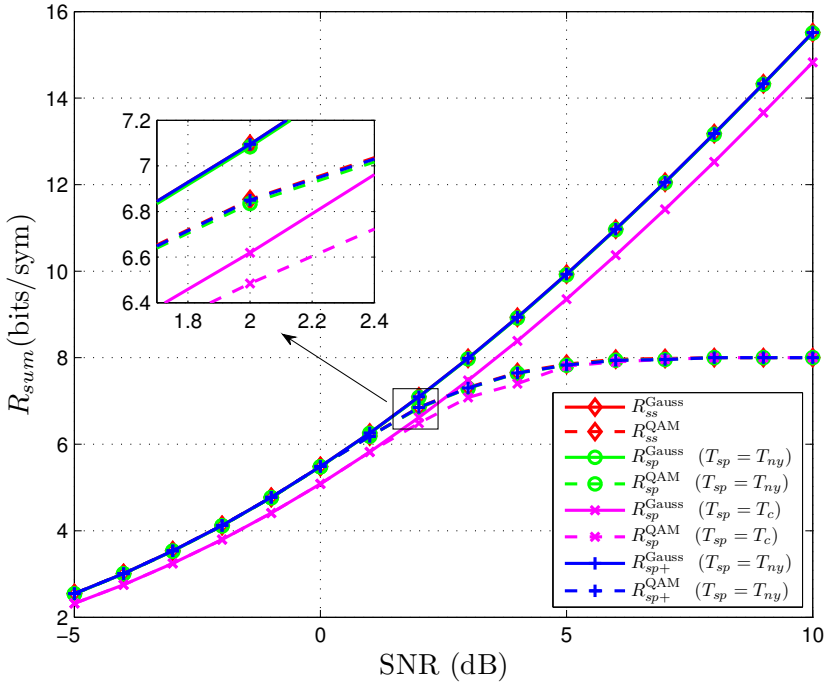


Figure 5.5: Achievable sum-rates for different inputs and receiver structures with $N = 32$ and $M = 2$. R_{ss}^{Gauss} and R_{ss}^{QAM} denote the sum-rates achieved by the sufficient statistic with Gaussian input and 4-QAM input, respectively. R_{sp}^{Gauss} and R_{sp}^{QAM} denote the sum-rates achieved by sampling with the sampling window equal to the block length $t_n \in [0, NT_s]$. R_{sp+}^{Gauss} and R_{sp+}^{QAM} denote the sum-rates achieved by sampling with the sampling window extended by 2 symbol durations on each side, i.e., $t_n \in [-2T_s, (N+2)T_s]$. All the sum-rates are normalized by $1/N$.

Nyquist rate ($T_{sp} = T_c > T_{ny}$) and Nyquist rate ($T_{sp} = T_{ny}$) are considered. As expected, the sum-capacity achieved by the sufficient statistic is an upper bound for the sum-rates achieved by systems employing sampling. Moreover, even when samples are taken at Nyquist rate, there are still gaps between the sum-rates achieved by sampling ($R_{sp}^{\text{Gauss}}(T_{sp} = T_{ny})$ and $R_{sp}^{\text{QAM}}(T_{sp} = T_{ny})$) and the sum-capacities achieved by matched filtering/sufficient statistic (R_{ss}^{Gauss} and R_{ss}^{QAM}). These losses are due to the finite time limit of our sampling window as the Nyquist sampling theorem states that infinite samples are required to be able to perfectly recover a band-limited signal [Lap09, Theorem 8.4.3]. Fortunately, by extending the sampling window by only two symbols duration each side (for R_{sp+}^{Gauss} and R_{sp+}^{QAM}), these losses can be significantly reduced.

5.6 Asymptotic Performance

Recalling the rate constraint in (5.10) with $\mathcal{J} = \{1, \dots, K\}$, we have $\sum_{k=1}^K R_k \leq I(\mathbf{d}; \mathbf{z}) \leq \sum_{k=1}^K H(\mathbf{d}_k)$, i.e., the sum-capacity is upper bounded by sum of the sources entropies. However, the results in Figure 5.4 show that when $\text{SNR} \rightarrow \infty$, the individual capacities can be simultaneously achieved, i.e., the sum-capacity approaches the sum of the source entropies. In this section, we provide a deeper analysis on this by characterizing the asymptotic behavior of the sum-capacity. For convenience, we begin with a simple MAC model, and then extend the result to the uplink WCDMA system in the following.

5.6.1 Simple K -User MAC Model

Firstly, we start from the asymptotic sum-capacity of a simple K -user MAC, where each user transmits only one data stream. This setup corresponds to our uplink WCDMA system with $M = 1$ and $N = 1$ in a frequency-non-selective channel. The results are mainly based on the following theorem.

Theorem 5.6.1. Consider the received signal model of a K -user MAC

$$y(t) = \sum_{k=1}^K d_k s_k(t) + n(t), \quad (5.37)$$

where d_1, \dots, d_K are the unit power transmitted symbols, which are independent and transmitted using K normalized signature waveforms $s_1(t), \dots, s_K(t)$ and $n(t)$ denotes the Gaussian noise process with psd $\frac{1}{\text{SNR}}$. When $\text{SNR} \rightarrow \infty$, the asymptotic sum-capacity of channel (5.37), $C_{\text{sum}}^{\text{as}} = \sum_{k=1}^K H(d_k)$, is achieved if the vector space $\mathcal{S}_K = \text{span}\{s_1(t), \dots, s_K(t)\}$ has the dimension K .

The proof of Theorem 5.6.1 is given by Appendix 5.8.B. The idea for the proof can be briefly presented as follow. First, we show that the received signal passing through a bank of matched filters, which are matched to the signature waveforms, yields a sufficient statistic for decoding $\mathbf{d} = [d_1, \dots, d_K]$ based on $y(t)$. Then we show that \mathbf{d} can be uniquely decoded, i.e., the decoder is able to decode the messages correctly from this sufficient statistic when $\text{SNR} \rightarrow \infty$ if $\dim(\mathcal{S}_K) = K$. Based on the uniquely decodable property we then prove that the asymptotic sum-capacity $C_{\text{sum}}^{\text{as}}$ approaches sum of the source entropies if the signature waveforms are linearly independent of each other, i.e., $\dim(\mathcal{S}_K) = K$.

5.6.2 Uplink WCDMA System

Next, we extend the results from the above simple K -user MAC to the asymptotic sum-capacity of the uplink WCDMA system. Let us recall the transmitted signal from user k of the uplink WCDMA system in (5.1), and take into account all K

users. The transmitted signal can be considered as the one of an equivalent KNM users MAC in (5.37) using KNM signature waveforms $s_{ki}^m(t - \lambda_k)$, $k = 1, \dots, K$, $i = 1, \dots, N$, and $m = 1, \dots, M$. The following corollaries, which can be derived from Theorem 1, specify the asymptotic sum-capacity of the uplink WCDMA system in different channel environments considering frequency-non-selective ($L = 1$) and frequency-selective ($L \geq 2$) channels.

Corollary 5.6.1. The asymptotic sum-capacity of the frequency-non-selective uplink WCDMA channel as described in (5.2) with $L = 1$ is $C_{\text{sum,nsec}}^{\text{as}} = \sum_{k=1}^K H(\mathbf{d}_k)$ if the dimension of the signature waveforms space $\mathcal{S}_T = \text{span}\{s_{11}^1(t - \lambda_1), \dots, s_{KN}^M(t - \lambda_K)\}$ is KNM .

The proof for Corollary 5.6.1 is given in Appendix 5.8.C. The intuition behind Corollary 5.6.1 can be expressed as: K users transmit KNM symbols and the receiver performs matched filtering with KNM fingers. Although the uplink WCDMA multi-user channel corresponds to a K -user SISO MAC, the RAKE receiver virtually converts this to an equivalent $KNM \times KNM$ MIMO channel. Thus, by appropriately choosing the signature waveforms and matched fingers, which yield a full-rank equivalent channel matrix \mathbf{H} , the transmitted symbols, $\mathbf{d}_1, \dots, \mathbf{d}_K$, can be perfectly (i.e., error-free) recovered from \mathbf{z} as SNR goes to infinity. In other words, a K -user uplink WCDMA channel can asymptotically achieve the capacity of KNM parallel channels as long as $\dim(\mathcal{S}_T) = KNM$.

Corollary 5.6.2. The asymptotic sum-capacity of the frequency-selective uplink WCDMA channel as described in (5.2) is $C_{\text{sum,sec}}^{\text{as}} = \sum_{k=1}^K H(\mathbf{d}_k)$ if $\dim(\overline{\mathcal{S}}) = KNM$, where $\overline{\mathcal{S}} = \text{span}\{\bar{s}_{11}^1(t), \dots, \bar{s}_{KN}^M(t)\}$ is the vector space spanned by the effective signature waveform $\bar{s}_{ki}^m(t) = \sum_{l=1}^L g_{kl} s_{ki}^m(t - \lambda_k - \tau_{kl})$.

The proof for Corollary 5.6.2 is given in Appendix 5.8.D. Unlike the frequency-non-selective channel case, the sufficient condition for achieving the asymptotic sum-capacity in frequency-selective channel case is based on the *effective signature waveforms*, which includes the impact of the channel gains $\{\mathbf{g}_k\}_k$ and delays $\{\tau_{kl}\}_{k,l}$. This implies that the multi-path channel may help the equivalent channel matrix \mathbf{H} to achieve full-rank. For instance, if $\dim(\mathcal{S}_T) < KNM$, \mathbf{H} is obviously singular when $L = 1$. However, \mathbf{H} can still be invertible when $L > 1$. Indeed, when $L > 1$, due to the effects of the channel selectivity and the potential offset in the multi-path environment, $\dim(\overline{\mathcal{S}})$ is possible to be equal to KNM and \mathbf{H} is invertible.⁷ This is particularly helpful in an overloaded CDMA system [MM12, YC10], where the number of users exceeds the spreading factor.

⁷When $L > 1$, the channel gain matrix \mathbf{G} is not a square matrix anymore. The invertible property of \mathbf{H} does not depend only on rank of the correlation matrix \mathbf{R} but also on \mathbf{G} .

5.6.3 Necessary Condition

Corollaries 5.6.1 and 5.6.2 state sufficient conditions such that the transmitted messages can be uniquely decoded when $\text{SNR} \rightarrow \infty$, which holds for all kinds of input signals including both finite and infinite constellation signals. However, the conditions in Corollaries 5.6.1 and 5.6.2 can be relaxed in certain scenarios with finite constellation inputs. In this subsection, we first consider a simple example where the conditions in Corollaries 5.6.1 and 5.6.2 can be relaxed. The necessary condition for the unique decoding with finite constellation input is then studied in the following.

For instance, let us consider an example with two different setups of channel (5.37) with $K = 2$ and binary transmitted signals $\mathbf{d}_a = [d_{a1} \ d_{a2}]^T$ and $\mathbf{d}_b = [d_{b1} \ d_{b2}]^T$, i.e.,

$$\begin{aligned} y_a(t) &= d_{a1}s_1(t) + d_{a2}s_2(t) + n_a(t), \\ y_b(t) &= d_{b1}s_1(t) + d_{b2}s_2(t) + n_b(t), \end{aligned}$$

where $n_a(t)$ and $n_b(t)$ denote additive Gaussian noise processes. We assume that the same signature waveform space $\mathcal{S}_2 := \text{span}\{s_1(t), s_2(t)\}$ is used in both setups. However, the transmitted symbols are uniformly and randomly picked up from different input constellation sets: $d_{a1}, d_{a2} \in \{0, 1\}$ and $d_{b1} \in \{-1/\sqrt{2}, 1/\sqrt{2}\}$, $d_{b2} \in \{0, 1\}$. The corresponding sufficient statistic models are then given by

$$\begin{aligned} Y_a &= d_{a1} + d_{a2} + N_a, \\ Y_b &= d_{b1} + d_{b2} + N_b, \end{aligned}$$

where Y_a, Y_b denote the sufficient statistics and N_a, N_b are the equivalent noises. We can see that when the noise power becomes zero (or $\text{SNR} \rightarrow \infty$), \mathbf{d}_a (and so (d_{a1}, d_{a2})) cannot be uniquely decoded from Y_a since the conditional entropy $H(d_{a1}, d_{a2} | Y_a) = 0.5 > 0$ when $\text{SNR} \rightarrow \infty$. However, (d_{b1}, d_{b2}) can be uniquely decoded from Y_b since $H(d_{b1}, d_{b2} | Y_b) = 0$ when $\text{SNR} \rightarrow \infty$ even though $\dim(\mathcal{S}_2) = 1 < 2$. It shows that the condition $\dim(\mathcal{S}_K) = K$ can be relaxed for certain signal constellation structures. Therefore, it is expected that necessary conditions for achieving the unique decoding with finite constellation input have to take both the signature waveforms and the structure of the signal constellation into account.

Let us assume that $\mathbf{d} \in \mathcal{M}^{KNM}$, where \mathcal{M} is a set of constellation points and is finite. In order to derive the sufficient condition for the unique decoding, we refer to the equivalent channel in (5.8.C.2) of Appendix 5.8.C

$$\mathbf{z} = \mathbf{H}\mathbf{E}\mathbf{d} + \mathbf{n}. \quad (5.38)$$

When $\text{SNR} \rightarrow \infty$, the transmitted vector \mathbf{d} can be uniquely decoded from \mathbf{z} if and only if the mapping

$$\begin{aligned} f : \mathcal{M}^{KNM} &\mapsto \mathcal{C}^{KNM} \\ \mathbf{d} &\mapsto \mathbf{H}\mathbf{E}\mathbf{d} \end{aligned}$$

is an one-to-one mapping. In particular, for any pair of $\mathbf{d}^i, \mathbf{d}^j \in \mathcal{M}^{KNM}$ and $\mathbf{d}^i \neq \mathbf{d}^j$, the condition $\mathbf{H}\mathbf{E}\mathbf{d}^i \neq \mathbf{H}\mathbf{E}\mathbf{d}^j$ is needed for the unique decoding. Therefore, by defining $\mathbf{v}_{ij} = \mathbf{d}^i - \mathbf{d}^j$, the condition for the unique decoding becomes

$$\mathbf{H}\mathbf{E}\mathbf{v}_{ij} \neq 0, \forall i \neq j. \quad (5.39)$$

In other words, the necessary condition for the unique decoding is that any vector \mathbf{v}_{ij} with $i \neq j$ is not in the null space of matrix $\mathbf{H}\mathbf{E}$. This necessary condition includes the impact of signal constellation reflected via \mathbf{v}_{ij} .

Remark 5.2. This result is consistent with the sufficient conditions in Corollaries 5.6.1 and 5.6.2. Indeed, when the (effective) signature waveform space has dimension KNM and \mathbf{H} is invertible, the null space of $\mathbf{H}\mathbf{E}$ is empty. Thus, the condition in (5.39) holds for any set of vector \mathbf{v}_{ij} and the unique decoding is achieved for any kind of input signal.

5.7 Chapter Conclusion

In this chapter, we have studied the spectral efficiency, i.e., capacity limit of the uplink WCDMA channel whose setup has been chosen to reflect a real CDMA cellular network. A framework was developed which can be used to see how close to the theoretical fundamental limit a practical system can achieve. To this end, sufficient statistics for decoding the transmitted messages were derived using a bank of matched filters, each of which is matched to the signature waveform. An equivalent discrete-time channel model based on the derived sufficient statistics is provided which can be used to analyze the capacity of the system. The capacity regions for finite constellation input and Gaussian distributed input signals have been both analytically and numerically characterized. A comparison with the sampling capacity showed that sampling within the transmission time window might cause a capacity loss even if the sampling was performed at Nyquist rate. Fortunately, this loss could be significantly diminished by extending the sampling window by only two symbol durations. An approximation algorithm inspired by sphere decoding has also been constructed to reduce the computation complexity for the system with large dimensions. Moreover, the asymptotic analysis showed that for proper choices of the (effective) signature waveforms, a K -user uplink WCDMA channel can be decoupled so that each user achieves a point-to-point channel capacity when SNR goes to infinity. The presented framework and results provide valuable insights for the design and further development of current and future WCDMA systems.

5.8 Appendices

5.8.A Derivation of equivalent noise statistic

Since $n(t)$ is a zero mean complex Gaussian random process, the equivalent noises after a bank of linear filters (matched filters), $n_{ki}^{ml} = \int_{-\infty}^{\infty} n(t) s_{ki}^m(t - \lambda_k - \tau_{kl})^* dt$,

$\forall k, i, m, l$, are zero mean joint Gaussian random variables [Gal68, Chap. 8], with the correlation coefficient given by

$$\begin{aligned}\mathbb{E} \left\{ n_{ki}^{ml} n_{k'i'}^{m'l'*} \right\} &= \mathbb{E} \left\{ \int_{-\infty}^{\infty} n(t) s_{ki}^m(t - \lambda_k - \tau_{kl})^* dt \int_{-\infty}^{\infty} n(t')^* s_{k'i'}^{m'}(t' - \lambda_{k'} - \tau_{k'l'}) dt' \right\} \\ &= \int_{-\infty}^{\infty} \int_{-\infty}^{\infty} \mathbb{E} \left\{ n(t) n(t')^* \right\} s_{ki}^m(t - \lambda_k - \tau_{kl})^* s_{k'i'}^{m'}(t' - \lambda_{k'} - \tau_{k'l'}) dt dt',\end{aligned}$$

where $\mathbb{E} \left\{ n(t) n(t')^* \right\} = \sigma^2 \delta(t - t')$. Thus, we have

$$\begin{aligned}\mathbb{E} \left\{ n_{ki}^{ml} n_{k'i'}^{m'l'*} \right\} &= \int_{-\infty}^{\infty} \int_{-\infty}^{\infty} \sigma^2 \delta(t - t') s_{ki}^m(t - \lambda_k - \tau_{kl})^* s_{k'i'}^{m'}(t' - \lambda_{k'} - \tau_{k'l'}) dt dt' \\ &= \sigma^2 \int_{-\infty}^{\infty} s_{ki}^m(t - \lambda_k - \tau_{kl})^* \left[\int_{-\infty}^{\infty} \delta(t - t') s_{k'i'}^{m'}(t' - \lambda_{k'} - \tau_{k'l'}) dt' \right] dt \\ &= \sigma^2 \int_{-\infty}^{\infty} s_{ki}^m(t - \lambda_k - \tau_{kl})^* s_{k'i'}^{m'}(t - \lambda_{k'} - \tau_{k'l'}) dt \\ &= \sigma^2 \rho_{(kiml)}^{(k'i'm'l')}.\end{aligned}$$

Accordingly, the equivalent noises $n_{ki}^m = \sum_{l=1}^L g_{kl}^* n_{ki}^{ml}$, $\forall k, i, m$ are zero mean joint Gaussian random variables with correlation coefficient

$$\begin{aligned}\mathbb{E} \left\{ n_{ki}^m n_{k'i'}^{m'*} \right\} &= \sum_{l=1}^L \sum_{l'=1}^L g_{kl}^* g_{k'l'} \mathbb{E} \left\{ n_{ki}^{ml} n_{k'i'}^{m'l'*} \right\} \\ &= \sigma^2 \sum_{l=1}^L \sum_{l'=1}^L g_{kl}^* g_{k'l'} \rho_{(kiml)}^{(k'i'm'l')}.\end{aligned}$$

Moreover, we have the (a, b) th element of \mathbf{H} expressed as

$$\mathbf{H}[a, b] = \sum_{l=1}^L \sum_{l'=1}^L g_{kl}^* g_{k'l'} \rho_{(kiml)}^{(k'i'm'l')}, \quad (5.8.A.1)$$

where the indices are given by

$$\begin{aligned}a &= (k - 1)NM + (i - 1)M + m, \\ b &= (k' - 1)NM + (i' - 1)M + m'.\end{aligned}$$

As a result, \mathbf{n} is a complex Gaussian random vector with zero mean and covariance matrix $\sigma^2 \mathbf{H}$.

5.8.B Proof of Theorem 5.6.1

The proof of Theorem 1 consists of two parts:

- Part 1: We first show that the received signal passed through a bank of matched filters, which match to the signature waveforms, yields a sufficient statistic for decoding $\mathbf{d} = [d_1, \dots, d_K]^T$ based on $y(t)$. Moreover, when $\text{SNR} \rightarrow \infty$, \mathbf{d} can be uniquely decoded if $\dim(\mathcal{S}_K) = K$.
- Part 2: Based on the uniquely decodable property, we then derive the asymptotic sum-capacity.

Part 1: Part 1 is resulted from the following lemma

Lemma 5.1. Consider a signal model as in (5.37). Let the received signal $y(t)$ passed through a bank of matched filters, where $y(t)$ is matched with each signature waveform $s_k(t)$, i.e.,

$$y_k = \langle y(t), s_k(t) \rangle = \int_{-\infty}^{\infty} y(t) s_k^*(t) dt, \quad k = 1 \dots K.$$

Then $\mathbf{y} = [y_1, \dots, y_K]^T$ is a sufficient statistic for decoding \mathbf{d} based on $y(t)$. Moreover, if the vector space $\mathcal{S}_K = \text{span}\{s_1(t), \dots, s_K(t)\}$ has dimension of K , \mathbf{d} can be uniquely decoded from the sufficient statistic \mathbf{y} as $\text{SNR} \rightarrow \infty$.

Proof. Following similar steps as in Section II.B, it can be shown that \mathbf{y} is a sufficient statistic for decoding \mathbf{d} based on $y(t)$.

It remains to show that \mathbf{d} can be uniquely decoded from \mathbf{y} when $\text{SNR} \rightarrow \infty$. Let us denote \mathbf{R}_s as the correlation matrix of the signature waveforms $\{s_k(t)\}_k$, where $\mathbf{R}_s[i, j] = \langle s_i(t), s_j(t) \rangle$. Therewith, we have the equivalent matrix expression

$$\mathbf{y} = \mathbf{R}_s \mathbf{d} + \tilde{\mathbf{n}},$$

where $\tilde{\mathbf{n}}$ is the equivalent noise vector.

Since $\dim(\mathcal{S}_K) = K$, we can rewrite $\{s_1(t), \dots, s_K(t)\}$ as

$$\begin{bmatrix} s_1(t) \\ \vdots \\ s_K(t) \end{bmatrix} = \mathbf{A} \begin{bmatrix} e_1(t) \\ \vdots \\ e_K(t) \end{bmatrix}$$

where $\{e_1(t), \dots, e_K(t)\}$ is an orthonormal basis of \mathcal{S}_K and \mathbf{A} is a $K \times K$ full rank matrix.

Consider the correlation matrix \mathbf{R}_e where

$$\mathbf{R}_e[i, j] = \langle e_i(t), e_j(t) \rangle.$$

Then we have $\mathbf{R}_e = \mathbf{I}_K$ since $\{e_1(t), \dots, e_K(t)\}$ is an orthonormal basic. Moreover,

$$\mathbf{R}_s = \mathbf{A} \mathbf{R}_e \mathbf{A}^\dagger = \mathbf{A} \mathbf{A}^\dagger.$$

Thus,

$$\text{rank}(\mathbf{R}_s) = \text{rank}(\mathbf{A}\mathbf{A}^\dagger) = \text{rank}(\mathbf{A}) = K.$$

Therefore, when $\dim(\mathcal{S}_K) = K$, \mathbf{R}_s is invertible and \mathbf{d} can be uniquely decoded from \mathbf{y} when $\text{SNR} \rightarrow \infty$ since $\lim_{\text{SNR} \rightarrow \infty} \mathbf{R}_s^{-1}\mathbf{y} = \mathbf{d}$. \square

Part 2: We next derive the asymptotic sum-capacity based on the sufficient statistic from Part 1.

The sum-capacity of the channel (5.37) is given by

$$C_{\text{sum}} = I(\mathbf{d}; y(t)). \quad (5.8.B.1)$$

From Lemma 1, we know that \mathbf{y} is a sufficient statistic for decoding \mathbf{d} based on $y(t)$. Thus,

$$I(\mathbf{d}; y(t)) = I(\mathbf{d}; \mathbf{y}), \quad (5.8.B.2)$$

where

$$I(\mathbf{d}; \mathbf{y}) = H(\mathbf{d}) - H(\mathbf{d}|\mathbf{y}). \quad (5.8.B.3)$$

When $\dim(\mathcal{S}_K) = K$, following from Part 1, \mathbf{R}_s is invertible and $\lim_{\text{SNR} \rightarrow \infty} \mathbf{R}_s^{-1}\mathbf{y} = \mathbf{d}$. Therefore,

$$\lim_{\text{SNR} \rightarrow \infty} H(\mathbf{d}|\mathbf{y}) = H(\mathbf{R}_s^{-1}\mathbf{y}|\mathbf{y}) = 0. \quad (5.8.B.4)$$

Let us define the asymptotic sum-capacity as $C_{\text{sum}}^{\text{as}} = \lim_{\text{SNR} \rightarrow \infty} C_{\text{sum}}$, combining (5.8.B.1)–(5.8.B.4), we have

$$C_{\text{sum}}^{\text{as}} = H(\mathbf{d}) = \sum_{k=1}^K H(d_k).$$

This completes the proof for Theorem 1. \blacksquare

5.8.C Proof of Corollary 5.6.1

Corollary 1 is proved in three steps:

- *Step 1:* We first re-formulate (5.9) by an equivalent input-output model, in which \mathbf{H} is decomposed into a multiplication of multiple matrices including a matrix that depends only on the signature waveform correlation coefficients. To this end, we rewrite the equivalent channel $\mathbf{H}_k^{k'}$ in (5.7) as

$$\mathbf{H}_k^{k'} = \mathbf{G}_k^\dagger \mathbf{R}_k^{k'} \mathbf{G}_{k'} \in \mathbb{C}^{NM \times NM},$$

where $\mathbf{G}_k = \text{blkdiag}\left(\underbrace{\bar{\mathbf{G}}_k, \dots, \bar{\mathbf{G}}_k}_{N \text{ matrices}}\right) = \text{blkdiag}\left(\underbrace{\mathbf{g}_k, \dots, \mathbf{g}_k}_{MN \text{ vectors}}\right)$, and

$$\mathbf{R}_k^{k'} = \begin{bmatrix} \mathbf{R}_{k1}^{k'1} & \mathbf{R}_{k1}^{k'2} & \cdots & \mathbf{R}_{k1}^{k'N} \\ \mathbf{R}_{k2}^{k'1} & \mathbf{R}_{k2}^{k'2} & \cdots & \mathbf{R}_{k2}^{k'N} \\ \vdots & \vdots & \vdots & \vdots \\ \mathbf{R}_{kN}^{k'1} & \mathbf{R}_{kN}^{k'2} & \cdots & \mathbf{R}_{kN}^{k'N} \end{bmatrix} \in \mathbb{C}^{NML \times NML}.$$

Therefore,

$$\mathbf{H}_k = \begin{bmatrix} \mathbf{G}_1^\dagger \mathbf{R}_1^k \mathbf{G}_k \\ \mathbf{G}_2^\dagger \mathbf{R}_2^k \mathbf{G}_k \\ \vdots \\ \mathbf{G}_K^\dagger \mathbf{R}_K^k \mathbf{G}_k \end{bmatrix} \in \mathbb{C}^{KNM \times NM}.$$

Moreover,

$$\mathbf{H} = [\mathbf{H}_1, \dots, \mathbf{H}_K] = \begin{bmatrix} \mathbf{G}_1^\dagger \mathbf{R}_1^1 \mathbf{G}_1 & \mathbf{G}_1^\dagger \mathbf{R}_1^2 \mathbf{G}_2 & \cdots & \mathbf{G}_1^\dagger \mathbf{R}_1^K \mathbf{G}_K \\ \mathbf{G}_2^\dagger \mathbf{R}_2^1 \mathbf{G}_1 & \mathbf{G}_2^\dagger \mathbf{R}_2^2 \mathbf{G}_2 & \cdots & \mathbf{G}_2^\dagger \mathbf{R}_2^K \mathbf{G}_K \\ \vdots & \vdots & \vdots & \vdots \\ \mathbf{G}_K^\dagger \mathbf{R}_K^1 \mathbf{G}_1 & \mathbf{G}_K^\dagger \mathbf{R}_K^2 \mathbf{G}_2 & \cdots & \mathbf{G}_K^\dagger \mathbf{R}_K^K \mathbf{G}_K \end{bmatrix}$$

can be rewritten as

$$\mathbf{H} = \mathbf{G}^\dagger \mathbf{R} \mathbf{G}, \quad (5.8.C.1)$$

where

$$\mathbf{G} = \text{blkdiag}\left(\mathbf{G}_1, \dots, \mathbf{G}_K\right) \in \mathbb{C}^{KNML \times KNM},$$

and

$$\mathbf{R} = \begin{bmatrix} \mathbf{R}_1^1 & \mathbf{R}_1^2 & \cdots & \mathbf{R}_1^K \\ \mathbf{R}_2^1 & \mathbf{R}_2^2 & \cdots & \mathbf{R}_2^K \\ \vdots & \vdots & \vdots & \vdots \\ \mathbf{R}_K^1 & \mathbf{R}_K^2 & \cdots & \mathbf{R}_K^K \end{bmatrix} \in \mathbb{C}^{KNML \times KNML}.$$

Thus, we have the equivalent input-output model as

$$\mathbf{z} = \mathbf{H} \mathbf{E} \mathbf{d} + \mathbf{n}, \quad (5.8.C.2)$$

where

$$\mathbf{E} = \text{diag}\left(\underbrace{\sqrt{E_1}, \dots, \sqrt{E_1}}_{NM \text{ elements}}, \dots, \underbrace{\sqrt{E_K}, \dots, \sqrt{E_K}}_{NM \text{ elements}}\right).$$

- *Step 2:* We show that \mathbf{H} is invertible when $L = 1$ and $\dim(\mathcal{S}_T) = KNM$.

Following the same arguments as for the proof of Theorem 1, we have \mathbf{R} is full-rank since $\dim(\mathcal{S}_T) = KNM$. Since $\mathbf{H} = \mathbf{G}^\dagger \mathbf{R} \mathbf{G}$, where \mathbf{G}, \mathbf{R} are the square matrices with full rank, it follows that \mathbf{H} is invertible.

- *Step 3:* Lastly, we can conclude on the asymptotic capacity of the channel (5.9). Since \mathbf{z} in (5.8.C.2) is a sufficient statistic for decoding \mathbf{d} based on $y(t)$ (from Section II.E) and \mathbf{H} is invertible, similarly to the proof in Part 2 of Theorem 1, it follows that

$$C_{\text{sum,nsec}}^{\text{as}} = H(\mathbf{d}) = \sum_{k=1}^K H(\mathbf{d}_k). \quad (5.8.C.3)$$

This completes the proof for Corollary 1. ■

5.8.D Proof of Corollary 5.6.2

Let us define $\bar{\rho}_{kim}^{k'i'm'}$ as the inner product between $\bar{s}_{ki}^m(t)$ and $\bar{s}_{k'i'}^{m'}(t)$, i.e.,

$$\begin{aligned} \bar{\rho}_{kim}^{k'i'm'} &= \langle \bar{s}_{ki}^m(t), \bar{s}_{k'i'}^{m'}(t) \rangle \\ &= \sum_{l=1}^L \sum_{l'=1}^L g_{kl}^* \langle s_{ki}^m(t - \lambda_k - \tau_{kl}), s_{k'i'}^{m'}(t - \lambda_k - \tau_{k'l'}) \rangle g_{k'l'} \\ &= \sum_{l=1}^L \sum_{l'=1}^L g_{kl}^* \rho_{kiml}^{k'i'm'l} g_{k'l'}. \end{aligned} \quad (5.8.D.1)$$

Define $\mathbf{R}_{\bar{\mathcal{S}}}$ as the correlation matrix of $\bar{\mathcal{S}}$, where

$$\mathbf{R}_{\bar{\mathcal{S}}}[a, b] = \bar{\rho}_{kim}^{k'i'm'}, \quad (5.8.D.2)$$

and the coefficient indices are given by

$$\begin{aligned} a &= (k-1)NM + (i-1)M + m, \\ b &= (k'-1)NM + (i'-1)M + m'. \end{aligned}$$

Since $\mathbf{R}_{\bar{\mathcal{S}}}$ is the correlation matrix of $\bar{\mathcal{S}}$, following similar steps as for the proof in Part 1 of Theorem 1, we arrive at $\text{rank}(\mathbf{R}_{\bar{\mathcal{S}}}) = KNM$ if $\dim(\bar{\mathcal{S}}) = KNM$.

Moreover, combining (5.8.A.1) with (5.8.D.1) and (5.8.D.2), we have

$$\mathbf{H} = \mathbf{R}_{\bar{\mathcal{S}}}.$$

Thus, $\text{rank}(\mathbf{H}) = KNM$ and \mathbf{H} is invertible.

Finally, similar to the proof in Part 2 of Theorem 1, given \mathbf{H} is invertible, the asymptotic sum-capacity is given by

$$C_{\text{sum,sec}}^{\text{as}} = H(\mathbf{d}) = \sum_{k=1}^K H(\mathbf{d}_k). \quad (5.8.D.3)$$

This completes the proof for Corollary 2. ■

Uplink WCDMA Channel with Imperfect CSIR

In Chapter 5, the capacity region of an uplink WCDMA channel has been derived assuming that perfect CSI is available at the receiver. In order to realize the capacity region in Chapter 5 the receiver needs to know the CSI to: i) perform matched filtering and ii) implement an optimal decoding scheme based on the transition pdf of the channel. In this chapter, we continue with the capacity limit of the uplink WCDMA channel but assume that only *imperfect CSI* is available at the receiver. Accordingly, the receiver first discretizes the continuous-time received signal using the mismatched filtering based on the imperfect CSIR. The resulting discrete-time signals are then decoded considering two different decoding strategies, i.e., an optimal decoding strategy based on the specific statistics of channel estimation error and a sub-optimal decoding strategy treating the signal associated with channel estimation error as additive noise with worst-case distribution. The achievable rate regions achieved by the proposed decoding strategies are characterized to exemplify the benefit of exploiting the knowledge on the statistics of the channel estimation error. Numerical simulations also assess the effect of the CSI imperfectness on the achievable rate, which reveals that finite constellation inputs are less sensitive to the estimation accuracy than Gaussian input, especially in the high SNR regime.

6.1 Related Works and Motivation

In most studies on channel capacity, it is common to assume that channel state is perfectly known at the receiver and/or the transmitter. However, in realistic scenarios, perfect CSI is hard to acquire due to various practical limitations such as limited resources and time-variance of nature [CJKR10]. In practice, the CSIR is typically obtained using training sequences, which often lead to the estimation errors due to time-varying nature of the channel, especially in wireless communications. Therefore, the channel capacity with imperfect CSIR is important for

the assessment of real systems and has received substantial attention over the recent decade [HH03, YG06, CJKR10, Méd00, LSK12]. For instance, a lower bound on the information theoretic capacity, i.e., achievable rate, achieved with a training-based scheme was derived in [HH03], where the effect of the training interval on the achievable rate was also studied. In [YG06], lower and upper bounds on the capacity under channel estimation errors were analyzed assuming MMSE channel estimation at the receiver. In [CJKR10], ergodic achievable rates of a fading multi-user MIMO broadcast channel with imperfect CSI have been characterized based on downlink training and CSI feedback.

In [HH03, YG06, CJKR10], the channel estimates are modeled as Gaussian random variables. An alternative approach is to consider the channel estimates as deterministic values, e.g., mean values of random channel coefficients [Méd00, LSK12]. For example, in [Méd00], the authors derived upper and lower bounds on the mutual information considering deterministic channel estimates and investigated the effect of the CSI imperfectness through the gap between the upper and lower bounds, while the imperfectness is described by variance of the channel estimation error. In [LSK12], the effect of CSI knowledge was studied for a MIMO channel with interference from other terminals when the estimated channel at the receiver is assumed to be deterministic.

In addition, most previous studies on the channel capacity with imperfect CSIR have been performed under the assumption that the input signal follows a Gaussian distribution, which often enables to derive closed-form capacity bounds, convenient for the analysis. However, in real cellular networks finite constellation inputs (e.g., PSK, QAM, etc) usually with uniform distribution are used. Motivated from a more practical perspective, in this chapter we analyze the capacity of an uplink WCDMA system with imperfect CSIR considering finite constellation inputs.

In the following, we model the channel estimates as deterministic parameters, i.e., mean values of the channel parameters, which are obtained at the receiver. Then, the receiver performs decoding based on this CSI knowledge. Since the receiver structure is implemented based on the imperfect CSI, this leads to mismatched decoding at the receiver. There have been some studies on the capacity with mismatched decoding at the receiver [Lap96, GLT00, KSS93, SMF14]. The capacity with the mismatched decoding including the optimization of the input distribution is unknown and a difficult open problem. In our setup, the optimization over the input distribution is not considered since we focus on a standard WCDMA cellular network where uniformly distributed finite modulation schemes are assumed [3GPP]. Consequently, in this chapter, we derive achievable rate regions, i.e., capacity inner bounds, for the uplink WCDMA system considering imperfect CSIR and finite constellation inputs. For comparison, the corresponding achievable rate regions for inputs with arbitrary distributions and Gaussian input are also provided in this chapter.

In particular, we derive an *equivalent*¹ discrete-time MIMO MAC model assum-

¹ Throughout this chapter, the term “equivalent” is used for the *equivalent matrix represen-*

ing mismatched filtering at the receiver. The following achievable rate regions are then characterized based on the equivalent discrete-time channel considering two different decoding strategies. Firstly, we derive an achievable rate region achieved by optimal decoding² at the receiver. Since a closed-form expression is not available for arbitrary distributions of the channel estimation errors, the computation of this achievable rate region requires Monte Carlo simulations with a high complexity. By assuming the equivalent channel estimation errors follow Gaussian distributions, we derive a simpler expression for the achievable rate region, which only depends on the covariance matrices of the equivalent channel estimation errors and can be computed with less complexity. Secondly, we derive an achievable rate region assuming sub-optimal decoding, in which the receiver simply treats the signal associated with the channel estimation error as additive noise with worst-case distribution, i.e., additive Gaussian noise [HH03, YG06].

Numerical results are then provided to show that performance gains can be obtained by exploiting the knowledge on the statistics of the channel estimation errors instead of simply treating them as additive Gaussian noise. We also numerically evaluate the effect of imperfectness and the sensitivity of the achievable rates with respect to the estimation accuracy.

The rest of this chapter is organized as follows: In Section 6.2, the considered signal model, which leads to the discrete-time equivalent channel, is presented. In Section 6.3, achievable rate regions corresponding to the optimal and sub-optimal decoding schemes are characterized. Numerical results are provided in Section 6.4. Finally, Section 6.5 concludes the chapter.

6.2 Problem Setup

Similar to Chapter 5, we begin with a signal model reflecting the practical operation of the uplink WCDMA PHY based on the 3GPP release 11 specification [3GPP]. Accordingly, we consider a K -user uplink WCDMA channel with M streams for each I/Q branch and spreading factor N_{sf} . The transmitted signal for user k is given by

$$x_k(t) = \sqrt{E_k} \sum_{i=1}^N \sum_{m=1}^M d_{ki}^m s_{ki}^m(t), \quad (6.1)$$

where N denotes the number of transmitted symbols from each user, E_k is the transmit power of user k , d_{ki}^m is the i -th symbol of the m -th stream for user k with $\mathbb{E}\{|d_{ki}^m|^2\} = 1$, and $s_{ki}^m(t) = \frac{1}{\sqrt{N_{\text{sf}}}} \sum_{n=0}^{N_{\text{sf}}-1} c_{ki}^m[n] p(t - (i-1)T_s - nT_c)$ is the signature waveform for the i -th symbol of the m -th stream for user k . $p(t)$ is the chip waveform with unit power and finite bandwidth, T_c is the chip duration, and

tation of the discrete-time signal resulting from the mismatched filtering.

² Optimal decoding is done using the equivalent channel of the discrete-time signal resulting from the mismatched filtering.

$T_s = N_{\text{sf}}T_c$ is the symbol duration. $c_{ki}^m[n]$ denotes the spreading sequence which satisfies $\sum_{n=0}^{N_{\text{sf}}-1} |c_{ki}^m[n]|^2 = N_{\text{sf}}$. We consider a CDMA system with long scrambling codes, in which a different spreading sequence $\{c_{ki}^m[n]\}_n$ is used for each transmitted symbol d_{ki}^m .

We also assume a tapped-delay line channel model with L multi-paths [Ver98, Chap. 2] for each user, i.e.,

$$h_k(t) = \sum_{l=1}^L g_{kl} \delta(t - \tau_{kl}),$$

where g_{kl} and τ_{kl} denote the channel coefficient and the propagation delay for the l -th path of user k , respectively. The received signal is then given by

$$\begin{aligned} r(t) &= \sum_{k=1}^K h_k(t) * x_k(t - \lambda_k) + n(t) \\ &= \sum_{k=1}^K \sum_{i=1}^N \sum_{m=1}^M \sqrt{E_k} d_{ki}^m \sum_{l=1}^L g_{kl} s_{ki}^m(t - \lambda_k - \tau_{kl}) + n(t), \end{aligned} \quad (6.2)$$

where λ_k denotes the time delay of the transmitted signal from user k , $*$ denotes the convolution operation, and $n(t)$ represents the additive complex Gaussian random noise with zero mean and power spectral density $N_0/2 = \sigma^2$.

6.2.1 Mismatched filtering

It has been shown in the previous chapter that the received signal $r(t)$ passing through a bank of matched filters, where $r(t)$ is matched to the signature waveforms $\{s_{ki}^m(t - \lambda_k - \tau_{kl})\}_{k,m,i,l}$, followed by MRC using the channel gains $\{g_{kl}\}_{k,l}$ as weighting factors, results in a sufficient statistic for decoding $\mathbf{d} = [d_{11}^1, \dots, d_{KN}^M]^T$ based on $r(t)$. However, in order to perform the matched filtering and MRC, the receiver needs to have perfect knowledge on $\{s_{ki}^m(t - \lambda_k - \tau_{kl})\}_{k,m,i,l}$ and $\{g_{kl}\}_{k,l}$, which is not easy to obtain in practice. Especially in an environment where the channel gains $\{g_{kl}\}_{k,l}$ vary quickly and/or the estimation precision requirements are high. For instance in high data rate systems, a very high speed timing is required, which makes accurate estimation of λ_k and τ_{kl} difficult.

Therefore, we assume that only partial CSI is available at the receiver. In particular, we assume that the channel coefficient g_{kl} is random and the receiver does not have the realization of g_{kl} but only the distribution of g_{kl} . Let us assume that

$$g_{kl} = \hat{g}_{kl} + \varepsilon_{kl},$$

where \hat{g}_{kl} is the mean value, which is deterministic, corresponds to the estimated channel, and is known at the receiver and ε_{kl} is the random channel estimation error. Similarly for the timing, we assume that

$$\lambda_k + \tau_{kl} = \hat{\lambda}_k + \hat{\tau}_{kl} + \gamma_{kl},$$

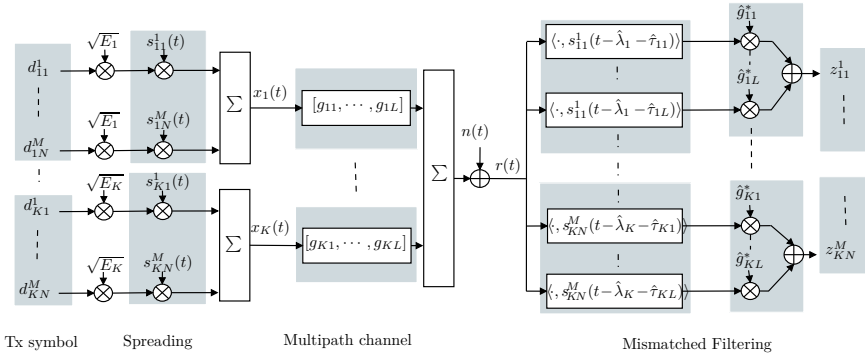


Figure 6.1: Transceiver block diagram of an uplink WCDMA system with imperfect CSIR.

where the estimated timing $\hat{\lambda}_k + \hat{\tau}_{kl}$ is deterministic and available at the receiver and γ_{kl} is the random timing error including the timing errors of both user delay and multi-path delay.

By keeping the same receiver structure as used for the perfect CSIR case in Chapter 5 case but replacing the signature waveforms and channel coefficients by their corresponding estimated versions $\{s_{ki}^m(t - \hat{\lambda}_k - \hat{\tau}_{kl})\}_{k,m,i,l}$ and $\{\hat{g}_{kl}\}_{k,l}$, we arrive at the system model with imperfect CSIR and mismatched filtering as shown in Figure 6.1. The received signal corresponding to the i -th symbol of the m -th stream of user k is given by

$$\begin{aligned}
 z_{ki}^m &= \sum_{l=1}^L \hat{g}_{kl}^* \int_{-\infty}^{\infty} r(t) s_{ki}^m(t - \hat{\lambda}_k - \hat{\tau}_{kl})^* dt \\
 &= \sum_{l=1}^L \sum_{k'=1}^K \sum_{i'=1}^N \sum_{m'=1}^M \sum_{l'=1}^L \sqrt{E_{k',i'}} d_{k',i'}^{m'} \hat{g}_{kl}^* g_{k'l'} \tilde{\rho}_{(k'im'l')}^{(k'i'm'l')} + n_{ki}^m, \quad (6.3)
 \end{aligned}$$

where $\tilde{\rho}_{(k'im'l')}^{(k'i'm'l')}$ is the mismatched correlation coefficient, given by

$$\tilde{\rho}_{(k'im'l')}^{(k'i'm'l')} = \int_{-\infty}^{\infty} s_{ki}^m(t - \lambda_k - \tau_{kl})^* s_{k'i'}^{m'}(t - \hat{\lambda}_{k'} - \hat{\tau}_{k'l'}) dt$$

and n_{ki}^m is the equivalent noise term associated with z_{ki}^m , i.e.,

$$n_{ki}^m = \sum_{l=1}^L \hat{g}_{kl}^* \int_{-\infty}^{\infty} n(t) s_{ki}^m(t - \hat{\lambda}_k - \hat{\tau}_{kl})^* dt.$$

As the received signal after the mismatched filtering $\{z_{ki}^m\}_{k,m,i}$ may no longer be a sufficient statistic, we derive achievable rate regions of the uplink WCDMA

system with imperfect CSIR. Even if those are *only* capacity inner bounds, they are still very useful results since the underlying assumptions correspond to a typical receiver structure in practical WCDMA systems. Moreover, since the receiver is constructed based on the optimal assumption, those achievable rate regions approach the capacity region when the estimation errors tend to zero, which is practically interpreted as sufficiently small.

6.2.2 Matrix representation

A matrix canonical form is useful to characterize the channel capacity. By following similar steps as in [DOKP14], a matrix canonical form of the equivalent channel with imperfect CSIR using mismatched receiver can be obtained from (6.3) as

$$\mathbf{z} = \sum_{k=1}^K \sqrt{E_k} \tilde{\mathbf{H}}_k \mathbf{d}_k + \mathbf{n}, \quad (6.4)$$

where $\mathbf{z} := [z_{11}^1, \dots, z_{KN}^M]^T \in \mathbb{C}^{KNM \times 1}$, $\mathbf{d}_k := [d_{k1}^1, \dots, d_{kN}^M]^T \in \mathbb{C}^{NM \times 1}$, and $\mathbf{n} := [n_{11}^1, \dots, n_{KN}^M]^T \in \mathbb{C}^{KNM \times 1}$. In (6.4), the equivalent mismatched channel $\tilde{\mathbf{H}}_k$, *unknown*³ at the receiver is given by

$$\tilde{\mathbf{H}}_k = \begin{bmatrix} \hat{\mathbf{G}}_1^\dagger \tilde{\mathbf{R}}_k^1 \mathbf{G}_k \\ \vdots \\ \hat{\mathbf{G}}_K^\dagger \tilde{\mathbf{R}}_k^K \mathbf{G}_k \end{bmatrix} \in \mathbb{C}^{KNM \times NM},$$

where \mathbf{G}_k is the channel gain matrix for user k , defined by

$$\mathbf{G}_k = \text{blkdiag} \left(\underbrace{\mathbf{g}_k, \dots, \mathbf{g}_k}_{MN \text{ vectors}} \right) \in \mathbb{C}^{LNM \times NM}$$

with $\mathbf{g}_k = [g_{k1}, \dots, g_{kL}]^T \in \mathbb{C}^{L \times 1}$. The mismatched correlation matrix $\tilde{\mathbf{R}}_k^{k'}$ is defined as

$$\tilde{\mathbf{R}}_k^{k'} = \begin{bmatrix} \tilde{\rho}_{(k111)}^{(k'111)} & \dots & \tilde{\rho}_{(k11L)}^{(k'11L)} & \dots & \tilde{\rho}_{(k111)}^{(k'NML)} \\ \tilde{\rho}_{(k112)}^{(k'111)} & \dots & \tilde{\rho}_{(k112)}^{(k'i'1L)} & \dots & \tilde{\rho}_{(k112)}^{(k'NML)} \\ \vdots & \vdots & \vdots & \vdots & \vdots \\ \tilde{\rho}_{(kNML)}^{(k'111)} & \dots & \tilde{\rho}_{(kNML)}^{(k'11L)} & \dots & \tilde{\rho}_{(kNML)}^{(k'NML)} \end{bmatrix} \in \mathbb{C}^{NML \times NML}, \quad (6.5)$$

and the estimated channel gain matrix $\hat{\mathbf{G}}_k$ is obtained by replacing g_{kl} by \hat{g}_{kl} in \mathbf{G}_k .

³ For distinction, throughout this chapter the tilde notation ($\tilde{\cdot}$) is used to denote a *mismatched* parameter, which is effected by the estimation error, unknown at the receiver, whereas the hat notation ($\hat{\cdot}$) is used to denote an *estimated* parameter, which is known at the receiver.

Given that $\{s_{ki}^m(t - \hat{\lambda}_k - \hat{\tau}_{kl})\}_{k,m,i,l}$ and $\{\hat{g}_{kl}\}_{k,l}$ are available at the receiver, the equivalent estimated channel

$$\hat{\mathbf{H}}_k = \begin{bmatrix} \hat{\mathbf{G}}_1^\dagger \hat{\mathbf{R}}_k^1 \hat{\mathbf{G}}_k \\ \vdots \\ \hat{\mathbf{G}}_K^\dagger \hat{\mathbf{R}}_k^K \hat{\mathbf{G}}_k \end{bmatrix} \in \mathbb{C}^{KNM \times NM}$$

is *known* at the receiver, where the estimated correlation matrix $\hat{\mathbf{R}}_k^k$, is obtained by replacing the mismatched correlation coefficient $\hat{\rho}_{(k' i' m' l')}^{(k' i' m' l')}$ by the estimated correlation coefficient $\hat{\rho}_{(k i m l)}^{(k' i' m' l')} = \int_{-\infty}^{\infty} s_{ki}^m(t - \hat{\lambda}_k - \hat{\tau}_{kl})^* s_{k' i'}^{m'}(t - \hat{\lambda}_{k'} - \hat{\tau}_{k' l'}) dt$ in $\hat{\mathbf{R}}_k^{k'}$ from (6.5). Let us denote $\Delta \mathbf{H}_k := \hat{\mathbf{H}}_k - \hat{\mathbf{H}}_k$ as the equivalent channel estimation error, the signal model in (6.4) can be rewritten as

$$\mathbf{z} = \sum_{k=1}^K (\sqrt{E_k} \hat{\mathbf{H}}_k \mathbf{d}_k + \sqrt{E_k} \Delta \mathbf{H}_k \mathbf{d}_k) + \mathbf{n}. \quad (6.6)$$

Moreover, by following the similar steps as in Appendix 5.8.A from Chapter 5, we can show that \mathbf{n} is a zero-mean Gaussian random vector with covariance matrix $\sigma^2 \hat{\mathbf{H}}$, i.e., $\mathbf{n} \sim \mathcal{CN}(0, \sigma^2 \hat{\mathbf{H}})$, where $\hat{\mathbf{H}} = [\hat{\mathbf{H}}_1 \cdots \hat{\mathbf{H}}_K] \in \mathbb{C}^{KNM \times KNM}$.

The signal model in (6.6) corresponds to a traditional discrete-time channel model for a channel with imperfect CSI [HH03, YG06, CJKR10, Méd00, LSK12], in which the transmitted signal is divided into two parts: one is associated with the estimated channel ($\sum_{k=1}^K \sqrt{E_k} \hat{\mathbf{H}}_k \mathbf{d}_k$) and the other is associated with the channel estimation error ($\sum_{k=1}^K \sqrt{E_k} \Delta \mathbf{H}_k \mathbf{d}_k$). Typically, the signal associated with the channel estimation error is treated as extra noise combined with \mathbf{n} . In this chapter, we next consider two different decoding strategies categorized based on the way that $\sum_{k=1}^K \sqrt{E_k} \Delta \mathbf{H}_k \mathbf{d}_k$ is treated: The first one is to do the optimal decoding by exploiting the true statistic of $\sum_{k=1}^K \sqrt{E_k} \Delta \mathbf{H}_k \mathbf{d}_k$. The second one is the simple approach where the receiver simply treats $\sum_{k=1}^K \sqrt{E_k} \Delta \mathbf{H}_k \mathbf{d}_k$ as additional noise.

Remark 6.1. It is worth noting that the covariance matrix of the equivalent noise \mathbf{n} depends on the estimated channel, i.e., $\hat{\mathbf{H}}$. The literature often studies the performance of communication systems using discrete-time model only, which leads to the situation that the impact of imperfect CSIR on the noise is neglected. Since the channel estimation influences the matched filtering and MRC, in our setup the impacts of the imperfect CSIR both on the desired signal and equivalent noise are taken into account.

Remark 6.2 (Optimality of the mismatched filtering). If the receiver has perfect knowledge on the timing offset (no timing estimation error, only channel gain estimation errors) and performs joint decoding the channel gains $\mathbf{g} := [g_{11}, \dots, g_{KL}]^T \in \mathbb{C}^{KL \times 1}$ and the transmitted messages $\mathbf{d} := [d_{11}^M, \dots, d_{KN}^M]^T \in \mathbb{C}^{KM \times 1}$, it can be

shown that the proposed receiving structure is optimal. Indeed, when the timing error vanishes, the proposed mismatched filtering becomes the receiver structure for the maximum likelihood sequence estimation (MLSE) for an unknown channel as in [CP96], by following similar arguments as in [CP96], we can show that the resulting discrete-time signal vector \mathbf{z} is a sufficient statistic for joint estimating and decoding (\mathbf{g}, \mathbf{d}) from $r(t)$, i.e., $(\mathbf{g}, \mathbf{d}) - \mathbf{z} - r(t)$ forms a Markov chain. From the properties of Markov chains, it follows that $\mathbf{d} - \mathbf{z} - r(t)$ is also a Markov chain. Therefore, \mathbf{z} is a sufficient statistic for optimal decoding \mathbf{d} from $r(t)$, and thus, the proposed receiver structure is optimal.

6.3 Achievable Rate Regions

In this section, based on the equivalent channel (6.6) we derive achievable rate regions for the uplink WCDMA channel with imperfect CSIR considering two different assumptions on the decoding scheme at the receiver.

6.3.1 Optimal decoding

First, we derive an achievable rate region achieved by optimal decoding at the receiver. To this end, we compute the transition pdf $p(\mathbf{z}|\mathbf{d}_1, \dots, \mathbf{d}_K)$ of the equivalent channel (6.6), which is used for the decoding criterion at the receiver. This transition pdf depends on statistics of the equivalent channel matrices $\tilde{\mathbf{H}}_k = \hat{\mathbf{H}}_k + \Delta\mathbf{H}_k$, $k = 1, \dots, K$. Since the estimates $(\hat{\lambda}_k + \hat{\tau}_{kl})$ and \hat{g}_{kl} are fixed and given at the receiver, the equivalent estimated channels $\hat{\mathbf{H}}_k$, $k = 1, \dots, K$, are deterministic. Thus, one only needs to average over the randomness of the equivalent channel estimation errors $\Delta\mathcal{H} := [\Delta\mathbf{H}_1, \dots, \Delta\mathbf{H}_K]$. We assume that $\Delta\mathcal{H}$ is independent of \mathbf{d} and \mathbf{n} , then the transition pdf can be written as

$$p(\mathbf{z}|\mathbf{d}_1, \dots, \mathbf{d}_K) = \mathbb{E}_{\Delta\mathcal{H}} \left\{ p(\mathbf{z}|\mathbf{d}_1, \dots, \mathbf{d}_K, \Delta\mathcal{H}) \right\}.$$

Given $(\mathbf{d}_1, \dots, \mathbf{d}_K, \Delta\mathcal{H})$, $\mathbf{z} = \sum_{k=1}^K \sqrt{E_k} (\hat{\mathbf{H}}_k + \Delta\mathbf{H}_k) \mathbf{d}_k + \mathbf{n}$ is a complex Gaussian random vector with mean $\sum_{k=1}^K \sqrt{E_k} (\hat{\mathbf{H}}_k + \Delta\mathbf{H}_k) \mathbf{d}_k$ and covariance matrix $\hat{\mathbf{R}}_{\mathbf{n}} = \sigma^2 \hat{\mathbf{H}}$. Therefore, the transition pdf can be computed as

$$p(\mathbf{z}|\mathbf{d}_1, \dots, \mathbf{d}_K) = \mathbb{E}_{\Delta\mathcal{H}} \left\{ p_{\mathcal{N}}(\mathbf{z}; \sum_{k=1}^K \sqrt{E_k} (\hat{\mathbf{H}}_k + \Delta\mathbf{H}_k) \mathbf{d}_k, \hat{\mathbf{R}}_{\mathbf{n}}) \right\}, \quad (6.7)$$

where $p_{\mathcal{N}}(\mathbf{x}; \mathbf{m}, \Phi)$ denotes the pdf of a complex Gaussian random vector \mathbf{x} with mean \mathbf{m} and covariance matrix Φ , i.e.,

$$p_{\mathcal{N}}(\mathbf{x}; \mathbf{m}, \Phi) = \frac{\exp(-(\mathbf{x} - \mathbf{m})^\dagger \Phi^{-1} (\mathbf{x} - \mathbf{m}))}{\pi^{KMN} \det \Phi}.$$

Assuming that the optimal decoding strategy (maximum a posteriori (MAP) decoding) based on the transition pdf $p(\mathbf{z}|\mathbf{d}_1, \dots, \mathbf{d}_K)$ is employed at the receiver.

The capacity region of the equivalent channel (6.6), provides an achievable rate region for the WCDMA system with imperfect CSIR in (5.2) and follows from the capacity region of a discrete memoryless MAC [Ahl71], [CT06, Chapter 15].

Let us define \mathcal{C} as the capacity region of the uplink WCDMA channel with imperfect CSIR in (5.2), then \mathcal{C} is the closure of the convex hull of the rate vectors (R_1, R_2, \dots, R_K) , where R_1, R_2, \dots, R_K are the maximal number of bits that can be reliably transmitted from user 1, user 2, ..., user K per block of N symbols⁴. Accordingly, an achievable rate region for the uplink WCDMA system with imperfect CSIR, $\mathcal{R} \subseteq \mathcal{C}$ is given by the following lemma.

Lemma 6.1 (Achievable rate region - \mathcal{R}). *An achievable rate region \mathcal{R} for the uplink WCDMA channel with imperfect CSIR in (5.2) is given by the closure of the convex hull of the union of all achievable rate vectors (R_1, R_2, \dots, R_K) satisfying*

$$\sum_{k \in \mathcal{J}} R_k \leq I(\mathbf{d}_{\mathcal{J}}; \mathbf{z} | \mathbf{d}_{\mathcal{J}^c}), \quad (6.8)$$

for all $\mathcal{J} \subseteq \{1, \dots, K\}$ and joint probability mass function (pmf) $p(\mathbf{d}) = \prod_{k=1}^K p(\mathbf{d}_k)$, where \mathcal{J}^c is the complement set of \mathcal{J} and $\mathbf{d}_{\mathcal{J}} = \{\mathbf{d}_k : k \in \mathcal{J}\}$.

The proof of Lemma 6.1 is straight-forward from the achievability proof for the capacity region of the MAC in [Ahl71], [CT06, Chapter 15]. We now use the result from Lemma 6.1 to derive the achievable rate regions of the uplink WCDMA system with imperfect CSIR considering two different assumptions on the distribution of $\Delta \mathbf{H}_k, k = 1, \dots, K$: arbitrary distribution and Gaussian distribution.

Arbitrary Channel Estimation Errors

For arbitrary distributions of the equivalent channel estimation errors $\Delta \mathbf{H}_k, k = 1, \dots, K$, an achievable rate region of the uplink WCDMA system with imperfect CSIR can be characterized as follows:

Theorem 6.3.1 (Arbitrary estimation errors - \mathcal{R}_{ab}). *Let the estimation errors $\Delta \mathbf{H}_k, k = 1, \dots, K$, be independent of \mathbf{d} and \mathbf{n} . An achievable rate region \mathcal{R}_{ab} for the uplink WCDMA channel with imperfect CSIR in (5.2) is given by the closure of the convex hull of the union of all achievable rate vectors (R_1, R_2, \dots, R_K) satisfying*

$$\begin{aligned} \sum_{k \in \mathcal{J}} R_k \leq & -\mathbb{E}_{\mathbf{z}_{\mathcal{J}}, \mathbf{d}_{\mathcal{J}^c}} \left[\log \mathbb{E}_{\Delta \mathcal{H}, \mathbf{d}_{\mathcal{J}}} \left\{ p_{\mathcal{N}} \left(\mathbf{z}_{\mathcal{J}}; \sum_{k \in \mathcal{J}} \sqrt{E_k} \hat{\mathbf{H}}_k \mathbf{d}_k + \sum_{k=1}^K \sqrt{E_k} \Delta \mathbf{H}_k \mathbf{d}_k, \hat{\mathbf{R}}_{\mathbf{n}} \right) \right\} \right] \\ & + \mathbb{E}_{\mathbf{z}_{\text{en}}, \mathbf{d}} \left[\log \mathbb{E}_{\Delta \mathcal{H}} \left\{ p_{\mathcal{N}} \left(\mathbf{z}_{\text{en}}; \sum_{k=1}^K \sqrt{E_k} \Delta \mathbf{H}_k \mathbf{d}_k, \hat{\mathbf{R}}_{\mathbf{n}} \right) \right\} \right], \end{aligned} \quad (6.9)$$

⁴Here, the capacity region is defined for a given channel impulse response and the assumption that a message is coded over sufficiently many blocks of N symbols using the same spreading sequences for all blocks while neglecting the effect of inter-block interference.

for all $\mathcal{J} \subseteq \{1, \dots, K\}$ and joint pmf $p(\mathbf{d}) = \prod_{k=1}^K p(\mathbf{d}_k)$, where $\mathbf{z}_{\mathcal{J}}$ and \mathbf{z}_{en} are given by $\mathbf{z}_{\mathcal{J}} = \sum_{k \in \mathcal{J}} \sqrt{E_k} \hat{\mathbf{H}}_k \mathbf{d}_k + \sum_{k=1}^K \sqrt{E_k} \Delta \mathbf{H}_k \mathbf{d}_k + \mathbf{n}$, $\mathbf{z}_{\text{en}} = \sum_{k=1}^K \sqrt{E_k} \Delta \mathbf{H}_k \mathbf{d}_k + \mathbf{n}$.

Proof. Refer to Appendix 6.6.A. □

Theorem 6.3.1 implies that the rate constraints in (6.8) can be evaluated by taking the expectations of the specific Gaussian pdfs over $\Delta \mathcal{H}$, \mathbf{d} , and \mathbf{z} as in (6.9). However, a closed-form expression for (6.9) is not easy to obtain. Even the numerical characterization of (6.9) via Monte Carlo simulation may require a very high computational complexity for arbitrary distribution of $\Delta \mathcal{H}$, especially in a large system. Thus, we derive a simpler expression for the achievable rate region assuming that the elements of $\Delta \mathcal{H}$ are complex Gaussian random variables.

Remark 6.3. Even though Theorem 6.3.1 characterizes the achievable rate region of the uplink WCDMA system with standard finite constellation inputs, the result in Theorem 6.3.1 holds for inputs with arbitrary distributions (e.g., Gaussian) by replacing the pmf $p(\mathbf{d})$ in Theorem 6.3.1 by a pdf representing the corresponding input.

Gaussian Equivalent Channel Estimation Errors

For further analysis, we now assume that the entries of the equivalent channel estimation error matrices $\Delta \mathbf{H}_k$, $k = 1, \dots, K$ follow zero mean complex Gaussian distributions, which are expressed as $\Delta \mathbf{H}_k \sim \mathcal{MN}(0, \mathbf{U}_k \otimes \mathbf{V}_k)$, $k = 1, \dots, K$ by using the matrix-variate normal distribution notation [GN99, Chap. 2]. In other words, $\text{vec}(\Delta \mathbf{H}_k^T) \sim \mathcal{CN}(0, \mathbf{U}_k \otimes \mathbf{V}_k)$, where $\mathbf{U}_k \in \mathbb{C}^{KNM \times KNM} \succeq 0$ is the row covariance matrix and $\mathbf{V}_k \in \mathbb{C}^{NM \times NM} \succeq 0$ is the column covariance matrix of $\Delta \mathbf{H}_k$. The correlation coefficient between the (m_1, n_1) th and (m_2, n_2) th elements of $\Delta \mathbf{H}_k$ is given by $\mathbb{E}\{(\Delta \mathbf{H}_k)_{m_1, n_1} (\Delta \mathbf{H}_k)_{m_2, n_2}^*\} = (\mathbf{U}_k)_{m_1, m_2} (\mathbf{V}_k)_{n_1, n_2}$. By this assumption, an achievable rate region for the uplink WCDMA channel with imperfect CSIR can be derived using the covariance matrices of $\Delta \mathbf{H}_k$ (i.e. \mathbf{U}_k and \mathbf{V}_k), $k = 1, \dots, K$, as in the following theorem.

Theorem 6.3.2 (Gaussian estimation errors - \mathcal{R}_{ge}). *Let the equivalent channel estimation errors be Gaussian distributed $\Delta \mathbf{H}_k \sim \mathcal{MN}(0, \mathbf{U}_k \otimes \mathbf{V}_k)$, $k = 1, \dots, K$, and independent of \mathbf{d}_k and \mathbf{n} . An achievable rate region \mathcal{R}_{ge} for the uplink WCDMA channel with imperfect CSIR in (5.2) is given by the closure of the convex hull of the union of all achievable rate vectors (R_1, R_2, \dots, R_K) satisfying*

$$\begin{aligned} \sum_{k \in \mathcal{J}} R_k \leq & - \mathbb{E}_{\mathbf{z}_{\mathcal{J}}, \mathbf{d}_{\mathcal{J}^c}} \left[\log \mathbb{E}_{\mathbf{d}_{\mathcal{J}}} \left\{ p_{\mathcal{N}} \left(\mathbf{z}_{\mathcal{J}}; \sum_{k \in \mathcal{J}} \sqrt{E_k} \hat{\mathbf{H}}_k \mathbf{d}_k, \Psi(\mathbf{d}) \right) \right\} \right] \\ & + \mathbb{E}_{\mathbf{z}_{\text{en}}, \mathbf{d}} \left[\log \left\{ p_{\mathcal{N}} \left(\mathbf{z}_{\text{en}}; 0, \Psi(\mathbf{d}) \right) \right\} \right], \end{aligned} \quad (6.10)$$

for all $\mathcal{J} \subseteq \{1, \dots, K\}$ and joint pmf $p(\mathbf{d}) = \prod_{k=1}^K p(\mathbf{d}_k)$, where $\Psi(\mathbf{d})$ is the equivalent estimation error signal plus noise covariance matrix, given by

$$\Psi(\mathbf{d}) = \sum_{k=1}^K E_k \mathbf{U}_k \text{tr}(\mathbf{d}_k \mathbf{d}_k^\dagger \mathbf{V}_k) + \hat{\mathbf{R}}_n,$$

and $\mathbf{z}_{\mathcal{J}}$ and \mathbf{z}_{en} are defined as in Theorem 6.3.1.

Proof. Refer to Appendix 6.6.B. □

By assuming that the elements of $\Delta\mathcal{H}$ are complex Gaussian random variables, the expectations over $\Delta\mathcal{H}$ in (6.9) can be analytically evaluated. This leads to a simpler expression for the achievable rate region, which can be efficiently computed and related to the channel estimation errors via the covariance matrices of $\Delta\mathbf{H}_k$, $k = 1, \dots, K$. Moreover, for an uplink WCDMA system with finite constellation input signal, the inner expectation of the first term in the rate constraint (6.10) becomes the pdf of a *Gaussian mixture* random vector, i.e.,

$$\begin{aligned} \mathbb{E}_{\mathbf{d}_{\mathcal{J}}} \left\{ p_{\mathcal{N}} \left(\mathbf{z}_{\mathcal{J}}; \sum_{k \in \mathcal{J}} \sqrt{E_k} \hat{\mathbf{H}}_k \mathbf{d}_k, \Psi(\mathbf{d}) \right) \right\} = \\ \sum_{\bar{\mathbf{d}}_{\mathcal{J}}} p(\mathbf{d}_{\mathcal{J}} = \bar{\mathbf{d}}_{\mathcal{J}}) \cdot p_{\mathcal{N}} \left(\mathbf{z}_{\mathcal{J}}; \sum_{k \in \mathcal{J}} \sqrt{E_k} \hat{\mathbf{H}}_k \mathbf{d}_k, \Psi(\mathbf{d}) \right) \Big|_{\mathbf{d}_{\mathcal{J}} = \bar{\mathbf{d}}_{\mathcal{J}}}, \end{aligned} \quad (6.11)$$

where $\bar{\mathbf{d}}_{\mathcal{J}}$ is a realization of $\mathbf{d}_{\mathcal{J}}$ and the summation with respect to $\bar{\mathbf{d}}_{\mathcal{J}}$ is over the feasible set of $\mathbf{d}_{\mathcal{J}}$. Therefore, the computation of the rate constraints in (6.10) can be computed similarly as done for the ones with perfect CSIR as in Chapter 5. However, the computation task is slightly different from the perfect CSIR case because each component of the Gaussian mixture distribution in (6.11) corresponding to an input vector \mathbf{d} can have a *different covariance matrix* $\Psi(\mathbf{d})$ due to the effect of the channel estimation errors.

It is worth noting that in order to realize the achievable rate regions in Theorems 6.3.1, 6.3.2, the receiver needs to be capable to exploit the explicit statistics of $\Delta\mathcal{H}$ and employs the optimal decoding scheme based on the transition pdf $p(\mathbf{z}|\mathbf{d}_1, \dots, \mathbf{d}_K)$ in (6.7). In the next sub-section, we derive another achievable rate region, which can be achieved without exploitation the explicit statistics of $\Delta\mathcal{H}$.

Remark 6.4. If the entries of $\Delta\mathbf{H}_k$ follow independent and identically distributed (i.i.d.) zero mean complex Gaussian distribution, it can be considered as a special case of Theorem 6.3.2 with $\mathbf{U}_k \otimes \mathbf{V}_k = \sigma_e^2 \mathbf{I}_{KN^2M^2}$ where σ_e^2 is the error variance. This is a common setup in the relevant literature [HH03, YG06].

6.3.2 Sub-optimal decoding

In this sub-section, we derive another achievable rate region, achieved by a sub-optimal decoding scheme at the receiver, in which the received signal associated with channel estimation errors is treated as additive noise with worst-case distribution.

Let us recall that \mathcal{R}_{ab} in Theorem 6.3.1 is an achievable rate region which is achieved by the optimal decoding based on the transition pdf of the mismatched channel in (6.6). Now, we assume that the receiver simply treats the received signal terms associated with the channel estimation errors in (6.6) (i.e., $\sum_{k=1}^K \sqrt{E_k} \Delta \mathbf{H}_k \mathbf{d}_k$) as additional noise. This yields in an achievable rate region. Let us denote this rate region as \mathcal{R}_{en} , we then have

$$\mathcal{R}_{\text{en}} \subseteq \mathcal{R}_{\text{ab}} \subseteq \mathcal{C}. \quad (6.12)$$

Moreover, it has been shown in [HH03, YG06] that \mathcal{R}_{en} is inner bounded by the capacity region of the corresponding channel with worst-case noise of (6.6), which can be written as

$$\mathbf{z}_{\text{wn}} = \sum_{k=1}^K \sqrt{E_k} \widehat{\mathbf{H}}_k \mathbf{d}_k + \tilde{\mathbf{n}}, \quad (6.13)$$

where the received signal associated with the channel estimation errors plus noise $\mathbf{z}_{\text{en}} = \sum_{k=1}^K \sqrt{E_k} \Delta \mathbf{H}_k \mathbf{d}_k + \mathbf{n}$ is replaced by the worst-case noise, i.e., Gaussian noise with the same covariance matrix, i.e., $\tilde{\mathbf{n}} \sim \mathcal{CN}(0, \mathbf{R}_e + \widehat{\mathbf{R}}_n)$, which is independent of \mathbf{d} , and \mathbf{R}_e is the auto-correlation matrix of $\sum_{k=1}^K \sqrt{E_k} \Delta \mathbf{H}_k \mathbf{d}_k$. Let us denote the capacity region of the equivalent channel with the worst-case noise (6.13) by \mathcal{R}_{wn} . Then, we have

$$\mathcal{R}_{\text{wn}} \subseteq \mathcal{R}_{\text{en}} \subseteq \mathcal{R}_{\text{ab}} \subseteq \mathcal{C}. \quad (6.14)$$

It is expected that when the distribution of $\sum_{k=1}^K \sqrt{E_k} \Delta \mathbf{H}_k \mathbf{d}_k$ is not Gaussian, the achievable rate region with sub-optimal decoding \mathcal{R}_{wn} is smaller than \mathcal{R}_{ab} . However, in compensation, the rate region \mathcal{R}_{wn} can be achieved without requiring the explicit statistics of $\Delta \mathcal{H}$ since the receiver simply treats $\sum_{k=1}^K \sqrt{E_k} \Delta \mathbf{H}_k \mathbf{d}_k$ as additive Gaussian noise regardless of the actual distribution of $\Delta \mathcal{H}$.

Moreover, the achievable rate region with the worst-case noise \mathcal{R}_{wn} can be characterized as in the following theorem.

Theorem 6.3.3 (Worst-case noise - \mathcal{R}_{wn}). *Let the estimation errors $\Delta \mathbf{H}_k, k = 1, \dots, K$, be independent of \mathbf{d} and \mathbf{n} . An achievable rate region \mathcal{R}_{wn} for the uplink WCDMA channel with imperfect CSIR in (5.2) is given by the closure of the convex hull of the union of all achievable rate vectors (R_1, R_2, \dots, R_K) satisfying*

$$\sum_{k \in \mathcal{J}} R_k \leq -\mathbb{E}_{\mathbf{z}_{\text{wn}} \mathcal{J}} \left[\log \mathbb{E}_{\mathbf{d} \mathcal{J}} \left\{ p_{\mathcal{N}} \left(\mathbf{z}_{\text{wn}} \mathcal{J}; \sum_{k \in \mathcal{J}} \sqrt{E_k} \widehat{\mathbf{H}}_k \mathbf{d}_k, \Phi \right) \right\} \right] - \log(\det(\pi e \Phi)), \quad (6.15)$$

for all $\mathcal{J} \subseteq \{1, \dots, K\}$ and joint pmf $p(\mathbf{d}) = \prod_{k=1}^K p(\mathbf{d}_k)$, where $\mathbf{z}_{\text{wn}} \mathcal{J}$ is given by $\mathbf{z}_{\text{wn}} \mathcal{J} = \sum_{k \in \mathcal{J}} \sqrt{E_k} \widehat{\mathbf{H}}_k \mathbf{d}_k + \tilde{\mathbf{n}}$, $\tilde{\mathbf{n}} \sim \mathcal{CN}(0, \Phi)$, and $\Phi = \mathbf{R}_e + \widehat{\mathbf{R}}_n$.

Proof. Refer to Appendix 6.6.C. □

The rate region \mathcal{R}_{wn} is achievable for any arbitrary channel estimation error. Therefore, \mathcal{R}_{wn} is also an achievable rate region for the case of Gaussian equivalent channel estimation errors (in Theorem 6.3.2), i.e., $\mathcal{R}_{\text{wn}} \subseteq \mathcal{R}_{\text{ge}}$ holds for $\Delta \mathbf{H}_k \sim \mathcal{MN}(0, \mathbf{U}_k \otimes \mathbf{V}_k)$, $k = 1, \dots, K$. Moreover, when the input signal follows Gaussian distribution, a closed-form expression for the rate region in Theorem 6.3.3 can be obtained as given in the following corollary.

Corollary 6.3.1 (Worst-case noise with Gaussian input - $\mathcal{R}_{\text{wn}}^{\text{Gauss}}$). *Let the estimation errors $\Delta \mathbf{H}_k$, $k = 1, \dots, K$, be independent of \mathbf{d} and \mathbf{n} . When the input signal \mathbf{d} is Gaussian distributed, an achievable rate region $\mathcal{R}_{\text{wn}}^{\text{Gauss}}$ for the uplink WCDMA channel with imperfect CSIR in (5.2) is given by the closure of the convex hull of the union of all achievable rate vectors (R_1, R_2, \dots, R_K) satisfying*

$$\sum_{k \in \mathcal{J}} R_k \leq \log \det \left(\mathbf{I}_{NM} + \sum_{k \in \mathcal{J}} E_k \hat{\mathbf{H}}_k^\dagger (\mathbf{R}_e + \hat{\mathbf{R}}_n)^{-1} \hat{\mathbf{H}}_k \right).$$

for all $\mathcal{J} \subseteq \{1, \dots, K\}$ and joint pmf $p(\mathbf{d}) = \prod_{k=1}^K p(\mathbf{d}_k)$.

The proof for Corollary 6.3.1 is straight-forward from Theorem 6.3.2 considering Gaussian distributed input signals. When the entries of $\Delta \mathbf{H}_k$ follow i.i.d. zero mean complex Gaussian distributions (i.e., $\mathbf{U}_k \otimes \mathbf{V}_k = \sigma_e^2 \mathbf{I}_{KN^2M^2}$ and $\mathbf{R}_e = \sum_{k \in \mathcal{J}} \sqrt{E_k} \sigma_e^2 \mathbf{I}_{KNM}$), the result in Corollary 6.3.1 corresponds to the results obtained in [HH03, YG06, Méd00], where i.i.d Gaussian estimation errors and Gaussian input signals are assumed.

6.4 Numerical Results

In this section, we numerically compare the performances of the different decoding strategies and evaluate the effect of the imperfect CSIR on the achievable rate. In particular, we evaluate the achievable sum-rate of a two-user uplink WCDMA example⁵.

6.4.1 Parameters Setup

Similarly to Chapter 5, we set the parameters which are close to those in a real uplink UMTS system specified in [3GPTm]: time-variant CDMA with OVSF codes and Gold sequence, spreading factor $N_{\text{sf}} = 4$, squared-root-raised-cosine pulse chip waveform $p(t)$ with roll-off factor 0.22, uniform power allocation $E_1/\sigma^2 = E_2/\sigma^2 =$

⁵In this chapter, we only show the numerical results of a sample setup with two users to exemplify the performance trends. The framework can be used to evaluate the performance of certain real cellular networks by adjusting the system parameters accordingly.

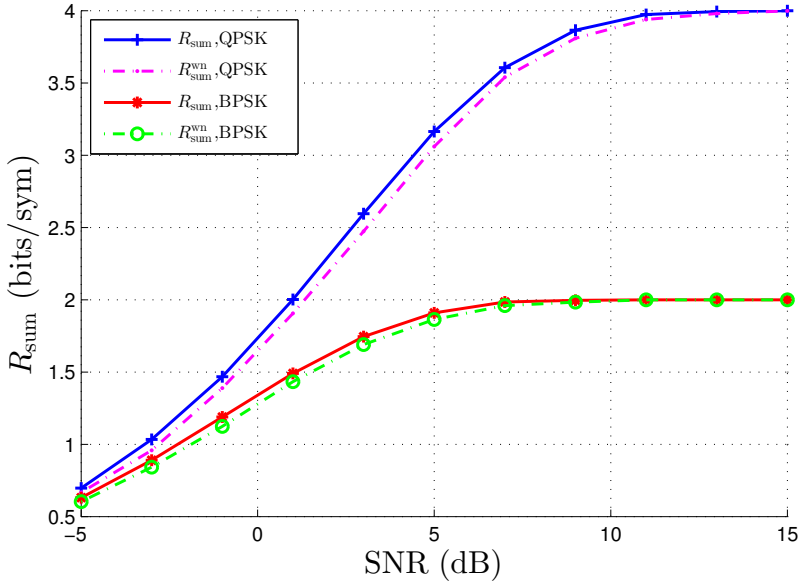


Figure 6.2: Achievable sum-rates with $N = 1$ and $\sigma_e^2 = 0.01$. R_{sum} denotes the achievable sum-rate with the optimal decoding (c.f. Theorem 6.3.2), $R_{\text{sum}}^{\text{wn}}$ denotes the achievable sum-rate when treating the estimation errors as the worst-case noise (c.f. Theorem 6.3.3). All rates are normalized by $1/NM$.

SNR. We assume a frequency-selective channel with $L = 3$ taps, relative path-amplitude vector $[0, -1.5, -3]$ dB, relative path-phase vector $[0, \frac{\pi}{3}, \frac{2\pi}{3}]$, $\|\mathbf{g}_1\|^2 = 2\|\mathbf{g}_2\|^2 = 1$, path-delay vector $[0, \frac{T_c}{2}, T_c]$, uniform random user delay $\lambda_k \sim \mathcal{U}(0, T_s)$.

For the estimation errors, the entries of $\Delta\mathbf{H}_k$ are assumed to be i.i.d complex Gaussian random variables, i.e., $\text{vec}(\Delta\mathbf{H}_k) \sim \mathcal{CN}(0, \sigma_e^2 \mathbf{I}_{KN^2M^2})$. From our independent numerical experiments in which the estimation errors are generated based on a uniform random timing offset error $\gamma_{kl} \sim U[-\frac{\delta}{T_c}, \frac{\delta}{T_c}]$ and a Gaussian random channel coefficient error $\varepsilon_{kl} \sim \mathcal{CN}(0, 10^{-2})$ and $\varepsilon_{kl} \sim \mathcal{CN}(0, 10^{-4})$, the order of variance of each element in the equivalent estimation error matrix $\Delta\mathbf{H}$ is approximately 10^{-2} and 10^{-4} , respectively. Therefore, in the following experiments (except the last one), we consider $\sigma_e^2 = 10^{-2}$ and $\sigma_e^2 = 10^{-4}$.

For the reproducible purpose, the realizations of the equivalent channels \mathbf{H} , which are used for the below experiments, are given in the Appendix 6.6.D.

6.4.2 Optimal and Sub-optimal Decoding Comparison

First, we evaluate the performance for different decoding schemes at the receiver for a simple setup with a 2×2 equivalent channel \mathbf{H} ($N = 1$) and $\sigma_e^2 = 10^{-2}$. A realization of \mathbf{H} in this experiment is given in Appendix 6.6.D.

Figure 6.2 illustrates the achievable sum-rates when the receiver employs the optimal decoding based on the transition pdf $p(\mathbf{z}|\mathbf{d}_1, \dots, \mathbf{d}_K)$ (c.f. Theorem 6.3.2) and when the receiver treats the signal associated with estimation errors as additive worst-case noise (c.f. Theorem 6.3.3). As expected, the achievable sum-rate with the optimal decoding R_{sum} is better than the one with the worst-case noise $R_{\text{sum}}^{\text{wn}}$ for both BPSK and QPSK input signals. This is because even though the estimation errors are unknown, the receiver can exploit knowledge about estimation error statistics instead of simply treating them as additional noise with worst-case distribution.

6.4.3 Impact of The Imperfectness CSIR

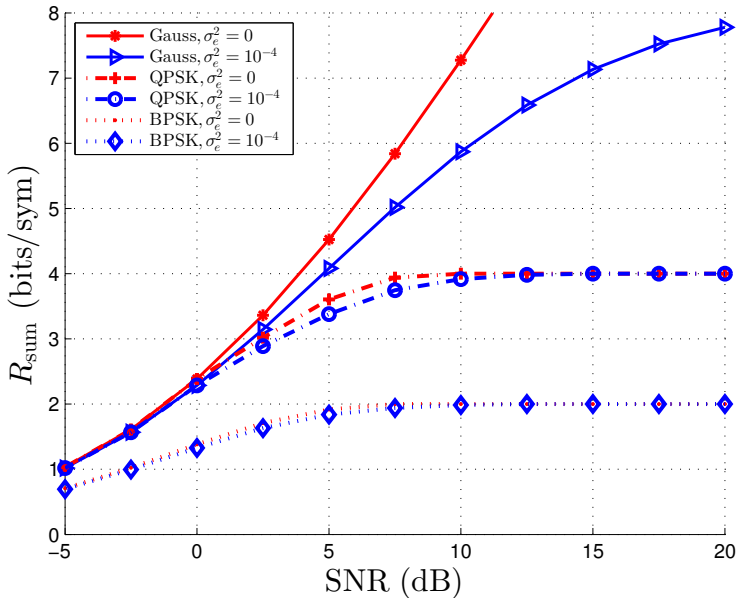


Figure 6.3: Achievable sum-rates with $N = 4$ and $\sigma_e^2 = 10^{-4}$. The dashed lines and dotted line are the achievable sum-rates with QPSK input and BPSK input (c.f. Theorem 6.3.3) and the solid lines are the achievable sum-rates with Gaussian input (c.f. Corollary 6.3.1). All rates are normalized by $1/NM$.

Next, we investigate the impact of the imperfectness of the CSIR on the achievable sum-rate for a larger setup with an 8×8 equivalent channel \mathbf{H} ($N = 4$). A realization of \mathbf{H} in this experiment is given in Appendix 6.6.D.

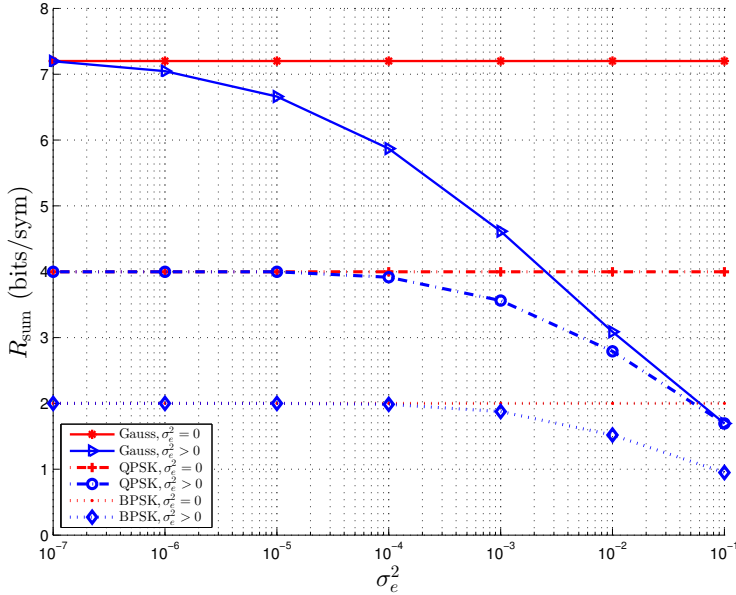


Figure 6.4: Achievable sum-rates according to different values of σ_e^2 with $N = 4$ and SNR = 10dB. The dashed lines and dotted line are the achievable sum-rates with QPSK input and BPSK input (c.f. Theorem 6.3.3) and the solid lines are the achievable sum-rates with Gaussian distributed input (c.f. Corollary 6.3.1). All rates are normalized by $1/NM$.

Figure 6.3 illustrates the achievable sum-rates evaluated using Theorem 6.3.3 with $\sigma_e^2 = 10^{-4}$. For comparison we also include the achievable sum-rates with no estimation errors $\sigma_e^2 = 0$ and Gaussian input signal (c.f. Corollary 6.3.1). Without channel estimation error, the achievable sum-rate with Gaussian input logarithmically increases with increasing SNR. However, the growth of the achievable sum-rates with respect to SNR is significantly degraded with channel estimation errors, since the power of the signal associated with channel estimation error grows linearly with the power of transmitted signal. This effect is reduced for BPSK and QPSK inputs because the capacities with finite constellation inputs saturate at the source entropy bounds in the high SNR regime.

Figure 6.4 shows the achievable sum-rates according to different values of σ_e^2 given that the SNR is fixed at 10dB. It shows that the achievable sum-rates with Gaussian distributed input are significantly degraded with an increasing error vari-

ance, while those with BPSK and QPSK input (at least for small error variances) are less sensitive with respect to the channel estimation error than the Gaussian distributed input case. This follows from the fact that when the SNR is high enough, e.g. SNR = 10dB, the achievable sum-rates with BPSK or QPSK inputs and small channel estimation error still approach the source entropy bound which is also the upper bound for the case without channel estimation error. Next, it is interesting to see that the achievable sum-rates with finite constellation inputs approach the achievable sum-rates with Gaussian distributed inputs as the channel estimation error increases. This behavior corresponds to the low SNR region (as the power of the equivalent additional noise is large) where the finite constellation inputs perform almost as good as the Gaussian.

6.5 Chapter Conclusion

In this chapter, we have investigated the capacity limit of an uplink WCDMA channel with the assumption of imperfect CSIR. The achievable rate regions have been derived considering two different assumptions on the decoding strategy at the receiver: the optimal decoding using the specific statistics of channel estimation error and the sub-optimal decoding treating the signal associated with channel estimation error as the worst-case noise. A simple expression for the achievable rate region when the equivalent channel estimation errors are Gaussian was also presented, which could reduce the numerical computation complexity remarkably. The results show how one can enhance the performance by exploiting the knowledge about the statistics of the estimation error signal instead of traditionally treating them as the additive Gaussian noise. It has also been shown that the impact from the imperfectness of CSIR becomes less sensitive for practical input signals, i.e., finite constellation input signals, compared to Gaussian input signal, especially in the high SNR regime.

6.6 Appendices

6.6.A Proof of Theorem 6.3.1

The proof follows from the rate constraint in (6.8) of Lemma 6.1 as

$$\begin{aligned}
 \sum_{k \in \mathcal{J}} R_k &\leq I(\mathbf{d}_{\mathcal{J}}; \mathbf{z} | \mathbf{d}_{\mathcal{J}^c}) \\
 &= h(\mathbf{z} | \mathbf{d}_{\mathcal{J}^c}) - h(\mathbf{z} | \mathbf{d}_{\mathcal{J}}, \mathbf{d}_{\mathcal{J}^c}) \\
 &= h\left(\sum_{k=1}^K (\sqrt{E_k} \hat{\mathbf{H}}_k \mathbf{d}_k + \sqrt{E_k} \Delta \mathbf{H}_k \mathbf{d}_k) + \mathbf{n} | \mathbf{d}_{\mathcal{J}^c}\right)
 \end{aligned}$$

$$-h\left(\sum_{k=1}^K(\sqrt{E_k}\widehat{\mathbf{H}}_k\mathbf{d}_k + \sqrt{E_k}\Delta\mathbf{H}_k\mathbf{d}_k) + \mathbf{n}|\mathbf{d}\right), \quad (6.6.A.1)$$

Since $\widehat{\mathbf{H}}_k, k = 1, \dots, K$, are deterministic, the first and second terms of (6.6.A.1) can be obtained as

$$\begin{aligned} h\left(\sum_{k=1}^K(\sqrt{E_k}\widehat{\mathbf{H}}_k\mathbf{d}_k + \sqrt{E_k}\Delta\mathbf{H}_k\mathbf{d}_k) + \mathbf{n}|\mathbf{d}_{\mathcal{J}^c}\right) = \\ h\left(\sum_{k \in \mathcal{J}}\sqrt{E_k}\widehat{\mathbf{H}}_k\mathbf{d}_k + \sum_{k=1}^K\sqrt{E_k}\Delta\mathbf{H}_k\mathbf{d}_k + \mathbf{n}|\mathbf{d}_{\mathcal{J}^c}\right) \end{aligned}$$

and

$$h\left(\sum_{k=1}^K(\sqrt{E_k}\widehat{\mathbf{H}}_k\mathbf{d}_k + \sqrt{E_k}\Delta\mathbf{H}_k\mathbf{d}_k) + \mathbf{n}|\mathbf{d}\right) = h\left(\sum_{k=1}^K\sqrt{E_k}\Delta\mathbf{H}_k\mathbf{d}_k + \mathbf{n}|\mathbf{d}\right).$$

Let us define $\mathbf{z}_{\mathcal{J}}$ and \mathbf{z}_{en} as $\mathbf{z}_{\mathcal{J}} := \sum_{k \in \mathcal{J}}\sqrt{E_k}\widehat{\mathbf{H}}_k\mathbf{d}_k + \sum_{k=1}^K\sqrt{E_k}\Delta\mathbf{H}_k\mathbf{d}_k + \mathbf{n}$, $\mathbf{z}_{\text{en}} := \sum_{k=1}^K\sqrt{E_k}\Delta\mathbf{H}_k\mathbf{d}_k + \mathbf{n}$, (6.6.A.1) can be rewritten as

$$\sum_{k \in \mathcal{J}} R_k \leq h(\mathbf{z}_{\mathcal{J}}|\mathbf{d}_{\mathcal{J}^c}) - h(\mathbf{z}_{\text{en}}|\mathbf{d}). \quad (6.6.A.2)$$

Now, let us start with the first term of (6.6.A.2), which can be expressed as

$$h(\mathbf{z}_{\mathcal{J}}|\mathbf{d}_{\mathcal{J}^c}) = -\mathbb{E}_{\mathbf{z}_{\mathcal{J}}, \mathbf{d}_{\mathcal{J}^c}} \left\{ \log p(\mathbf{z}_{\mathcal{J}}|\mathbf{d}_{\mathcal{J}^c}) \right\}, \quad (6.6.A.3)$$

where the conditional pdf $p(\mathbf{z}_{\mathcal{J}}|\mathbf{d}_{\mathcal{J}^c})$ can be computed by averaging over $\Delta\mathcal{H}$ and $\mathbf{d}_{\mathcal{J}}$ as

$$\begin{aligned} p(\mathbf{z}_{\mathcal{J}}|\mathbf{d}_{\mathcal{J}^c}) &= \mathbb{E}_{\Delta\mathcal{H}, \mathbf{d}_{\mathcal{J}}} \left\{ p(\mathbf{z}_{\mathcal{J}}|\mathbf{d}_{\mathcal{J}^c}, \mathbf{d}_{\mathcal{J}}, \Delta\mathcal{H}) \right\} \\ &= \mathbb{E}_{\Delta\mathcal{H}, \mathbf{d}_{\mathcal{J}}} \left\{ p(\mathbf{z}_{\mathcal{J}}|\Delta\mathcal{H}, \mathbf{d}) \right\}. \end{aligned} \quad (6.6.A.4)$$

For given $(\Delta\mathcal{H}, \mathbf{d})$, $\mathbf{z}_{\mathcal{J}}$ is a Gaussian random vector with mean $\sum_{k \in \mathcal{J}}\sqrt{E_k}\widehat{\mathbf{H}}_k\mathbf{d}_k + \sum_{k=1}^K\sqrt{E_k}\Delta\mathbf{H}_k\mathbf{d}_k$ and covariance matrix $\hat{\mathbf{R}}_{\mathbf{n}}$, i.e.,

$$p(\mathbf{z}_{\mathcal{J}}|\Delta\mathcal{H}, \mathbf{d}) = p_{\mathcal{N}}\left(\mathbf{z}_{\mathcal{J}}; \sum_{k \in \mathcal{J}}\sqrt{E_k}\widehat{\mathbf{H}}_k\mathbf{d}_k + \sum_{k=1}^K\sqrt{E_k}\Delta\mathbf{H}_k\mathbf{d}_k, \hat{\mathbf{R}}_{\mathbf{n}}\right). \quad (6.6.A.5)$$

Combining (6.6.A.3)–(6.6.A.5), we have

$$h(\mathbf{z}_{\mathcal{J}}|\mathbf{d}_{\mathcal{J}^c}) = \quad (6.6.A.6)$$

$$\mathbb{E}_{\mathbf{z}_{\mathcal{J}}, \mathbf{d}_{\mathcal{J}^c}} \left[\log \mathbb{E}_{\Delta\mathcal{H}, \mathbf{d}_{\mathcal{J}}} \left\{ p_{\mathcal{N}}\left(\mathbf{z}_{\mathcal{J}}; \sum_{k \in \mathcal{J}}\sqrt{E_k}\widehat{\mathbf{H}}_k\mathbf{d}_k + \sum_{k=1}^K\sqrt{E_k}\Delta\mathbf{H}_k\mathbf{d}_k, \hat{\mathbf{R}}_{\mathbf{n}}\right) \right\} \right].$$

Similarly, the second term of (6.6.A.2) can be computed as

$$h(\mathbf{z}_{\text{en}}|\mathbf{d}) = -\mathbb{E}_{\mathbf{z}_{\text{en}}, \mathbf{d}} \left[\log \mathbb{E}_{\Delta \mathcal{H}} \left\{ p_{\mathcal{N}} \left(\mathbf{z}_{\text{en}}; \sum_{k=1}^K \sqrt{E_k} \Delta \mathbf{H}_k \mathbf{d}_k, \hat{\mathbf{R}}_{\mathbf{n}} \right) \right\} \right]. \quad (6.6.A.7)$$

The rate constraints (6.9) are then obtained from (6.6.A.2), (6.6.A.6), and (6.6.A.7).

6.6.B Proof of Theorem 6.3.2

Let us recall from the proof of Theorem 6.3.1 that

$$\sum_{k \in \mathcal{J}} R_k \leq h(\mathbf{z}_{\mathcal{J}}|\mathbf{d}_{\mathcal{J}^c}) - h(\mathbf{z}_{\text{en}}|\mathbf{d}), \quad (6.6.B.1)$$

where

$$h(\mathbf{z}_{\mathcal{J}}|\mathbf{d}_{\mathcal{J}^c}) = -\mathbb{E}_{\mathbf{z}_{\mathcal{J}}, \mathbf{d}_{\mathcal{J}^c}} \left\{ \log p(\mathbf{z}_{\mathcal{J}}|\mathbf{d}_{\mathcal{J}^c}) \right\}. \quad (6.6.B.2)$$

Now we assume that the entries of $\Delta \mathbf{H}_k$ are zero mean complex Gaussian random variables, i.e., $\Delta \mathbf{H}_k \sim \mathcal{MN}(0, \mathbf{U}_k \otimes \mathbf{V}_k)$, $k = 1, \dots, K$. For given \mathbf{d}_k the random vector $\Delta \mathbf{H}_k \mathbf{d}_k$ is a zero mean complex Gaussian random vector with covariance matrix given by

$$\begin{aligned} \mathbb{E} \left\{ \Delta \mathbf{H}_k \mathbf{d}_k (\Delta \mathbf{H}_k \mathbf{d}_k)^\dagger \right\} &= \mathbb{E} \left\{ \Delta \mathbf{H}_k \mathbf{d}_k \mathbf{d}_k^\dagger \Delta \mathbf{H}_k^\dagger \right\} \\ &= \mathbf{U}_k \text{tr}(\mathbf{d}_k \mathbf{d}_k^\dagger \mathbf{V}_k), \end{aligned}$$

where the second equality comes from [GN99, Theorem 2.3.5]. Let us consider an alternative expression for $p(\mathbf{z}_{\mathcal{J}}|\mathbf{d}_{\mathcal{J}^c})$ in (6.6.A.4) as

$$p(\mathbf{z}_{\mathcal{J}}|\mathbf{d}_{\mathcal{J}^c}) = \mathbb{E}_{\mathbf{d}_{\mathcal{J}}} \{ p(\mathbf{z}_{\mathcal{J}}|\mathbf{d}) \}. \quad (6.6.B.3)$$

For given \mathbf{d} , $\mathbf{z}_{\mathcal{J}} = \sum_{k \in \mathcal{J}} \sqrt{E_k} \hat{\mathbf{H}}_k \mathbf{d}_k + \sum_{k=1}^K \sqrt{E_k} \Delta \mathbf{H}_k \mathbf{d}_k + \mathbf{n}$ is the summation of the deterministic vectors $\sum_{k \in \mathcal{J}} \sqrt{E_k} \hat{\mathbf{H}}_k \mathbf{d}_k$ with the Gaussian random vectors $\sqrt{E_k} \Delta \mathbf{H}_k \mathbf{d}_k$ and \mathbf{n} . Therefore, for given \mathbf{d} , $\mathbf{z}_{\mathcal{J}}$ is a complex Gaussian random vector with mean $\sum_{k \in \mathcal{J}} \sqrt{E_k} \hat{\mathbf{H}}_k \mathbf{d}_k$ and covariance $\Psi(\mathbf{d}) = \sum_{k=1}^K E_k \mathbf{U}_k \text{tr}(\mathbf{d}_k \mathbf{d}_k^\dagger \mathbf{V}_k) + \hat{\mathbf{R}}_{\mathbf{n}}$. Thus,

$$p(\mathbf{z}_{\mathcal{J}}|\mathbf{d}) = p_{\mathcal{N}} \left(\mathbf{z}_{\mathcal{J}}; \sum_{k \in \mathcal{J}} \sqrt{E_k} \hat{\mathbf{H}}_k \mathbf{d}_k, \Psi(\mathbf{d}) \right). \quad (6.6.B.4)$$

Combining (6.6.B.2), (6.6.B.3) and (6.6.B.4) we have

$$h(\mathbf{z}_{\mathcal{J}}|\mathbf{d}_{\mathcal{J}^c}) = -\mathbb{E}_{\mathbf{z}_{\mathcal{J}}, \mathbf{d}_{\mathcal{J}^c}} \left[\log \mathbb{E}_{\mathbf{d}_{\mathcal{J}}} \left\{ p_{\mathcal{N}} \left(\mathbf{z}_{\mathcal{J}}; \sum_{k \in \mathcal{J}} \sqrt{E_k} \hat{\mathbf{H}}_k \mathbf{d}_k, \Psi(\mathbf{d}) \right) \right\} \right]. \quad (6.6.B.5)$$

Similarly, we have

$$h(\mathbf{z}_{\text{en}}|\mathbf{d}) = -\mathbb{E}_{\mathbf{z}_{\text{en}}, \mathbf{d}} \left[\log \left\{ p_{\mathcal{N}} \left(\mathbf{z}_{\text{en}}; 0, \Psi(\mathbf{d}) \right) \right\} \right]. \quad (6.6.B.6)$$

The rate constraints (6.10) are then obtained from (6.6.B.1), (6.6.B.5) and (6.6.B.6).

6.6.C Proof of Theorem 6.3.3

Given that $\tilde{\mathbf{n}}$ is Gaussian noise, the capacity of (6.13), which is served as an achievable rate region in Theorem 6.3.3, can be characterized by

$$\begin{aligned} \sum_{k \in \mathcal{J}} R_k &\leq I(\mathbf{d}_{\mathcal{J}}; \mathbf{z}_{\text{wn}} | \mathbf{d}_{\mathcal{J}^c}) \\ &= h(\mathbf{z}_{\text{wn}} | \mathbf{d}_{\mathcal{J}^c}) - h(\mathbf{z}_{\text{wn}} | \mathbf{d}_{\mathcal{J}}, \mathbf{d}_{\mathcal{J}^c}) \\ &= h\left(\sum_{k=1}^K \sqrt{E_k} \hat{\mathbf{H}}_k \mathbf{d}_k + \tilde{\mathbf{n}} | \mathbf{d}_{\mathcal{J}^c}\right) - h\left(\sum_{k=1}^K \sqrt{E_k} \hat{\mathbf{H}}_k \mathbf{d}_k + \tilde{\mathbf{n}} | \mathbf{d}\right). \end{aligned} \quad (6.6.C.1)$$

Since $\hat{\mathbf{H}}_k, k = 1, \dots, K$, are deterministic and $\mathbf{d}_{\mathcal{J}}, \mathbf{d}_{\mathcal{J}^c}$, and $\tilde{\mathbf{n}}$ are independent, the first and second terms of (6.6.C.1) can be obtained as

$$\begin{aligned} h\left(\sum_{k=1}^K \sqrt{E_k} \hat{\mathbf{H}}_k \mathbf{d}_k + \tilde{\mathbf{n}} | \mathbf{d}_{\mathcal{J}^c}\right) &= h\left(\sum_{k \in \mathcal{J}} \sqrt{E_k} \hat{\mathbf{H}}_k \mathbf{d}_k + \tilde{\mathbf{n}}\right), \\ h\left(\sum_{k=1}^K \sqrt{E_k} \hat{\mathbf{H}}_k \mathbf{d}_k + \tilde{\mathbf{n}} | \mathbf{d}\right) &= h(\tilde{\mathbf{n}}). \end{aligned}$$

Therefore, (6.6.C.1) can be rewritten as

$$\sum_{k \in \mathcal{J}} R_k \leq h\left(\sum_{k \in \mathcal{J}} \sqrt{E_k} \hat{\mathbf{H}}_k \mathbf{d}_k + \tilde{\mathbf{n}}\right) - h(\tilde{\mathbf{n}}). \quad (6.6.C.2)$$

Let us start with the first term of (6.6.C.2), which can be expressed as follows

$$\begin{aligned} h\left(\sum_{k \in \mathcal{J}} \sqrt{E_k} \hat{\mathbf{H}}_k \mathbf{d}_k + \tilde{\mathbf{n}}\right) &= h(\mathbf{z}_{\text{wn}\mathcal{J}}) \\ &= -\mathbb{E}_{\mathbf{z}_{\text{wn}\mathcal{J}}} \{\log p(\mathbf{z}_{\text{wn}\mathcal{J}})\} \\ &= -\mathbb{E}_{\mathbf{z}_{\text{wn}\mathcal{J}}} \{\log \mathbb{E}_{\mathbf{d}_{\mathcal{J}}} \{p(\mathbf{z}_{\text{wn}\mathcal{J}} | \mathbf{d}_{\mathcal{J}})\}\}. \end{aligned}$$

Since $\tilde{\mathbf{n}} \sim \mathcal{CN}(0, \mathbf{R}_e + \hat{\mathbf{R}}_n)$, given $\mathbf{d}_{\mathcal{J}}, \mathbf{z}_{\text{wn}\mathcal{J}} = \sum_{k \in \mathcal{J}} \sqrt{E_k} \hat{\mathbf{H}}_k \mathbf{d}_k + \tilde{\mathbf{n}}$ is a complex Gaussian random vector with mean $\sum_{k \in \mathcal{J}} \sqrt{E_k} \hat{\mathbf{H}}_k \mathbf{d}_k$ and covariance $\Phi = \mathbf{R}_e + \hat{\mathbf{R}}_n$, i.e.,

$$p(\mathbf{z}_{\text{wn}\mathcal{J}} | \mathbf{d}_{\mathcal{J}}) = p_{\mathcal{N}}\left(\mathbf{z}_{\text{wn}\mathcal{J}}; \sum_{k \in \mathcal{J}} \sqrt{E_k} \hat{\mathbf{H}}_k \mathbf{d}_k, \Phi\right).$$

Therefore,

$$\begin{aligned} h\left(\sum_{k \in \mathcal{J}} \sqrt{E_k} \hat{\mathbf{H}}_k \mathbf{d}_k + \tilde{\mathbf{n}}\right) &= \\ &= -\mathbb{E}_{\mathbf{z}_{\text{wn}\mathcal{J}}} \left[\log \mathbb{E}_{\mathbf{d}_{\mathcal{J}}} \left\{ p_{\mathcal{N}}\left(\mathbf{z}_{\text{wn}\mathcal{J}}; \sum_{k \in \mathcal{J}} \sqrt{E_k} \hat{\mathbf{H}}_k \mathbf{d}_k, \Phi\right) \right\} \right]. \end{aligned} \quad (6.6.C.3)$$

Moreover, the second term of (6.6.C.2) is entropy of a complex Gaussian random vector, which can be obtained by

$$h(\bar{\mathbf{n}}) = \log(\det(\pi e \Phi)). \quad (6.6.C.4)$$

The rate constraints (6.15) are then obtained from (6.6.C.2), (6.6.C.4) and (6.6.C.4).

6.6.D Channel Realizations

The realization of \mathbf{H} used for the experiment in Section 6.4.2

$$\mathbf{H} = \begin{bmatrix} 1.004 + 0.000i & 0.167 - 0.297i \\ 0.167 + 0.297i & 0.692 + 0.000i \end{bmatrix}.$$

The realization of \mathbf{H} used for the experiment in Section 6.4.3

$$\mathbf{H} = \begin{bmatrix} 1.00+0.00i & 0.06+0.17i & 0.01+0.00i & 0.00+0.00i & 0.17-0.30i & -0.28+0.19i & -0.01+0.00i & 0.00+0.00i \\ 0.06-0.17i & 2.39+0.00i & -0.08-0.16i & -0.01-0.00i & 0.01-0.03i & 0.76+1.37i & 0.19+0.27i & 0.00+0.00i \\ 0.01+0.00i & -0.08+0.16i & 1.73+0.00i & 0.00+0.18i & 0.00-0.00i & -0.02-0.04i & -0.58+0.10i & 0.27-0.09i \\ 0.00-0.00i & -0.01+0.00i & 0.00-0.18i & 0.43+0.00i & 0.00-0.00i & 0.00-0.00i & -0.04+0.01i & -0.09-0.10i \\ 0.17+0.30i & 0.01+0.03i & 0.00+0.00i & 0.00+0.00i & 0.69+0.00i & -0.08+0.01i & -0.00+0.00i & 0.00+0.00i \\ -0.28-0.19i & 0.76-1.37i & -0.02+0.04i & 0.00+0.00i & -0.08-0.00i & 1.20+0.000 & 0.08-0.03i & 0.00+0.00i \\ -0.01+0.00i & 0.19-0.27i & -0.58-0.10i & -0.04-0.01i & -0.00+0.00i & 0.08+0.03i & 0.95+0.00i & -0.00+0.08i \\ 0.00+0.00i & -0.00-0.00i & 0.27+0.09i & -0.09+0.10i & 0.00+0.00i & 0.00+0.00i & 0.00-0.08i & 0.42+0.00i \end{bmatrix}.$$

Uplink WCDMA Channel with Decision Feedback Equalizer

It is implicitly understood that the achievable rate regions for the uplink WCDMA channels (with and without perfect CSIR) in Chapter 5 and Chapter 6 are obtained under the assumption that the transmitted symbols are jointly decoded at the receiver. However, the complexity of joint decoding grows exponentially with dimensions of the system such as the number of transmitted symbols and size of input constellation. In this chapter, we consider a low-complexity receiver for the uplink WCDMA channel, called decision feedback equalizer (DFE). The DFE decomposes the equivalent MIMO channel into a series of independent point-to-point channels (or streams) with interference pre-subtracted at the receiver. Motivated from the proposed decoding strategies in Chapter 6, we investigate the performance of the DFE when the streams are optimally decoded (using the true statistics of inter-stream interference) and sub-optimally decoded (treating the inter-stream interference as additive Gaussian noise). Numerical results show that although the MMSE DFE is optimal for Gaussian input signal, it is sub-optimal for finite constellation input signals. Moreover, one can also obtain performance gains by treating the inter-stream interference using its true statistics instead of simply treating it as additive Gaussian noise.

7.1 Related Works and Motivation

Typically, in order to achieve the capacity of multiplexing channels such as MAC channel or MIMO channel, the receivers have to decode the transmitted messages jointly [Ahl71, TV05]. However, the complexity of such an approach increases exponentially with dimensions of the system, which makes the decoding scheme difficult to implement in practice. In order to tackle this problem, the DFE [CDEF95a, CDEF95b, YC04], so called successive interference cancellation (SIC) [TV05] has been proposed. For instance, in [CDEF95a, CDEF95b] the MMSE DFE has been used to deal with the inter-symbol interference in linear dispersive channels by

subtracting the effect of each symbol in the remaining signal after it is decoded. In [TV05], performances of various DFEs including MMSE DFE, matched filter (MF) DFE, and decorrelator DFE in a Gaussian point-to-point MIMO channel have been presented. In [YC04], the MMSE DFE has been considered for a Gaussian vector broadcast channel, where coordination is allowed among transmit terminals, but not among receivers.

It has been shown that the MMSE DFE is optimal in the sense of achieving (sum-)capacities of the Gaussian linear dispersive channel [CDEF95a, CDEF95b], Gaussian point-to-point MIMO channel [TV05], and Gaussian vector broadcast channel [YC04] when the input signals follow Gaussian distributions, since then the inter-stream interference is Gaussian. However, the optimality of the DFE is not guaranteed in a more practical system, where the input signals are from finite constellations so that the inter-stream interference's distribution is no longer Gaussian. In this chapter, we investigate the performance of the DFE for the uplink WCDMA channel, in which the input is finite constellation signal. For comparison, the corresponding results for Gaussian input are also included.

We start with an MMSE DFE structure, which is a capacity achieving receiver for Gaussian distributed input. After showing that the MMSE DFE is optimal for a simple two-user setup, we generalize it to our uplink WCDMA channel. In addition to the MMSE DFE, we consider two other DFEs: MF DFE and decorrelator DFE. Since the inter-stream interference is not Gaussian in general, in this chapter we propose two decoding strategies for the DFE motivated from the strategies to deal with the undesired signal in Chapter 6: i) per-stream optimal decoding that uses the true transition pdf of each stream and ii) per-stream sub-optimal decoding that treats the inter-stream interference as Gaussian noise.

The rest of this chapter is organized as follows: Section 7.2 introduces the problem setup. In Section 7.3, we show the optimality of the MMSE DFE for Gaussian input signal. The achievable sum-rates for the DFE with per-stream optimal and per-stream sub-optimal decodings are derived in Section 7.4. Section 7.5 considers three different linear filters: MMSE, MF, and decorrelator for the DFE. Section 7.6 shows the numerical examples and Section 7.7 concludes the chapter.

7.2 Problem Setup

We continue from the continuous-time waveform transmitted signal of a K -user uplink WCDMA channel as in (5.2) from Chapter 5. Let us assume that perfect CSI is available at the receiver and RAKE receiver is used to obtain a sufficient statistic for optimal decoding based on the continuous-time received signal. Similar to other DFE literature, we also consider the achievable sum-rate as performance measurement. Accordingly, we consider the equivalent channel of the system in a compact matrix-form, which is given in (5.38) of Chapter 5 as

$$\mathbf{z} = \mathbf{H}\mathbf{e}\mathbf{d} + \mathbf{n}, \quad (7.1)$$

where $\mathbf{H} \in \mathbb{C}^{KNM \times KNM}$ is the equivalent channel matrix, $\mathbf{E} \in \mathbb{C}^{KNM \times KNM}$ is a diagonalized power allocation matrix, $\mathbf{d} \in \mathbb{C}^{KNM \times 1}$ denotes the input symbol vector, and $\mathbf{n} \in \mathbb{C}^{KNM \times 1}$ is the colored Gaussian random noise vector, $\mathbf{n} \sim \mathcal{CN}(0, \sigma^2 \mathbf{H})$. After noise pre-whitening, the equivalent whitened channel model becomes

$$\mathbf{z}_w = \mathbf{H}_w \mathbf{x} + \mathbf{n}_w, \quad (7.2)$$

where $\mathbf{x} = \mathbf{E}\mathbf{d}$, $\mathbf{z}_w = (\sigma^2 \mathbf{H})^{-1/2} \mathbf{z}$, $\mathbf{H}_w = (\sigma^2 \mathbf{H})^{-1/2} \mathbf{H}$, and $\mathbf{n}_w = (\sigma^2 \mathbf{H})^{-1/2} \mathbf{n}$ is a white Gaussian random noise vector, i.e., $\mathbf{n}_w \sim \mathcal{CN}(0, \mathbf{I})$. Since noise pre-whitening is a full rank linear operation, the capacity of the system is preserved [Gal68]. Throughout this chapter, we focus on the equivalent whitened channel model in (7.2), which can be depicted as in Figure 7.1.

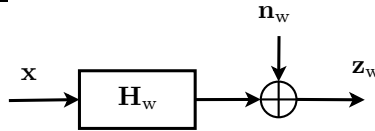


Figure 7.1: Simplified equivalent channel model of the uplink WCDMA system after noise pre-whitening.

Sum-capacity of the uplink WCDMA channel in (5.2) corresponds to the capacity of the equivalent point-to-point MIMO channel in (7.2). For convenience, let us define $N_t = KNM$ as the number of total transmitted symbols and $\mathbf{x} = [x_1 x_2 \dots x_{N_t}]^T$. Typically, the capacity of the uplink WCDMA channel is achieved when x_1, x_2, \dots, x_{N_t} are decoded jointly and optimally at the receiver. However, the complexity of joint decoding increases exponentially with the dimension of \mathbf{x} , i.e., N_t . In the following, we consider a less complexity decoding scheme, the DFE, which decodes x_1, x_2, \dots, x_{N_t} separately, and evaluate the achievable sum-rate achieved by this sub-optimal scheme.

7.3 MMSE DFE for Gaussian Input

In this section, we will show that the MMSE DFE preserves the sum-capacity of the equivalent point-to-point MIMO channel in (7.2) when the input is a Gaussian distributed signal. To this end, we first prove the optimality of the MMSE DFE for a simple two-user setup, then extend it to our uplink WCDMA channel.

7.3.1 MMSE DFE over a two-user setup

First of all, let us consider a two-user setup (i.e., a two-stream scenario) in which the transmitted vector can be expressed as $\mathbf{x} = [\mathbf{x}_1 \ \mathbf{x}_2]^T$ where $\mathbf{x}_1 \in \mathbb{C}^{n_1 \times 1}$ and $\mathbf{x}_2 \in \mathbb{C}^{n_2 \times 1}$. We assume that the received signal \mathbf{z}_w given in (7.2) is passed through

a linear MMSE filter as in Figure 7.2. In this aggregate channel model, the linear MMSE filter is obtained by [TV05]

$$\mathbf{F}_{\text{mmse}} = (\mathbf{H}_w^\dagger \mathbf{H}_w + \mathbf{R}_{xx}^{-1})^{-1} \mathbf{H}_w^\dagger, \quad (7.3)$$

where $\mathbf{R}_{xx} \in \mathbb{C}^{(n_1+n_2) \times (n_1+n_2)}$ is the autocorrelation matrix of the transmitted signal \mathbf{x} . Assuming that \mathbf{x}_1 and \mathbf{x}_2 are statistically independent, \mathbf{R}_{xx} can be rewritten as

$$\mathbf{R}_{xx} = \mathbb{E}\{\mathbf{x}\mathbf{x}^\dagger\} = \begin{bmatrix} \mathbf{R}_{x_1x_1} & \mathbf{0} \\ \mathbf{0} & \mathbf{R}_{x_2x_2} \end{bmatrix}, \quad (7.4)$$

where $\mathbf{R}_{x_1x_1} \in \mathbb{C}^{n_1 \times n_1}$ and $\mathbf{R}_{x_2x_2} \in \mathbb{C}^{n_2 \times n_2}$ are the autocorrelation matrices of \mathbf{x}_1 and \mathbf{x}_2 , respectively.

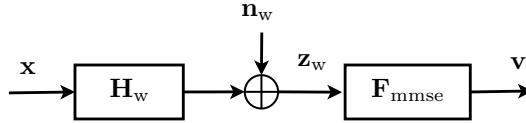


Figure 7.2: Channel model with a linear MMSE filter.

Let us define the error between the transmitted signal and the received signal after the linear MMSE filter by $\mathbf{e} := \mathbf{x} - \mathbf{v}$. By the properties of linear estimation theory [Kay93], the error \mathbf{e} has the following properties:

- \mathbf{e} is independent of \mathbf{v} .
- The covariance matrix of \mathbf{e} is determined by

$$\mathbf{R}_{ee} = (\mathbf{H}_w^\dagger \mathbf{H}_w + \mathbf{R}_{xx}^{-1})^{-1}. \quad (7.5)$$

- If \mathbf{x} is a Gaussian random vector, \mathbf{e} is a Gaussian random vector.

Due to the second property above, the linear MMSE filter \mathbf{F}_{mmse} in (7.3) can be splitted into two parts: the matching channel \mathbf{H}_w^\dagger part and the error covariance matrix \mathbf{R}_{ee} part. The equivalent channel model with the splitted linear MMSE filter is illustrated in Figure 7.3.

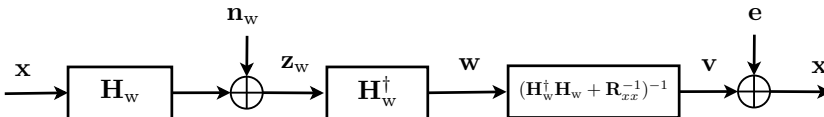


Figure 7.3: Equivalent channel model of the splitted linear MMSE filter.

Hereafter, by adopting the deriving methodology for a Gaussian vector broadcast channel in [YC04], we show that the MMSE DFE is an optimal receiver for decoding \mathbf{x} from \mathbf{v} in a stream-wise fashion for our channel model.

By performing the block Cholesky factorization on $\mathbf{H}_w^\dagger \mathbf{H}_w + \mathbf{R}_{xx}^{-1}$, the error covariance matrix \mathbf{R}_{ee} in (7.5) can be decomposed as

$$\mathbf{R}_{ee} = (\mathbf{U}^\dagger \Delta \mathbf{U})^{-1}, \quad (7.6)$$

where \mathbf{U} is an upper triangular matrix and Δ is a diagonal matrix, which can be expressed as follows

$$\mathbf{U} = \begin{bmatrix} \mathbf{I} & \mathbf{U}_{22} \\ \mathbf{0} & \mathbf{I} \end{bmatrix} \quad \text{and} \quad \Delta = \begin{bmatrix} \Delta_{11} & \mathbf{0} \\ \mathbf{0} & \Delta_{22} \end{bmatrix}, \quad (7.7)$$

in which $\Delta_{11} \in \mathbb{C}^{n_1 \times n_1}$, $\Delta_{22} \in \mathbb{C}^{n_2 \times n_2}$ are diagonal semi-definite positive matrices and $\mathbf{U}_{22} \in \mathbb{C}^{n_1 \times n_2}$. Let us define $\mathbf{e}' = [\mathbf{e}'_1 \mathbf{e}'_2]^T = \mathbf{Ue}$, i.e.,

$$\begin{bmatrix} \mathbf{e}'_1 \\ \mathbf{e}'_2 \end{bmatrix} = \begin{bmatrix} \mathbf{I} & \mathbf{U}_{22} \\ \mathbf{0} & \mathbf{I} \end{bmatrix} \begin{bmatrix} \mathbf{e}_1 \\ \mathbf{e}_2 \end{bmatrix}. \quad (7.8)$$

Then, \mathbf{e}'_1 and \mathbf{e}'_2 are uncorrelated since

$$\begin{aligned} \mathbf{R}_{e'e'} &= \mathbb{E}\{\mathbf{e}'\mathbf{e}'^\dagger\} = \mathbb{E}\{\mathbf{Ue}(\mathbf{Ue})^\dagger\} \\ &= \mathbf{UR}_{ee}\mathbf{U}^\dagger = \Delta^{-1}, \end{aligned} \quad (7.9)$$

where Δ and hereafter Δ^{-1} are diagonal matrices. Furthermore, the received signal over the backward channel from \mathbf{v} to \mathbf{x} in the equivalent channel model shown in Figure 7.3 can be derived as

$$\begin{aligned} \mathbf{x} &= \mathbf{v} + \mathbf{e} \\ \Leftrightarrow \mathbf{x} &= (\mathbf{U}^\dagger \Delta \mathbf{U})^{-1} \mathbf{w} + \mathbf{e} \\ \Leftrightarrow \mathbf{Ux} &= \Delta^{-1} \mathbf{U}^{-\dagger} \mathbf{w} + \mathbf{Ue} \\ \Leftrightarrow \mathbf{x} &= \Delta^{-1} \mathbf{U}^{-\dagger} \mathbf{w} + (\mathbf{I} - \mathbf{U})\mathbf{x} + \mathbf{e}'. \end{aligned} \quad (7.10)$$

Following from (7.10), the equivalent channel can be described using the MMSE DFE structure as in Figure 7.4. Moreover, substituting (7.7) into (7.10) and defining $\mathbf{x}' = [\mathbf{x}'_1 \mathbf{x}'_2]^T = \Delta^{-1} \mathbf{U}^{-\dagger} \mathbf{w} + (\mathbf{I} - \mathbf{U})\mathbf{x}$, the individual \mathbf{x}_2 and \mathbf{x}_1 are obtained by

$$\mathbf{x}_2 = \Delta_{22}^{-1} (-\mathbf{U}_{22}^\dagger \mathbf{w}_1 + \mathbf{w}_2) + \mathbf{e}'_2 = \mathbf{x}'_2 + \mathbf{e}'_2, \quad (7.11)$$

$$\mathbf{x}_1 = \Delta_{11}^{-1} \mathbf{w}_1 - \mathbf{U}_{22} \mathbf{x}_2 + \mathbf{e}'_1 = \mathbf{x}'_1 + \mathbf{e}'_1. \quad (7.12)$$

This implies that once \mathbf{x}_2 is decoded correctly from its sub-channel (7.11), $\mathbf{U}_{22} \mathbf{x}_2$ can be subtracted from the sub-channel for \mathbf{x}_1 as in (7.12) before decoding \mathbf{x}_1 .

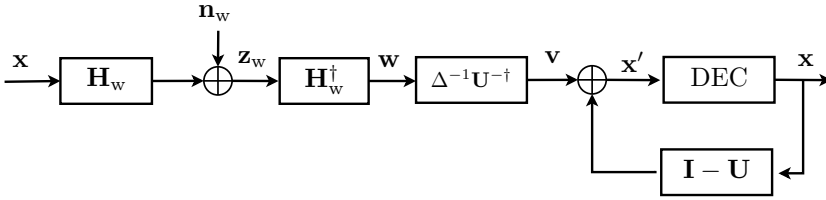


Figure 7.4: Equivalent channel model for the MMSE DFE. The DEC represents a decoding block which is based on successive decoding operation.

We have introduced the structure and decoding procedure of the MMSE DFE. Now, we derive the achievable sum-rate achieved by the MMSE DFE in order to show that the proposed receiver structure is sum-capacity achieving. For the optimal decoding without any post-processing at the receiver, the sum-capacity is given by the mutual information between the input \mathbf{x} and received \mathbf{z}_w , i.e.,

$$R_s = I(\mathbf{x}; \mathbf{z}_w). \quad (7.13)$$

From the fact that the MMSE filter is an invertible linear transformation and does not change the mutual information, we can write

$$R_s = I(\mathbf{x}; \mathbf{z}_w) = I(\mathbf{x}; \mathbf{v}). \quad (7.14)$$

Moreover, due to the properties of the error \mathbf{e} , the backward channel $\mathbf{x} = \mathbf{v} + \mathbf{e}$ is a conventional MIMO Gaussian channel, whose mutual information corresponding to the sum-capacity is given by

$$I(\mathbf{x}; \mathbf{v}) = \log \frac{\det \mathbf{R}_{xx}}{\det \mathbf{R}_{ee}}. \quad (7.15)$$

On the other hand, the achievable sum-rate, which is achieved by the MMSE DFE, is given by

$$R'_s = I(\mathbf{x}_1; \mathbf{x}'_1) + I(\mathbf{x}_2; \mathbf{x}'_2) \quad (7.16)$$

since the MMSE DFE structure decomposes the original channel into two sub-channels that are independently encoded and decoded. The achievable sum-rate in (7.16) can be further expressed as

$$\begin{aligned} R'_s &= \log \frac{\det \mathbf{R}_{x_1 x_1}}{\det \mathbf{R}_{e'_1 e'_1}} + \log \frac{\det \mathbf{R}_{x_2 x_2}}{\det \mathbf{R}_{e'_2 e'_2}} \\ &= \log \frac{\det \mathbf{R}_{x_1 x_1} \mathbf{R}_{x_2 x_2}}{\det \mathbf{R}_{e'_1 e'_1} \mathbf{R}_{e'_2 e'_2}}. \end{aligned} \quad (7.17)$$

In addition, since \mathbf{R}_{xx} and $\mathbf{R}_{e'e'}$ are both diagonal as shown in (7.4) and (7.9), we have the following equalities

$$\begin{aligned}\det \mathbf{R}_{x_1x_1} \mathbf{R}_{x_2x_2} &= \det \mathbf{R}_{xx}, \\ \det \mathbf{R}_{e'_1e'_1} \mathbf{R}_{e'_2e'_2} &= \det \Delta_{11}^{-1} \det \Delta_{22}^{-1} = \det \Delta^{-1}, \\ \det \mathbf{R}_{ee} &= \det(\mathbf{U}^\dagger \Delta \mathbf{U})^{-1} = \det \Delta^{-1}.\end{aligned}$$

Therefore, we finally arrive at

$$\begin{aligned}R'_s &= \log \frac{\det \mathbf{R}_{x_1x_1} \mathbf{R}_{x_2x_2}}{\det \mathbf{R}_{e'_1e'_1} \mathbf{R}_{e'_2e'_2}} \\ &= \log \frac{\det \mathbf{R}_{xx}}{\det \mathbf{R}_{ee}} = R_s.\end{aligned}\tag{7.18}$$

This implies that the MMSE DFE structure preserves the sum-capacity for a two-stream setup when the input signal \mathbf{x} follows a Gaussian distribution.

7.3.2 MMSE DFE over the Uplink WCDMA Channel

Based on the result from the simple two-user setup, we now generalize the MMSE DFE structure to the uplink WCDMA channel, in which we decompose the equivalent channel into N_t point-to-point channels at the receiver. Accordingly, \mathbf{U} and Δ in (7.7) are generalized as

$$\mathbf{U} = \begin{bmatrix} \mathbf{I} & \mathbf{U}_{12} & \mathbf{U}_{13} & \cdots & \mathbf{U}_{1N_t} \\ 0 & \mathbf{I} & \mathbf{U}_{23} & \cdots & \mathbf{U}_{2N_t} \\ \vdots & \vdots & \ddots & \vdots & \vdots \\ 0 & 0 & \cdots & \mathbf{I} & \mathbf{U}_{(N_t-1)N_t} \\ 0 & 0 & \cdots & 0 & \mathbf{I} \end{bmatrix},\tag{7.19}$$

$$\Delta = \begin{bmatrix} \Delta_1 & 0 & 0 & \cdots & 0 \\ 0 & \Delta_2 & 0 & \cdots & 0 \\ \vdots & \vdots & \ddots & \vdots & \vdots \\ 0 & 0 & \cdots & \Delta_{N_t-1} & 0 \\ 0 & 0 & \cdots & 0 & \Delta_{N_t} \end{bmatrix}.\tag{7.20}$$

Then, the equivalent received signal vector is the same as (7.10) in a matrix form and explicitly derived as

$$\begin{aligned}
\begin{bmatrix} \mathbf{x}_1 \\ \mathbf{x}_2 \\ \vdots \\ \mathbf{x}_{N_t-1} \\ \mathbf{x}_{N_t} \end{bmatrix} &= \begin{bmatrix} \Delta_1^{-1} & 0 & 0 & \cdots & 0 \\ -\Delta_2^{-1} \mathbf{U}_{(N_t-1)N_t}^\dagger & -\Delta_2^{-1} & 0 & \cdots & 0 \\ \vdots & \vdots & \vdots & \vdots & \vdots \\ -\Delta_{N_t-1} \mathbf{U}_{2N_t}^\dagger & -\Delta_{N_t-1} \mathbf{U}_{2(N_t-1)}^\dagger & \cdots & \Delta_{N_t-1}^{-1} & 0 \\ -\Delta_{N_t} \mathbf{U}_{1N_t}^\dagger & -\Delta_{N_t} \mathbf{U}_{1(N_t-1)}^\dagger & \cdots & -\Delta_{N_t} \mathbf{U}_{12}^\dagger & \Delta_{N_t}^{-1} \end{bmatrix} \times \\
&\begin{bmatrix} \mathbf{w}_1 \\ \mathbf{w}_2 \\ \vdots \\ \mathbf{w}_{N_t-1} \\ \mathbf{w}_{N_t} \end{bmatrix} - \begin{bmatrix} \mathbf{U}_{12}\mathbf{x}_2 + \mathbf{U}_{13}\mathbf{x}_3 + \cdots + \mathbf{U}_{1N_t}\mathbf{x}_{N_t} \\ \mathbf{U}_{23}\mathbf{x}_3 + \cdots + \mathbf{U}_{2N_t}\mathbf{x}_{N_t} \\ \vdots \\ \mathbf{U}_{(N_t-1)N_t}\mathbf{x}_{N_t} \\ 0 \end{bmatrix} + \begin{bmatrix} \mathbf{e}'_1 \\ \mathbf{e}'_2 \\ \vdots \\ \mathbf{e}'_{N_t-1} \\ \mathbf{e}'_{N_t} \end{bmatrix} \\
&:= \begin{bmatrix} \mathbf{x}'_1 \\ \mathbf{x}'_2 \\ \vdots \\ \mathbf{x}'_{N_t-1} \\ \mathbf{x}'_{N_t} \end{bmatrix} + \begin{bmatrix} \mathbf{e}'_1 \\ \mathbf{e}'_2 \\ \vdots \\ \mathbf{e}'_{N_t-1} \\ \mathbf{e}'_{N_t} \end{bmatrix}. \tag{7.21}
\end{aligned}$$

The DFE structure is then similar to one in Figure 7.4 and the decoding procedure is performed inductively from \mathbf{x}_{N_t} to \mathbf{x}_1 . The optimality of the MMSE DFE for the uplink WCDMA channel is also easily verified as follows.

Since \mathbf{R}_{xx} and $\mathbf{R}_{e'e'}$ are both diagonal, we have

$$\det \mathbf{R}_{xx} = \prod_{i=1}^{N_t} \det \mathbf{R}_{x_i x_i}$$

and

$$\begin{aligned}
\det \mathbf{R}_{ee} &= \det(\mathbf{U}^\dagger \Delta \mathbf{U})^{-1} = \det \Delta^{-1} \\
&= \prod_{i=1}^{N_t} \det \Delta_i^{-1} = \prod_{i=1}^{N_t} \det \mathbf{R}_{e'_i e'_i}. \tag{7.22}
\end{aligned}$$

Therefore, the achievable sum-rate of the uplink WCDMA system, achieved by the MMSE DFE for Gaussian distributed inputs is given by

$$R'_s = \sum_{i=1}^{N_t} I(\mathbf{x}_i; \mathbf{x}'_i) = \sum_{i=1}^{N_t} \log \frac{\det \mathbf{R}_{x_i x_i}}{\det \mathbf{R}_{e'_i e'_i}}$$

$$\begin{aligned}
&= \log \prod_{i=1}^{N_t} \frac{\det \mathbf{R}_{x_i x_i}}{\det \mathbf{R}_{e'_i e'_i}} = \log \frac{\prod_{i=1}^{N_t} \det \mathbf{R}_{x_i x_i}}{\prod_{i=1}^{N_t} \det \mathbf{R}_{e'_i e'_i}} \\
&= \log \frac{\det \mathbf{R}_{xx}}{\det \mathbf{R}_{ee}} = R_s.
\end{aligned} \tag{7.23}$$

This implies that the sum-capacity is preserved for the uplink WCDMA system with the MMSE DFE when the inputs are Gaussian distributed. This result is expected and similar to the optimality of the MMSE DFE for the Gaussian linear dispersive channel or the Gaussian vector broadcast channel [CDEF95a, CDEF95b, YC04]. Next, we exemplify the optimality of the DFE for finite constellation input.

7.4 DFE for Finite Constellation Input

In this section, we analyze the performance of the DFE when the input signals are from finite constellations. We derive the achievable sum-rates of the uplink WCDMA channel considering two decoding strategies, which use the true transition pdf of the channel or treat multi-user and inter-symbol interference (equivalently, inter-stream interference) as worst-case noise.

Let us denote $\mathbf{h}_i \in \mathbb{C}^{N_t \times 1}$ as the i -th column vector of \mathbf{H}_w , the equivalent channel model in (7.2) can be rewritten as

$$\mathbf{z}_w = \mathbf{H}_w \mathbf{x} + \mathbf{n}_w = \sum_{i=1}^{N_t} \mathbf{h}_i x_i + \mathbf{n}_w, \tag{7.24}$$

where x_i denotes the i -th element of the transmitted symbol vector \mathbf{x} . Instead of jointly decoding x_1, \dots, x_{N_t} , the receiver decodes each transmit signal x_i separately using the DFE structure.

It has been shown in [GC01], [TV05, Chapter 8] that the receiver structure of a Vertical Bell Laboratories Layered Space-Time (V-BLAST) system is equivalent to the DFE described in the previous section. We investigate the achievable sum-rate of the DFE using the V-BLAST structure, which can be depicted as in Figure 7.5. Accordingly, the receiver consists of a bank of separate filters to estimate the transmitted symbols per stream independently. We observe that the receiver performs the SIC process, i.e., once a stream is successfully decoded, its associated signal is subtracted from the received signal before the next stream is decoded. Without loss of generality, we assume that the decoding order is from the 1st stream to the N_t -th stream as depicted in Figure 7.5. In this figure, $\mathbf{v}_i \in \mathbb{C}^{N_t \times 1}$, $i = 1, \dots, N_t$ are the filtering vectors and y_i , $i = 1, \dots, N_t$ are the scalar output signals, which are given by

$$y_i = \mathbf{v}_i^\dagger \left(\mathbf{z}_w - \sum_{j=1}^{i-1} \mathbf{h}_j x_j \right) = \mathbf{v}_i^\dagger \left(\sum_{j=i}^{N_t} \mathbf{h}_j x_j + \mathbf{n}_w \right)$$

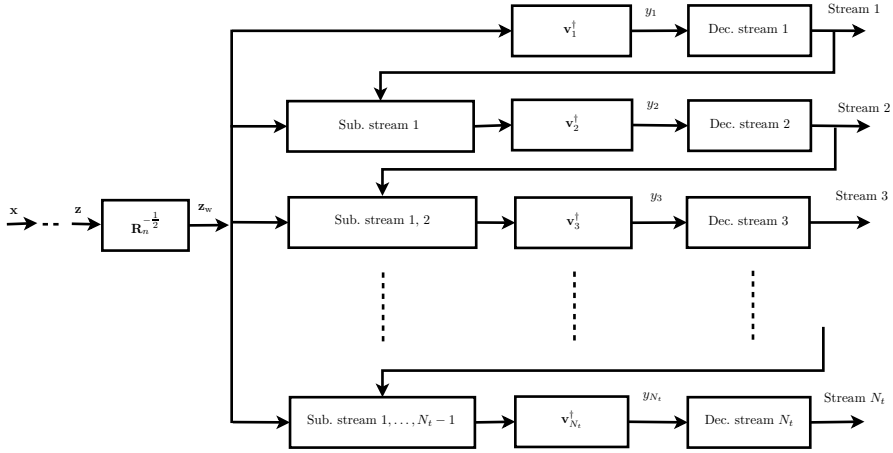


Figure 7.5: The receiver structure of a V-BLAST system equivalent to the DFE.

$$= \mathbf{v}_i^\dagger \mathbf{h}_i x_i + \sum_{j=i+1}^{N_t} \mathbf{v}_i^\dagger \mathbf{h}_j x_j + \mathbf{v}_i^\dagger \mathbf{n}_w, i = 1, \dots, N_t, \quad (7.25)$$

where the first term in the right hand side of (7.25) is the desired signal, the second term is the residual inter-stream interference. When \mathbf{x} is not Gaussian distributed input, $\sum_{j=i+1}^{N_t} \mathbf{v}_i^\dagger \mathbf{h}_j x_j$ is not a Gaussian signal in general.

Motivated from the strategies to deal with the undesired signal in Chapter 6, we propose two decoding strategies for the DFE: i) *per-stream optimal decoding* which performs a MAP criterion using the true transition pdf of each stream based on the true statistics of the residual inter-stream interference and ii) *per-stream sub-optimal decoding* which simply treats the residual inter-stream interference as worst-case noise.

7.4.1 Per-stream Optimal Decoding

Assuming that in order to decode x_i from on y_i , the optimal decoding criterion MAP is used with the true statistics of the inter-stream interference plus noise ($\sum_{j=i+1}^{N_t} \mathbf{v}_i^\dagger \mathbf{h}_j x_j + \mathbf{v}_i^\dagger \mathbf{n}_w$). The achievable sum-rate for the uplink WCDMA channel is then given by

$$R_s = \sum_{i=1}^{N_t} R_i, \quad (7.26)$$

where R_i is the achievable rate for the i -th stream, which is given by the capacity of a point-to-point channel, i.e.,

$$R_i = I(x_i; y_i)$$

$$\begin{aligned}
&= h(y_i) - h(y_i|x_i) \\
&= h\left(\sum_{j=i}^{N_t} \mathbf{v}_i^\dagger \mathbf{h}_j x_j + \mathbf{v}_i^\dagger \mathbf{n}_w\right) - h\left(\sum_{j=i+1}^{N_t} \mathbf{v}_i^\dagger \mathbf{h}_j x_j + \mathbf{v}_i^\dagger \mathbf{n}_w\right) \quad (7.27)
\end{aligned}$$

since each stream is decoded optimally and independently after the interference pre-subtraction.

Similar to the case of joint decoding in Section 6.3.1, a closed form for the achievable rate in (7.27) is not easy to obtain, especially for finite constellation inputs. The achievable rates R_i and R_s are numerically evaluated using Monte Carlo simulations, where each term in the right hand side of (7.27) is the entropy of a Gaussian mixture distribution with $M_c^{N_t}$ components (M_c is the finite constellation size).

7.4.2 Per-stream Suboptimal Decoding

Now, we assume that instead of employing the optimal decoding for each stream, the receiver simply treats inter-stream interference plus estimation errors as the additive Gaussian noises, i.e., worst-case noises with the same covariances. Using the same argument as in Section 6.3.2, the achievable rate of the i -th stream is obtained by

$$R_{i,\text{wn}} = h(\mathbf{v}_i^\dagger \mathbf{h}_i x_i + n_i) - h(n_i), \quad (7.28)$$

where $n_i \sim \mathcal{CN}(0, \sum_{j=i+1}^{N_t} E_j |\mathbf{v}_i^\dagger \mathbf{h}_j|^2 + |\mathbf{v}_i^\dagger \mathbf{v}_i|)$ is the corresponding worst-case noise.

Similarly to the case of joint decoding as in Section 6.3.2, a closed form of the achievable sum-rate can be obtained for Gaussian input signals as

$$R_{s,\text{wn}}^{\text{Gauss}} = \sum_{i=1}^{N_t} \log \left(1 + \frac{E_i |\mathbf{v}_i^\dagger \mathbf{h}_i|^2}{\sum_{j=i+1}^{N_t} E_j |\mathbf{v}_i^\dagger \mathbf{h}_j|^2 + |\mathbf{v}_i^\dagger \mathbf{v}_i|} \right). \quad (7.29)$$

7.5 Linear Filters

In addition to the decoding strategy, the performance of the DFE highly depends on the linear filter vectors \mathbf{v}_i , $i = 1, \dots, N_t$. In the following, we consider three familiar linear filters, i.e., MMSE filter, MF and decorrelator filter.

7.5.1 MMSE DFE

First, we consider the MMSE filter, which is shown to be optimal for Gaussian input in the previous section. For the MMSE DFE, the filter vector for the i -th stream is given by

$$\mathbf{v}_i^{\text{mmse}} = \mathbf{K}_i^{-1} \mathbf{h}_i, \quad i = 1, \dots, N_t, \quad (7.30)$$

where $\mathbf{K}_i = \mathbf{I}_{N_t} + \sum_{j=i+1}^{N_t} E_j \mathbf{h}_j \mathbf{h}_j^\dagger$ is the covariance matrix of the inter-stream interference plus noise of the i -th stream. When the MMSE filter is used, the corresponding signal-to-interference-plus-noise ratio (SINR) of the i -th stream is given by

$$\rho_i^{\text{mmse}} = E_i \mathbf{h}_i^\dagger \mathbf{K}_i^{-1} \mathbf{h}_i, \quad i = 1, \dots, N_t. \quad (7.31)$$

Moreover, the achievable sum-rate for Gaussian distributed input is obtained as in (7.29) by

$$R_{\text{s,mmse}}^{\text{Gauss}} = \sum_{i=1}^{N_t} \log \left(1 + E_i \mathbf{h}_i^\dagger \mathbf{K}_i^{-1} \mathbf{h}_i \right). \quad (7.32)$$

It is worth noting that for Gaussian distributed input, the achievable sum-rates with per-stream optimal and per-stream sub-optimal decodings are the same since the inter-stream interference already has the worst-case distribution, i.e., Gaussian distribution. The achievable sum-rates for finite constellation inputs with per-stream optimal and per-stream sub-optimal decodings are derived from (7.27) and (7.28) by applying the MMSE filter, i.e., $\mathbf{v}_i = \mathbf{v}_i^{\text{mmse}}$.

7.5.2 MF DFE

In the second case, we consider the MF which aims for maximizing the energy of the desired stream without taking the inter-stream interference into consideration. This is the optimal filter for single-input multiple-output (SIMO) channels. The MF for the i -th stream is simply given by

$$\mathbf{v}_i^{\text{mf}} = \mathbf{h}_i, \quad i = 1, \dots, N_t. \quad (7.33)$$

The corresponding SINR of the i -th stream is obtained as

$$\rho_i^{\text{mf}} = \frac{E_i |\mathbf{h}_i^\dagger \mathbf{h}_i|^2}{|\mathbf{h}_i^\dagger \mathbf{h}_i| + \sum_{j=i+1}^{N_t} E_j |\mathbf{h}_i^\dagger \mathbf{h}_j|^2}. \quad (7.34)$$

Then, the achievable sum-rate for Gaussian distributed input (for both per-stream optimal and per-stream sub-optimal decodings) is given by

$$R_{\text{s,mf}}^{\text{Gauss}} = \sum_{i=1}^{N_t} \log \left(1 + \frac{E_i |\mathbf{h}_i^\dagger \mathbf{h}_i|^2}{|\mathbf{h}_i^\dagger \mathbf{h}_i| + \sum_{j=i+1}^{N_t} E_j |\mathbf{h}_i^\dagger \mathbf{h}_j|^2} \right). \quad (7.35)$$

The achievable sum-rates for finite constellation inputs with per-stream optimal and per-stream sub-optimal decodings are derived from (7.27) and (7.28) by applying the MF, i.e., $\mathbf{v}_i = \mathbf{v}_i^{\text{mf}}$.

7.5.3 Decorrelator DFE

The decorrelator aims for the suppression of the inter-stream interference, that is, it completely nulls out the interference regardless of the energy of the desired stream. For the decorrelator DFE, the received filter for the i -th stream is given by [TV05]

$$\mathbf{v}_i^{\text{dc}} = (\mathbf{Q}_i^\dagger \mathbf{Q}_i) \mathbf{h}_i, \quad i = 1, \dots, N_t, \quad (7.36)$$

where \mathbf{Q}_i is a $(N_t - i) \times N_t$ matrix whose rows are orthogonal to the subspace spanned by the vectors $\mathbf{h}_{i+1}, \dots, \mathbf{h}_{N_t}$. This corresponds to the projection of \mathbf{h}_i onto the orthogonal complement of the subspace spanned by $\mathbf{h}_{i+1}, \dots, \mathbf{h}_{N_t}$. Therefore, the decorrelator filter can be further derived as

$$\mathbf{v}_i^{\text{dc}} = \left(\mathbf{I} - \mathbf{H}_{-i} (\mathbf{H}_{-i}^\dagger \mathbf{H}_{-i})^{-1} \mathbf{H}_{-i}^\dagger \right) \mathbf{h}_i, \quad (7.37)$$

where $\mathbf{H}_{-i} = [\mathbf{h}_{i+1}, \dots, \mathbf{h}_{N_t}]$. Note that since $\mathbf{v}_i^{\text{dc}\dagger} \mathbf{h}_i = (\mathbf{Q}_i \mathbf{h}_i)^\dagger \mathbf{Q}_i \mathbf{h}_i$, the decorrelator filter can be interpreted as a combination of two components: the zero-forcing (ZF) filter \mathbf{Q}_i that nulls out the interference from the other streams and the MF of $\mathbf{Q}_i \mathbf{h}_i$ that maximizes the output SNR after the interference nulling. The corresponding SINR for the i -th stream is then given by

$$\rho_i^{\text{dc}} = E_i \left\| \left(\mathbf{I} - \mathbf{H}_{-i} (\mathbf{H}_{-i}^\dagger \mathbf{H}_{-i})^{-1} \mathbf{H}_{-i}^\dagger \right) \mathbf{h}_i \right\|^2. \quad (7.38)$$

Thus, the achievable sum-rate for Gaussian distributed input is obtained as

$$R_{\text{s,dc}}^{\text{Gauss}} = \sum_{i=1}^{N_t} \log \left(1 + E_i \left\| \left(\mathbf{I} - \mathbf{H}_{-i} (\mathbf{H}_{-i}^\dagger \mathbf{H}_{-i})^{-1} \mathbf{H}_{-i}^\dagger \right) \mathbf{h}_i \right\|^2 \right). \quad (7.39)$$

The achievable sum-rates for finite constellation inputs with per-stream optimal and per-stream sub-optimal decodings are given in (7.27) and (7.28) by applying the decorrelator filter, i.e., $\mathbf{v}_i = \mathbf{v}_i^{\text{dc}}$.

From the results in the literature, the MMSE filter requires the largest complexity since it involves a matrix inversion operation but provides the best performance for Gaussian input signal. The MF and decorrelator filters are simpler but only work well in the low SNR and high SNR regime, respectively. It is expected the similar performance trend for the finite constellation inputs, we will exemplify this by the numerical results in the next section.

7.6 Numerical Examples

In this section, we numerically evaluate the achievable sum-rates of three different DFEs (MMSE DFE, MF DFE, decorrelator DFE) for both per-stream optimal and sub-optimal decodings. Similarly to Chapter 5, we set the parameters which are close to those in a real uplink UMTS system as specified in [3GPTm] (specific details

on the signature waveform, spreading sequences, etc. can be found in Section 5.5 of Chapter 5). For comparison, the achievable sum-rates with Gaussian distributed input and optimal joint decoding are also included.

For Gaussian distributed input: The sum-capacity of the optimal joint decoding is computed by $C_s^{\text{Gauss}} = \log \det(\mathbf{I} + \mathbf{H}_w \mathbf{R}_{xx} \mathbf{H}_w^\dagger)$. The achievable sum-rates with the DFEs are obtained by (7.29), which are the same for per-stream optimal and per-stream sub-optimal decodings as we discussed in Section 7.5.1.

For finite constellation inputs: The sum-capacities of the optimal joint decoding are computed as $C_s^{\text{QAM}} = h(\mathbf{z}_w) - h(\mathbf{z}_w|\mathbf{x}) = h(\mathbf{H}_w \mathbf{x} + \mathbf{n}_w) - h(\mathbf{n}_w)$. The achievable sum-rates for the DFEs with per-stream optimal decoding and per-stream sub-optimal decoding are obtained by (7.27) and (7.28), respectively.

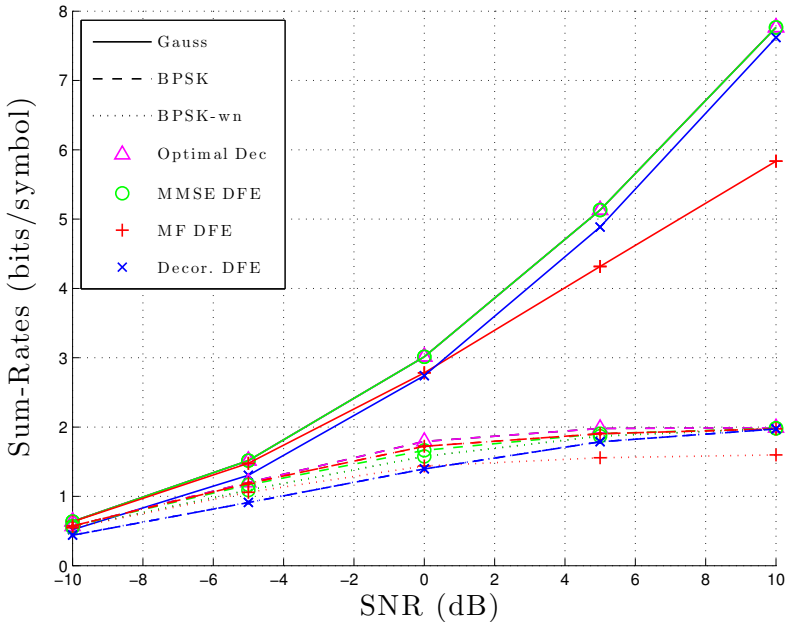


Figure 7.6: Achievable sum-rates of various DFEs when $N_t = 4$ ($K = 2$, $M = 1$, $N = 2$) and $L = 3$ for Gaussian distributed and BPSK inputs. All rates are normalized by $1/NM$.

Figure 7.6 shows the achievable sum-rates of the proposed DFEs for both Gaussian distributed and BPSK inputs when $N_t = 4$. For Gaussian distributed input, the achievable sum-rate of the MMSE DFE is the same as the sum-capacity of the optimal joint receiver. That is, the low-complexity MMSE DFE structure is optimal for Gaussian distributed input, since then the inter-stream interference is Gaussian distributed. The MF DFE and the decorrelator DFE show a tradeoff in terms of

the achievable sum-rate with respect to SNR. While the achievable sum-rate of the MF DFE is close to the optimal one at low SNR, the decorrelator DFE performs better at high SNR. For BPSK input, we can see a gap between the achievable sum-rates achieved by the MMSE DFE and by the optimal joint decoding, i.e., the MMSE DFE structure is no longer optimal, a fact which is often off one's mind. As expected, the DFEs with per-stream optimal decoding outperforms the DFEs with per-stream sub-optimal decoding. In this setup, the MF DFE also outperforms the MMSE DFE and decorrelator DFE for BPSK input. Interestingly, for the decorrelator DFE with BPSK input, both per-stream optimal decoding and per-stream sub-optimal decoding provide the same performance. This can be explained as follows: The decorrelator filter completely removes the inter-stream interferences which leads to the same noise terms for both cases regardless the assumed statistics of the inter-stream interference.

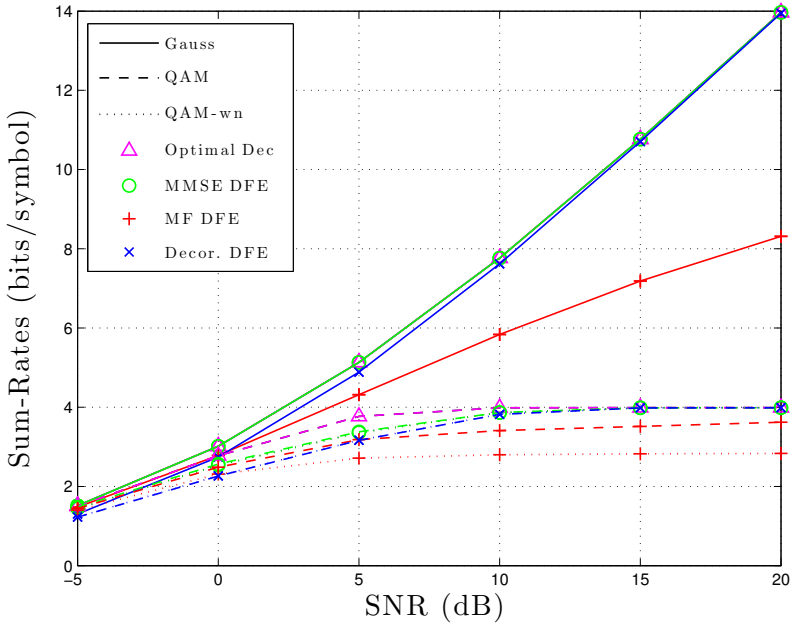


Figure 7.7: Achievable sum-rates of various DFEs when $N_t = 2$ ($K = 2, M = 1, N = 1$) and $L = 3$ for Gaussian distributed and 4-QAM inputs. The index “-wn” represents the per-stream sub-optimal decoding with worst-case noise. All rates are normalized by $1/NM$.

Figure 7.7 shows the achievable sum-rates of the proposed DFEs for Gaussian distributed and 4-QAM inputs when $N_t = 2$. The performance trends for Gaussian distributed input are the same to those in Figure 7.6. However, unlike the results in

Figure 7.6, for this setup, among the DFEs with per-stream optimal decoding, the MMSE DFE outperforms the MF DFE and decorrelator DFE. This implies that although MMSE filter is shown to be the best linear filter for Gaussian distributed input, the optimal linear filter for finite constellation input is still unknown.

In addition, from Figure 7.6 and Figure 7.7, we can see that the performance gap between per-stream optimal decoding and per-stream sub-optimal decoding is smaller for 4-QAM input compared to the one of BPSK input. This can be explained as follows: when a higher modulation scheme is used, the approximation by Gaussian distribution becomes better due to the law of large number and central limit theorem. Therefore, in practice when the modulation constellation used at the transmitter is high enough, the sub-optimal decoding strategy can be used at the receiver to reduce the complexity without sacrificing much on the performance.

Figure 7.8 shows the achievable sum-rates of the proposed DFEs for Gaussian distributed and BPSK inputs with a larger number of streams $N_t = 8$. The trends of the achievable sum-rates are similar to those in Figure 7.7. As shown in the figure, the MMSE DEF achieves the best sum-rate in this setup.

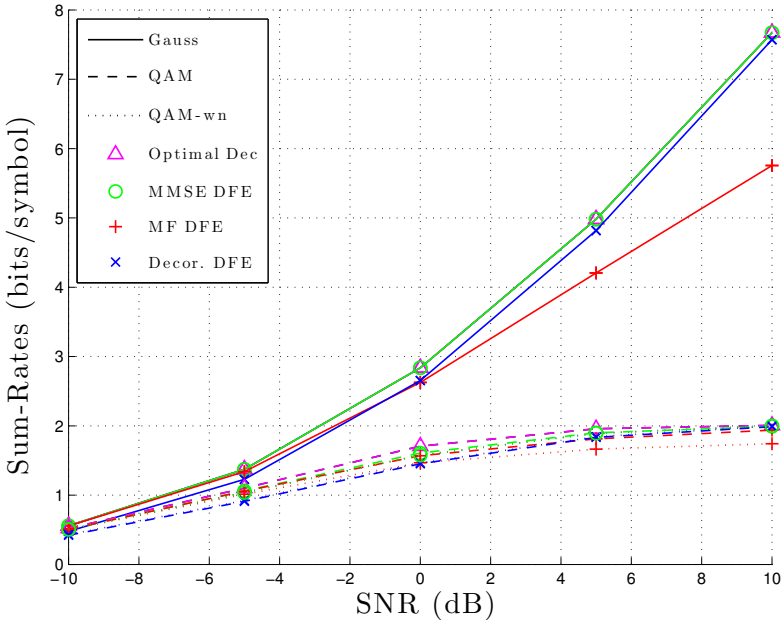


Figure 7.8: Achievable sum-rates of various DFEs when $N_t = 8$ ($K = 2, M = 1, N = 4$) and $L = 3$ for Gaussian distributed and BPSK inputs. The index “-wn” represents the per-stream sub-optimal decoding with worst-case noise. All rates are normalized by $1/NM$.

7.7 Chapter Conclusion

In this chapter, the performance of the DFE has been studied for the uplink WCDMA channel. Following the literature, we showed that the MMSE DFE, which has a low-complexity structure compared to the optimal receiver, is sum-capacity lossless for Gaussian distributed input and applied it to our uplink WCDMA channel. In addition to the MMSE DFE, we consider two other DFEs: MF DFE and decorrelator DFE. Motivated from the decoding strategies for the uplink WCDMA channel with imperfect CSIR in Chapter 6, we investigated the performance of the DFE when the streams are optimally decoded using the true statistics of the inter-stream interference and sub-optimally decoded treating the inter-stream interference as additive Gaussian noise. Throughout MATLAB simulations, we provided the performance comparison among three different DFEs for both per-stream optimal decoding and per-stream sub-optimal decoding. Numerical results show that although the MMSE DFE is optimal for Gaussian input signal, it is sub-optimal for finite constellation input signals. Moreover, one can obtain performance gains by treating the inter-stream interference using its true statistics instead of simply treating it as worst-case noise.

Conclusion

8.1 Summary

In this thesis, we have investigated some fundamental limits in wireless wideband networking. In particular, we have studied the energy efficiency and bandwidth efficiency aspects of two classes of wireless wideband networks: Gaussian MIMO bidirectional broadcast channels and uplink wideband CDMA channels. In the following, we summarize the main results in this thesis.

- In Chapter 3, we have studied the energy efficiency of a *single user-pair Gaussian MIMO bidirectional broadcast channel*. We derived an optimal transmit strategy for the system in the wideband regime. It has been shown that:

- In the wideband regime (or low SNR regime), a closed-form solution of the optimal transmit strategy for the Gaussian MIMO bidirectional broadcast channel can be obtained, which was impossible in the moderate SNR regime.
- Beamforming along the principal eigenvector of the equivalent channel matrix is optimal in the low SNR regime. This result is similar to the single beam optimality of a point-to-point MIMO channel in the low SNR regime, i.e., the optimal policy is to allocate all power to the strongest eigenmode.
- For MISO channels the optimal beamforming vector can be expressed as the linear combination of channel directions.
- The vector optimization problem formulation allows us to take the fairness issues into account when designing the transmit strategy.
- The proposed transmit strategy can achieve the individual wideband slope of a point-to-point Gaussian channel (2 bits/s/Hz/3dB). The highest system wideband slope (4 bits/s/Hz/3dB) can be obtained with the max-min fairness strategy.

- In Chapter 4, we have extended the study in Chapter 3 to a *multiple user-pair Gaussian MIMO bidirectional broadcast channel*. We proposed a simple transmit

scheme for the multi-pair bidirectional broadcast channel in the wideband regime, which is motivated from the optimal transmit strategy for the single user-pair case. It has been shown that:

- A closed-form solution of the optimal transmit strategy in sense of maximizing the achievable wideband weighted sum-rate can be derived.
- The operation points on the boundaries of the achievable wideband rate and EpB regions can be achieved by serving only a selected user-pair with full power.
- Similar to the single user-pair setup, single beam transmit strategy is also optimal in the wideband regime.
- Although the wideband capacity and MEpB regions of a multi-pair MIMO bidirectional broadcast channel have not been derived, the proposed scheme can achieve the corner points in the boundaries of the wideband capacity and MEpB regions.

- In Chapter 5, we have studied the spectral efficiency of an *uplink wideband CDMA channel with perfect CSIR*. Various realistic assumptions have been included into the problem, which make the framework and results valuable for the performance assessment of real cellular networks. It has been shown that:

- A sufficient statistic for decoding the transmitted messages can be obtained by a bank of matched filters at the receiver. An equivalent discrete-time channel model can be then expressed based on the sufficient statistics.
- The capacity regions for finite constellation inputs and Gaussian distributed input can be both analytically and numerically characterized using the equivalent discrete-time channel model.
- Sampling within the transmission time window may cause a capacity loss even if sampling was performed at Nyquist rate. However, this loss can be significantly diminished by extending the sampling window by only few symbol durations.
- With proper choices of the (effective) signature waveforms, a multi-user uplink WCDMA channel can be decoupled so that each user achieves a point-to-point channel capacity when SNR tends to infinity.

- In Chapter 6, we have extended the study of Chapter 5 to an *uplink wideband CDMA channel with imperfect CSIR*. We first discretized the continuous-time received signal using the concept of mismatched filtering based on the imperfect CSIR. We then proposed two decoding strategies for the resulting discrete-time signals: the optimal decoding strategy based on the specific statistics of channel estimation errors and the sub-optimal decoding strategy treating the estimation errors as worst-case noise. It has been shown that:

- When the equivalent estimation errors follow Gaussian distributions, a simple expression for the achievable rate region can be obtained, which significantly reduces the computation complexity.
- Although the estimation errors are unknown at the receiver, one can enhance the performance by exploiting the knowledge about the statistics of the estimation errors instead of traditionally treating them as additive Gaussian noise.
- Finite constellation inputs are less sensitive to the estimation accuracy than Gaussian input, especially in the high SNR regime.

- In Chapter 7, we have studied an *uplink wideband CDMA channel with DFE*. We have considered a low-complexity receiver for the uplink WCDMA system based on the DFE, which decomposes the equivalent MIMO channel into a series of point-to-point channels with interference pre-subtraction at the receiver. Motivated from the decoding strategies for the uplink WCDMA channel with imperfect CSIR, we have investigated the performance of the DFE when the streams were optimally decoded (using the true statistics of the inter-stream interference) and sub-optimally decoded (treating the inter-stream interference as Gaussian noise). It has been shown that:

- The low-complexity MMSE DFE is sum-capacity lossless for Gaussian distributed input but is sub-optimal for finite constellation inputs.
- Unlike in a system with Gaussian input, the MMSE DFE does not always outperform the MF DFE or decorrelator DFE in systems with finite constellation inputs.
- For the DFE, one can also obtain performance gains by treating the inter-stream interferences with their true statistics instead of simply treating them as Gaussian noise while decoding the streams.

8.2 Discussion

Fundamentally, the study in this thesis has been constructed from theoretical analysis and computer simulation. However, we have built up our study around system models that can capture important characteristics of practical networks, and yet are tractable to analyze. To this end, we organized the flow of the thesis from a simple and theoretical setup to more complex and as close as possible to practical setups. For instance, in the first part of the thesis, we have studied from a simple single user-pair network to a multiple user-pair network, which can better describe the nature a cellular network, where many user-pairs want to communicate together with support of a base station under the presence of interference from other user-pairs. In the second part of the thesis, we started from an uplink WCDMA system with some ideal assumptions (perfect CSIR, optimal joint decoding), then add more and more practical assumptions (imperfect CSIR, sub-optimal DFE) in the following. Of

course, the study still has its own limits. For example, some other assumptions have not been included such as inter-cell interference, fading environment, etc. However, we expect that the framework and results in this thesis will be useful for the assessment of real cellular networks to identify potentials for performance improvements in practical design.

Bibliography

- [3GPTm] 3GPP, *3GPP Specification series: 25-series 3GPP TSG RAN (Release 11)*, 2012. [Online]: <http://www.3gpp.org/DynaReport/25-series.htm>.
- [AH13] J. Ahmed and K. A. Hamdi, "Spectral efficiency of asynchronous MC-CDMA with frequency offset over correlated fading," *IEEE Trans. Veh. Technol.*, vol. 62, no. 7, pp. 3423–3429, Sep. 2013.
- [Ahl71] R. Ahlswede, "Multi-way communication channels," in *Proc. 2nd. Int. Symp. Infor. Theory (ISIT)*, Sep. 1971.
- [AK12] Y. Avrithis and Y. Kalantidis, "Approximate gaussian mixtures for large scale vocabularies," in *Proc. 12th European conference on Computer Vision*, Oct. 2012.
- [AKSH09] A. S. Avestimehr, M. A. Khajehnejad, A. Sezgin, and B. Hassibi, "Capacity region of the deterministic multi-pair bi-directional relay network," in *Proc. IEEE Information Theory Workshop*, Jun. 2009, pp. 57–61.
- [ASDG06] A. Abdel-Samad, T. N. Davidson, and A. B. Gershman, "Robust transmit eigen beamforming based on imperfect channel state information," *IEEE Trans. Signal Process.*, vol. 54, no. 5, pp. 1596 – 1609, May 2006.
- [Aul10] T. Aulin, "Signal processing in digital communications - the fall of science," in *Proc. 7th Inter. Symp. on Wire. Commun. Systems (ISWCS)*, Sep. 2010, pp. 112–114.
- [Bon95] P. K. Bondyopadhyay, "Guglielmo Marconi - the father of long distance radio communication - an engineer's tribute," in *25th European Microwave Conference*, vol. 2, Sep. 1995, pp. 879–885.
- [BS08] H. Boche and M. Schubert, "The structure of general interference functions and applications," *IEEE Trans. Inf. Theory*, vol. 54, no. 11, pp. 4980 –4990, Nov. 2008.

- [BV04] S. Boyd and L. Vandenberghe, *Convex Optimization*. Cambridge Univ. Press., 2004.
- [BXX08] M. Boko, J. Xavier, and V. A. N. Barroso, “Further results on the capacity and error probability analysis of noncoherent MIMO systems in the low SNR regime,” *IEEE Trans. Signal Process.*, vol. 56, no. 7, pp. 2915–2930, Jul. 2008.
- [CDEF95a] J. M. Cioffi, G. P. Dudevoir, M. V. Eyuboglu, and G. D. Forney, “MMSE decision-feedback equalizers and coding I: Equalization results,” *IEEE Trans. Commun.*, vol. 43, no. 10, pp. 2582–2594, Oct. 1995.
- [CDEF95b] J. M. Cioffi, G. P. Dudevoir, M. V. Eyuboglu, and G. Forney, “MMSE decision-feedback equalizers and coding II: Coding results,” *IEEE Trans. Commun.*, vol. 43, no. 10, pp. 2595–2604, Oct. 1995.
- [CDL09] Y. Cai and R. C. De Lamare, “Space-time adaptive MMSE multiuser decision feedback detectors with multiple-feedback interference cancellation for CDMA systems,” *IEEE Trans. Veh. Technol.*, vol. 58, no. 8, pp. 4129–4140, Oct. 2009.
- [CJKR10] G. Caire, N. Jindal, M. Kobayashi, and N. Ravindran, “Multiuser MIMO achievable rates with downlink training and channel state feedback,” *IEEE Trans. Inf. Theory*, vol. 56, no. 6, pp. 2845–2866, Jun. 2010.
- [CMD10] L. Cottatellucci, R. Muller, and M. Debbah, “Asynchronous CDMA systems with random spreading - part I: Fundamental limits,” *IEEE Trans. Inf. Theory*, vol. 56, no. 4, pp. 1477–1497, Apr. 2010.
- [CP96] K. M. Chugg and A. Polydoros, “MLSE for an unknown channel part i: Optimality considerations,” *IEEE Trans. Commun.*, vol. 44, no. 7, pp. 836–846, Jul. 1996.
- [CT06] T. M. Cover and J. A. Thomas, *Elements of Information Theory, 2nd Ed.* Wiley-Interscience, 2006.
- [CTV04] G. Caire, D. Tuninetti, and S. Verdú, “Suboptimality of TDMA in the low-power regime,” *IEEE Trans. Inf. Theory*, vol. 50, no. 4, pp. 608–620, Apr. 2004.
- [CWPS11] D. F. Crouse, P. Willett, K. Pattipati, and L. Svensson, “A look at gaussian mixture reduction algorithms,” in *Proc. IEEE FUSION*, 2011.

- [CY09] M. Chen and A. Yener, “Multiuser two-way relaying: detection and interference management strategies,” *IEEE Trans. Wireless Commun.*, vol. 8, no. 8, pp. 4296–4305, Aug. 2009.
- [DBK⁺98] E. Dahlman, P. Beming, J. Knutsson, F. Ovesjo, M. Persson, and C. Roobol, “WCDMA—the radio interface for future mobile multimedia communications,” *IEEE Trans. Veh. Technol.*, vol. 47, no. 4, pp. 1105–1118, Nov. 1998.
- [DGC03] M. O. Damen, H. E. Gamal, and G. Caire, “On maximum-likelihood detection and the search for the closest lattice point,” *IEEE Trans. Inf. Theory*, vol. 49, no. 10, pp. 2389–2402, Oct. 2003.
- [DKOP15] T. T. Do, S. M. Kim, T. J. Oechtering, and G. Peters, “Capacity analysis of uplink WCDMA systems with imperfect channel state information,” in *Proc. 81th IEEE Veh. Technol. Conf. (VTC2015-Spring)*, May 2015.
- [DKO⁺ed] T. T. Do, S. M. Kim, T. J. Oechtering, M. Skoglund, and G. Peters, “Waveform domain framework for capacity analysis of uplink WCDMA systems,” *EURASIP Journal on Wireless Commun. and Networking*, 2015, conditionally accepted.
- [DOKP14] T. T. Do, T. J. Oechtering, S. M. Kim, and G. Peters, “Capacity analysis of continuous-time time-variant asynchronous uplink wideband CDMA system,” in *Proc. 80th IEEE Veh. Technol. Conf. (VTC2014-Fall)*, Sep. 2014.
- [DOK⁺ed] T. T. Do, T. J. Oechtering, S. M. Kim, M. Skoglund, and G. Peters, “Uplink waveform channel with imperfect channel state information and finite constellation inputs,” *IEEE Trans. Wireless Commun.*, 2015, submitted.
- [DOS11] T. T. Do, T. J. Oechtering, and M. Skoglund, “Optimal transmission for the MIMO bidirectional broadcast channel in the wideband regime,” in *Proc. 12th IEEE Int. Workshop on Signal Process. Adv. in Wireless Commun. (SPAWC2011)*, Jun. 2011, pp. 356–360.
- [DOS12] —, “Achievable energy per bit for the multi-pair MIMO bidirectional broadcast channel,” in *Proc. 18th European Wireless Conference (EW2012)*, Apr. 2012.
- [DOS13] —, “Optimal transmission for the MIMO bidirectional broadcast channel in the wideband regime,” *IEEE Trans. Signal Process.*, vol. 61, no. 20, pp. 5103–5116, Oct. 2013.
- [DPSB08] E. Dahlman, S. Parkvall, J. Sköld, and P. Beming, *3G Evolution: HSPA and LTE for Mobile Broadband, 2nd Ed.* Elsevier, 2008.

- [FBW06] C. Fragouli, J.-Y. L. Boudec, and J. Widmer, “Network coding: An instant primer,” *SIGCOMM Comput. Commun. Rev.*, vol. 36, no. 1, pp. 63–68, 2006.
- [FCC⁺09] T. L. Fulghum, D. Cairns, C. Cozzo, Y.-P. E. Wang, and G. E. Bottomley, “Adaptive generalized rake reception in DS-CDMA systems,” *IEEE Trans. Wireless Commun.*, vol. 8, no. 7, pp. 3464–3474, Jul. 2009.
- [Gal68] R. G. Gallager, *Information theory and reliable communication*. John Wiley & Sons, 1968.
- [GC01] G. Ginis and J. M. Cioffi, “On the relation between V-BLAST and the GDFE,” *IEEE Commun. Letters*, vol. 5, no. 9, pp. 364–366, Sep. 2001.
- [GLT00] A. Ganti, A. Lapidoth, and I. E. Telatar, “Mismatched decoding revisited: general alphabets, channels with memory, and the wide-band limit,” *IEEE Trans. Inf. Theory*, vol. 46, no. 7, pp. 2315–2328, Nov. 2000.
- [GN99] A. K. Gupta and D. K. Nagar, *Matrix variate distributions*. CRC Press, 1999.
- [Gra72] R. M. Gray, “On the asymptotic eigenvalue distribution of Toeplitz matrices,” *IEEE Trans. Inf. Theory*, vol. 18, no. 6, pp. 725–730, Nov. 1972.
- [Gra09] —, *Probability, Random Processes, and Ergodic Properties*, 2nd ed. Springer-verlag US, 2009.
- [GYGP13] D. Gündüz, A. Yener, A. Goldsmith, and H. V. Poor, “The multiway relay channel,” *IEEE Trans. Inf. Theory*, vol. 59, no. 1, pp. 51–63, Jan. 2013.
- [HBDWH08] M. F. Huber, T. Bailey, H. Durrant-Whyte, and U. D. Hanebeck, “On entropy approximation for gaussian mixture random vectors,” in *Proc. IEEE Multisensor Fusion and Integration for Intelligent Systems (MFI)*, 2008.
- [HH03] B. Hassibi and B. M. Hochwald, “How much training is needed in multiple-antenna wireless links?” *IEEE Trans. Inf. Theory*, vol. 49, no. 4, pp. 951–963, Apr. 2003.
- [HH08] M. F. Huber and U. D. Hanebeck, “Progressive gaussian mixture reduction,” in *Proc. IEEE FUSION*, 2008.

- [HM88] W. Hirt and J. L. Massey, "Capacity of the discrete-time Gaussian channel with intersymbol interference," *IEEE Trans. Inf. Theory*, vol. 34, no. 3, pp. 38–38, May 1988.
- [HM10] A. Høst-Madsen, "Minimum energy per bit in wireless networks with correlated information," in *Proc. IEEE Int. Symp. on Inform. Theory 2010*, Jun. 2010, pp. 2358–2362.
- [HT04] H. Holma and A. Toskala, *WCDMA for UMTS*. John Wiley & Sons, Ltd, 2004.
- [HtB03] B. M. Hochwald and S. ten Brink, "Achieving near-capacity on a multiple-antenna channel," *IEEE Trans. Commun.*, vol. 51, no. 3, pp. 389–399, Mar. 2003.
- [HV05] B. Hassibi and H. Vikalo, "On the sphere-decoding algorithm i. expected complexity," *IEEE Trans. Signal Process.*, vol. 53, no. 8, Aug. 2005.
- [ITU14] ITU, *The World in 2014: ICT Facts and Figures*. ITU releases 2014 ICT figures, 2014.
- [JBN10] E. Jorswieck, H. Boche, and S. Naik, "Energy-aware utility regions: Multiple access Pareto boundary," *IEEE Trans. Wireless Commun.*, vol. 9, no. 7, pp. 2216–2226, Jul. 2010.
- [JKV09] A. Jain, S. R. Kulkarni, and S. Verdú, "Minimum energy per bit for Gaussian broadcast channels with common message and cooperating receivers," in *Proc. 47th Annual Allerton Conf.*, Oct. 2009, pp. 740–747.
- [JKV11] A. Jain, S. Kulkarni, and S. Verdú, "Multicasting in large wireless networks: Bounds on the minimum energy per bit," *IEEE Trans. Inf. Theory*, vol. 57, no. 1, pp. 14–32, Jan. 2011.
- [JL05] L. B. Jiang and S. C. Liew, "Proportional fairness in wireless LANs and ad hoc networks," in *Proc. of IEEE Wireless Commun. and Networking Conf. (WCNC '05)*, vol. 3, Mar. 2005, pp. 1551–1556.
- [JO05] J. Jaldén and B. Ottersten, "On the complexity of sphere decoding in digital communications," *IEEE Trans. Signal Process.*, Apr. 2005.
- [Kay93] M. S. Kay, *Fundamentals of statistical signal processing, volume I: Estimation theory*. Englewood Cliffs: Prentice Hall PTR, 1993.
- [KDOP14] S. M. Kim, T. T. Do, T. J. Oechtering, and G. Peters, "Sphere decoding inspired approximation method to compute the entropy of large Gaussian mixture distributions," in *2014 IEEE Stat. Signal Process. Workshop (SSP'14)*, Jul. 2014.

- [KDOP15] —, “On the entropy computation of large complex gaussian mixture distributions,” *IEEE Trans. Signal Process.*, vol. 63, no. 17, pp. 4710–4723, Sep. 2015.
- [Kel97] F. P. Kelly, “Charging and rate control for elastic traffic,” *Eur. Trans. Telecommun.*, vol. 8, no. 1, pp. 33–37, Jan. 1997.
- [KMT08] S. J. Kim, P. Mitran, and V. Tarokh, “Performance bounds for bidirectional coded cooperation protocols,” *IEEE Trans. Inf. Theory*, vol. 54, no. 11, pp. 5235–5241, Nov. 2008.
- [KSD10] S. J. Kim, B. Smida, and N. Devroye, “Capacity bounds on multi-pair two-way communication with a base-station aided by a relay,” in *Proc. IEEE Int. Symp. on Inform. Theory 2010*, Jun. 2010, pp. 425–429.
- [KSS93] G. Kaplan and S. Shamai (Shitz), “Information rates and error exponents of compound channels with application to antipodal signaling in a fading environment,” *AEÜ-International Journal of Electronics and Communication*, vol. 47, no. 4, pp. 228–230, 1993.
- [Lap96] A. Lapidoth, “Mismatched decoding and the multiple-access channel,” *IEEE Trans. Inf. Theory*, vol. 42, no. 5, pp. 1439–1452, Sep. 1996.
- [Lap09] —, *A Foundation in Digital Communication*. Cambridge, 2009.
- [LGW04] Q. Li, C. N. Georghiadis, and X. Wang, “Blind multiuser detection in uplink CDMA with multipath fading: A sequential EM approach,” *IEEE Trans. Commun.*, vol. 52, no. 1, Jan. 2004.
- [LJS06] P. Larsson, N. Johansson, and K. E. Sunell, “Coded bi-directional relaying,” in *Proc. 63th IEEE Veh. Technol. Conf.*, vol. 2, May 2006, pp. 851–855.
- [LSK12] N. Lee, O. Simeone, and J. Kang, “The effect of imperfect channel knowledge on a MIMO system with interference,” *IEEE Trans. Commun.*, vol. 60, no. 8, pp. 2221–2229, Aug. 2012.
- [LTV03] A. Lozano, A. M. Tulino, and S. Verdú, “Multiple-antenna capacity in the low-power regime,” *IEEE Trans. Inf. Theory*, vol. 49, no. 10, pp. 2527–2544, Oct. 2003.
- [LUE05] J. Luo, S. Ulukus, and A. Ephremides, “Optimal sequences and sum capacity of symbol asynchronous CDMA systems,” *IEEE Trans. Inf. Theory*, vol. 51, no. 8, pp. 2760–2769, Aug. 2005.

- [Méd00] M. Médard, “The effect upon channel capacity in wireless communications of perfect and imperfect knowledge of the channel,” *IEEE Trans. Inf. Theory*, vol. 46, no. 3, pp. 933–946, May 2000.
- [MGDC06] A. D. Murugan, H. E. Gamal, M. O. Damen, and G. Caire, “A unified framework for tree search decoding: rediscovering the sequential decoder,” *IEEE Trans. Inf. Theory*, vol. 52, no. 3, Mar. 2006.
- [MLTV10] P. Memmolo, M. Lops, A. M. Tulino, and R. A. Valenzuela, “Up-link multi-user MIMO capacity in low-power regime,” in *Proc. IEEE Int. Symp. on Inform. Theory 2010*, Jun. 2010, pp. 2308–2312.
- [MM12] O. Mashayekhi and F. Marvasti, “Uniquely decodable codes with fast decoder for overloaded synchronous CDMA systems,” *IEEE Trans. Commun.*, vol. 60, no. 11, pp. 3145–3149, Nov. 2012.
- [OJWB09] T. J. Oechtering, E. A. Jorswieck, R. F. Wyrembelski, and H. Boche, “On the optimal transmit strategy for the MIMO bidirectional broadcast channel,” *IEEE Trans. Commun.*, vol. 57, no. 12, pp. 3817–3826, Dec. 2009.
- [OKJ10] L. Ong, C. M. Kellett, and S. J. Johnson, “Capacity theorems for the AWGN multi-way relay channel,” in *Proc. IEEE Int. Symp. on Inform. Theory 2010*, Jun. 2010, pp. 664–668.
- [OSBB08] T. J. Oechtering, C. Schnurr, I. Bjelakovic, and H. Boche, “Broadcast capacity region of two-phase bidirectional relaying,” *IEEE Trans. Inf. Theory*, vol. 54, no. 1, pp. 454–458, Jan. 2008.
- [OWB09] T. J. Oechtering, R. F. Wyrembelski, and H. Boche, “Multiantenna bidirectional broadcast channels—optimal transmit strategies,” *IEEE Trans. Signal Process.*, vol. 57, no. 5, pp. 1948–1958, May 2009.
- [Poo94] H. V. Poor, *An Introduction to Signal Detection and Estimation, 2nd Ed.* Springer-Verlag, 1994.
- [Pro95] J. G. Proakis, *Digital communications, 3rd Ed.* McGraw-Hill, New York, 1995.
- [PRS03] S. I. Park, V. Raghunathan, and M. B. Srivastava, “Energy efficiency and fairness tradeoffs in multi-resource, multi-tasking embedded systems,” in *Proc. ACM Int’l Symp. Low Power Electronics and Design*, Aug. 2003, pp. 469–474.
- [PZSY13] P. Pan, Y. Zhang, Y. Sun, and L.-L. Yang, “On the asymptotic spectral efficiency of uplink MIMO-CDMA systems over rayleigh fading channels with arbitrary spatial correlation,” *IEEE Trans. Veh. Technol.*, vol. 62, no. 2, pp. 679–691, Feb. 2013.

- [RM94] M. Rupf and J. Massey, "Optimum sequence multisets for synchronous code-division multiple-access channels," *IEEE Trans. Inf. Theory*, vol. 40, no. 4, pp. 1261–1266, 1994.
- [RW07] B. Rankov and A. Wittneben, "Spectral efficient protocols for half-duplex fading relay channels," *IEEE J. Sel. Areas Commun.*, vol. 25, no. 2, pp. 379–389, Feb. 2007.
- [SH09] D. Schieferdecker and M. F. Huber, "Gaussian mixture reduction via clustering," in *Proc. IEEE FUSION*, 2009.
- [SMF14] J. Scarlett, A. Martinez, and A. G. i. Fàbregas, "Mismatched decoding: Error exponents, second-order rates and saddlepoint approximations," *IEEE Trans. Inf. Theory*, vol. 60, no. 5, pp. 2647–2666, May 2014.
- [SSBNS08] O. Simeone, O. Somekh, Y. Bar-Ness, and U. Spagnolini, "Throughput of low-power cellular systems with collaborative base stations and relaying," *IEEE Trans. Inf. Theory*, vol. 54, no. 1, pp. 459–467, Jan. 2008.
- [TH99] D. N. C. Tse and S. V. Hanly, "Linear multiuser receivers: effective interference, effective bandwidth and user capacity," *IEEE Trans. Inf. Theory*, vol. 45, no. 2, pp. 641–657, Mar. 1999.
- [TV05] D. Tse and P. Viswanath, *Fundamentals of Wireless Communication*. Cambridge Univ. Press., 2005.
- [UY04] S. Ulukus and R. D. Yates, "User capacity of asynchronous CDMA systems with matched filter receivers and optimum signature sequences," *IEEE Trans. Inf. Theory*, vol. 50, no. 5, pp. 903–909, May 2004.
- [UYHMX10] M. Uppal, Z. Yang, A. Høst-Madsen, and Z. Xiong, "Cooperation in the low power regime for the MAC using multiplexed rateless codes," *IEEE Trans. Signal Process.*, vol. 58, no. 9, pp. 4720–4734, Sep. 2010.
- [VA99] P. Viswanath and V. Anantharam, "Optimal sequences and sum capacity of synchronous CDMA systems," *IEEE Trans. Inf. Theory*, vol. 45, no. 6, Sep. 1999.
- [Ver89] S. Verdú, "The capacity region of the symbol-asynchronous Gaussian multiple-access channel," *IEEE Trans. Inf. Theory*, vol. 35, no. 4, pp. 733–751, Jul. 1989.
- [Ver98] —, *Multiuser Detection*. The Press of Syndicate of the University of Cambridge, 1998.

- [Ver02] —, “Spectral efficiency in the wideband regime,” *IEEE Trans. Inf. Theory*, vol. 48, no. 6, pp. 1319–1343, Jun. 2002.
- [VS99] S. Verdú and S. Shamai, “Spectral efficiency of CDMA with random spreading,” *IEEE Trans. Inf. Theory*, vol. 45, no. 2, pp. 622–640, Mar. 1999.
- [WCK05] Y. Wu, P. A. Chou, and S. Y. Kung, “Information exchange in wireless networks with network coding and physical-layer broadcast,” in *Proc. 39th Conf. Inf. Sci. Syst.*, vol. 2, Mar. 2005, pp. 16–18.
- [WJ65] J. M. Wozencraft and I. M. Jacobs, *Principles of communication engineering, Vol. 1*. New York: Wiley, 1965.
- [WOB⁺08] R. F. Wyrembelski, T. J. Oechtering, I. Bjelakovic, C. Schnurr, and H. Boche, “Capacity of Gaussian MIMO bidirectional broadcast channels,” in *Proc. IEEE Int. Symp. on Inform. Theory 2008*, Jul. 2008, pp. 584–588.
- [WP99] X. Wang and H. V. Poor, “Space-time multiuser detection in multipath CDMA channels,” *IEEE Trans. Signal Process.*, vol. 47, no. 9, pp. 2356–2374, Sep. 1999.
- [Wyn66] A. D. Wyner, “The capacity of the band-limited Gaussian channel,” *Bell Syst. Tech. J.*, vol. 45, pp. 359–395, 1966.
- [YC04] W. Yu and J. M. Cioffi, “Sum capacity of gaussian vector broadcast channels,” *IEEE Trans. Inf. Theory*, vol. 50, no. 9, pp. 1875–1892, Sep. 2004.
- [YC10] Y. H. Yun and J. H. Cho, “On sum capacity of continuous-time overloaded CDMA systems,” in *Proc. Inf. Theory and Appl. Workshop (ITA)*, Feb. 2010.
- [YG06] T. Yoo and A. Goldsmith, “Capacity and power allocation for fading MIMO channels with channel estimation error,” *IEEE Trans. Inf. Theory*, vol. 52, no. 5, pp. 2203–2214, May 2006.
- [YYU02] A. Yener, R. D. Yates, and S. Ulukus, “CDMA multiuser detection: A nonlinear programming approach,” *IEEE Trans. Commun.*, vol. 50, no. 6, Jun. 2002.
- [ZJW⁺10] C. Zhong, S. Jin, K.-K. Wong, M. S. Alouini, and T. Ratnarajah, “Low SNR capacity for MIMO rician and Rayleigh-Product fading channels with single co-channel interferer and noise,” *IEEE Trans. Commun.*, vol. 58, no. 9, pp. 2549–2560, Sep. 2010.